FOOT BEHAVIOR DURING WALKING BASED ON FOOT KINETICS AND KINEMATICS

WANG XUE

（B. ENG）

A THESIS SUBMITTED

FOR THE DEGREE OF DOCTOR OF PHILOSOPHY

DEPARTMENT OF MECHANIMCAL ENGINEERING

NATIONAL UNIVERSITY OF SINGAPORE

2012

DECLARATION

I hereby declare that the thesis is my original work and it has been written by me in its entirety. I have duly acknowledged all the sources of information which have been used in the thesis.

This thesis has also not been submitted for any degree in any university previously.

Wang Xue 25 Mar 2013

Wang Xue

March 25th, 2013

ABSTRACT

As most falls of aging population occur during walking, evaluation of walking behavior is important to understand the falls. Other clinical problems related to walking also require standard and improved methods for gait analysis. Many previous studies focused on gait analysis related to hip, knee and ankle motion and considered the foot as one rigid segment; however the foot is composed of multi-segments and joints. The foot behavior during walking is not yet well investigated. Useful information or features obtained from the foot dynamic behavior study could help to indicate normal and pathological gait, and will benefit clinical issues related to walking problems or foot dysfunctions. Hence, the objective of this thesis is to study the foot behavior during walking based on foot kinetics and kinematics, to extract useful foot dynamic features, and to model the foot dynamics.

For the foot kinetics, as foot pressure is much related to walking behavior, some features are extracted from foot pressure to depict the whole foot pressure changes during walking. These features could reflect kinetic information such as the foot center of pressure trajectory, and the foot pressure repeatability between strides. The foot pressure features are further applied for quantitative walking stability evaluation. Results show that some of the proposed foot pressure features work well in foot behavior characteristics description. In addition, the whole foot pressure is divided into sub-areas to investigate the segment pressure changes for foot behavior. However, the foot pressure is only 2D information. Thus, 3D foot motion is also analyzed for better understanding of foot behavior.

For the foot kinematics study, the 3D foot motion features are extracted. The foot motion features include joint rotation angles between sub-defined foot segments, and some proposed functional angles for describing the whole foot physical features of

walking. The results show that time-histories of the joint rotation angles present good agreement with previous literature. The results of four proposed functional angles are consistent with walking physics and can more intuitively describe foot kinematic behavior with good repeatability. Angle values at the mid-stance are proposed as dynamic reference positions, which perform well for reducing variance among subjects. In addition, different conditions are designed to enable subjects to walk in less stable conditions. Extracted foot motion features are applied to designed different walking conditions for their effectiveness on describing foot behavior characteristics. The current study provides evidence that the values of some foot motion features present significant difference in different walking conditions. Data of selected motion features are further processed with pattern recognition method for automatically classifying these walking conditions.

Finally, to better understand the foot kinetics and kinematics during walking, the relationship between foot segment pressure/force and motion is studied through modeling of the multi-segment foot. For foot dynamic function, modeling and simulation can be a good choice. For this purpose, a multi-segment foot model is built with LifeMOD biomechanics modeling toolbox. One normal walking and one abnormal walking are modeled. The simulated results from detailed foot model match well with the experiment data. This simulation provides a better visualized, relatively convenient, and thorough method for analyzing and understanding relationship among foot segment kinetic features, foot segment kinematic features and walking behaviors.

In conclusion, the foot dynamic behavior characteristics are studied through foot dynamic features extraction. The study could benefit many applications such as foot function investigation, shoe design industry, and clinical issues related to the foot.

ACKNOWLEDGEMENT

First and foremost, the author would like to express her deepest gratitude to Professor Lu Wen Feng, for his dedicated supervision, patient guidance and great support. This project would not have possibly reached this stage without his counsel support and guidance. Professor Lu Wen Feng is always very helpful and considerate. He is not only a great supervisor, but also a good friend, who shares life experiences and instrumental suggestions on all perspectives of life.

The author would like to express her most sincere appreciation to Professor Wong Yoke San and Professor Loh Han Tong, for their invaluable advices and continuous guidance. They have been very helpful throughout the process by giving critical advices and concerns for the project. Due to discussion with them, the author could have smooth and controlled research progress.

The author is very grateful to Singapore Polytechnic's Lecturer, Dr. Ong Fook Rhu, for his valuable advices, great support and sharing his knowledge. He is very experienced in using the equipment and his advices have been vital in data collection and analysis. Without his aid, this project would not have been successful.

The author would also like to thank Singapore Polytechnic's Lab officers, Mr. Lawrence and Mr. Yu Boon Tat, for their assistance in operations of the facilities in Singapore Polytechnic Biomechanics Lab.

The author would also like to thank the final-year project students, Mr. Julian Yeo, Mr. Ong Wua Wei, Mr. Lim Boon Tah, Ms. Shifali Jamwal and Mr. Nadzri Hussain for useful discussions and help.

The author would like to thank Mr. Huynh Kim Tho, Ms. Khatereh Hajizadeh, and Ms. Huang Meng Jie for their sharing research experience of LifeMOD modeling.

The author would like to thank Ms. Wang Jinling, Ms. Wang Yan, Mr. Wang Jingjing, Mr. Zheng Fei, Ms. Asma Perveen, Ms. Li Hai Yan, Mr. Indraneel Biswas, Mr. Hesamoddin Ahmadi and all the other labmates for their companion, support and encouragement.

The author also would like to thank Mr. Chen Xue Tao, for his understanding, encouragement and support. He takes pressure from the author and brings happiness. Finally the author would express her deepest appreciation to her parents Mr. Wang Fu Lin and Ms. Wo Su Rong. With their love and support, the author could overcome the most difficult time during the PhD study. Although they are far away in China, but the author can feel their support and encouragement anytime, anywhere and feel they are always by her side.

CONTENTS

LIST OF TABLES

LIST OF FIGURES

CHAPTER 1 INTRODUCTION

1.1 Background

As the population demographics shift during these several decades, aging and associated health risks are becoming increasingly important. Falls are a large cause of morbidity and mortality in the elderly people. Approximately 35% to 40% of healthy elderly people fall annually. Around 40-60% of falls results in injuries [1]. As most falls occur during walking, evaluation of walking behavior could be essential and helpful. Poor stability during walking leads to decreased life quality. Two methods of evaluating walking behavior are mostly used at present: one is through qualitative observation from experiences of physical therapists; the other one is through quantitative measurement of gait analysis by motion cameras. For quantitative measurement of gait analysis, many studies have been done for the whole body gait analysis or lower body gait analysis, which are more focused on the hip, knee and ankle motion study and consider the foot as one rigid body [2, 3].

In fact, the foot behavior is quite complex and closely related to the lower body function. 52 bones are in the feet, which are nearly one quarter of all body bones. The unique foot structure allows it to absorb the shock during foot strike and is rigid enough to push off the ground at the end of the stance phase. It works in conjunction with the lower body: ankle, knee, hip and lower back. While only a few studies are focused on the foot behavior, the foot is not yet well investigated for its behavior during walking. For foot dynamic behavior study, many experimental techniques were developed and employed, such as pressure sensing platforms [4], gait analysis [5, 6] and cadaveric anatomic experiments [7]. The first two methods are relatively easier

implemented. Most of the foot dynamic behavior studies have concentrated on the kinetic analysis and kinematic analysis. The kinetic analysis is processed with force and pressure plates for the force or pressure distribution during walking. On the other hand, the kinematic gait analysis could include dorsi-flexion/plantar-flexion, inversion/eversion, and abduction/adduction movements of fore-foot, mid-foot and hind-foot. Both the foot kinetics and foot kinematics are very important and could be measured with commercial equipment and further analyzed. Focusing on the foot dynamic behavior will benefit clinical problems related to walking problems or foot dysfunctions. To best describe foot behavior characteristics, foot kinetics and kinematics features could be extracted. To identify the features for foot dynamic behavior characteristics is very important and quite difficult, because the foot has complex structure and function. Useful features obtained from the foot dynamic behavior study could be accumulated to form database. The database could contain foot kinetic or kinematic features to indicate normal and pathological gait. For example, the diabetic patients tend to have higher pressure under metatarsals and different dorsi/plantar-flexion [8]. This will be very clinically important and helpful for disease prescription and solution. The feature data base could also provide useful information for customized shoe design industry. Once you know what type of foot you have, such as the foot with over pronation tendency, shoes that complement your feet should be selected.

For the foot kinetics, foot plantar pressure can be measured and analyzed to provide kinetic information. One main advantage of studying foot pressure is that the foot pressure could be relatively easily measured and the equipment is portable and relatively cheap. During the past several decades, foot plantar pressure information has been used in diverse fields such as in commercial shoe design, clinical applications and

sports medicine [9-11]. One of the most popular applications of foot plantar pressure research is to reduce the peak plantar pressure for comfortable walking of normal people and ulcers prevention for diabetic patients. Foot plantar pressure information is also widely used as a part of gait analysis for disease detection for patients with walking problems [12]. Different people would have different foot pressure during various behaviors. Foot plantar pressure can be an important indication of the foot kinetics and walking behavior. However, the foot pressure is only providing the 2D information and is a bit indirect and implicit, thus the 3D foot motion also needs to be measured and analyzed for studying the foot dynamic behavior characteristics.

Compared with the 2D plantar pressure, the 3D foot motions are more intuitional understood because they are directly reflecting the walking behavior by showing different attitude of the foot. On the other hand, the 3D foot motion could provide useful foot kinematics information. Since these foot motions are greatly influenced by the person's control ability and lower body function, the foot motions should be able to perform as an indication of the walking behavior. Traditional approach would consider the foot as one rigid segment although the foot has complex intrinsic structure and interactions. In recent studies, the foot is divided into multi-segments such as the metatarsals, toes, and calcaneus for 3D foot motion study [13]. Since the 3D foot motion study is a relatively new area, it is still in its infancy. There are complex motions between the adjacent segments of the foot during walking. Although large variances of the motions exist, some consistent motions can be identified for certain group of people.

Besides the experimental methods, many empirical and physical-based computational models, such as mathematical models, finite element models and kinematic models have been developed [14]. For gaining insight to the function of

specific foot structures, very complex models are useful, while for gaining overall foot dynamic function, simple kinematic models can be a good choice. Modeling and simulation of foot force and motion could provide better visualization. Through the model, simultaneously looking into foot kinetics and kinematics could help to better understand foot dynamic behavior from a new perspective. The dynamic foot model could present the relationship between foot force and foot motion, and combined function of foot kinetic and kinematic features. As a result, the foot dynamic behavior characteristic could be analyzed from the developed foot model's point of view. Furthermore, with verified foot dynamic model, various simulations with different kinematics could be investigated. The activities of some muscles or tendons, which are difficult to be obtained through real experiments, could also be possibly simulated. Thus, to enhance the understanding of foot dynamic behavior, a modeling method could be used to integrate foot kinetics and kinematics features.

1.2 Problem identification

As mentioned in Section 1.1, the foot kinetics and kinematics behavior characteristics during walking are not yet well investigated, although many studies were performed for walking behavior description. To describe foot dynamic behavior characteristics, features that can best depict foot behavior characteristics need to be extracted from both foot kinetic and kinematic studies. The features of foot dynamic behavior could possibly be collected to form a foot feature database for healthy gait and pathological gait. As more data will be collected into the feature database, pattern recognition method could also be proposed and applied to automatically classify healthy/pathological gait pattern. If a person's walking features are identified through pattern recognition as similar to one group of patients' in the feature database, this person could be considered to have similar foot behavior or disease with quantitative

proof. Thus, investigation of foot dynamic behavior could benefit clinical foot/walking related disease identification and solution. Moreover, useful foot features could also be possibly measured and integrated in shoes to provide real time walking behavior information. In a word, the foot dynamic features extraction could benefit multiple areas such as foot function investigation, shoe design industry and clinical issues related to the foot.

Since the study of foot dynamic behavior is very important with many benefits, this thesis will focus on foot dynamic behavior based on foot kinetics and foot kinematics. For best describing foot dynamic behavior characteristics, effort will be put on extracting effective features from both the foot plantar pressure for the foot kinetics, and foot motion for the foot kinematics. Additionally, combined foot kinetic and kinematic features, as well as the relationship between foot kinetic and kinematic features need to be investigated. However, the foot dynamic features are not easy to be extracted because of the complexity in the foot structure and dynamics. Considering the difficulties, foot could be investigated from both one whole foot's function, and foot multi-segments' function, for studying the foot kinetic and kinematic behavior characteristics.

For the foot kinetics, features could be extracted to describe the whole foot function and foot segment kinetic function. Foot pressure during walking can be directly recorded as foot plantar pressure patterns through commercial pressure measurement equipment. Some features extracted from plantar pressure might provide useful foot kinetic information. However, the effectiveness of these foot pressure features still needs to be investigated and more effective foot pressure features need to be extracted. Although some kinetic features could be extracted from the foot plantar pressure pattern, the foot plantar pressure only provides 2D information and is not

sufficient, thus further feature extraction from the 3D foot motion is required. For the foot kinematics study, some motion features could also be extracted by looking into the whole foot motion and foot segment motion. Considering the foot as a whole, some features could be extracted to describe some important foot behavior characteristics. The foot has multiple bones and joints with complex interactions. A single-segment foot model cannot fulfill the requirements of dynamic modeling of foot and ankle, as well as clinical problems regarding the kinematics of foot and ankle. Thus it requires improved methods for investigation of foot and ankle kinematics. Multi-segment foot model method should be considered for detailed foot motion description. However, the foot motion study is still in its infancy. There is still no consensus on the multi-segment foot motion measurement protocol. It is still not well known the best way to extract most useful foot motion features. Additionally, little study is done on variation of values of these foot motion features during different walking conditions. Thus extraction and investigation of foot motion features are required. If the obtained motion feature data is overwhelming and the pattern of the data is not distinctive, some pattern recognition methods are necessary to link the motion features with corresponding walking conditions.

Besides the individual study of foot kinetic features and foot kinematic features, the integrated aspect of foot kinetics and kinematics might provide a convincing assessment. A method to better interpret relationship between foot kinetic features and kinematic features is needed. To investigate the relationship between foot pressure/force and foot motion, modeling method could be used. With the help of the model, integrated foot kinematics and kinetics features could be better visualized and interpreted. Previous modeling of the foot was usually performed by finite element analysis (FEA) method. FEA can achieve the detailed foot modeling with good

reliability, but this method demands great computing and is more suitable for static analysis. So, some other detailed foot behavior modeling method, which could both easier conducted and provide overall foot dynamic function, is required.

1.3 Objective

In view of the above gaps, the objective of this thesis is to study the foot behavior during walking based on foot kinetics and kinematics, to extract useful foot dynamic features and to model the foot dynamics. To achieve this, some foot kinetic features are extracted from foot pressure for describing both the whole foot pressure function and multi-segment foot pressure. Effective features of the foot pressure could show consistent differences between different walking behaviors. Furthermore, foot kinematic features are extracted from foot motion for describing both the whole foot motion function and multi-segment foot motion. Obtained motion features are also applied in designed walking conditions. If the feature data are not clear enough, pattern recognition method can be applied to automatically sort data of motion features of different walking conditions. In addition, an innovative multi-segment foot model is built with LifeMOD biomechanics modeler to combine foot kinetic and kinematic information for enhanced visualization and better understanding of foot segment features. Thus in this thesis, the foot dynamic behavior characteristics are studied through extracting effective foot kinetic and kinematics features.

1.4 Organization of the Thesis

This thesis consists of seven chapters. Chapter 1 introduces the background of the research problems, the research motivation and objectives, as well as the organization of this thesis. Chapter 2 provides the literature review on foot pressure, foot multi-segment motions and dynamic modeling of foot kinematics and kinetics. Chapter

3 depicts the general framework for the whole research study. In Chapter 4, features are identified and extracted from foot plantar pressure. The effectiveness of these foot pressure features are further tested in the application of walking stability. In Chapter 5, features are identified and extracted from foot motion for normal walking condition. Considering the multi-segment foot motion function, foot segment motions are measured with a multi-segment foot model and regarded as motion features. Considering the whole foot motion function, new functional angles are additionally proposed as foot motion features. Chapter 6 applies the foot motion features for both normal walking and less stable walking conditions. This study provides evidence that some motion features show significant differences during various walking stability conditions. Pattern recognition method is also applied to classify gait patterns of different walking conditions. Chapter 7 investigates the dynamic foot behavior with a multi-segment foot model built with LifeMOD Biomechanics Modeler. This model combines the foot kinetics and foot kinematics and explains the dynamic relationship between the changes of foot pressure features/force and foot motion features. Then Chapter 8 provides the conclusions and future works for this study. Lastly, the reference and three appendixes are listed.

CHAPTER 2 LITERATURE REVIEW

This study would solely focus on the foot dynamic behavior. The literature review includes three parts: a review on foot pressure related issues, a review on foot multi-segment motions and a review on dynamic modeling of foot kinematics and kinetics.

2.1 Foot pressure related issues

2.1.1 Foot pressure relief

The use of therapeutic foot orthoses has been found to be effective in plantar pressure relief and foot ulceration prevention. H Chen et al. [9] investigated the relationship between the foot pressure distribution and running shoe comfort. Cavanagh, P. R. et al. [15, 16] generated a three dimensional insole which aligns the foot shape and reduces plantar pressure distribution and later investigated the performance of a great number of designs for reducing plantar pressure maximally by building a two-dimensional plane strain finite element model. Later Cheung [17] used a combined finite element and Taguchi statistical method to identify the sensitivity of five design factors of foot orthosis for reducing plantar pressure. Actis, R. L. et al. [10] modified a typical total contact inserts by inserting cylindrical plugs of softer materials in the high pressure regions based on the results of finite element analyses. For the prevention of foot ulcers, suitable design of accommodative in-shoe orthoses is needed to reduce plantar pressure levels at locations of bony prominences, particularly under the metatarsal heads. Lemmon, D et al. [18] investigated alterations in pressure under the second metatarsal head. Cheung et al. [19] evaluated the effect of material stiffness of insoles on both plantar pressures and stress distribution in the bony structures during

standing. Custom-moded foot orthoses are routinely prescribed in clinical practice to avoid or treat foot ulcers in diabetes by relieve the peak plantar pressure in certain foot region such as the metatarsals. In these applications, obtaining foot pressure information is very important. Besides orthoses design to redistribute foot plantar pressure, many researchers are evaluating the effectiveness of different foot insoles. Chen et al. [20] and Tsung et al. [21] investigated the effects of total contact insoles on the plantar stress redistribution. Bus, S. A. et al. [8] and Guldemond, N. A. et al. [22] studied the effects of customized insoles on plantar pressure redistribution in diabetic patients with foot deformity. Zequera, M. et al. [23] evaluated the effect of different insoles made by the computer model system which they proposed previously on a random group of diabetes mellitus patients in the early stages of the disease.

The pressure reduction is one of the main concerns of higher living quality for both healthy people and patient with diabetic foot. Foot pressure experimental measurement and modeling (FEA or other modeling methods) could indicate the pressure reduction in different foot regions, such as the hallux, metatarsals, mid-foot and the heel, etc. However, the FEA modeling is mainly suitable for static modeling.

2.1.2 Foot pressure analysis for diagnoses

Since diabetes could alter the normal biomechanics of the foot, leading to high pressure areas at the metatarsal heads, heel and toe regions. Foot pressure analysis is most widely used for diagnosing diabetic foot. M. L. Zequera et al. [24] did a descriptive study of the pressure distribution on the foot insoles both in static position and during gait of normal people, type I and type II diabetic patients and found the type of diabetes combined with neuropathies might affect the plantar pressure distribution behavior.

Aiming for distinguishing flat foot, R. Karkokli et al. [25] developed a cost

effective plantar pressure distribution analysis which is suitable for clinical podiatry. Jay Goldberg et al. [26] divided the foot into different regions and identified peak pressure during walking for each foot to examine the foot pressure patterns during pregnancy. The pregnant women had significantly higher hind-foot pressures and lower maximal fore-foot pressures than the non-pregnant women. The peak pressures were higher in both the mid-feet and on the lateral side of the right fore-foot in the pregnant women. The contact area of the foot with the pressure plate was greater in the pregnant women than in the non-pregnant women.

Foot pressure is also used widely for walking stability evaluation. The most frequently investigated features related to stability problems are center of foot pressure (COP) and center of body mass (COM). P. R. Rougier [27] did a review on the major aspects of the understanding of center of pressure trajectories during undisturbed erect stance control. Murray et al. [28] explained COM and COP biomechanically. Human body has a given mass and the COM positions change according to changes in the positions and movements of the body segments. The COP is the center of the distribution of the total force applied to the supporting surface. COP trajectory is one essential pressure feature for dynamic walking description.

During standing, in order to maintain balance, human body is swaying insignificantly. Sway is the in the anterior-posterior (AP) and medial-lateral (ML) planes. This variable is not measurable in a direct way, although it is frequently indicated with the COP that could be typically measured by a force platform or a pressure mat [27]. According to many previous publications [29], sway is believed to be an indication of human’s posture stability.

However static stability is far from enough. Dynamic stability measurement is necessary to evaluate human performance over a variety of locomotor environment to

ensure a high quality of life [30]. Most falls happen during human walking. Thus both static and dynamic stability measures are essential to assess one's ability to prevent a fall. The well-known condition for standing stability is that the vertical projection of the COM should be within the base of support (BOS) in static situations. A. L. Hof [31] also investigated the condition for dynamic stability from a pendulum model. Since COP, COM and their relationship are responsible for dynamic stability, Heng-Ju Lee and Li-Shan Chou [32] [33] did a control study to conclude that instantaneous COM-COP inclination angles during gait could be a sensitive measure of dynamic stability in the elderly. Kevin P. Granata and Thurmon E. Lockhart [34] also did a study to identify dynamic stability differences between elderly individuals who are at a high risk of falling, and healthy elderly adults. Bih-Jen Hsue et al. [35, 36] did a study which demonstrated that COM-COP divergence can characterize the dynamic balance of the CP children in walking and assist in differentiating and comparing stability patterns. Shier-Chieg Huang et al. [37] investigated the height and age effects on the COM and COP inclination angles and angular velocities during obstacle crossing.

However, the fundamental limitation of using the body COM for balance assessment is that it is not directly accessible [38-40]. The advantages of using the COP are that it is directly measured, easily quantified, and sensitive to conditions that disturb balance.

Foot plantar pressure is directly related to lower body activities and abnormal foot pressure patterns may indicate different kinds of unhealthy body conditions. So investigating foot pressure is valuable for human health monitoring. The COP can be obtained from foot pressure measurement and can be considered as a key feature extracted from foot pressure information.

2.1.3 Pressure related gait analysis

Karkokli, R. et al. [25] designed a low cost plantar pressure analysis system to closely measure and analyze the pressure distribution along each foot during dynamic movements of the feet. Chao and Yin [41] present a novel six component force sensor system for measuring the loading on the feet during a gait cycle. Savelberg [42] and de Lange applied an artificial neural network to map insole pressures and ground reaction forces and conclude that artificial neural network can be used to map their relationship. Ion P. I. Pappas et al. [43-45] presented a new gait phase detection sensor and a rule-based detection algorithm that reliably identified the transitions between gait phases: stance, heel off, swing, and heel strike. Robert E. Morley et al. [46] designed and developed an electronic system in a shoe that can give an extended measurement of the environmental conditions in the shoe of a subject such as reliable force, temperature, and humidity data. Joseph Paradiso et al. [47] designed and fabricated a cybershoe as an interface for a dancer's feet. This system can illustrate dancer's performance. Foot force/pressure information is reflecting the body movement. Foot pressure measurement and analysis are potential to be integrated in shoes for different applications.

Many studies have considered the gait patterns to get health information, reduce and prevent injury, evaluate the function of footwear and improve performance. Ceri E. Diss [48] assessed the reliability of 24 kinetic and kinematic variables to represent normal running gait from three synchronized systems. To investigate whether normal gait patterns are consistent, Ann L. Revill et al. [49] evaluate the repeatability of components of the ground reaction force, percent of ground reaction force, and peak force loading rate across repeated walking trials. They suggest that baseline impact force measurements are stable and do not need to be recorded between experimental

conditions in walking studies. Brian T. Smith [50] used force sensing resistors to detect the transitions between five main phases of gait for the control of electrical stimulation while walking with seven children with spastic diplegia, cerebral palsy. Meg E. Morris et al. [51, 52] studied the biomechanics and motor control of gait in Parkinson disease. Stefan Kimmeskamp and Ewald M. Hennig [52] analyzed plantar pressures to determine characteristics of the heel to toe motion of the foot in Parkinson patients in a mild or moderate stage of the disease during walking. They found that Parkinson patients show significant changes in heel to toe motion of the foot during free walking, which may be due to adaptive mechanisms of the patients to prevent unsteadiness during walking.

Pressure analysis was also used for walking stability in some studies. Edward D. Lemaire et al. [30, 53] picked up six parameters for dynamic walking stability analysis. Such a measure only used plantar foot pressure data detected by Tekscan insole sensors. These parameters are supposed to be combined most consistently effectively to identify dynamic gait stability using a fuzzy logic method. However, out of 15 tested subjects, only 7 subjects' experiments showed expected results. More information from foot pressure and more effective pressure parameters need to be extracted.

From previous literature review, pressure information is widely applied in different applications with different methods. However, the foot dynamic pressure has not been well investigated. Some studies have looked into real time force/pressure distributions in sub-divided foot areas and pressure transitions during walking, while the analyzed foot pressure features and information are still limited. Although many studies are related to foot pressure, features from foot pressure are not thoroughly extracted and well investigated.

Additionally, the foot plantar pressure measured with pressure mat is only 2D information which provides some foot kinetics, but could hardly show any foot kinematics. This may be relatively indirect and implicit for dynamic foot behavior study during different walking conditions. 3D foot motion could be an advance to provide foot kinematics information and it could be more intuitively linked with lower body movement and walking stability. The foot motion could serve as an advancement for better understanding foot kinetics, kinematics during walking. Next will be a literature review on foot motion studies.

2.2 Foot multi-segment motions

In traditional gait analysis method, the foot was regarded as one rigid segment with no intrinsic motion and efforts are more on the study of hip, knee and ankle kinematics [2, 3, 54-56]. However, the foot has multiple bones and joints with complex interactions. A single-segment foot model cannot fulfill the requirements of dynamic modeling of foot and ankle, as well as clinical problems regarding the kinematics of foot and ankle. Thus it requires improved methods for investigation of foot and ankle kinematics.

In the past two decades, an increased interest in foot multi-segment kinematics analysis by stereo photogrammetry was documented in the literature. In 1990s, S. M. Kidder [57] and A. Leardini [58] designed techniques individually for describing foot segment kinematics. They mainly focused on the technique exploration. In 2000s, different multi-segment foot models are further developed. Bruce A. MacWilliams, et al. [59] used 19 retro reflective markers for 9-segment foot model to determine 3D angles, moments and powers in eight joints or joint complexes and provided normative foot joint angles, moments and powers during adolescent gait. They also presented a complete set of sagittal, coronal and transverse plane results which contribute to a

better understanding of normal joint kinematics during gait. Buczek, F. L. [60] reported the impact of median-lateral segmentation on a multi-segment foot model by investigating the forces and moments between mediolaterally adjacent segments. T. R. Jenkyn and A. C. Nicol [6] divided the foot into 6 segments and defined 6 functional joints. Their results indicate that the most repeatable motions are ankle and subtalar joint motions and twisting of the fore-foot, while the least repeatable ones are the hind-foot motions, both inter- and intra- subjects.

The more investigated movements are the four major articulations in the foot, the ankle, subtalar, midtarsal and metatarsophalangeal joints. A. Leardini, et al. [5] used 14 markers to record three-dimensional joint rotations and planar angles by tracking a large number of foot segments during the stance phase of gait. Although many studies were performed for foot motion measurement, there is no standard agreement on the selection of the foot segments, the design of the marker set and anatomical reference, and the calculation of the kinematics.

Curtis, D. J. [61] examined possible variations in the repeatability during the foot roll over process of children. They concluded that repeatability were best in the sagittal plane and were poorest in the transverse plane. Repeatability was consistent throughout the gait cycle, but varied significantly between planes and segments. Rao, S., et al. [62] also did a study on foot multi-segment motions and compared the differences between normal control subjects and patients with mid-foot arthritis during walking and step descent. They investigated the peak and total range of motion (ROM) differences in the variables of 1^{st} metatarso-phalangeal dorsiflexion, 1^{st} metatarsal plantar flexion, ankle dorsiflexion, calcaneal eversion and fore-foot abduction. Their results presented both the differences in foot segment motions between normal walking and step decent, and the differences between control people and patients with mid-foot

arthritis.

Publications are relating the use of different foot models on normal adolescents' walking, and a few clinical populations. It is essential to investigate how foot segments function during walking. Some segments show consistent movements and can be used as features of walking of normal people and certain group of patients. However, studies on foot multi-segment motions and applications are still in its infancy. These are vital to determine which of the available methods are the most clinically significant. It is needed to find a better method for foot detailed motion measurement and useful foot motion features for dynamic foot behavior characteristics description.

2.3 Dynamic modeling of foot kinematics and kinetics

Previous literature reviews are focused on foot motion and foot pressure individually, which are all experimental works. Experiments can be designed to obtain particular kinds of data, using corresponding equipment. However, if more information is required, you may need to redesign and conduct experiments even involving other equipment. Computational modeling offers a cost-effective alternative to study the behavior of the human body mechanisms. Modeling and simulation method could also enhance the visualization of the problem in discussion.

Many empirical and physical-based computational models, such as mathematical models [63, 64] and finite element models [65, 66] have been developed. These mathematical models are generally quite complex. For gaining insight to the function of specific foot structures, very complex models are useful, while for gaining overall foot dynamic function, simple kinematic models can be a good choice. Recently, many software applications have been developed for biomechanical analysis, impact and movement simulation. The software enables users to perform human body dynamic modeling and simulation. One popular method for foot modeling is the Finite Element

Analysis method. As discussed in Section 2.1.1, FEA method could indicate the pressure in specific foot regions with a finely defined foot model. However, the FEA modeling is mainly applied for static modeling [14]. For the dynamic modeling, one leading simulation tool for human body modeling is the LifeMOD Biomechanics Modeler.

The LifeMOD Biomechanics Modeler is used to perform multi-body analysis and is a plug-in module to the ADAMS (Automatic Dynamic Analysis of Mechanical Systems). The LifeMOD Biomechanics Modeler has many good features. The models could be built with good efficiency and accuracy with complexity. It can also model human with interaction with environment, such as the foot with the ground during walking. Generally, it is a user friendly and fast modeling tool. LifeMOD is one powerful biomechanics modeling software, which is used by many researchers in recent years.

J Z Li, et al. developed a validated multi body dynamic human model of the lower extremities by LifeMOD. The motion data from experiments of walking and jump-landing was imported into the model to teach the joint servos which were later used to drive the model in forward dynamic analysis. Zultowski, I. and A. Aruin investigated the effect that load magnitude, load location, and the dimensions that the base of support have on postural sway in standing while wearing a backpack, single strapped bag, briefcase, or purse. Their findings suggest the importance of considering the way we carry loads in order not only to place less strain on the body and to minimize our efforts, but to optimize postural control as well [67]. Hyunho Choi, et al. generated a LifeMOD model to investigate biomechanical effects on the body center of mass (COM) and joint moments of lower extremity as the weight of sided load in walking. Their results showed that the ankle and hip joint of loading side is used to

support the body and the knee joint of unloading side is used to progress the walking with keeping the balance of the body [68]. Some others also used the results from LifeMOD modeling as input conditions to finite element models of specific human body part for injury prediction studies. R. Al Nazer, et al. estimated tibial strains during walking using a numerical approach based on flexible multi-body dynamics. They firstly developed a lower body musculoskeletal model by LifeMOD biomechanics modeling software, with motion capture data as input to LifeMOD modeling. The motion capture data were used in inverse dynamics simulation to train the model to replicate the motion in forward dynamics simulation. Their results are in line with literature values from in vivo measurements [69].

Through the papers, LifeMOD is a very power tool for human body dynamic modeling, as well as interacting with the environments. A general idea of LifeMOD modeling application and process of inverse-dynamic and forward-dynamic simulation is introduced. However, in these previous studies, foot was always modeled as one rigid segment, which is different in the real case. A more detailed foot model to be built with LifeMOD is needed. With the modeling tool, foot kinetics and kinematics during walking could be better visualized and integrated.

2.4 Summary

Many previous studies focused on gait analysis related to hip, knee and ankle motion. However, few studies have been focused on the foot behavior and the foot is not yet well investigated for its dynamic behavior characteristics. The foot dynamic behavior during walking is very important and essential for walking behavior investigation and clinical applications related to foot dysfunctions. In order to draw the holistic view of foot dynamic behavior, literatures about the three perspectives of foot dynamic behavior, which are foot pressure, foot motion and the modeling of foot

pressure and foot motion, are reviewed.

From the literature review of foot pressure studies, pressure information is widely applied in different applications. Some studies were performed for static foot pressure analysis; however, the foot dynamic pressure has not been well investigated. Although a few studies have looked into dynamic force/pressure distributions in sub-divided foot areas and pressure transitions during walking, information of analyzed foot pressure features are quite limited and critical features are not fully extracted from foot pressure. Although some features have been identified from plantar pressure and might provide walking information, the effectiveness of these foot pressure features still needs to be verified. In addition, more effective foot pressure features need to be extracted for walking behavior description. A better method to quantitatively analyze foot dynamic pressure is needed.

From the literature review of foot motion studies, a single-segment foot model cannot fulfill the requirements of dynamic modeling of foot and ankle, as well as clinical problems regarding the kinematics of foot and ankle. Thus it requires improved methods for investigation of foot and ankle kinematics. Although many studies were performed for foot motion measurement, there is no standard agreement on the selection of the foot segments, the design of the marker set, and the calculation of the kinematics. It is needed to find a better method for detailed foot motion measurement, and to find useful foot motion features for dynamic walking description. Furthermore, the foot motion measurement is a relatively new research field and it is not well known how the detailed foot motions are related to different walking conditions.

Except the studies on either foot pressure and foot motion, few studies are investigating their combined information and relationship during walking. The combined information of foot kinetics and kinematics could help to better understand

foot dynamic behavior from a new perspective. Dynamic modeling of the foot could simultaneously investigate foot pressure and motion and link them. From the literature review of dynamic modeling for foot kinetics and kinematics, LifeMOD Biomechanics Modeler is a very powerful tool for simulating overall foot dynamic function. Multi-segment foot model could be built with LifeMOD, and the segment features could be better investigated with the integrated segment force and motion information. Thus, simulation of foot pressure and motion could provide better visualization and understanding foot multi-segment dynamic behavior. However, most previous LifeMOD modeling studies consider the foot as one rigid segment. This does not meet the foot's multi-segment structure and complex interactions. A multi-segment foot model built with LifeMOD is required to better understand integrated foot pressure/force and foot motion features and their relationship for each foot segment.

Thus, to thoroughly study the foot behavior during walking, based on these research gaps, the research strategy will be described in the Chapter 3.

CHAPTER 3 PROPOSED FRAMEWORK

The objective of this thesis is to study the foot behavior during walking based on foot kinetics and kinematics, and to extract useful foot dynamic features and model the foot dynamics. In this thesis, the foot dynamic behavior characteristics are studied through foot dynamic features extraction, shown in Figure 3.1. The foot dynamic behavior includes the foot kinetics and kinematics. From both the foot kinetics and foot kinematics, features will be extracted for describing both the whole foot function and multi-segment foot function. A multi-segment foot model will also be built with LifeMOD for the foot segment features, which combines the segment force and motion information. The obtained foot dynamic features could be applied to many applications, such as foot function investigation, shoe design industry and clinical issues related to the foot.

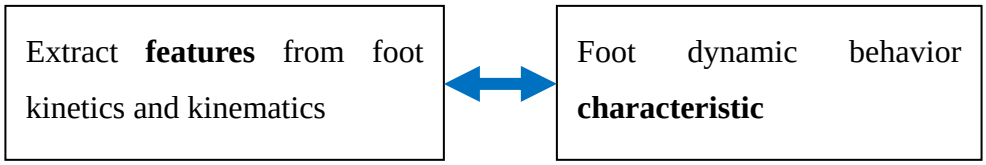

Figure 3.1: The theme of this study

Figure 3.2 presents the general framework of the whole research project. To study the foot behavior during walking, this study starts from foot kinetics and foot kinematics. For the foot kinetics, foot pressure features are extracted for walking behavior description. After the foot plantar pressure is recorded during walking, foot pressure data could be obtained. The whole foot plantar pressure could be measured with commercial equipment. The next step is to extract features from plantar pressure information for walking behavior description. The foot function could be inspected from the whole foot function perspective, and foot segment function perspective. For

the whole foot pressure behavior, one of the key foot pressure features is the center of foot pressure (COP). The sampled pressure patterns will be divided into strides and one stride is the period between two adjacent heel strikes. COP motion within a stride can provide much information. With certain proposed algorisms, several features could be extracted from the pressure information for illustrating foot behavior during walking. The details of the algorithms and meaning of each feature will be presented in the following chapter. For the foot segment pressure behavior, pressure values under the segments of heel, mid-foot, metatarsals and toes will be calculated and presented. In addition, it is also very important to check whether these features could successfully describe foot functions and walking behavior in different walking conditions. In this study, the application is to evaluate walking stability with obtained foot pressure features.

However, plantar pressure insoles can only provide sampled 2D pressure patterns during walking which may not be sufficient to describe foot behavior characteristics during walking. For foot kinematics study, the foot motion could also be measured and analyzed. The foot motion could be measured with Vicon motion cameras. The foot motion data collected will be used for further processing. The foot motion features can also be extracted to describe the whole foot motion function and segment motion function. For extracting foot multi-segment motion features, a multi-segment foot model is used. In the foot model, the foot and ankle can be divided into shank, calcaneus, mid-foot, and metatarsus segments. In the data analysis, the first step is to set up axes system for joint rotations between segments. This is followed by the investigation of the 3D rotations of the joints in all sagittal, coronal and transverse planes. The 3D rotations of the joints are regarded motion features, which include the ankle complex, calcaneus (heel) with respect to shank (Shank_Heel), mid-foot with

respect to heel (Heel_Mid), metatarsus with respect to mid-foot (Mid_Met) and metatarsus with respect to calcaneus (Heel_Met). For the whole foot function, some functional angles which could reflect whole foot motion characteristics will also be investigated as additional motion features. After obtaining all the foot motion features from normal walking conditions, the obtained features could also be applied to evaluate walking stability. Motion features could be further analyzed with pattern recognition methods, such as fuzzy logic system to automatically classify different walking conditions. Fuzzy logic system has the advantage of combining human knowledge and machine learning. Investigating the 3D foot and ankle motions is still in the infancy. The detailed foot and ankle motion is not yet applied to many clinical problems, such as the elderly people and patients with walking difficulties. The advantage of foot motion measurement is that it is more explicit for walking behavior and foot function explanation.

Considering the close relationship between the foot kinetics and foot kinematics, the foot pressure and motion could be simultaneously measured, simulated and analyzed. With the individually obtained foot segment pressure and multi-segment foot motion, a multi-segment foot model could be built to further study the foot multi-segment kinetic and kinematic features simultaneously. Modeling and simulation of foot segment pressure/force and motion could provide better visualization and understanding of the foot segment dynamic behavior. Furthermore, various simulations of different walking conditions could be investigated with verified foot multi-segment dynamic model. Thus, a multi-segment foot model will be built with LifeMOD biomechanics modeler to study segment kinetic features, segment kinematic features and their relationship during normal and abnormal walking conditions. Foot pressure/force features and foot motion features could be better visualized,

synchronized, and investigated through LifeMOD. LifeMOD is a good tool for dynamic walking modeling and simulation. The LifeMOD Biomechanics Modeler will be used to study the foot multi-segment behavior of walking through the linkage of foot segment kinetics and kinematics features.

In summary, referring to Figure 3.2, for foot kinetics, foot plantar pressure will be recorded during designed walking experiments. Then, foot pressure features will be identified by observing the 2D foot plantar pressure patterns. The effectiveness of these pressure features will be further tested in the application of evaluation of walking stability. For foot kinematics, 3D foot motions will be recorded and analyzed. Joint rotation angles between foot segments will be calculated as foot motion features with a multi-segment foot model. New functional angles will also be proposed as foot motion features for the whole foot kinematic behavior description. These motion features will be applied for walking stability evaluation. For the simulation of foot dynamics, a multi-segment foot model will be built with LifeMOD for the better understanding of foot segments' dynamic features. A normal and an abnormal walking conditions will be modeled and simulated for foot kinetics and kinematics study. Foot pressure features, foot motion features, and their relationship will be explained and investigated from both physics and modeling perspectives. Thus in this thesis, the foot dynamic behavior characteristics will be studied through foot dynamic features extraction.

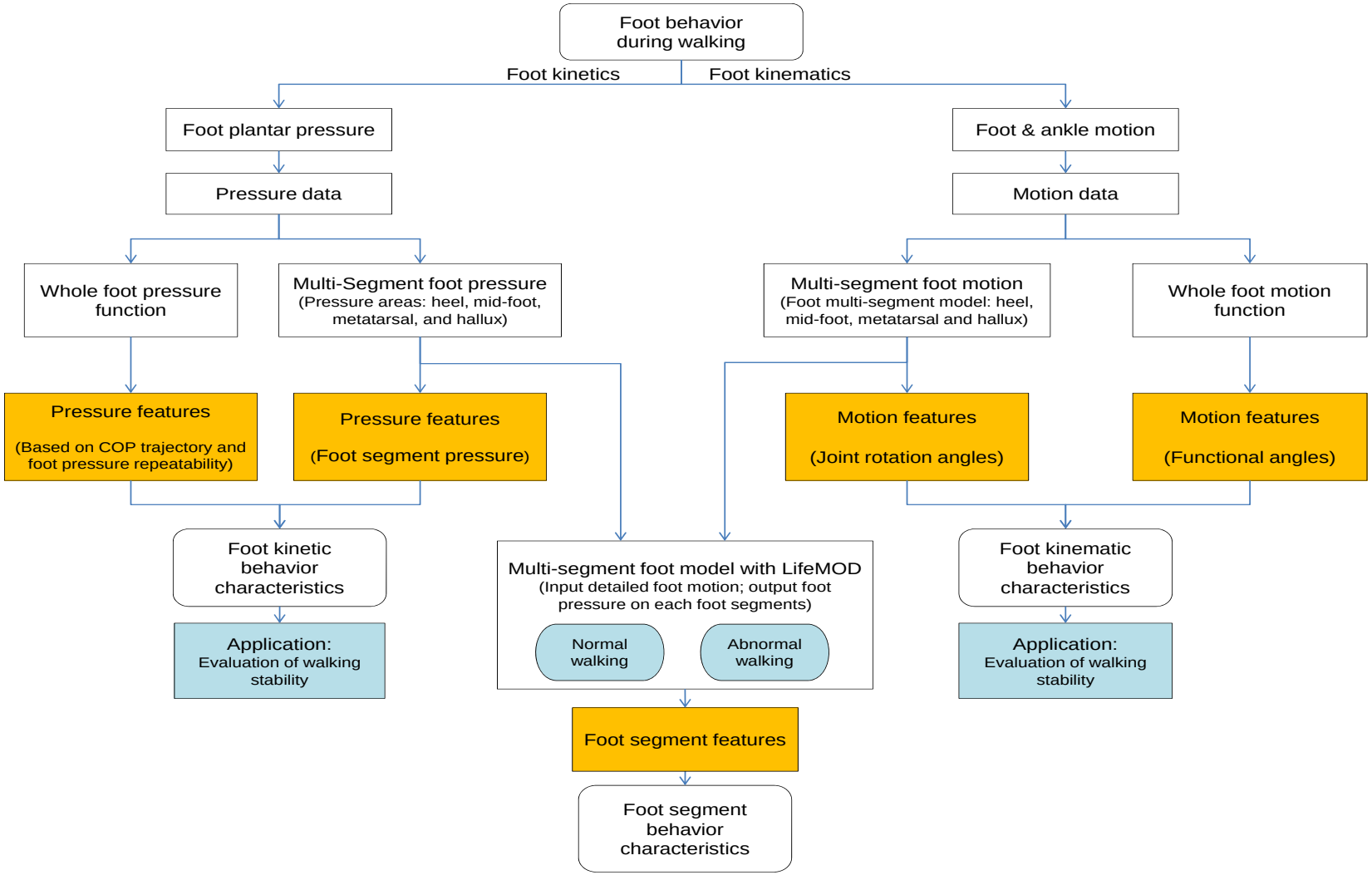

Figure 3.2: A main framework of the whole project

CHAPTER 4 IDENTIFY FEATURES FROM FOOT PLANTAR PRESSURE PATTERNS

This chapter focuses on the studies of extracting features from foot plantar pressure patterns for foot function and walking behavior. As discussed in previous chapters, the foot pressure could be easily measured as the equipment of measuring foot pressure is portable. Walking behavior could be indicated by the analysis of the foot plantar pressure during a gait cycle using pressure sensing shoe insoles. For the whole foot function, center of foot pressure (COP) reflects ankle moment adjustments, which is influenced by the whole body movement during walking, and thus can be analyzed for foot function and walking behavior. In a normal gait cycle, COP under the foot should follow a smooth progression. An abnormal gait would be indicated by erratic progression of the COP. To depict the COP trajectory during walking, studies involving plantar pressures are needed, and pressure features could be extracted for walking behavior description. In addition, foot pressure could also be divided into smaller sub-segments, and in different walking conditions, the segment foot pressure might also be different. Thus the segment foot pressure will also be calculated and investigated.

A general block diagram of this chapter is shown in Figure 4.1. Foot pressure data could be collected by the commercial available portable equipment: Tekscan F-scan Mobile system. Data collected with such a system can be analyzed using vendor software, or exported to other software for further analysis. After analyzing data resulting from gait experiments, it could be possible to extract pressure features that could indicate characteristics of the transition of COP during walking, and thus illustrate walking behavior. One stride is from one heel strike to the subsequent heel

strike. Some foot pressure features will be proposed both within one stride for the COP trajectory, and between strides for pressure repeatability to explain the whole foot dynamic function and walking behavior. In addition, foot segment pressure will also be calculated and analyzed. As an application, these extracted pressure features will be applied to describe walking conditions with different stability scenarios.

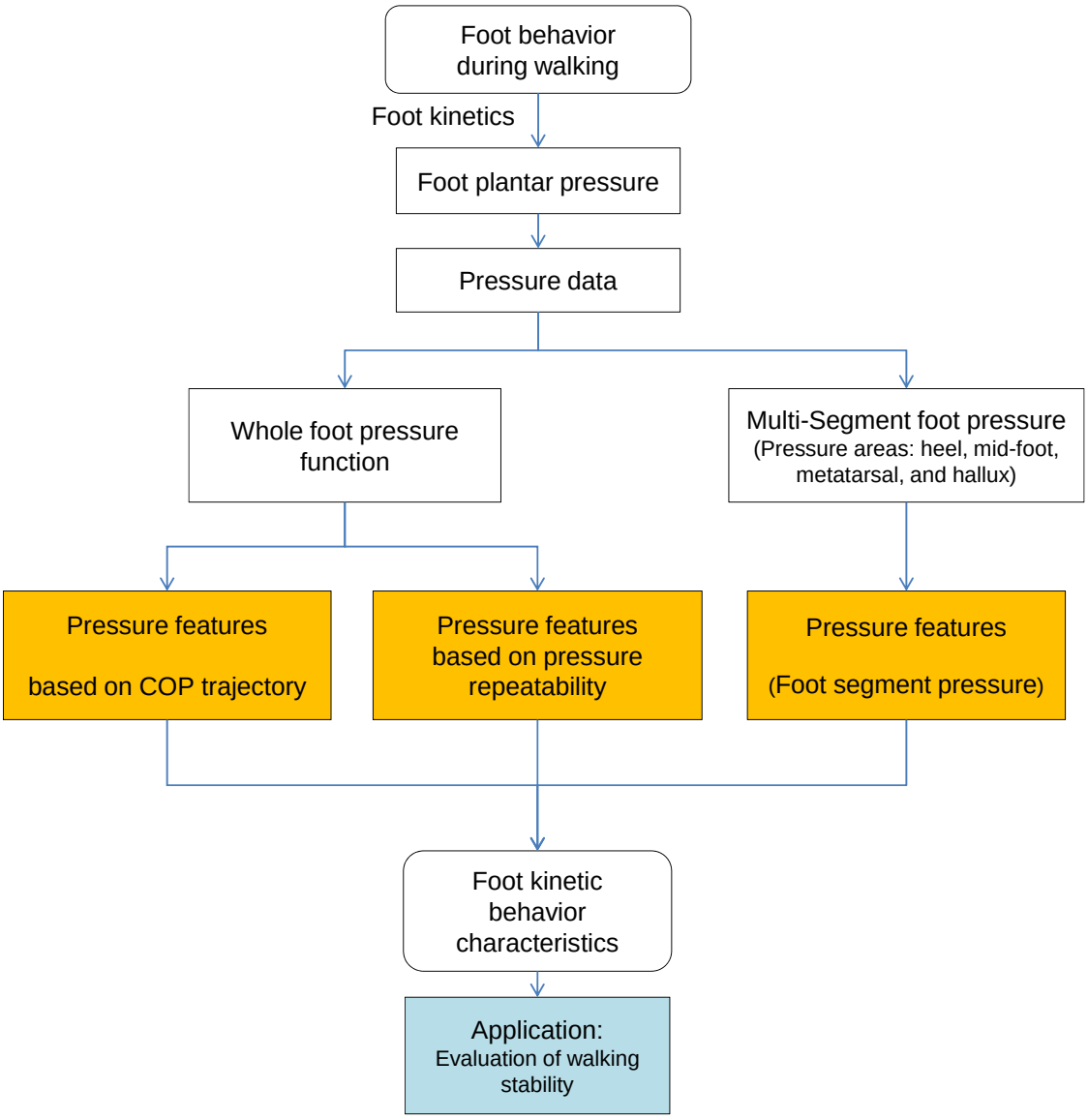

Figure 4.1: A general diagram of foot pressure features extraction for foot behavior description

4.1 Foot pressure features based on COP trajectory

4.1.1 Proposed pressure features

According to a study of Biswas et al. [30], several features could possibly be used to indicate a person's gait. These features could be obtained by analyzing raw data from the Tekscan F-scan Mobile system, and are supposed to provide the changes of the center of foot pressure (COP) in one stride. The performance and effectiveness of the obtained features need to be testified.

In a normal stride, the center of foot pressure COP starts in the phase of heel strike and ends after the toe off phase. The COP should transit smoothly in the anterior-posterior direction from the heel to the fore-foot. In the medial-lateral direction, the COP proceeds laterally from the heel strike phase to the heel off phase, and changes direction at mid-stance to move medially during the heel off and toe off phases. With such COP trajectory, each area of the foot is ideally in contact with the ground only once in a stride for normal walking. In a normal and stable stride, the person's center of mass (COM) stays close to the medial plane. Thus the largest lateral placement of COP remains smaller than that of abnormal stride, where the COP may deviate away from the medial plane and is more irregular. In addition, abnormal strides generally have a larger stride time and longer double support time as compared to normal strides. Thus, the following features are proposed in one stride as characteristics from the foot plantar pressure for potentially quantitative walking behavior studies:

1) Anterior-posterior (AP) Motion: Count number of occurrences of AP-COP motion moving towards the heel during a stride, normalized by stride time.

For a normal stride, COP is supposed to move smoothly from heel to fore-foot and the count is low. This feature presents the degree of body sway of anterior

posterior direction.

2) Medial-lateral (ML) Stability: Number of times COP velocity in the ML direction crosses a certain threshold after a change in sign, normalized by stride time.

In a normal walking stride, COP motion in the ML direction is expected to move laterally first and then back in the medial direction. A sign change followed by a threshold crossing indicates large and irregular body sway in the ML direction.

3) Medial-lateral range of COP: The difference between maximum lateral and medial placement of the COP in a stride.

Large medial-lateral ranges of COP are indicative of a swaying COM in the medial-lateral direction.

4) Cell Triggering: Highest number of times any section of the foot comes into contact with the ground in a single stride, normalized by stride time. For an ideal normal walking, any section of the foot should come into contact of the ground only once; multiple contacts are an indication of abnormal weight shifting.

5) Stride Time: Time period from heel strike to the following heel strike of the same foot. Stride time is supposed to increase when the subject's gait becomes more unstable.

6) Double Support Time: Time period with both feet exerting pressure on the ground in a stride. Double support time is supposed to increase when the subject's gait becomes more unstable.

4.1.2 Experiment set-up

To test the effectiveness of the six foot pressure features, experiments are designed and conducted to apply these features for walking stability evaluation as one of the important characteristics of walking behavior. By manipulating the tested subjects' visual factors (walking with eyes open or closed) and causation of dizziness

factors (with or without spinning before walking), less stable walking conditions could be obtained. Tekscan F-Scan Mobile is used to detect foot plantar pressures at fixed time intervals and the sampling frequency is chosen as 200Hz. This equipment can give the exact pressure values on each cell of the insoles. F-scan Research (version 6.30) software, shown in Figure 4.2, is able to calculate the position of the COP at each interval of pressure collection. Finally, Matlab and Microsoft Excel are used to analyze the pressure data exported from F-scan research software. Subjects are used in experiments only if they are not known to suffer any gait disorders or possess ambulatory problems.

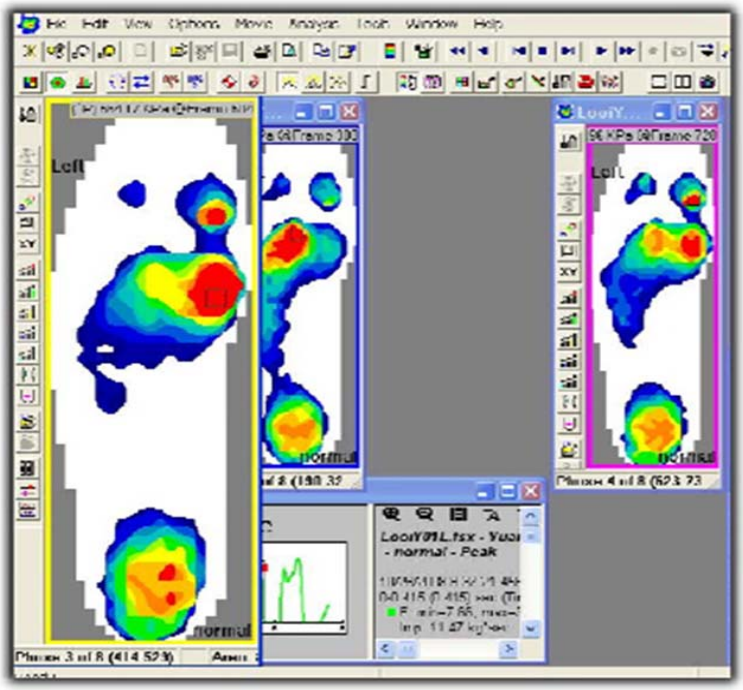

Figure 4.2: F-Scan research software interface

The experiment procedure is as follows.

1) Pressure insoles are trimmed to the size of the subject's feet, in accordance with guidelines recommended by Tekscan's user manual, and are attached to the bottom of the subject's feet. Socks are worn over the insoles and feet.

2) The subject wears the F-scan Mobile equipment, as shown in Figure 4.3, and

the combined weight of the subject, the equipment, and his/her clothing is measured on a digital weighing scale.

3) F-scan Mobile equipment is turned on and synchronized with F-scan Research software. Calibration and conditioning of the sensors must be carried out before data collation.

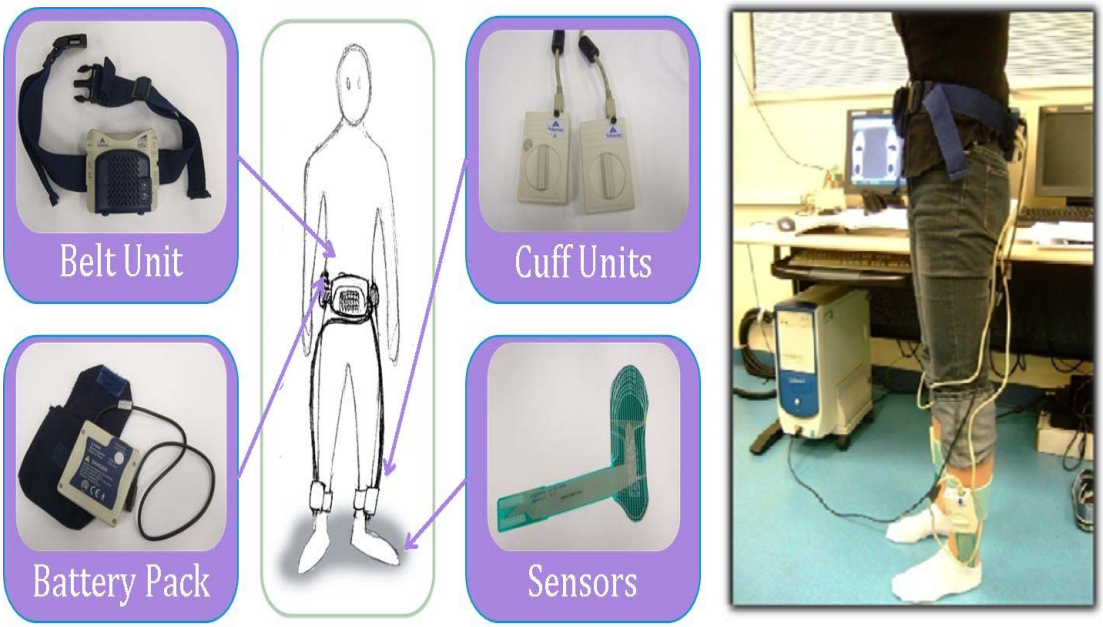

Figure 4.3: Experiment set-up using Tekscan equipment measuring foot plantar pressure

4) Data acquisition frequency is set at 200 Hz, which is enough for the pressure data analysis.

5) To test the effectiveness of pressure features, four experiments are conducted, being increasingly less stable for the subject during walking from Experiments A to D. The conditions of the four experiments are listed in Table 4.1.

Table 4.1: Experimental conditions

	A (Stable)	B (Less stable 1)	C (Less stable 2)	D (Less stable 3)
Visual	Eyes open	Eyes closed	Eyes open	Eyes closed
Dizziness	No spinning	No spinning	Spinning	Spinning

For each experiment, the subject is instructed to walk at a comfortable pace for at least five complete strides in as straight a line as they can manage. Each experiment requires the subject to make the five strides with or without their eyes open, and in a dizzy or non-dizzy condition, as shown in Table 1. For experiments requiring spinning, the subject sits in an office chair and is spun for 10 revolutions with the speed of once per second.

6) After each experiment, Mobile receiver unit is reconnected to the PC to log data from the experiment. Multiple runs of each experiment are carried out according to how well the subject felt after each run.

7) At the end of each session, the equipment is packaged according to procedures recommended by Tekscan.

8) Data from all experiments is exported into ASCII files and run through a customized Matlab program to obtain the six features, which are subsequently exported into Microsoft Excel for analysis.

4.1.3 Experiment data analysis methods and calculations

In this study, totally six subjects are tested (three females and three males; mean age 23.3 years (20-24 years); mean weight 65.8 kg (52-77 kg); mean height 173cm (161-183 cm)). Subjects with a history of foot injury or obvious gait abnormality are excluded. The subjects were instructed to walk at a comfortable pace for at least five complete strides. Each experiment requires the subject to make five strides with or without their eyes open, and in a dizzy or non-dizzy condition, as shown previously in Table 4.1.

For each experiment, two different ASCII files are obtained from Tekscan files. The first contains sampled frames of pressure magnitudes for 60 rows and 21 columns of pressure sensor cells. The second ASCII file contains the coordinate of the position

of the COP for each sampled frame, of the form COP = (*r, c*), where *r* is the row coordinate and *c* is the column coordinate. Figure 4.4 shows an example of data from the cell pressure magnitude file while Figure 4.5 shows an example of data from the COP coordinate file.

A median filter is firstly applied across each frame of data, and a new frame of data is created from an average of several frames of data in a period of time. This method aims to reduce noise in the initial data collection. Figure 4.6 shows some sampled plantar pressure frame patterns analyzed and plotted by Matlab.

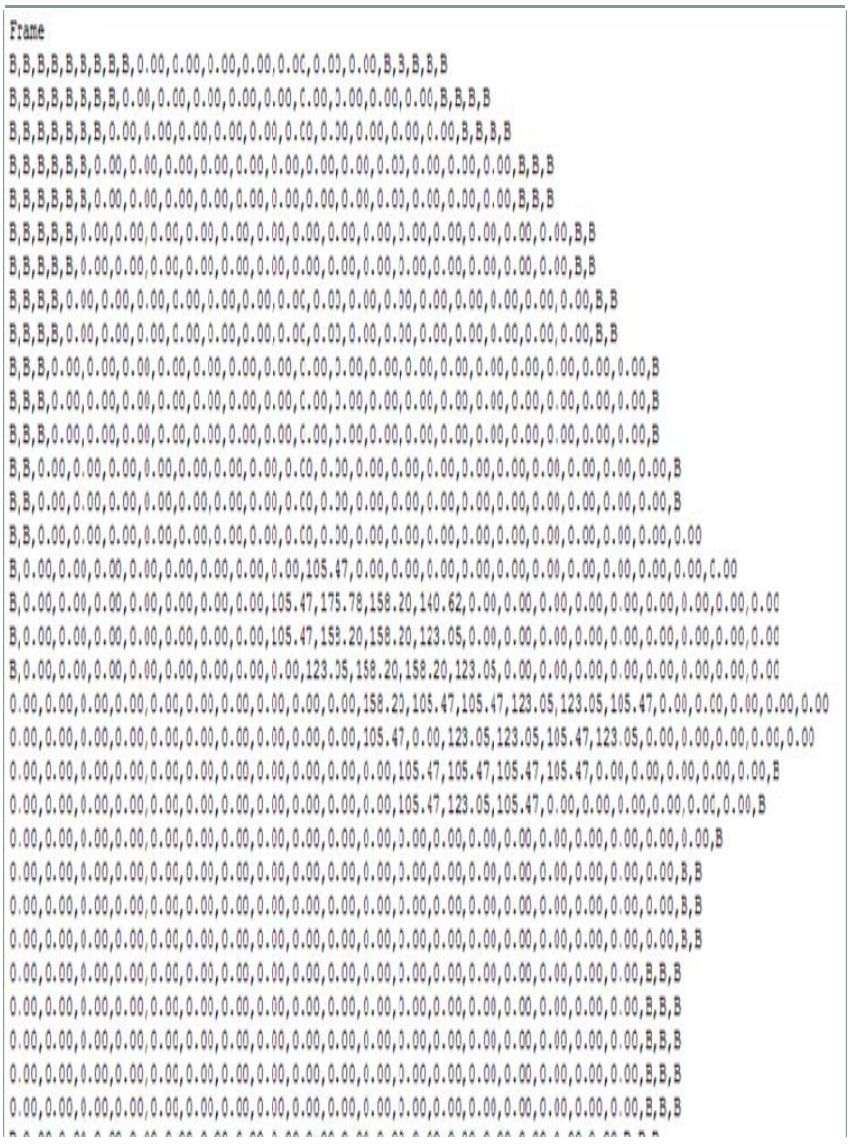

Figure 4.4: Pressure magnitude of sampled frame data

```
START_FRAME 1
END_FRAME 1729
COMMENTS Frame #, Time, Row, Column
ASCII_DATA @@

1, 0, 48.56, 10.37
2, 0.005, 48.55, 10.29
3, 0.01, 48.53, 10.34
4, 0.015, 48.48, 10.26
5, 0.02, 48.52, 10.34
6, 0.025, 48.62, 10.40
7, 0.03, 48.51, 10.34
8, 0.035, 48.75, 10.41
9, 0.04, 48.51, 10.34
10, 0.045, 48.55, 10.26
11, 0.05, 48.52, 10.34
12, 0.055, 48.54, 10.27
13, 0.06, 48.46, 10.32
14, 0.065, 48.66, 10.41
15, 0.07, 48.50, 10.37
16, 0.075, 48.61, 10.40
17, 0.08, 48.50, 10.39
18, 0.085, 48.64, 10.42
19, 0.09, 48.37, 10.42
20, 0.095, 48.63, 10.37
21, 0.1, 48.44, 10.37
22, 0.105, 48.48, 10.32
23, 0.11, 48.42, 10.38
24, 0.115, 48.60, 10.34
25, 0.12, 48.48, 10.41
26, 0.125, 48.53, 10.40
27, 0.13, 48.29, 10.34
28, 0.135, 48.50, 10.38
29, 0.14, 48.35, 10.43
30, 0.145, 48.48, 10.39
31, 0.15, 48.31, 10.40
32, 0.155, 48.54, 10.43
33, 0.16, 48.38, 10.38
34, 0.165, 48.41, 10.39
```

Figure 4.5: COP coordinates data

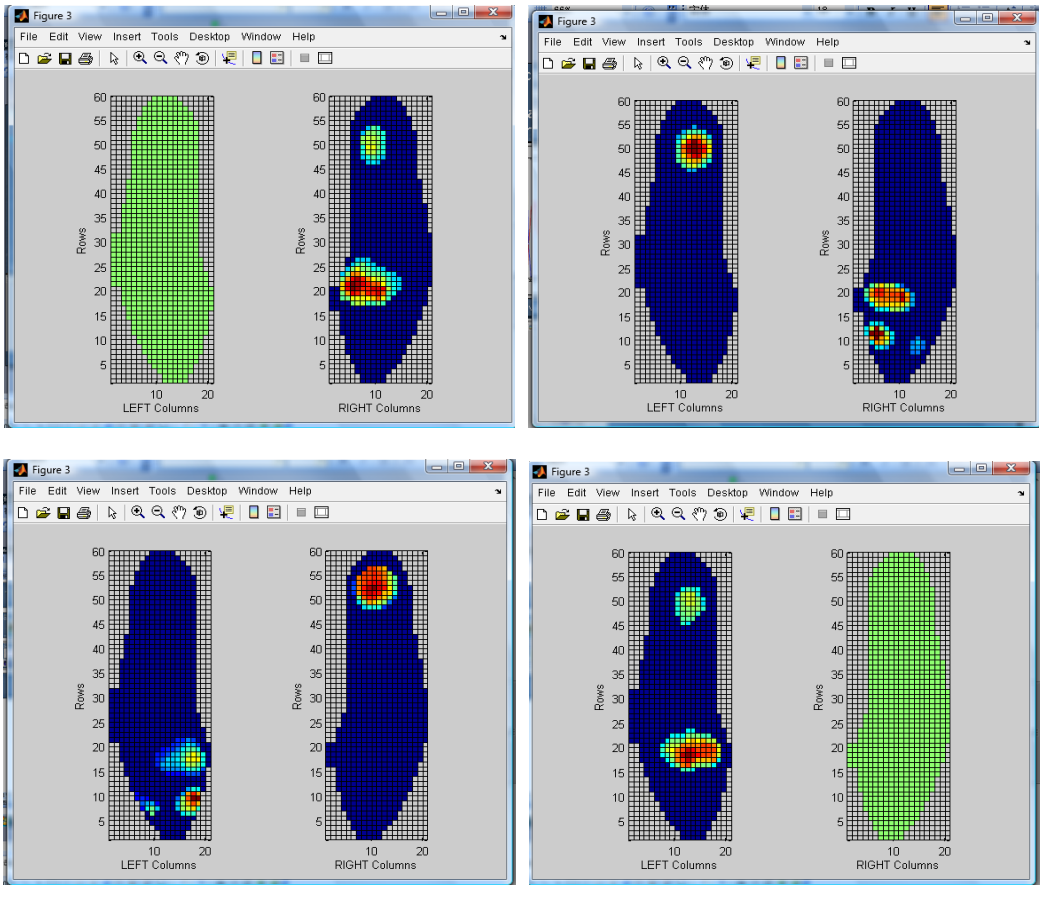

Figure 4.6: Sampled foot plantar pressure frame patterns

The following equation is obtaining total force in each frame.

$$Total\ \ force\ exerted\ in\ Frame\ k,\ F_k = \sum_{i}^{60}\sum_{j}^{21}(P_{i,j} \times A_{cell}) \qquad (4.1)$$

Where i = row number, j = column number, $P_{i,j}$ = sensor cell pressure on row i column j, and A_{cell} = surface area of sensor cell.

The next step is to split frames into strides. After obtaining the total force exerted in each frame, a graph of "Total Force" versus "Frames" is plotted. As an example, the plot of walking condition A (normal walking) and D (walking after being spun with eyes closed) is shown in Figure 4.7. The frames are grouped into strides by identifying the starting frame of the stride, which occurs when $F_k > 0$ and $F_{k-1} = 0$, where k is the frame number. The strides can be identified as $S_n(FR_n)$, where S_n is the Stride number $(1,2,\ldots,n)$ and FR_n is the starting frame number of the stride n.

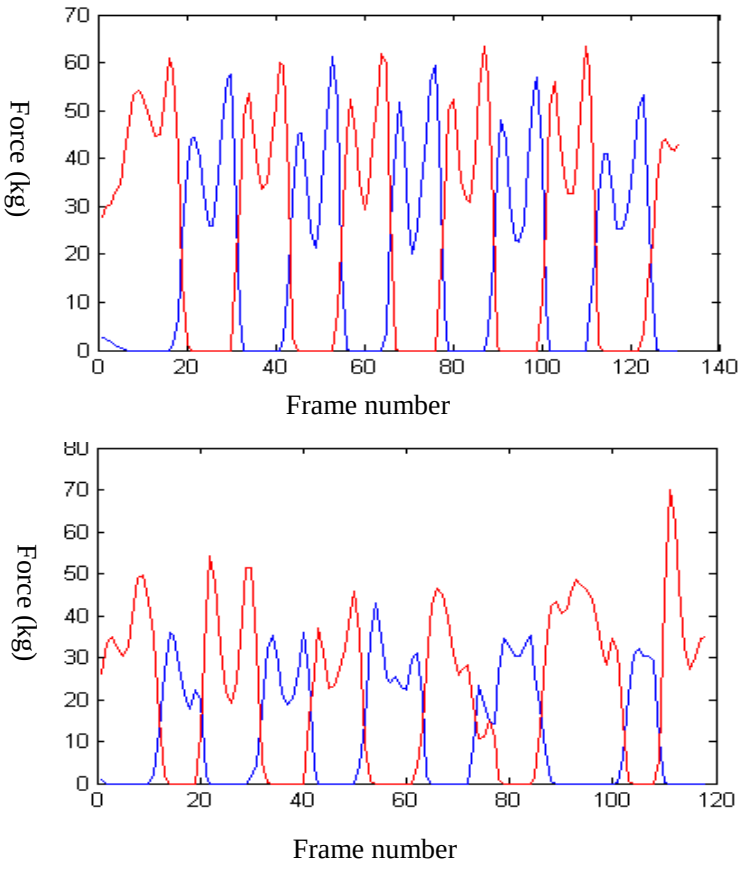

Figure 4.7: Total force exerted versus frame number; Experiment A (top) and D (bottom)

For each subject, an average of five sets of data from both feet for five strides was obtained. Only data from the middle three strides were considered with the assumption that the first and last strides may contain irregular data. This is due to the fact that the subject might be accelerating from a halt and decelerating to a stop respectively. Thus the unwanted strides are eliminated.

With these data, previous six foot pressure features could be extracted and calculated.

AP Motion: To obtain Feature 1, the row coordinate, *r* values of COP_k in each stride are analyzed. Each time the *r* value between frames decreases, the count accumulates, and then normalized by stride time. Here, the COP_k is the COP position in the frame number *k*.

ML Motion: Feature 2 is found by analyzing the 1st differential of the column coordinate *c* values of COP_k in a stride. The count accumulates when the 1st differential of the *c* values exceeds 0.5 after a change in sign, and then normalized by stride time.

ML Range: Each *c* value of COP_k within a stride is examined to obtain the maximum COP_k lateral position c_{max} ; and the minimum COP_k medial position c_{min}. The Feature 3 is calculated as follows.

$$ML\ Range = c_{\max} - c_{\min} \tag{4.2}$$

Cell Triggering: Every single cell is examined and the number of times each cell is triggered (turned on after being off) is counted. Feature 4 is simply the highest trigger times among all the cells in a stride.

Stride Time: Stride time is the number of frames in a stride multiplied by the pre-set period between frames. Thus Feature 5 is calculated as

$$Stride\ Time = (FR_n - FR_{n-1}) \times T \tag{4.3}$$

where T = Time between frames, FR_n is the starting frame number in stride n.

Double Support Time: It is the time period in a stride when F_k of the both feet is non-zero. It is obtained by checking F_k for both feet simultaneously.

4.1.4 Results and discussion

The results of the six features which show the characteristics within a stride were investigated [70]. Combined mean values and standard deviations for each feature are obtained from raw feature data from all three strides of the left and right foot as well as repeated runs of experiments. Graphs were plotted for each individual feature to observe the trends of mean and standard deviations across the four walking conditions. The results from two subjects' calculated experiment values are listed in Tables 4.2 and 4.3. Table 4.2 and Figure 4.8 contain the six feature's combined data of Test subject 1, ZengJ. Table 4.3 and Figure 4.9 show the six features' combined data of Test subject 2, LooiY. Results of the other four subjects are listed in Appendix A.

As to the anterior-posterior (AP) Motion feature, the study by Biswas et al. [30] suggested that AP motion feature should increase with higher levels of instability. The value of the AP feature is the count number of occurrences of AP-COP motion moving towards the heel during a stride, normalized by stride time. From the AP values in Table 4.2 for Subject 1, the mean of AP value is 1.308 for Condition A and rises gradually in Conditions B and C to 1.507 and 2.138. The value increases dramatically to 5.278 in Condition D with least stable walking condition. As for

Subject 2, the AP mean is 1.905 for Condition A, while it drops slightly in Condition B, but rises in Conditions C and D at the value of 3.322. For all the other tested subjects, the values of AP feature show similar trend. It generally increases from Conditions A to D, indicating more backward motion during walking. This increase in AP motion of center of pressure, from walking Conditions A to D, was under our expectation that the more the value is, the less stable the gait is.

Table 4.2: Combined data for six features; Test subject 1

EXPERIMENT:		A	B	C	D
FEATURE 1: AP MOTION, NORMALISED	MEAN	1.308	1.507	2.138	5.278
	STD DEV	0.654	0.616	1.078	1.775
FEATURE 2: ML MOTION, NORMALISED	MEAN	1.862	1.959	2.665	3.680
	STD DEV	0.503	0.657	0.487	1.099
FEATURE 3: ML RANGE	MEAN	5.766	6.519	6.112	6.187
	STD DEV	1.202	2.205	0.403	1.559
FEATURE 4: CELL TRIGGERING, NORMALISED	MEAN	1.447	1.414	1.158	2.315
	STD DEV	0.370	0.432	0.365	0.798
FEATURE 5: STRIDE TIME	MEAN	1.208	1.113	1.000	0.875
	STD DEV	0.051	0.071	0.045	0.129
FEATURE 6: DOUBLE SUPPORT TIME	MEAN	0.354	0.338	0.233	0.217
	STD DEV	0.033	0.038	0.026	0.041

The higher AP value indicates the instability in anterior-posterior sway. Except the mean value of AP feature, we did not find clear correlation between stability conditions with the other calculation of AP feature, such as its standard deviation. Because the mean value of AP motion increases with less stable walking conditions, it could be

regarded as one effective feature for foot dynamic behavior characteristics.

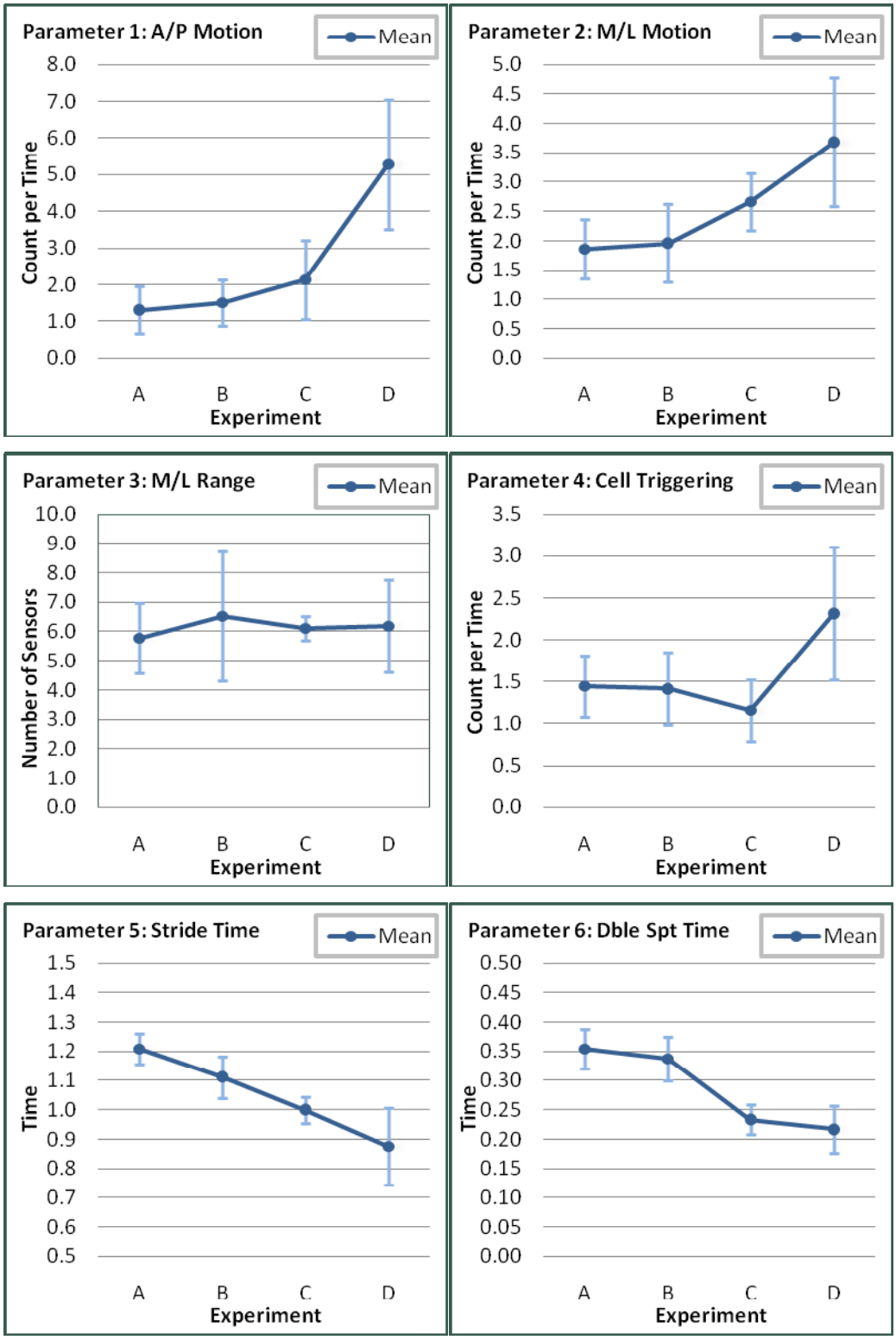

Figure 4.8: Mean and standard deviation of Features 1 to 6 across experimental conditions A to D; Test subject 1

Table 4.3: Combined data for six features; Test subject 2

EXPERIMENT:		A	B	C	D
FEATURE 1: AP MOTION, NORMALISED	MEAN	1.905	1.638	2.413	3.322
	STD DEV	1.205	1.250	1.667	0.971
FEATURE 2: ML MOTION, NORMALISED	MEAN	2.230	1.839	1.929	2.556
	STD DEV	1.143	0.794	0.588	1.035
FEATURE 3: ML RANGE	MEAN	5.600	5.604	5.060	6.408
	STD DEV	2.071	2.950	2.640	2.172
FEATURE 4: CELL TRIGGERING, NORMALISED	MEAN	1.437	1.527	0.968	1.888
	STD DEV	0.513	0.434	0.025	0.496
FEATURE 5: STRIDE TIME	MEAN	1.042	1.083	1.033	1.050
	STD DEV	0.020	0.068	0.026	0.089
FEATURE 6: DOUBLE SUPPORT TIME	MEAN	0.292	0.292	0.258	0.233
	STD DEV	0.020	0.038	0.038	0.026

The ML motion value should also goes higher for increasing instability for the medial-lateral (ML) Motion from the physics point of view. For subject 1, the ML value increases from Conditions A to D, but this does not show in subject 2. The standard deviation, the mean and standard deviation of combined value all cannot present clear indication for different stability conditions. This feature does not work as expected in this study. This may due to the definition of the feature and limited experiment conditions.

For the ML range feature, it is expected to increase from walking conditions A to D; however, the ML range feature values for the first three conditions do not have a clear trend. This feature does not work as expected in this study. The cell triggering feature has similar phenomenon with the ML range feature. The cell triggering values for the first three conditions are mixed together. For these features, comparing the

results of the tested subjects, it is difficult to find any good indication for decreasing walking stability. The values of these features are not having changes as expected for the four walking conditions.

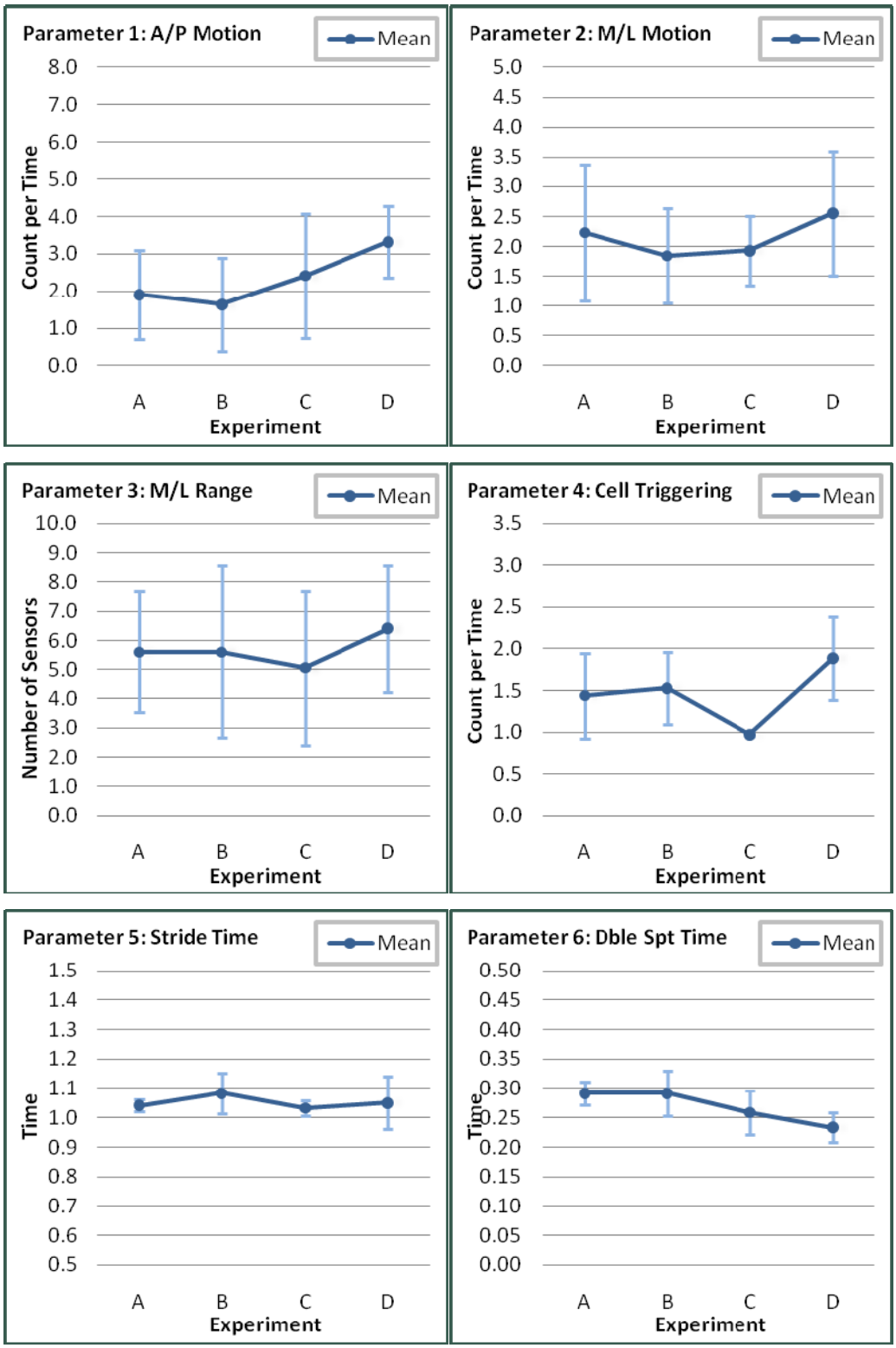

Figure 4.9: Mean and standard deviation of Features 1 to 6 across experimental conditions A to D; Test subject 2

For the stride time feature, the subject tends to walk even faster for less stable walking conditions, especially walking after being spun. The subject was trying to avoid the dizziness brought by the spinning right after he/she started walking. The changes of the stride time might due to the effect of the spinning speed; here one revolusion per second is used. The double support time is also smaller for the designed less stable walking conditions. This might also due to the smaller stride time and the spinning effect of the designed walking conditions. The stride time feature and double support time feature could indicate the differences brought by the less stability during walking. However, the differences are small with less than 0.1 second and it is a bit difficult to recognize.

In conclusion, the features extracted within one stride are not as good as expected for stability indication, except the AP feature. More effective foot pressure features are needed to perform better foot behavior description. Although six features were extracted from foot pressure, the foot pressure information is not yet fully investigated.

4.2 Foot pressure features based on pressure repeatability between strides

To find more useful information from foot pressure, more careful investigation is required. The aforementioned features are all calculated within a stride. There is no consideration of pressure relations between strides. This section aims to identify effective features calculated between strides to describe walking behavior and apply the new features to evaluate walking stability.

4.2.1 Proposed pressure features

A normal walking should have a more consistent force pattern exerted between strides, and the force should be more periodic than abnormal walking. During normal

walking, the differences between repetitive strides are expected to be small; thus cross correlation between successive strides is proposed as it can reveal the variations between strides.

Cross-correlation is a measure of similarity of two waveforms as a function of a time-lag between them, also known as a sliding dot product. It is often used to identify a shorter, known feature in a long duration signal, and also has applications in pattern recognition.

The correlation coefficient *corr(X,Y)* between two random variables X and Y with expected values μ_X and μ_Y and standard deviations σ_X and σ_Y is defined as:

$$corr(X,Y) = \frac{\mathrm{cov}(X,Y)}{\sigma_X \sigma_Y} = \frac{E\left((X-\mu_X)(Y-\mu_Y)\right)}{\sigma_X \sigma_Y} \tag{4.4}$$

where E is the expected value operator and cov is the covariance. Autocorrelation is the correlation of a signal with itself.

A feature named as normalized cross-correlation of subsequent strides (NCSS) is proposed. This feature indicates the similarity between total force patterns of two consecutive strides. The cross-correlation of the two consecutive strides is calculated to present their similarity and repeatability. NCSS is proposed to quantitatively evaluate characteristics between strides.

Normalized cross-correlation of subsequent strides (NCSS): The total force under each foot of two subsequent strides is calculated individually. Each stride is sampled by 200 evenly distributed points. NCSS is calculated according to Equation (4.5):

$$NCSS = \frac{max\left(corr\left(S_n, S_{n+1}\right)\right)}{\sqrt{max\left(corr\left(S_n, S_n\right)\right) \cdot max\left(corr\left(S_{n+1}, S_{n+1}\right)\right)}} \tag{4.5}$$

4.2.2 Experiment design

To check the effectiveness of the proposed feature, similar experiments were designed to apply the NCSS for walking stability evaluation. Experiments were designed for normal healthy young people to perform both stable and less stable/unstable walking. For simplicity, three walking conditions are used and each condition being increasingly less stable for the subject, as shown in Table 4.4.

The NCSS values are expected to decrease from stable walking to less stable conditions, assuming that the more stable the gait is, the more correlated the two subsequent strides are, and the values of the NCSS would therefore be higher. Since the NCSS is normalized, greater stability is expected for an NCSS value closer to one.

Here we hypothesis that the NCSS should decrease from stable to less stable walking conditions, whereas the standard deviation of the NCSS among experiments should increase from stable to less stable walking conditions.

Table 4.4: Experimental conditions

	Walking condition 1	Walking condition 2	Walking condition 3
Visual	Eyes open	Eyes closed	Eyes closed
dizziness	No spinning	No spinning	Spinning

The study was conducted on six young healthy volunteers (three females and three males; mean age 25 years (23-28 years); mean weight 67 kg (45-78 kg); mean height 174 cm (158-183 cm)).

The Tekscan F-Scan Mobile [71] was used to detect foot plantar pressures at fixed time intervals during walking. The experimental set-up and procedure are same as the ones in Section 4.1.

Every subject repeats the same experiment at least three times under each walking condition. For each experiment, the subject is instructed to walk at a comfortable pace

for at least five complete strides in as straight a line as they can manage. Each experiment requires the subjects to make five strides with or without their eyes open, and in a dizzy or non-dizzy condition, as stated in Table 4.4. For experiments requiring spinning, the subjects sit on an office chair and are spun around for 10 revolutions at a rate of 60 rpm.

4.2.3 Results and discussion

Data sets from the experiments are exported to ASCII files and analyzed using a specially developed Matlab program, with the results exported to Microsoft Excel. A median filter is firstly applied across each frame of data to reduce noise in the initial data collection. The filtered data is analyzed further to obtain the proposed pressure features. Figures 4.10 to 4.11 are samples of the total force exerted on both feet during multiple strides of each walking condition.

Figure 4.10 shows the consistency of successive strides of both left foot and right foot during normal walking. This subject's left foot force (solid line) is larger than the right foot force (dotted line) in Figure 4.10. This indicates that the tested subject might be a left foot walker. Although different subjects have different walking styles, the periodic feature between subsequent strides of normal walking is similar for all subjects being tested.

As shown in Figure 4.11, in the case of walking with eyes closed, the consistency of walking is less obvious compared with normal walking. However, it is much better compared with walking with eyes closed after being spun, as shown in Figure 4.12, in which the force value and periodicity change significantly. From these observations, normalized cross-correlation between subsequent strides (NCSS) is hence considered

to be suitable as a feature to indicate the differences in walking quantitatively in our study.

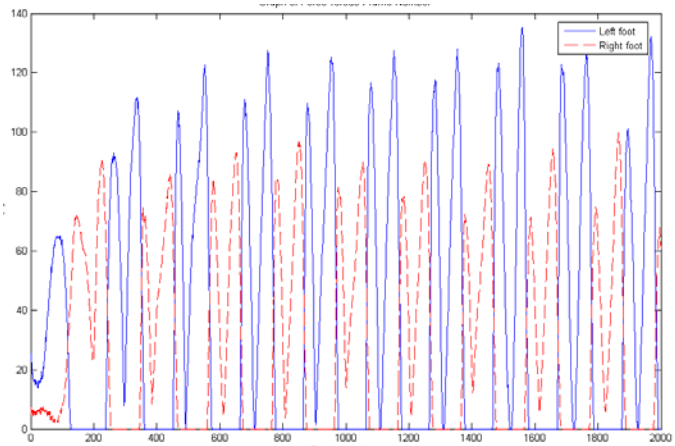

Figure 4.10: Total force (kg) exerted during multiple strides of condition 1 (normal walking) Left foot (real line), right foot (dash line)

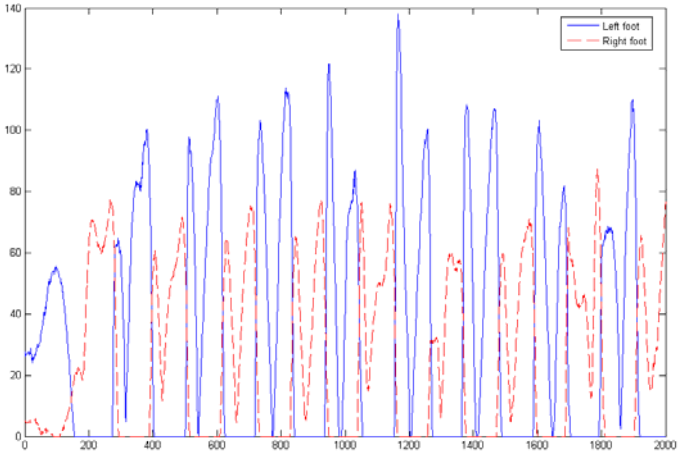

Figure 4.11: Total force (kg) exerted during multiple strides of condition 2 (eye closed) Left foot (real line), right foot (dash line)

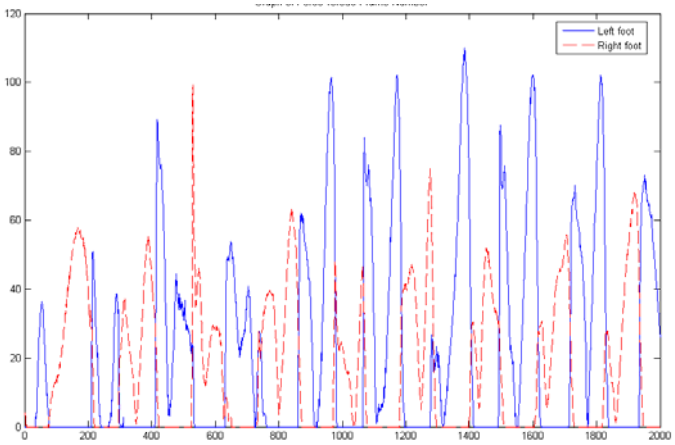

Figure 4.12: Total force (kg) exerted during multiple strides of condition 3 (eye closed after being spun) Left foot (real line), right foot (dash line)

Figures 4.13, 4.14 and 4.15 show samples of total forces over two subsequent strides for walking conditions 1, 2, and 3 respectively.

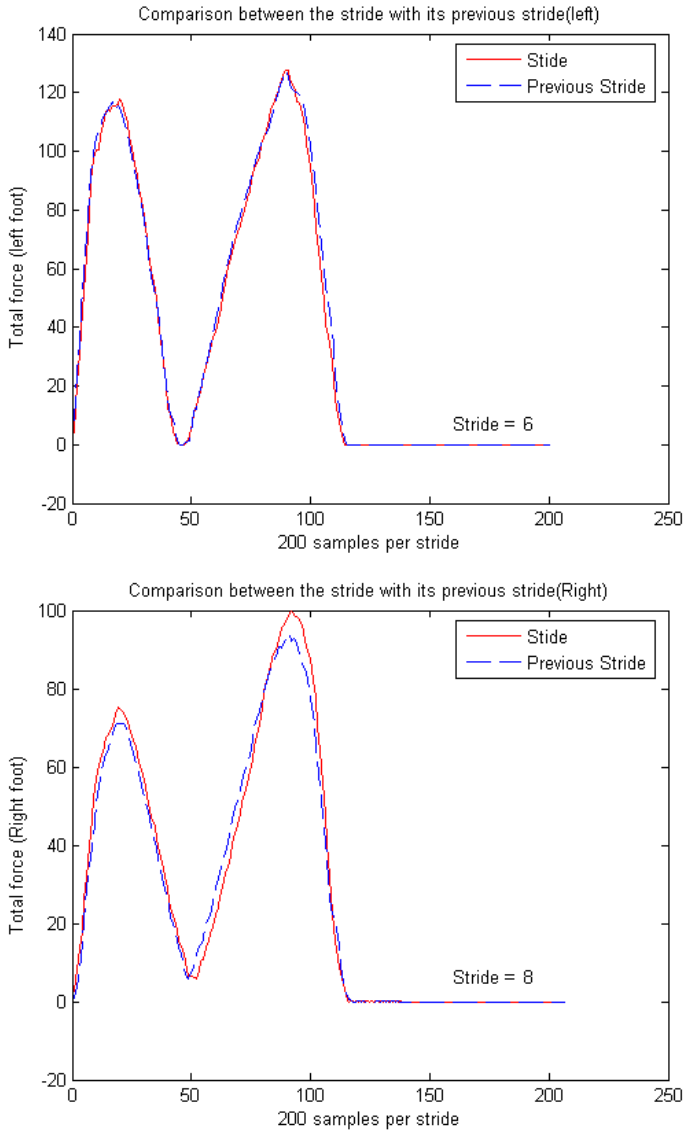

Figure 4.13: Example of comparison between two subsequent strides of condition 1

There are observable differences in the force signals obtained from the sensors for the three kinds of walking. For normal walking (condition 1), the successive strides match quite well as shown in Figure 4.13. For walking with eyes closed after being spun (condition 3), the successive strides show little correlation. For walking with eyes closed (condition 2), the strides match with each other to some extent, much better than condition 3 but worse than condition 1. The left foot and right foot has similar

patterns, but with different amplitudes. This is normal phenomenon, as most of people tend to use one foot more than the other. According to these figures, comparison between subsequent strides is important to indicate the differences of these three walking conditions.

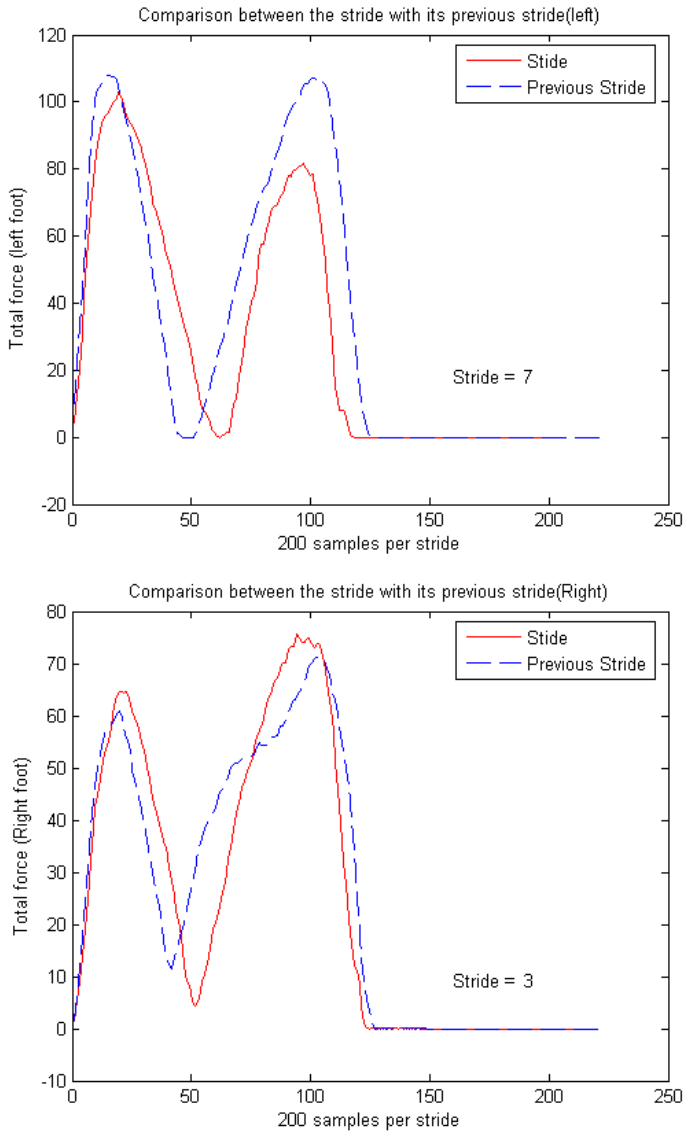

Figure 4.14: Example of comparison between two subsequent strides of condition 2

Thus normalized cross-correlation between subsequent strides (NCSS) is calculated for all walking trials of normal and less stable walking. The calculated results of NCSS

and its standard deviation (STD) for all six subjects being tested are shown in Figure 4.16. The triangular marks indicate means of the correlation of every two subsequent left foot strides; the diamond ones are means of the correlations of every two subsequent right foot strides. For the X axis, 1 denotes the walking experiment condition 1, 2 denotes condition 2, and 3 denotes condition 3.

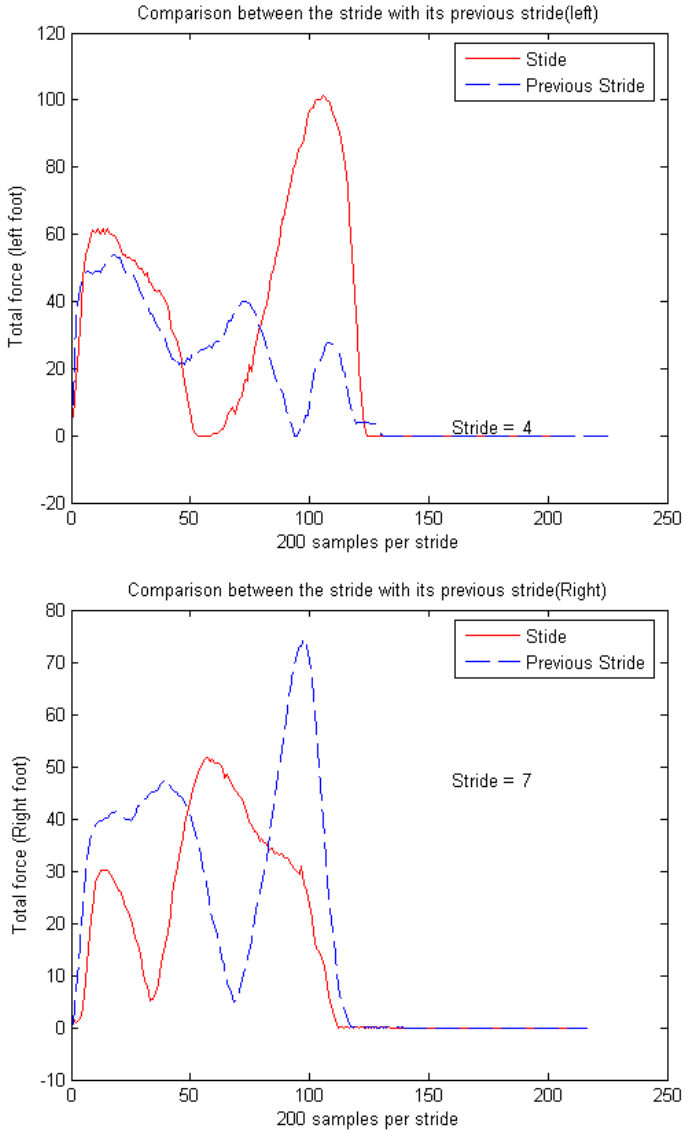

Figure 4.15: Example of comparison between two subsequent strides of condition 3

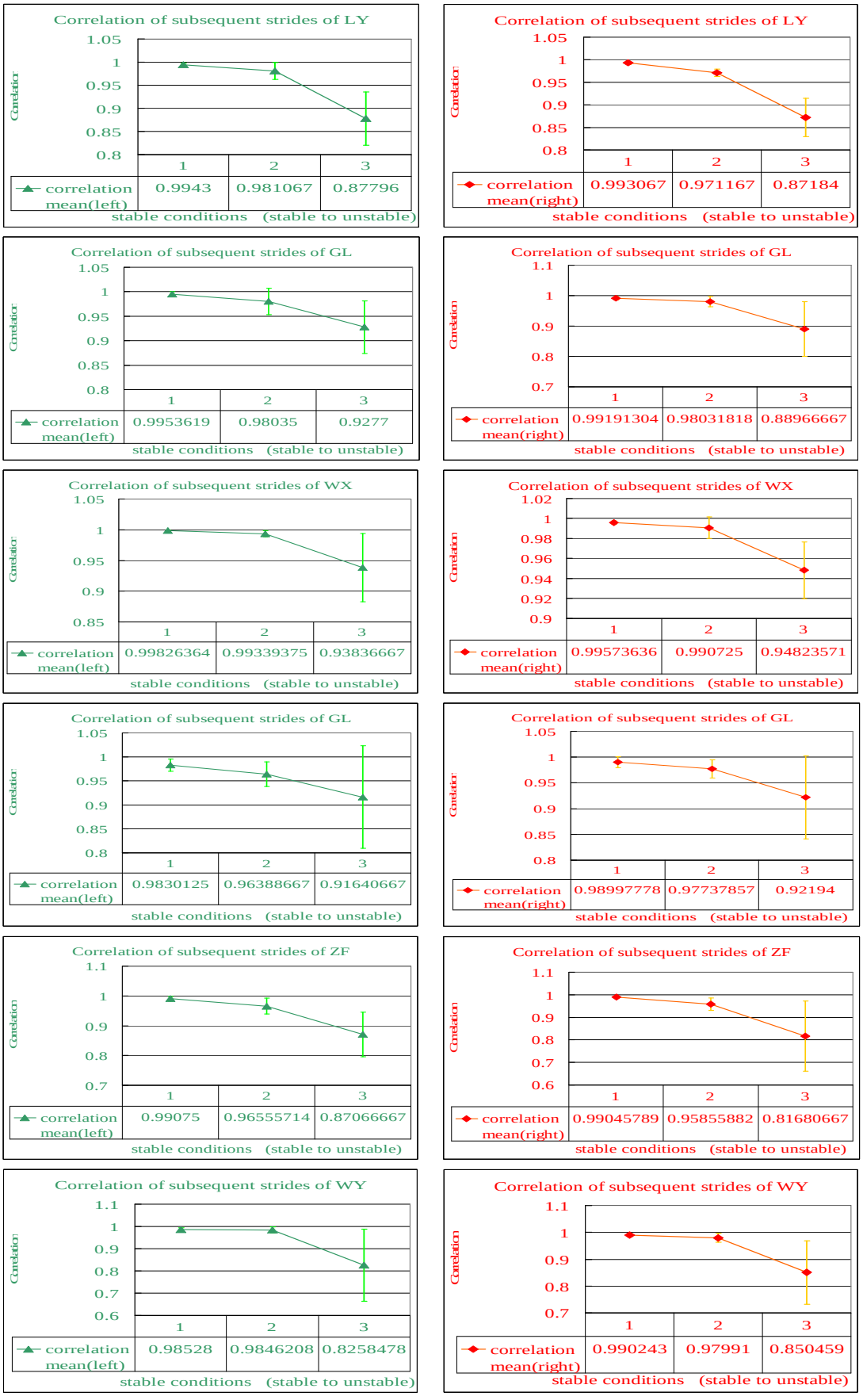

Figure 4.16: Mean and std of NCSS of six subjects (triangle: left foot; diamond: right foot)

From the data of all subjects being tested, the mean of NCSS values of both the left foot strides and right foot strides decreases as the gait goes from normal walking to less stable walking from conditions 1 to 3, as shown in Figure 4.16. For example, the top left graph is the mean and the standard deviation of NCSS of subject LY's left foot. It shows the mean values at 0.994 for condition 1, 0.981 for condition 2, and 0.878 for condition 3. The top right graph shows the mean and standard deviation of NCSS of subject LY's right foot. The mean value is 0.993 for condition 1, 0.971 for condition 2, and 0.871 for condition 3. Thus the mean of NCSS can indicate the stability information well and clearly. In Table 4.5, the standard deviation (STD) of condition 1 is very small, and the STD of condition 2 is relatively much larger compared with the one of condition 1. It also shows that the STD of NCSS values of both the left foot strides and right foot strides increase as the gait goes from normal walking to less stable walking, from conditions 1 to 3.

However, different people have different ability to adapt to the designed walking conditions. Some subjects show relatively good adaption for walking with eyes closed, such as subject 3 in Table 4.5. The NCSS mean of subject 3 does not change much from walking condition 1 to 3 and the STD of NCSS also does not show much difference. Subject 3 shows relatively good adaption for walking with eyes closed after being spun. Thus this feature also has the potential to estimate the adaption ability of different people in the same condition.

Figure 4.17 shows 150 samples of NCSS values for walking conditions from 1 to 3. From the figure, it can be seen that the range of NCSS values for normal walking is quite narrow, with most values around 0.995. The range of NCSS values for the other two walking conditions is relatively wide. There are distinguishing differences between conditions 1 and 3. There is no obvious boundary for the NCSS values of

walking conditions 2 and 3. Due to different neural controllability of different people, values of NCSS change within a relatively wide range for less stable walking conditions. More subjects could be tested for the NCSS values during different walking conditions. Threshold might be found for the NCSS value for different group of subjects.

From experimental results, both mean and STD of NCSS are found to be good indicators for different walking behaviors. The means of NCSS values of both the left foot strides and right foot strides decrease as the gait goes from normal walking to less stable walking conditions, i.e. conditions 1 to 3. STD of NCSS values increases as the gait goes from normal walking to less stable walking conditions.

Table 4.5: Mean and std of NCSS of six tested subjects

		Condition 1		Condition 2		Condition 3	
		Mean	STD	Mean	STD	Mean	STD
Subject1	Left foot	0.98301	0.01259	0.96389	0.02568	0.91641	0.10664
	Right foot	0.98998	0.01086	0.97738	0.01773	0.92194	0.08019
Subject2	Left foot	0.99536	0.00470	0.98035	0.02718	0.9277	0.05322
	Right foot	0.99191	0.00534	0.98032	0.01631	0.88967	0.09015
subject 3	Left foot	0.99826	0.00099	0.99339	0.00489	0.93837	0.05569
	Right foot	0.99574	0.00165	0.99073	0.01073	0.94824	0.02846
subject 4	Left foot	0.99075	0.00775	0.96556	0.02674	0.87067	0.07390
	Right foot	0.99046	0.00542	0.95856	0.02751	0.81681	0.15545
subject 5	Left foot	0.9943	0.00416	0.98107	0.01820	0.87796	0.05796
	Right foot	0.99368	0.00367	0.97612	0.00828	0.8749	0.04275
subject 6	Left foot	0.98528	0.00862	0.98462	0.01419	0.82585	0.16282
	Right foot	0.99024	0.00574	0.97991	0.01760	0.85046	0.11837

For the left foot and right foot, the force patterns are similar for the normal walking. The force magnitudes are a bit different between left foot and right foot; this depends on whether the tested subject is left foot walker or right foot walker. For the

calculated NCSS values, same phenomenon appears on both the left foot and right foot. The NCSS values may depend on tested subjects, but not on the left or right side of the foot.

The NCSS is effective for evaluating walking stability conditions and it may also be applied to other studies such as evaluation of human neural adaption. More effective features might be extracted from foot plantar pressure measurement.

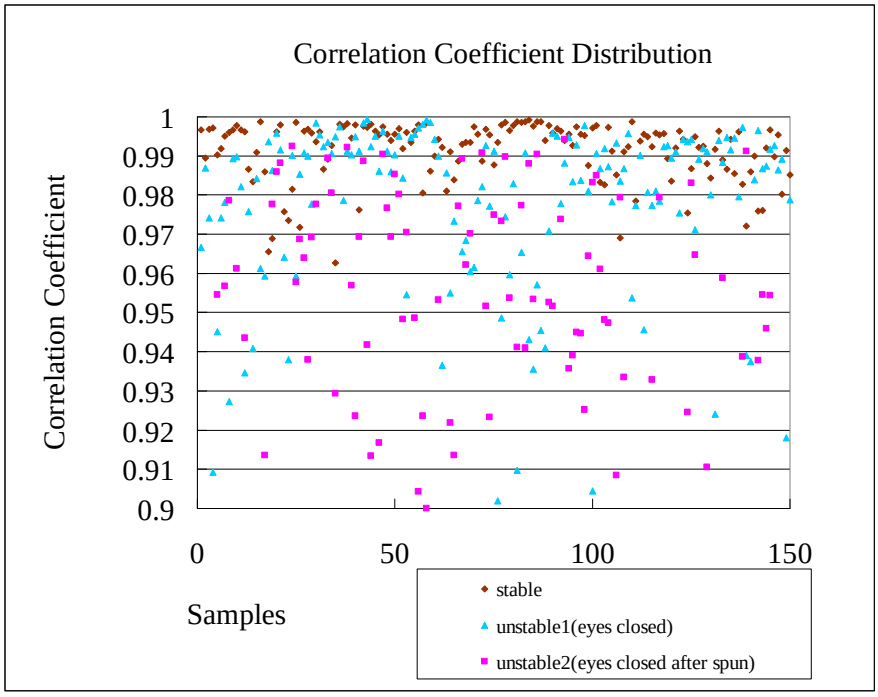

Figure 4.17: Correlation coefficient distribution for the three walking conditions

4.3 Multi-segment foot pressure

Besides investigating the whole foot pressure changes, the foot pressure could also be divided into different foot regions: heel, mid-foot, metatarsals and toes, shown in Figure 4.18. For different walking conditions, the foot segment pressure could possibly be different. So in this study, pressure under each foot segment will be calculated and discussed. By comparing the segment foot pressure changes, foot behavior characteristics could also be indicated. This section will give a brief

introduction about the multi-segment foot pressure function during walking.

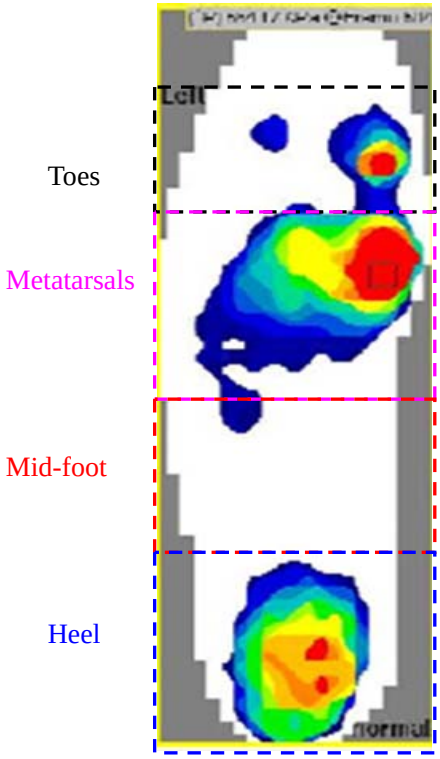

Figure 4.18: Multi-segment foot pressure regions

In different walking conditions, the pressure under heel, mid-foot, metatarsals and toes will be presented and analyzed. The multi-segment foot pressure for the normal walking is shown in the following Figure 4.19.

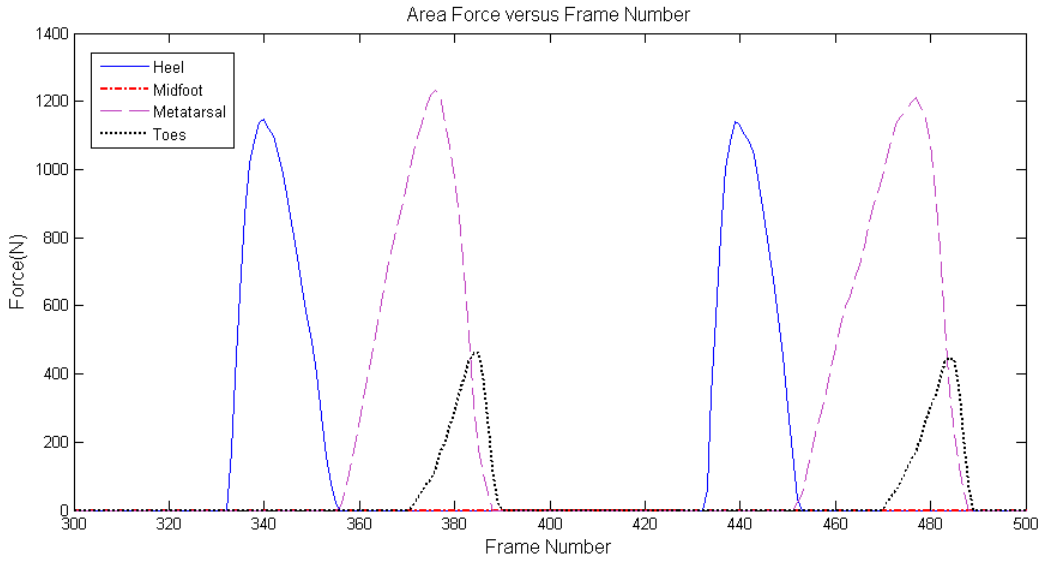

Figure 4.19: Multi-segment foot pressure for normal walking

We may notice that during the two strides shown in the figure, force patterns under all the four foot segments are quite repetitive. The force under mid-foot segment is zero throughout the period.

The multi-segment foot pressure for the walking with eyes closed after being spun in the chair is shown in the following Figure 4.20.

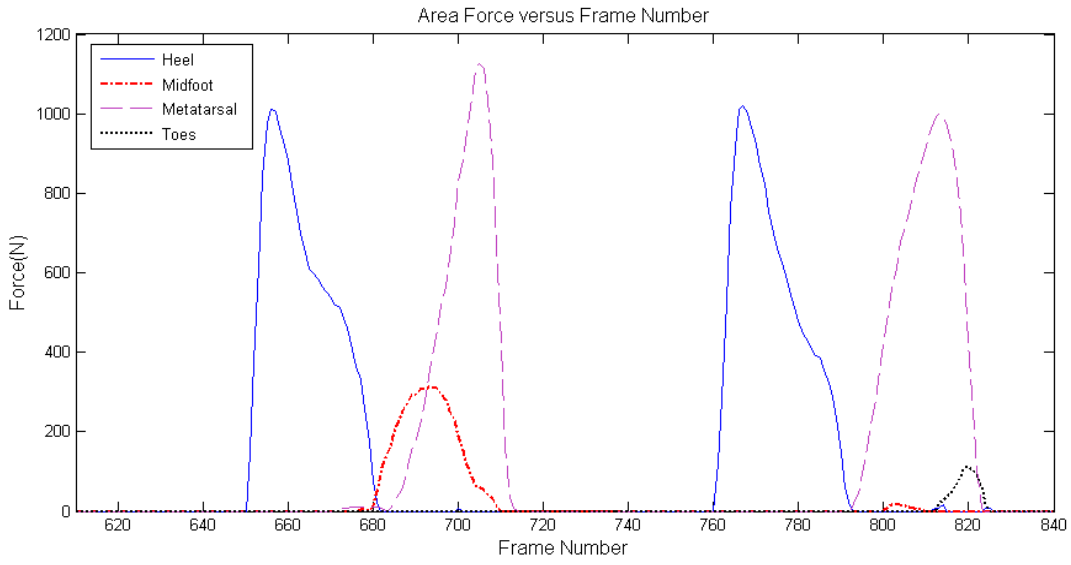

Figure 4.20: Multi-segment foot pressure for walking with eyes closed after being spun in the chair

Compared with the normal walking, the segment forces are less consistent between strides. The force on the mid-foot appears during walking, that may due to the instability caused by the dizziness and the mid-foot is helping to balance. In addition, the force on the toes greatly decreased. The force on the toes is mainly used for pushing off during toe off phase. This might because that the subject is more focused on walking steady, but not pushing off the ground for walking forward. Thus, for the less stable walking, the forces on each segment also changes for adjustment and better stability. The segment pressure study is valuable for the foot behavior description.

4.4 Summary

This study focused on the feature extraction from foot pressure for both the whole foot pressure function and segment foot pressure function. For the whole foot pressure function description, a general framework is shown in Figure 4.21 to conclude the foot pressure feature definition. With the foot pressure analysis, it was found that the center of foot pressure trajectory and graphs of force exerted versus frames are good qualitative tools to explain foot behavior. Center of pressure (COP) is influenced by the whole body movement during walking, and thus can be analyzed for foot function characteristics and walking behavior. Besides the COP transitions within one stride, the dynamic pressure characteristics of pressure repeatability among strides were also investigated. In the studies, seven pressure features were extracted both within stride and between strides from foot plantar pressure pattern for foot dynamic behavior study. From the above 2D foot plantar pressure analysis, AP-COP motion and NCSS can well indicate the walking stability differences. Results obtained for AP-COP and NCSS are in-line with theoretical expectations. Both features are effective indicators.

In addition, pressure under foot segments, including the heel, mid-foot, metatarsals and toes are also introduced. Different walking conditions will lead to different pressure distribution under foot segments. Thus segment foot pressure could also be regarded as features to indicate the foot kinetic behavior characteristics.

However, that is far from enough to fully understand walking behavior and foot dynamic characteristics. The foot pressure features are extracted from 2D foot pressure information, and these are indirect indication of the 3D foot behavior. Thus further study of the foot behavior is required. In fact, 3D foot motion could also be measured and analyzed for walking behavior description. Thus in the next chapter, measuring foot motions is proposed to help better investigate foot dynamic behavior during

walking. Motion features will be extracted from foot kinematic measurement and analysis. A study of the foot and ankle motion could also benefit the foot pressure information interpretation, because the foot pressure and foot motion are produced simultaneously and have close relationship.

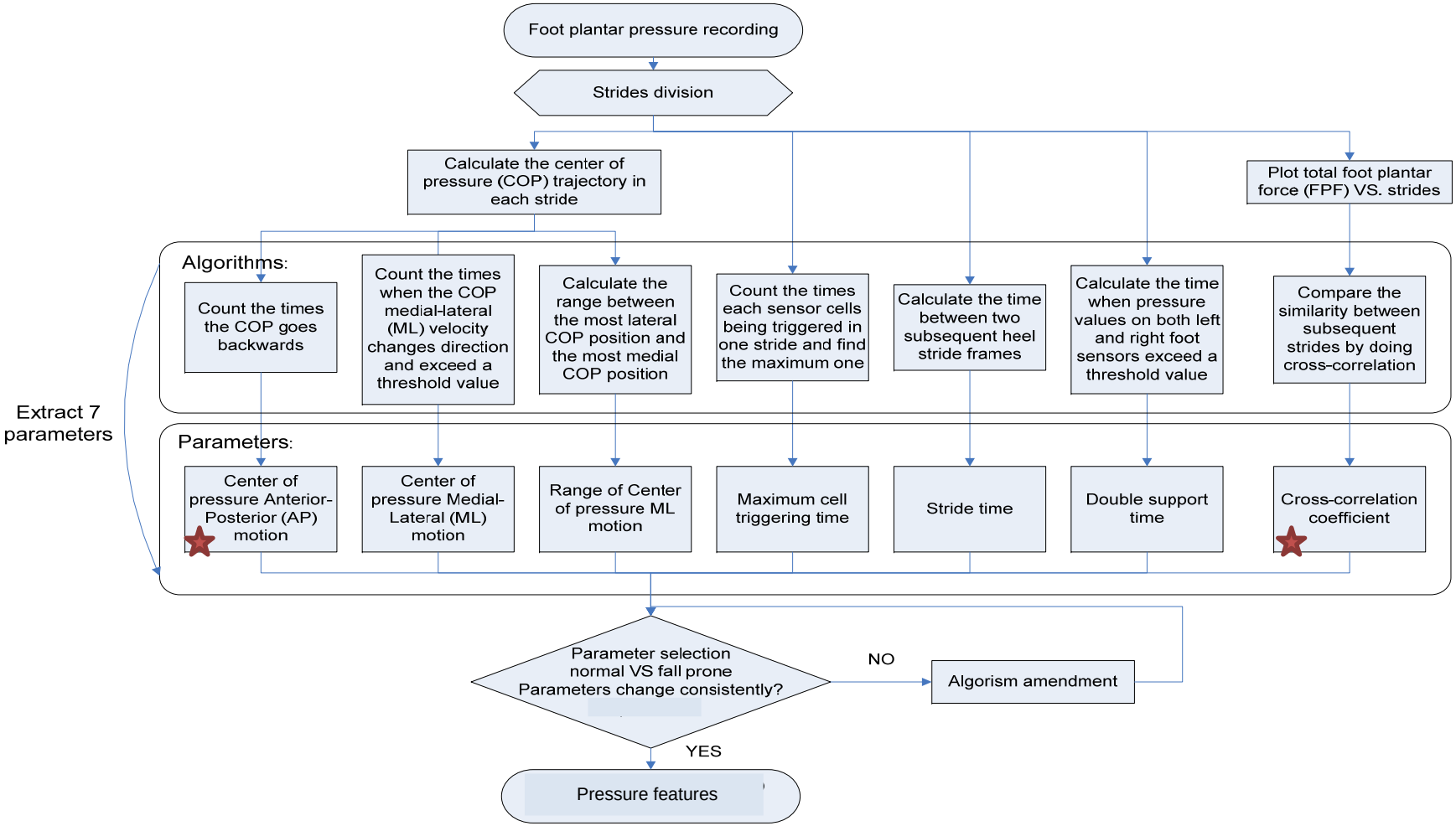

Figure 4.21: Details of the pressure features extracted from 2D plantar pressure for the application of walking stability

CHAPTER 5 IDENTIFY FEATURES FROM FOOT MOTIONS

Since foot pressure is only 2D information and is implicit, additional information, such as 3D foot motions will be measured and investigated in this chapter for the study of foot behavior during walking. Due to recent technology development, foot motion could be measured with motion cameras. 3D foot motion is more directly linked with lower body motion and easier understood. The purpose of this study is to investigate kinematic foot behavior during walking, and to identify foot motion features from detailed foot motion measurement and analysis. The foot motion features will be extracted for both the multi-segment foot motion function and the whole foot motion function.

5.1 Introduction

During the recent two decades, foot and ankle kinematics based on multi-segment foot models are getting more and more popular. A. Leardini, et al. [5] recorded three-dimensional foot joint motions and planar angles by tracking five rigid segments (shank, hind-foot, mid-foot, fore-foot and the whole foot) during the stance phase of gait. Although these models have different marker positions and definitions of joint rotation axis, they mainly divide the foot into segments of fore-foot, mid-foot and hind-foot. Some studies are interested in the fidelity and repeatability of the multi-segment foot and ankle model using skin mounted markers. M. P. Kadaba, et al. [72] proposed a coefficient of multiple correlation (CMC) to test the repeatability of kinematic data and concluded that the gait variables are quite repeatable. C. Nester, et al. [73] compared kinematic data obtained from bone and skin mounted markers. Nori Okita, et al. [13] used cadaver lower extremities to examine the validity of the rigid

body assumption and the magnitude of soft tissue artifact induced by skin-mounted markers. They concluded that the segmented model performs reasonably well overall. With these foot models, special studies were also performed on different groups of population, adolescent and certain patients [74-77].

According to previous studies in foot segment movements, it is essential to investigate how the foot functions during walking. The use of different foot models can be related to various clinical populations. Some segments show consistent movements and could be considered as walking features of normal people or certain groups of patients. However, there is currently no consensus on the number of segments division and joint motion definition. Different opinions exist on the selection of foot segments, the design of marker sets and anatomical reference, and the calculation of kinematic variables, etc. Investigations of the foot and ankle kinematics are still in the infancy and their clinical relevance remains unclear. This study investigates kinematic behaviors of foot and ankle during walking, and identifies foot motion features; including joint rotation angles between sub-defined rigid segments, and proposed angles for describing the whole foot physical features of walking.

5.2 Foot motion measurement

5.2.1 Foot structure and segments division

The single-rigid-body foot model does not provide sufficient information regarding the kinematic behavior of the foot in gait cycle. Unlike the shank, thigh etc., the foot is comprised of multiple joints and bones with complex interactions. The foot structure is shown in Figure 5.1. Different foot models are proposed dividing the foot into different segments [58-60, 72, 73], mostly separating the foot into hind-foot (heel), metatarsals, toes and sometimes mid-foot. Among these proposed models, the models having more sub-defined foot segments and measured with less skin-mounted markers

are preferred. In this study, the multi-segment model proposed by Leardini et al. [5] is adopted, involving five rigid segments: shank, hind-foot (calcaneus and talus/heel), mid-foot (cuboid, navicular, and three cuneiforms), fore-foot (metatarsals) and the whole foot. More effort will be focused on the three sub-defined foot segments: hind-foot, mid-foot and fore-foot. Here the whole foot is also regarded as one rigid segment to study the whole foot function. The motion of the whole foot segment is actually composed of the motions of sub-defined foot segments.

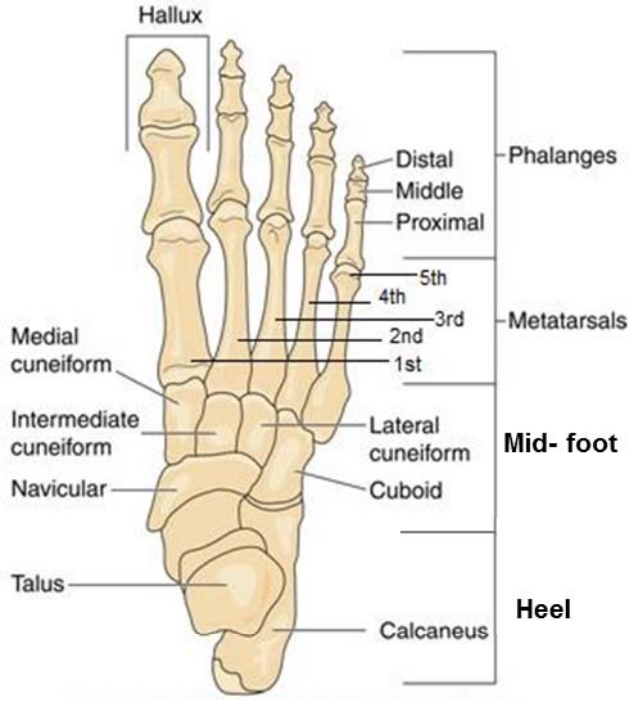

Figure 5.1: Foot bone structure

To measure each segment, at least three markers are needed on each segment to form a plane. In addition, extra markers are also needed to set up the local coordinates for angle definition. Figure 5.2 presents the foot structure, marker positions (black dots) and local coordinates on the three sub-defined foot segments. For each segment, the local axis system is defined to calculate relative motions between segments. The *X* axis is in the anterior-posterior direction, the *Y* axis is in the medial-lateral direction and the *Z* axis is in the proximal-distal direction.

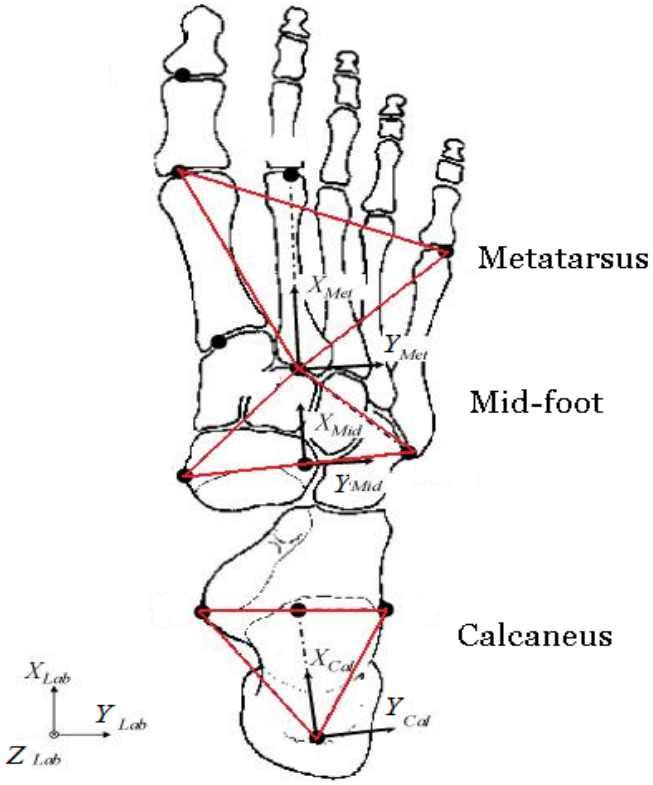

Figure 5.2: Foot segments and local coordinate

5.2.2 Experiment set-up

With the defined foot multi-segment model, experiment was set up for the measurement of foot motion. Video motion capture is one of the most useful tools in acquiring data for gait analysis. The main apparatus of the experiment consists of six Vicon cameras (Vicon MX13 Camera). The six cameras were mounted on the tripods and placed as shown in Figure 5.3. The height and angles of the camera were adjusted in order to optimize motion capture. The cameras were placed in such a way so that at every point of time at least two cameras capture each marker. The left lower leg and foot are tracked with the Vicon system sampling at 120 Hz. The captured volume is 2 m long, 1m wide and 0.7 m high. Before the experiment, system calibration is required. Accuracy is estimated at around 0.5 mm on calibration residuals. The calibration is exerted with the aid of the Vicon software, “Workstation”. There are two types of calibrations to be performed, static and dynamic calibration. For the static calibration,

eight markers are placed on the platform, shown in Figure 5.4.

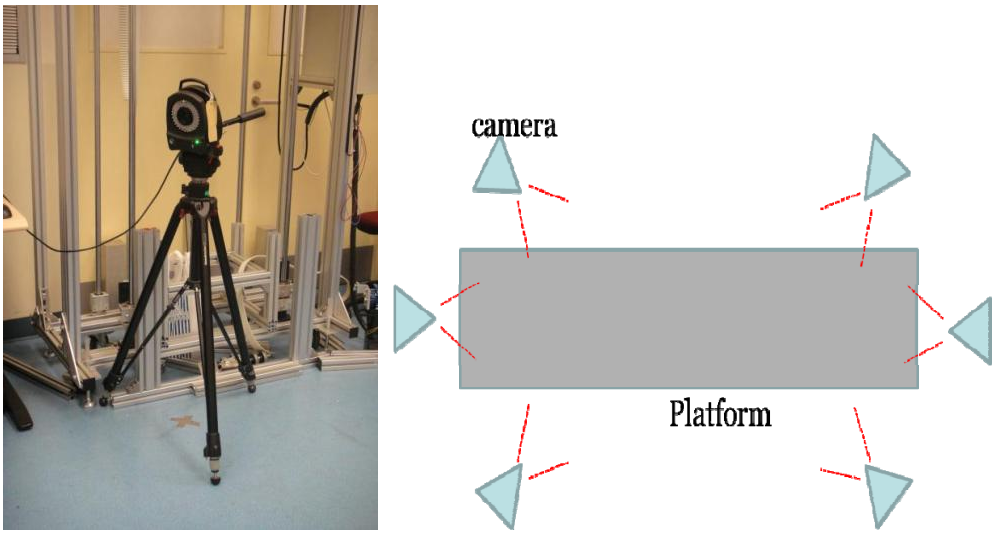

Figure 5.3: Vicon motion cameras and their positions during experiments

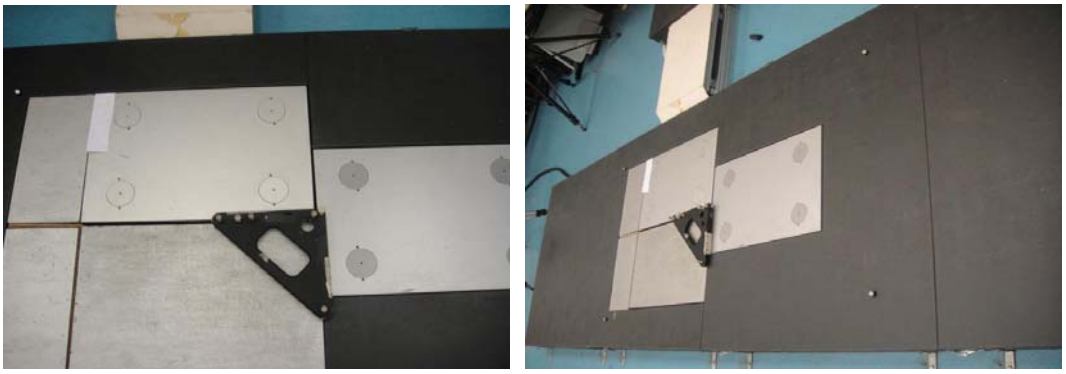

Figure 5.4: Positions of the markers for static calibration

With the aid of live monitor and diagnostics of Workstation, the cameras are adjusted in terms of height and angles such that all the eight markers are being seen clearly in the middle of the monitor. Noise threshold and strobe strength are also adjusted so that the camera can most efficiently capture the reflections of the eight markers. Due to the spacious issue in the lab, few cameras cannot be located further away from the platform, hence there is a need to make sure angles are adjusted so that the all the eight markers are seen. In addition, there is a need to make sure the position of the cameras can avoid the opposite camera's light.

After the static calibration, the dynamic wand is used for the dynamic calibration. The wand, shown in Figure 5.5, is moved in the “figure of 8” in the space of capture volume. After the dynamic calibration, Workstation will generate the visibility of the wand. In addition, the range of error will be calculated as well. In this study, experiment will then be carried out if the error is lesser than 0.7mm.

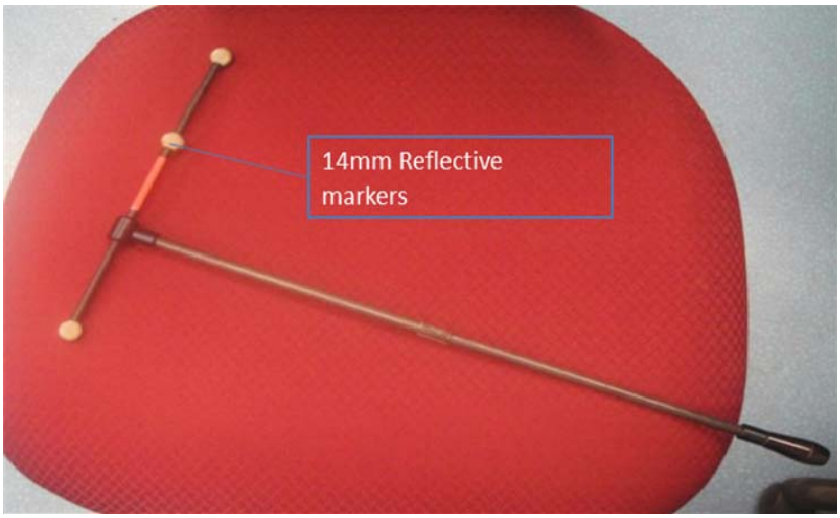

Figure 5.5: Standard wand with three reflective markers for dynamic calibration

Five subjects are tested during barefoot walking (mean age: 25 years, range: 23-27 years; mean body mass: 68 kg, range: 49-77 kg). Subjects with a history of foot injury or obvious gait abnormality are excluded. Each subject performs five walking trials at self-selected speed. Sixteen auto-reflective (9mm diameter) markers are mounted on the skin. The marker positions are shown in Table 5.1 and Figure 5.6 [4]. These markers are located at either proximal or distal positions of the anatomical bony structures. Since the markers are all put on the left foot side, all markers are named with initial letter “L”. For each segment, the local axis system is defined to calculate relative motions between segments. In Table 5.2, the local axes systems of all segments are listed, including the origin and three axes. The *X, Y, Z* directions are same as defined in Figure 5.2.

Table 5.1: Experiment marker sets

Markers	Description
LPM	Left Proximal Phalanx Marker of the Hallux
LFMH	Left 1st Metatarsal Head Marker
LSMH	Left 2nd Metatarsal Head Marker
LVMH	Left 5th Metatarsal Head Marker
LFMB	Left 1st Metatarsal Base Marker
LSMB	Left 2nd Metatarsal Base Marker
LTN	Left Medial Navicular Tuberosity Marker
LVMB	Left 5th Metatarsal Base Marker
LMM	Left Malleolus Medial Marker
LLM	Left Malleolus Lateral Marker
LCAM	Left Calcaneus Medial Marker
LCA	Left Central Ridge of the Calcaneus Posterior Surface Marker
LCAL	Left Calcaneus Lateral Marker
LPTM	Left Proximal Tibia Medial Marker
LPTT	Left Proximal Tibia Tuberosity Marker
LPTL	Left Proximal Tibia Lateral Marker

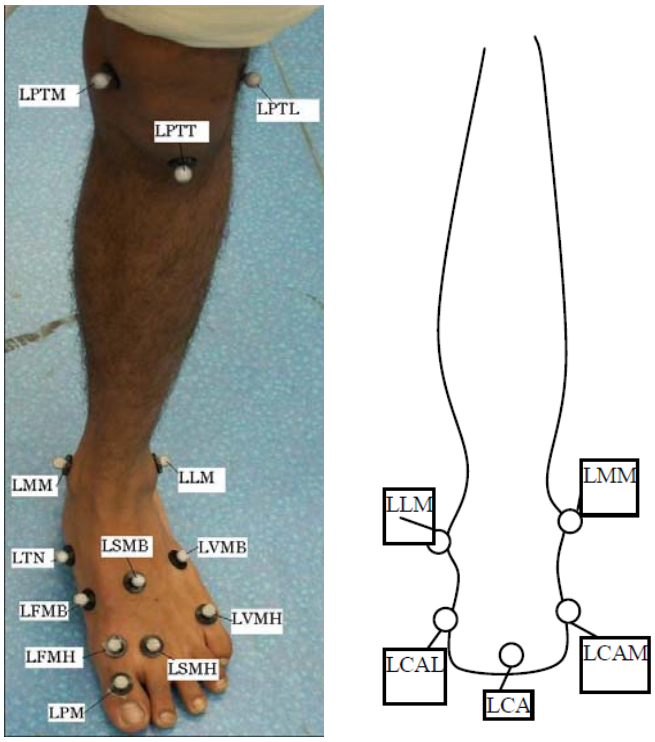

(a) (b)

Figure 5.6: Experiment marker set (a) anterior view (b) posterior view

Table 5.2: Defining vectors and origins used to establish the local segment-fixed reference system

Segment / Defining vectors	Shank	Hind-foot (heel)	Mid-foot	Fore-foot (metatarsals)	Foot
$\vec{v}_1$	$\vec{v}_2 \times \vec{v}_3$	LCA-LIC	LID-LSMB	LSMB-LSMH	LCA-LSMH
$\vec{v}_2$	LIM-LLM	LCAM-LIC	LTN-LID	LFMH-LVMH	LFMH-LVMH
$\vec{v}_3$	LIM-LIPT	$\vec{v}_1 \times \vec{v}_2$	$\vec{v}_1 \times \vec{v}_2$	$\vec{v}_1 \times \vec{v}_2$	$\vec{v}_1 \times \vec{v}_2$
O	LIM	LCA	LID	LSMB	LCA

Note: LIPT = (LPTM+LPTL)/2; LIM = (LMM+LLM)/2;
LIC = (LCAM+LCAL)/2; LID = (LTN+LVMB)/2; $\vec{v}_1$ is in the direction of *X* axis,
$\vec{v}_2$ is in the direction of *Y* axis and $\vec{v}_3$ is in the direction of *Z* axis

After the walking trial, foot motion data are recorded as all marker trajectories. From Workstation, the data could be viewed in three-dimension, shown below in Figure 5.7. The white dots are the markers positions in one time frame during the walking trial. The data will be discarded if most of the markers are missing in most of the frames. This could be due to poor calibration or poor layout of the positioning of the cameras. The next step is to label the markers in workstation and this could make it easier to find out whether the markers are missing. The labeled data is shown in Figure 5.8.

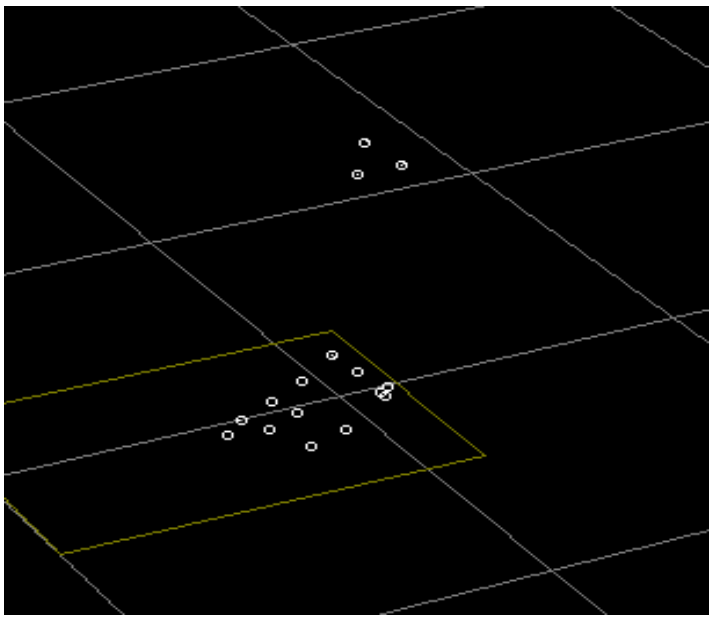

Figure 5.7: Captured raw marker positions in Workstation

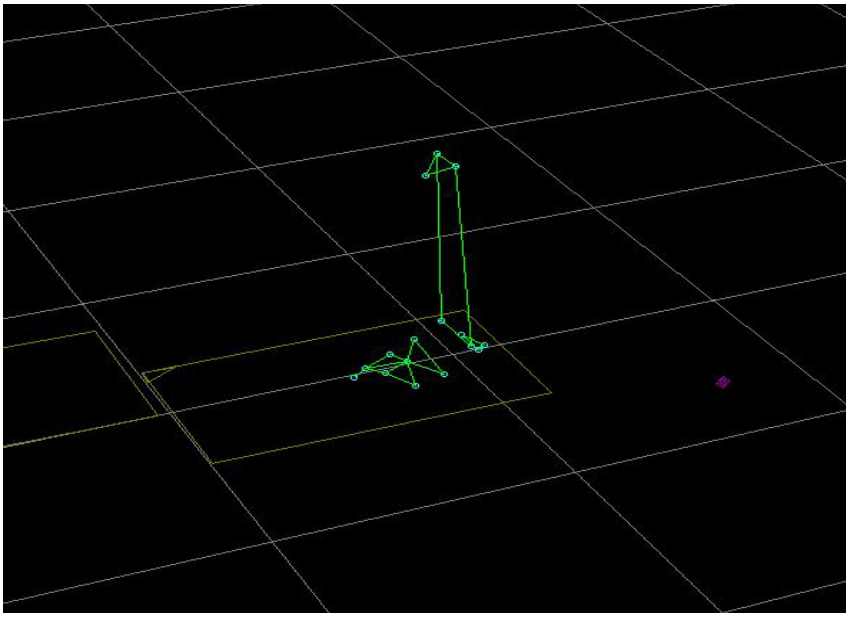

Figure 5.8: Labeled marker positions in Workstation

After all the labeling has been done for all markers in each frame, the file has to be opened in “Bodybuilder” for building the missing markers in every frame. Every marker can generate trajectories with respect to *x, y, z* axis. The trajectories depict the continuity of the markers. Hence, all charts are to be patched so that the video is complete, shown in Figure 5.9.

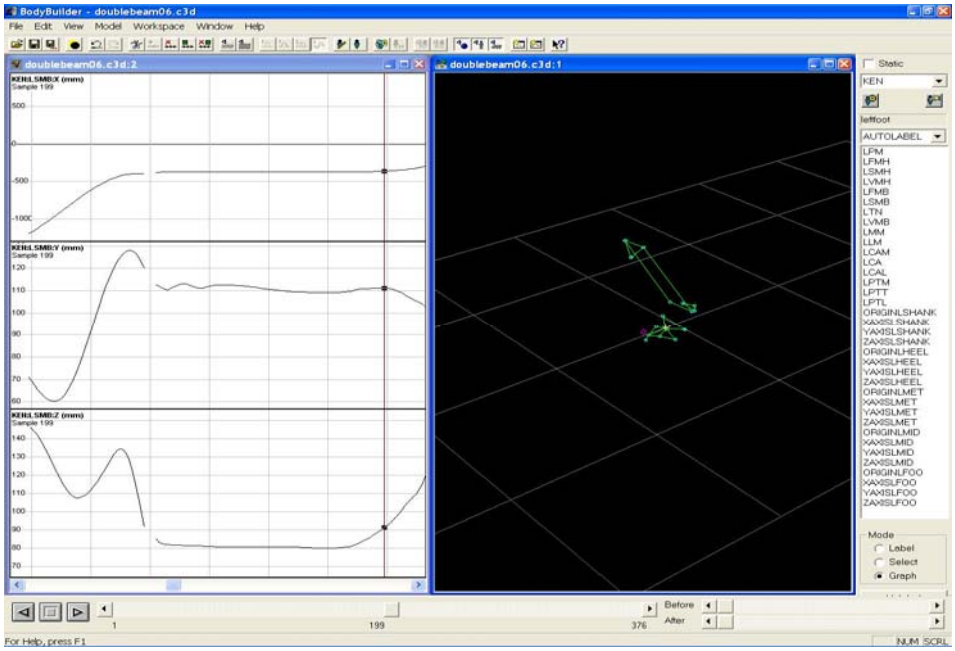

Figure 5.9: Patching up the trajectories in Bodybuilder

Then the local coordinate will be set up for each sub-segment, defining origin, *x*, *y* and *z* axis directions, by writing customized codes to be compiled in Bodybuilder. The defined local coordinates are shown in Figure 5.10.

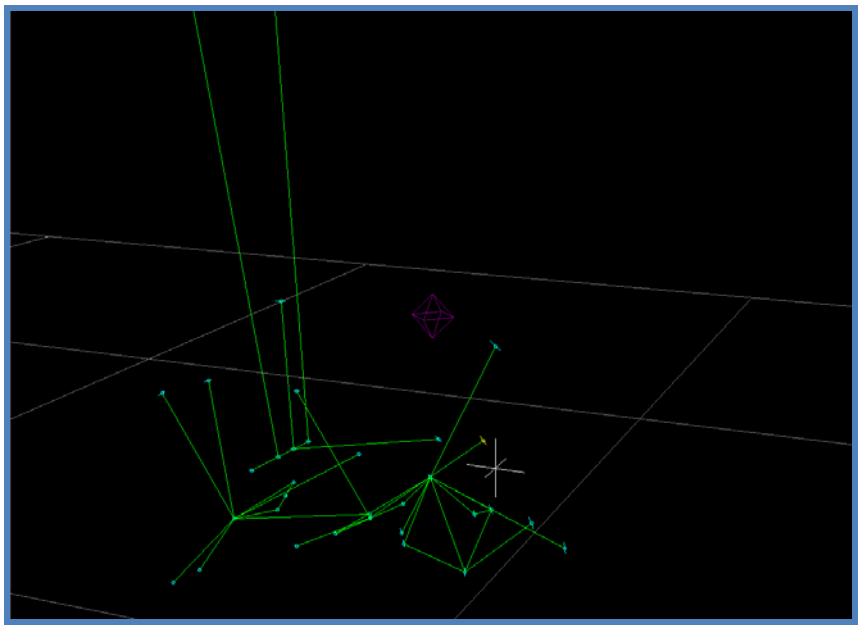

Figure 5.10: Setup five local coordinates on each foot segment in Bodybuilder

Joint angles between two segments or any particular angle formed by markers could be calculated with Bodybuilder software according to the Euler angle rule. The angle values could be exported into ASCII files for further analysis.

5.3 Foot motion features

5.3.1 Joint motions calculation

According to the introduced foot structure and sub-defined segments, to extract foot motion features, joint motions between foot segments are considered. In this study, the multi-segment model proposed by Leardini et al. [5] is adopted, involving five rigid segments: shank, hind-foot, mid-foot, fore-foot and the whole foot. This model can provide five joint motions, which are joint motions between shank and heel (Shank-Heel), heel and mid-foot (Heel-Mid), heel and metatarsals (Heel-Met), and

mid-foot and metatarsals (Mid-Met), as well as shank and the whole foot (Shank-Foot). Totally 15 joint rotation angles (JRAS) are calculated as motion features because each joint motion has joint rotation angles in sagittal (dorsi/plantar-flexion), coronal (eversion/inversion) and transverse (abduction/adduction) planes respectively, shown in Figure 5.11.

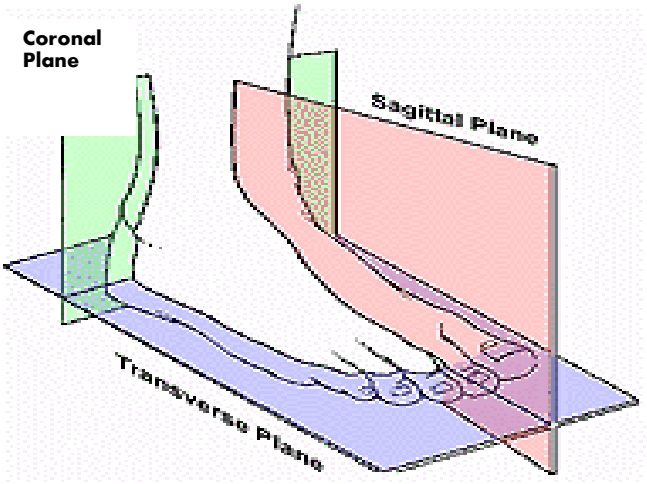

Figure 5.11: Motion in sagittal, coronal and transverse planes

These joint motions are calculated by Vicon software-“Bodybuilder”, further processed by “MATLAB”. All data were normalized in time through linear interpolation to 100% stance phase. The reference position for each trial is defined as the angle value at the mid-stance phase time during the dynamic walking as seen in Figure 5.12. In previous literature [5, 59], the reference position is mostly taken during the static trial (standing posture). When data from trials of different subjects is compared, a large amount of variance is due to off-set values. Considering the difference between foot gestures during standing and walking for different individuals, the mid-stance phase position is considered here as the new reference position for a dynamic study in the proposed work. The mid-stance time is chosen as the mid-time point when both LPM and LCA markers have zero vertical direction displacement (when both the hallux and heel are contacting the ground). This new reference position

can better reduce variance, because it is a dynamic reference and changes according to walking styles of tested individuals.

Figure 5.12: The three phases of a stance

Mean and standard deviation of fifteen joint rotation angles between segments are calculated. Each tested subject needs to go through 3 trials. To test intra-subject and inter-subject repeatability of the joint motions, averaged standard deviations (ASD) and coefficients of multiple correlations (CMC) [72] are calculated.

5.3.2 Functional angles calculation

Joint rotation angles can provide angular projections in the sagittal, coronal and transverse planes of the joint motion, but these projections are difficult to apply in the clinics because they are not directly describing foot dynamic functions. To solve this problem, additional four functional angles (Angle 1 to Angle 4) are proposed to represent specific physical features of whole foot motion function during walking. This could help to improve clinical applications of the available data and can be a supplementation of multi-segment method. These angles are calculated in Vicon software-“Bodybuilder” and reported in “Polygon”. In the “Bodybuilder”, Euler angles are used to determine the joint angles in 3D. “Polygon” is used to report the calculated angles and patterns.

Assume that the virtual marker LIM is the mid-point between LLM and LMM (Figure 5.13). To represent the arch changes during the stance phase of walking, the angle (angle 1), between vector of LCA to LIM and vector of LSMB to LIM, is proposed and calculated.

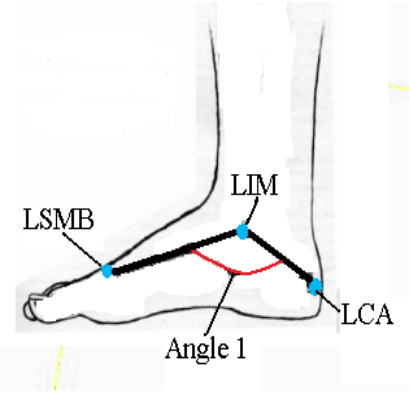

Figure 5.13: Definition of Angle 1 for weight bearing arch changes

The projection angle is defined as the angle between two vectors in the perspective view along the axis of rotation. Aiming for describing the windlass mechanism between fore-foot and hind-foot, the angle (angle 2) between vector of LFMH to LVMH and vector of LCAM to LCAL, which projected on the "quasi-coronal" plane, is calculated as shown in Figure 5.14. The quasi-coronal plane here is the dynamic plane with the normal vector as LCA to LSMH.

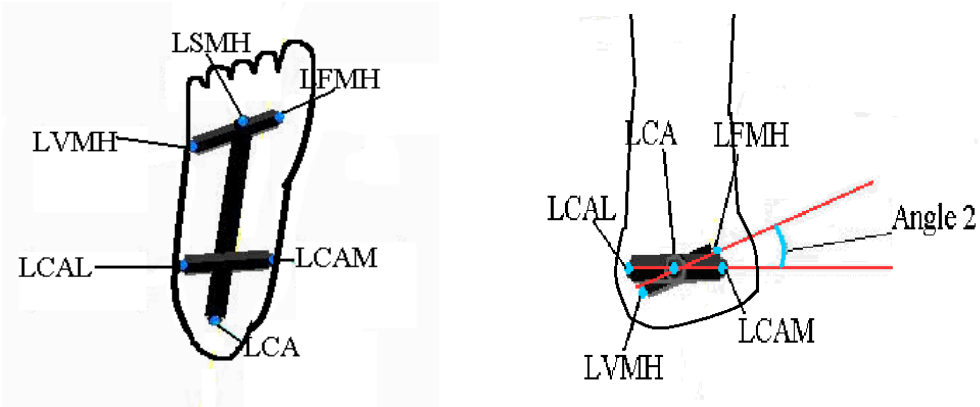

(a) (b)

Figure 5.14: Definition of Angle 2 for windless mechanism
(a) transverse plane view (b) coronal plane view

For indicating the push off feature at the late stance, the angle (angle 3) between vector of LFMH to LPM and vector of LCA to LSMH, which projected on the "quasi-sagittal" plane is calculated as shown in Figure 5.15. The quasi-sagittal plane here is the dynamic plane with the normal vector as LFMH to LSMH.

Assume that virtual marker LIPT is the mid-point between LPTL and LPTM. The angle (angle 4) is the angle between vector of LIM to LSMB and vector of LIM to LIPT. This angle is actually among previous joint rotation angles, but this angle is important to represent the feature of flexibility and controllability of the ankle joint during walking. For example, the ankle flexibility might decrease during aging, and the dynamic pattern of angle 4 should be able to present the changes. Thus angle 4 is regarded as a typical functional angle here, shown in Figure 5.16.

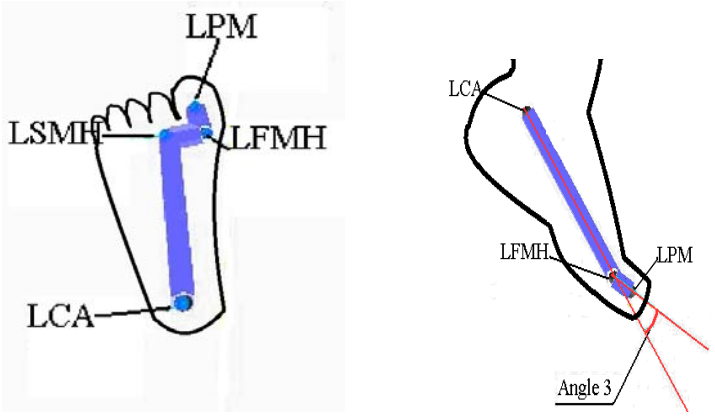

(a) (b)

Figure 5.15: Definition of Angle 3 for push off feature
(a) transverse plane view (b) sagittal plane view

5.4 Results

5.4.1 Joint motions

The five reported joint motions are normalized to one stance phase of the gait cycle. Figure 5.17 presents five joint motions of 3 trials from one tested subject. Figure

5.18 presents five joint motions of 15 trials from all five subjects. The thick lines represent the mean values. The thin lines indicate one standard deviation from the mean value.

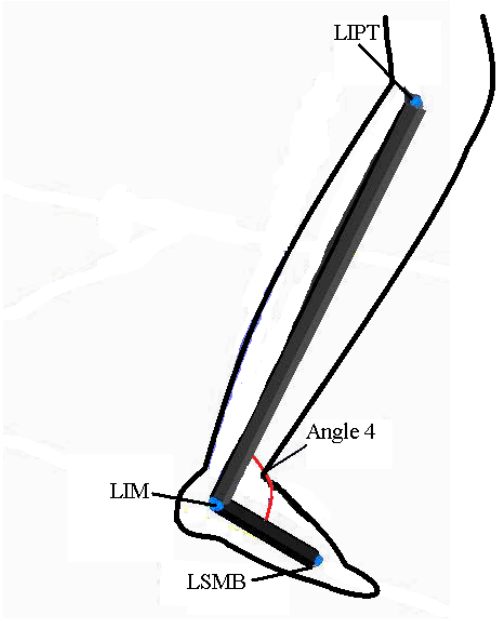

Figure 5.16: Definition of Angle 4 for ankle flexibility feature

In general, the variation is low for multi-trials of one subject as shown in Figure 5.17. The mean ±1 S.D. created a narrow corridor for each parameter. The motions for all subjects show relatively consistent patterns as seen in Figure 5.18. The consistency of these variables is also indicated by ASD and CMC in Table 5.3 and Table 5.4 separately. The rows headed by “Average” are the averaged ASD or CMC values of five above values of the five tested subjects. The rows headed by “ALL” are the ASD or CMC values comparing all trials from all tested subjects. Thus values in the “Average” row indicate the intra-subject variance (data from one subject) and values in the “All” row indicates the inter-subject variance (data from different subjects). Thus the values in the “All” row are generally larger than the ones in the “Average” row. Generally the smaller the ASD is, the larger the CMC is and the more consistent the

corresponding motion is. Since variables with consistent patterns among different subjects can be regarded as the characteristic of this group of subjects, those angles are more of our interest. ASD and CMC values can help to select those relatively consistent variables; however, there is still no consensus on the boundary value to define an absolute consistent motion due to different experiment protocols, equipment and conductors. According to our calculated ASD and CMC results, the averaged ASD values that are below “1” are bolded. The ASD for all subjects (the row headed by “ALL”) are naturally have larger values than the averaged ASD values (the row headed by “Average”). Thus the values that are below “1.5” are bolded. As to the CMC, those near or above 0.9 are bolded. From these bolded values, several joint rotation angles are selected for further studies: the shank-foot angles in three planes, shank-heel angles in three planes, heel-mid angles in coronal and transverse planes, mid-met angle in coronal planes and heel-met in coronal and transverse planes. All the angles are discussed referring to the angles of the mid-stance time. The angle is calculated from the distal segment relative to the proximal segment, e.g. Shank-Foot angle means the angle of the foot relative to the shank.

Figure 5.18 presents the joint motions during stance phase for all tested subjects. For the sagittal plane angle between shank and the whole foot (Shank-Foot) at the heel strike relative to the reference position (mid-stance phase position), the foot is plantar-flexed and reaches a peak plantar-flexed angle at around 10% of stance time. Until the mid-stance phase time, the Shank-Foot angle turns to dorsi-flexed and keeps on dorsi-flexing until propulsive phase at around 80% stance time. At the late stance phase (propulsive phase), the Shank-Foot angle goes quickly from most dorsi-flexed to most plantar-flexed. The average range of motion is more than 20 degree and this motion angle describes a key foot motion. Both the pattern and range of motion is

consistent with J. Simon's study [78]. For the Shank-Foot angle in the coronal plane, the foot is relatively inverted at the heel strike and reaches a peak inversion at around 7% of the stance time. The foot is everting till the mid-stance time. At the propulsive phase, the angle goes back inverting. The averaged range of motion is around 10 degrees. As to the Shank-Foot angle in the transverse plane, the average range of motion is around five degrees. The foot is slightly adducted at the very beginning and the end of the stance phase relative to the reference position. The coronal and transverse plane angles have less range of motion than the sagittal plane angle, and with good intra-subject and inter-subject consistency.

For the Shank-Heel angles in the sagittal, coronal and transverse planes, the angle patterns are quite similar with corresponding Shank-Foot ones. Only the range of motion is slightly smaller. This is because that the Shank-Heel motion is one key component of the Shank-Foot motion.

The Heel-Mid sagittal plane angle shows a small saddle shape. At the heel strike phase, the mid-foot is slightly dorsi-flexed relative to the heel. At the propulsive phase, the mid-foot is plantar-flexed relative to the heel. In the coronal plane, the mid-foot is everting smoothly at the first 20% stance phase and inverting smoothly at the late 20% stance phase relative to the heel. In the transverse plane, the mid-foot is slightly adducted (two degrees) at the very beginning of the stance phase and adducted obviously at the late 20% of stance phase, with the range of motion around 8 degrees. The Heel-Mid motion is relatively small for the normal walking; however, consistent motion exists among heel and mid-foot and this motion might exert some function on stabilization. This could be verified in future study conducting some less stable walking tasks.

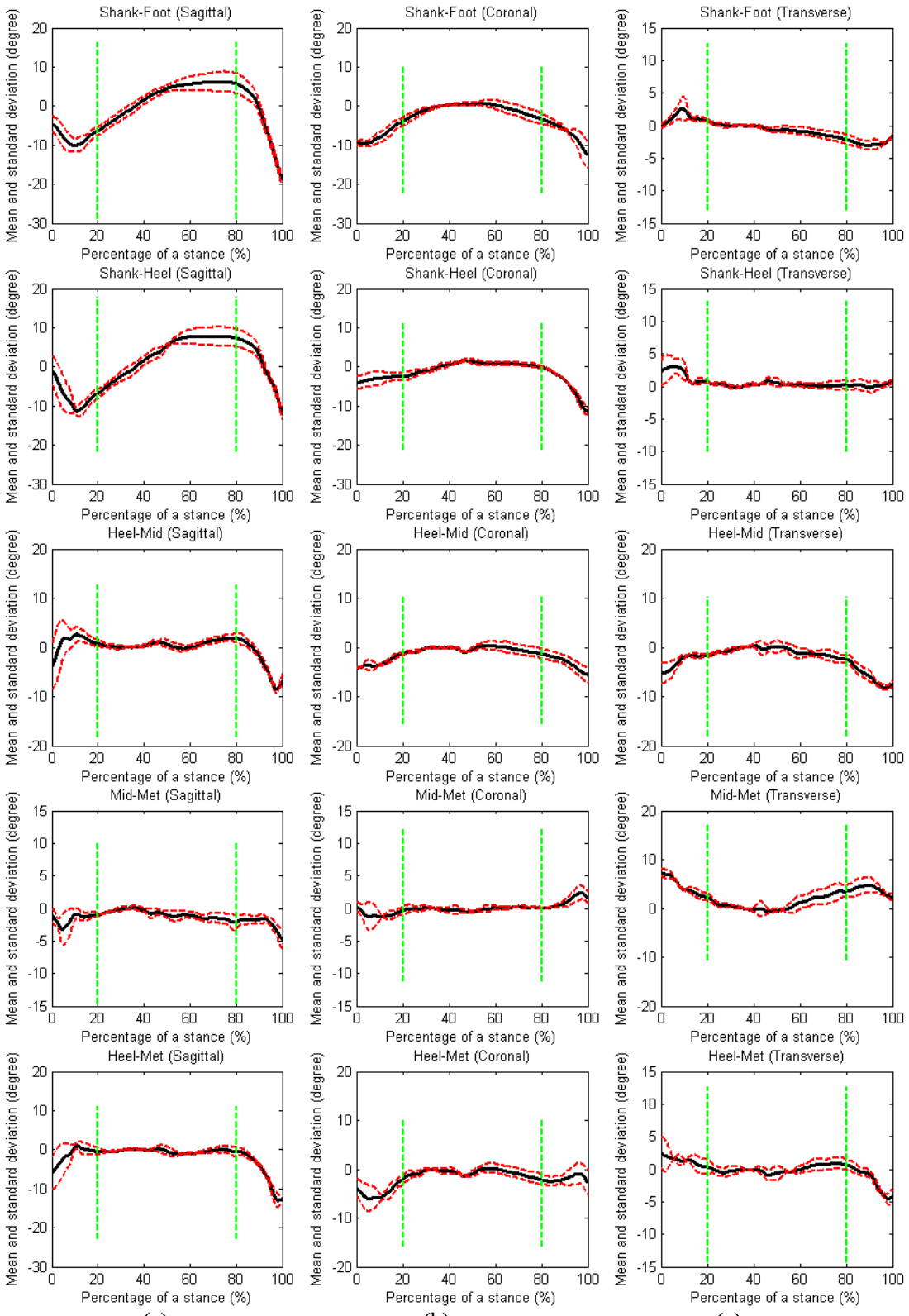

Figure 5.17: Five averaged joint motions of 3 trials from one subject in three planes. (a) Sagittal plane (positive: Dosi-flexion/negative: Plantar-flexion) (b) coronal plane (positive: Eversion/negative: Inversion) (c) transverse plane (positive: Abduction/negative: Adduction); Mean (real black line), ±1 S.D. (red dotted line), 20% and 80% mark (green vertical dotted line)

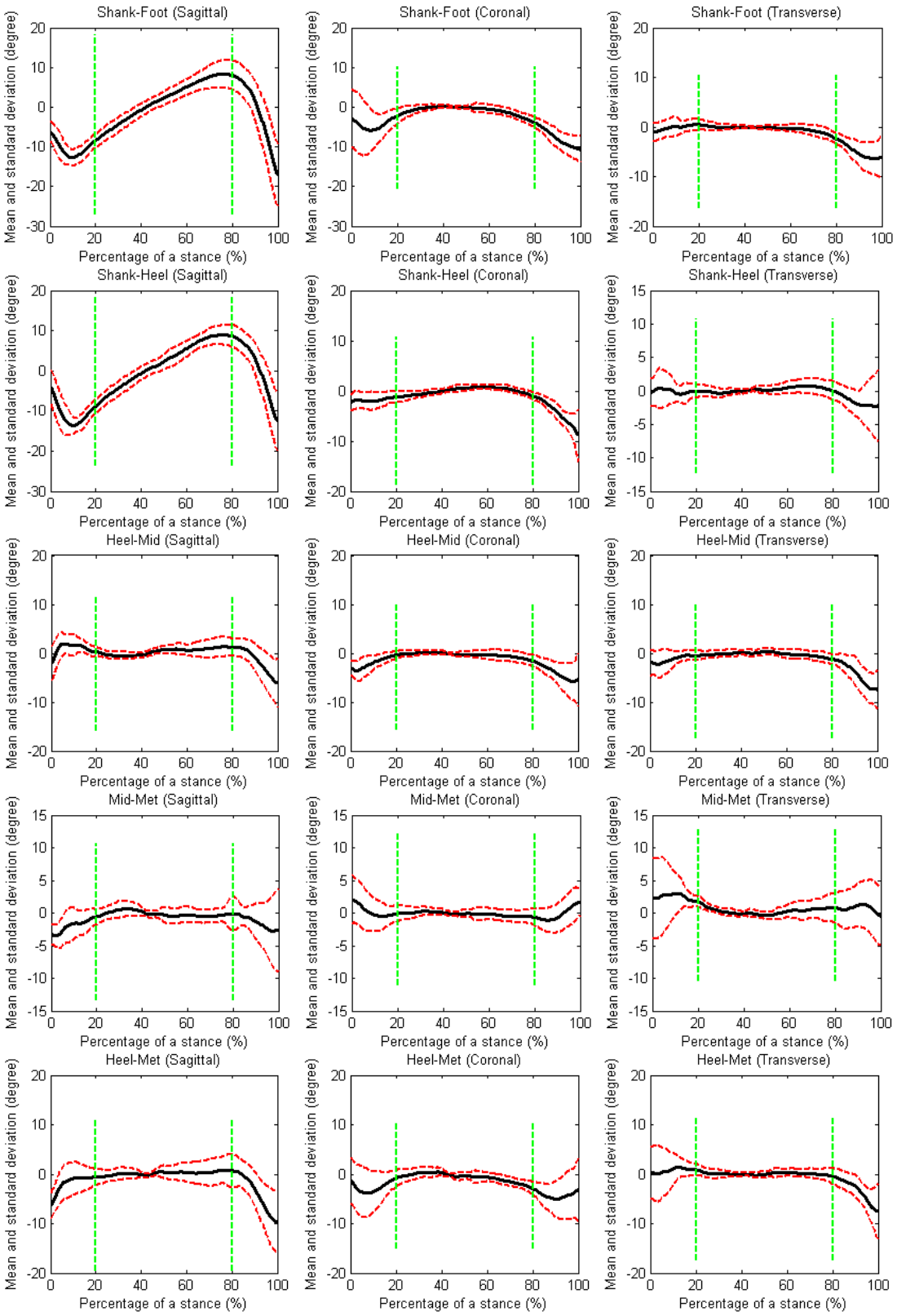

Figure 5.18: Five averaged joint motions of 15 trials from five subjects in three planes. (a) Sagittal plane (positive: Dosi-flexion/negative: Plantar-flexion) (b) coronal plane (positive: Eversion/negative: Inversion) (c) transverse plane (positive: Abduction/negative: Adduction); Mean (real black line), ±1 S.D. (red dotted line), 20% and 80% mark (green vertical dotted line)

Table 5.3: Averaged standard deviations (ASD) for five tested subjects and combined group of all subjects

	Shank-Foot			Shank-Heel			Heel-Mid			Mid-Met			Heel-Met		
	S	C	T	S	C	T	S	C	T	S	C	T	S	C	T
Subject 1	1.107	1.019	0.672	0.832	0.451	0.992	1.274	0.907	1.069	1.002	0.653	1.190	1.611	0.841	0.799
Subject 2	1.428	0.926	1.488	0.902	0.999	1.952	1.361	1.360	1.509	0.776	0.610	1.270	1.805	0.937	1.620
Subject 3	1.434	1.436	1.068	1.156	0.454	0.952	1.238	0.638	0.577	1.361	1.107	1.259	1.774	1.231	1.365
Subject 4	1.363	1.454	0.623	1.210	0.603	0.639	0.827	0.555	0.706	1.251	0.724	1.138	1.326	1.238	1.009
Subject 5	1.633	1.039	0.500	1.721	0.691	0.530	0.922	0.635	0.763	0.669	0.488	0.888	0.940	1.041	0.723
Average	1.393	1.175	**0.870**	1.164	0.640	1.013	1.124	**0.819**	**0.925**	1.012	**0.716**	1.149	1.491	1.058	1.103
ALL	2.536	1.568	**1.217**	2.409	**1.039**	**1.387**	1.706	**1.204**	**1.398**	1.668	**1.335**	1.768	2.162	1.821	**1.463**

S: Sagittal plane; C: Coronal plane; T: Transverse plane

Table 5.4: Coefficients of multiple correlations (CMC) for five tested subjects and combined group of all subjects

	Shank-Foot			Shank-Heel			Heel-Mid			Mid-Met			Heel-Met		
	S	C	T	S	C	T	S	C	T	S	C	T	S	C	T
subject1	0.991	0.986	0.991	0.993	0.998	0.989	0.648	0.959	0.904	0.628	0.928	0.740	0.670	0.963	0.921
subject2	0.979	0.988	0.973	0.989	0.983	0.929	0.671	0.861	0.851	0.932	0.958	0.911	0.795	0.947	0.791
subject3	0.970	0.944	0.987	0.980	0.997	0.989	0.889	0.973	0.977	0.659	0.810	0.627	0.729	0.878	0.824
subject4	0.961	0.957	0.994	0.976	0.996	0.995	0.824	0.920	0.898	0.785	0.944	0.915	0.892	0.898	0.964
subject5	0.964	0.984	0.995	0.956	0.992	0.994	0.838	0.968	0.967	0.673	0.922	0.961	0.900	0.925	0.972
Average	**0.973**	**0.972**	**0.988**	**0.979**	**0.993**	**0.979**	0.774	**0.936**	**0.919**	0.735	**0.912**	0.831	0.797	**0.922**	**0.894**
ALL	**0.935**	**0.966**	**0.980**	**0.941**	**0.987**	**0.976**	0.597	0.874	0.836	0.490	0.735	0.706	0.710	0.769	0.870

S: Sagittal plane; C: Coronal plane; T: Transverse plane

The Mid-Met sagittal plane angle is dorsi-flexing at the heel strike phase and plantar-flexing at the propulsive phase. In the coronal plane, the metatarsal segment is everted at the heel strike and inverting during the first 10% of stance time, then keeps unchanged during the foot flat phase, and goes around 5 degrees everted at the late 10% stance time.

In the transverse plane, the metatarsal segment is slightly adducting till the mid-stance, and then keeps abducting at the propulsive phase. This angle can also help to understand functions of the fore-foot, especially providing push off forces during propulsive phase. During the propulsive phase, fore-foot is plantar-flexed, everted and abducted.

The Heel-Met sagittal plane angle is plantar-flexed at heel strike and is dorsi-flexing at the first 10% stance phase, then keeps unchanged till 80% of stance phase and is plantar-flexing at the propulsive phase, with more than 10 degrees' range of motion. In the coronal plane, the metatarsal is from inversion to neutral at the very beginning of stance phase, and then inversion again at the late 20% of stance phase, with around 5 degrees' range of motion. In the transverse plane, the metatarsal is adducted obviously at the late 20% of stance phase, with around 7 degrees' range of motion. The Heel-Met motion could be regarded as the sum of Heel-Mid motion and Mid-Met motion. The combined motion of adjacent segments contributes to the whole foot motion during walking.

5.4.2 Functional angles

Angle 1 generally has a saddle shape and can clearly present the arch change feature. Figure 5.19 (a) is a sample of the angle 1 calculated during one stance of a subject. In the figure, the range of motion of the arch angle 1 is around 10 degrees, from 119 to 129 degrees. The patterns are relatively consistent with the overall mean range of motion as 9.3 degrees. Figure 5.19 (b) is a sample of the angle 1 calculated for three walking trials of one subject.

Angle 2 increases from heel strike to 7% of stance phase and decreases fast till foot flat, and becomes relatively steady during mid-stance, and increases fast from heel

rise to 90% of stance phase then decreases till toe off. The changes can help describe foot coronal plane motions; fore-foot with respect to the hind-foot from supination at the early stance phase to supination again at the toe off phase. The angle pattern is consistent both within a subject and among subjects with the mean range of motion as 9.1 degrees. The motion pattern is quite obvious to describe coronal plane foot motions. Figure 5.20 presents the angle pattern in detail and a sample of the angle 2 calculated for two walking trials of one tested subject.

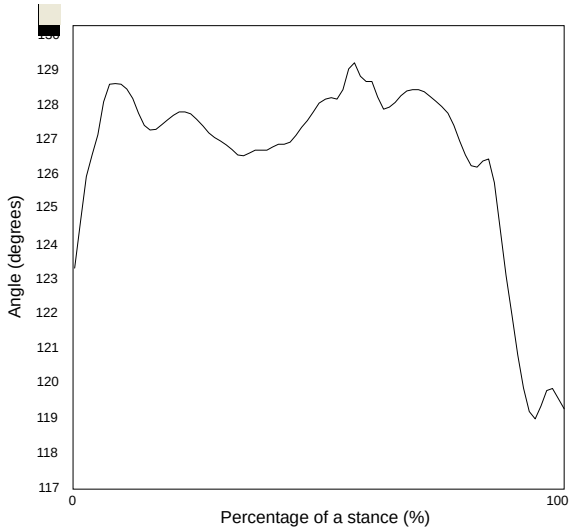

(a)

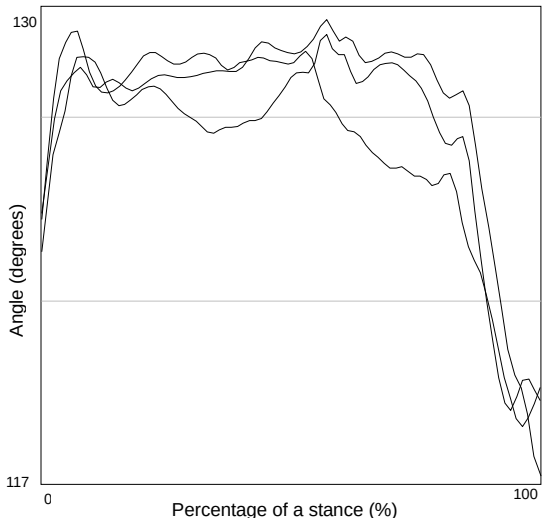

(b)

Figure 5.19: Angle 1 for foot arch dynamic feature
(a) one trial (b) three trials comparison

In Figure 5.21, angle 3 has consistent impulse pattern at the toe off phase (propulsive phase). By measuring relative magnitude of the impulse, push off feature can be represented. In the joint motion calculation section, only the metatarsal part of the fore-foot is concentrated, while the hallux motion is not described. Push off feature could help to describe motion between hallux and the whole foot. It could be a necessary compensation for fore-foot motion analysis.

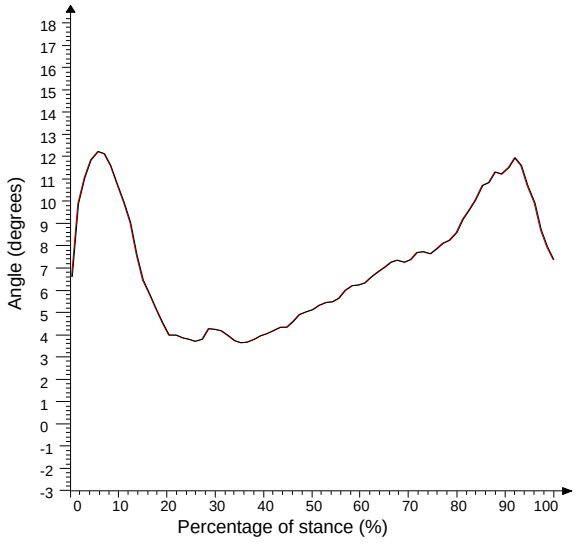

(a)

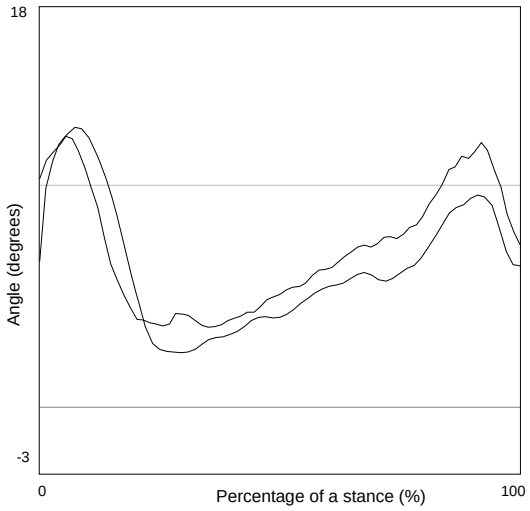

(b)

Figure 5.20: Angle 2 for fore-foot and hind-foot windless mechanism
(a) one trial (b) two trials comparison

For our tested subjects, the mean relative magnitude of the impulse is 44 degrees. The magnitude is quite large and this indicates that young healthy people (tested subjects) have very flexible hallux motion during push off and this could also result in great push off force opposite the ground. The angle has consistent pattern in trials of one subject and trials all subjects. Figure 5.21 shows the angle pattern in detail and the repeatability of the angle 3 for one tested subject.

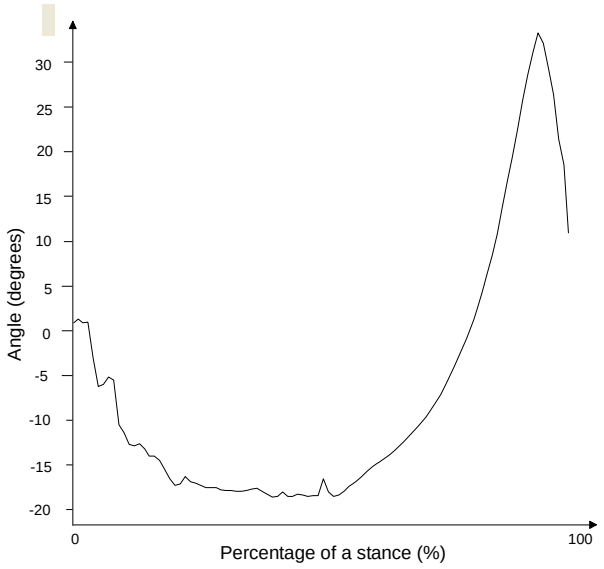

(a)

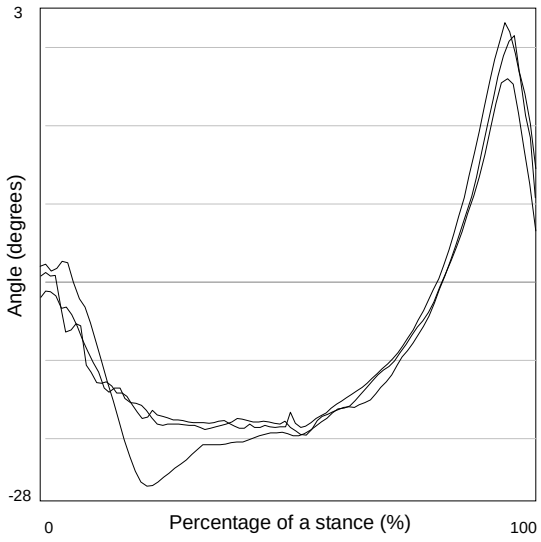

(b)

Figure 5.21: Angle 3 for push off feature (a) one trial (b) three trials comparison

Angle 4 has the overall average range of motion as 19 degrees. This angle pattern is very consistent between trials of one subject as shown in Figure 5.22. This angle can also clearly present the flexibility of the ankle during subjects' walking. Through life experience observation, the elderly people tend to have a dragging feature during walking. This may lead to smaller range of motion of angle 4 and this could be verified in future study.

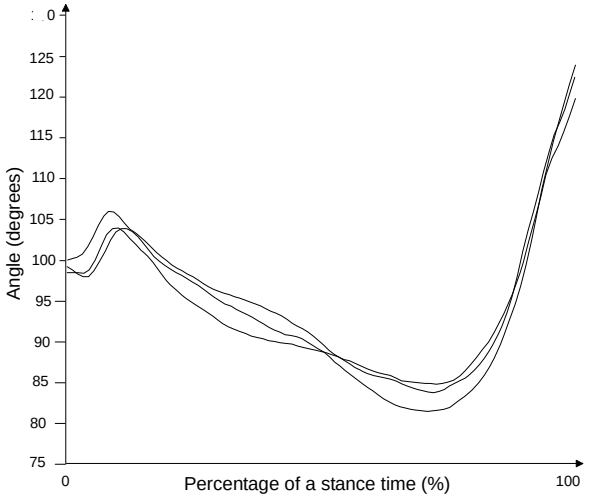

Figure 5.22: Angle 4 for ankle flexibility feature
(Comparison of three trials of one tested subject)

5.5 Discussion

Foot motion features including joint rotation angles and functional angles were identified and analyzed for foot kinematic behavior description.

The joint rotation angles were investigated in previous literature with different defined foot multi-segment models. Here we choose a model with relatively fewer markers and more defined segments. Thus motions among segments can be well studied with this model.

The reference position in this study is different with previous studies [5, 6], in which the marker positions taken during the standing trial (static trial) is used. The selection of reference position is very important for the comparison of different

walking trials from different subjects. The reference position taken from static trial can be very helpful to reduce the intrinsic biological variation among subjects. However, different tested subjects have their own walking styles, which might be quite different with their standing postures taken during the static trial. In this study, the reference position is taken during the dynamic walking trial, defined as the markers and angular positions at the mid-stance time. The mid-stance time is the mid-time of the foot flat phase.

A simple comparison was made between Shank-Heel joint rotation angles in the sagittal plane calculated with these two references as shown in Figure 5.23. The two upper figures are obtained from static reference. Obvious off-set values still exist between different subjects' trials (Figure 5.23.a) and this leads to large standard deviation (Figure 5.23.b). The two bottom figures are obtained from our proposed dynamic reference. Data from all trials of all subjects are mixed together (Figure 5.23.c) and this indicates that the off-set values are well reduced among subjects. Thus the standard deviation is also largely reduced with proposed reference (Figure 5.23.d). The dynamic reference position performs better for reducing the variances among trials of different subjects. The variance is largely reduced. Thus in this study all angles are discussed referring to the dynamic reference position, position of the mid-stance time.

All the joint motions are calculated in three planes: sagittal, coronal and transverse planes. According to some previous studies [59] the joint rotation angles in the sagittal plane are mostly consistent and should be investigated with priority. In this study, some joint rotation angles in the coronal and transverse planes have more consistent angular patterns as shown in Table 5.3 and Table 5.4,. For example, the Heel-Mid motion has higher values of CMC or lower values of ASD in the coronal and transverse planes.

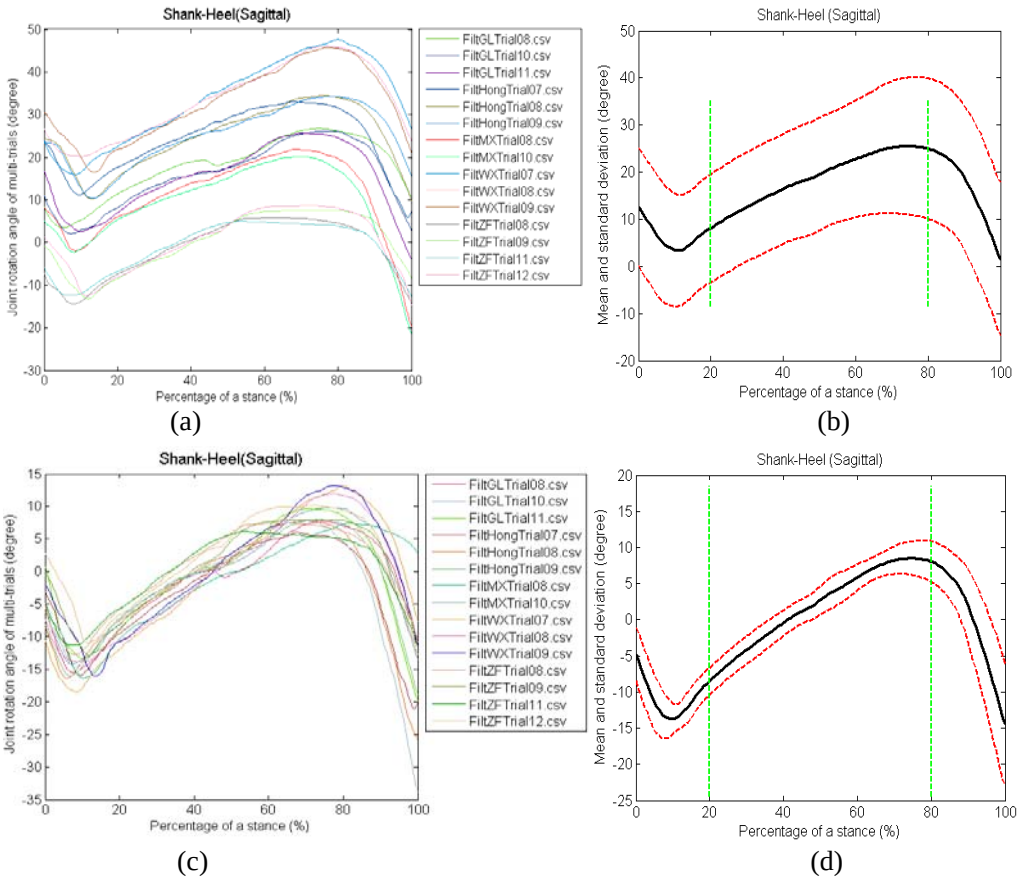

Figure 5.23: A comparison between Shank-Heel sagittal angle calculated with static and dynamic references (a) angles calculated with static reference (b) mean and STD calculated with static reference (c) angles calculated with dynamic reference (d) mean and STD calculated with dynamic reference

According to both Table 5.3 and Table 5.4, motions with good intra-subject repeatability are Shank-Foot motions in three planes, Shank-Heel motion in three planes, Heel-Mid motion in coronal and transverse planes, Mid-Met motion in coronal plane and Heel-Met motion in coronal and transverse planes. These motions all have higher averaged CMC values and relatively lower ASD values. In our study, the coronal plane motions have the best intra-subject repeatability, the repeatability between trials of one subject. While, not all of these motions have good inter-subject repeatability, that is the repeatability among trials from different subjects. For example, the Heel-Met motion in the coronal plane has high averaged CMC value at 0.9229, but quite low CMC value among all subjects at 0.7692. Thus motions with better

inter-subject repeatability are Shank-Foot motion, Shank-Heel motion, Heel-Mid motion in coronal and transverse planes and Heel-Met motion in the transverse plane. These motions have more consistent patterns among all trials of all tested subjects. More attentions could be focused on these motions since they are very consistent among tested subjects and can be treated as dynamic features for young healthy subjects' walking.

Most of the joint angles are showing similar patterns with results described in previous literature [5]. The Mid-Met and Heel-Met motions in the coronal and transverse planes are a bit different in our study. Since the Heel-Met motion can be regarded as the combination of Heel-Mid and Mid-Met motions. The greatest different angle pattern in these two studies is the Mid-Met motion. This might be due to the large intra- and inter- subject variation of the motion, and the small subject samples of our study. This also indicates that metatarsal segment motion has larger variance compared with the other segmental motions.

To fully extract foot motion features, this study focused on both foot segment joint rotation angles for the segment foot kinematic function, and functional angles for the whole foot kinematic function. The multi-segment foot models are well accepted methods for foot function evaluation, and this method shows the detailed foot joint motion in 3 planes. However, the segment definitions might need improvement to best describe foot kinematics. Thus new functional angles are proposed in this study as a compensation of joint rotation angles. Compared with the joint rotation angles, the functional angles proposed have advantages that they are not based on segments; thus fewer markers are needed for recording each functional angle. Further, the functional angles are more targeted on walking features. Functional angles have potential to represent walking features of a particular group of people such as the elderly people

for interested motions or foot functions. In this study, the functional angles provide good repetition; however, more subject samples are needed to verify these newly proposed functional angles.

Errors can come from maker positions and the repeatability of maker placement. Due to the limitation of the skin mounted method, surface markers cannot exactly present real bony structures of the foot, and thus it is another source of error. Cameras' position and resolution also bring small errors. According to a recent study, the largest errors come from marker positions; however according to discussions of the paper [79], the error is overall acceptable.

5.6 Summary

This study investigates kinematic behaviors of foot and ankle during normal walking. In this chapter, a relatively standard protocol is developed for the foot kinematics measurement and analysis. Foot motion features are identified and extracted from foot motion both for the segment foot kinematic function and the whole foot kinematic function. Foot segment motions are measured with a multi-segment foot model and regarded as motion features. Additionally new functional angles are proposed as foot motion features for the whole foot function.

A general framework of this chapter is shown in Figure 5.24. The joint rotation angle patterns are generally consistent with previous studies. Consistency and repetition of joint rotation angles are discussed according to ASD and CMC values. Sometimes angles in coronal and transverse planes present better intra-subject and inter-subject consistency than those in the sagittal plane. The proposed reference positions perform well for variance reduction among subjects. Additionally, functional angles are proposed for directly describing some foot mechanism during walking. The

functional angles are not based on segments and sagittal, coronal and transverse planes, and could be more flexible and intuitive for understanding foot mechanism.

In conclusion, the proposed method is a reasonable method to describe detailed foot kinematics with foot motion features for a group of people, here young healthy subjects. In order to test these extracted foot motion features for effectiveness of foot kinematic behavior characteristics, experiments on different walking conditions are needed and will be discussed in the next chapter.

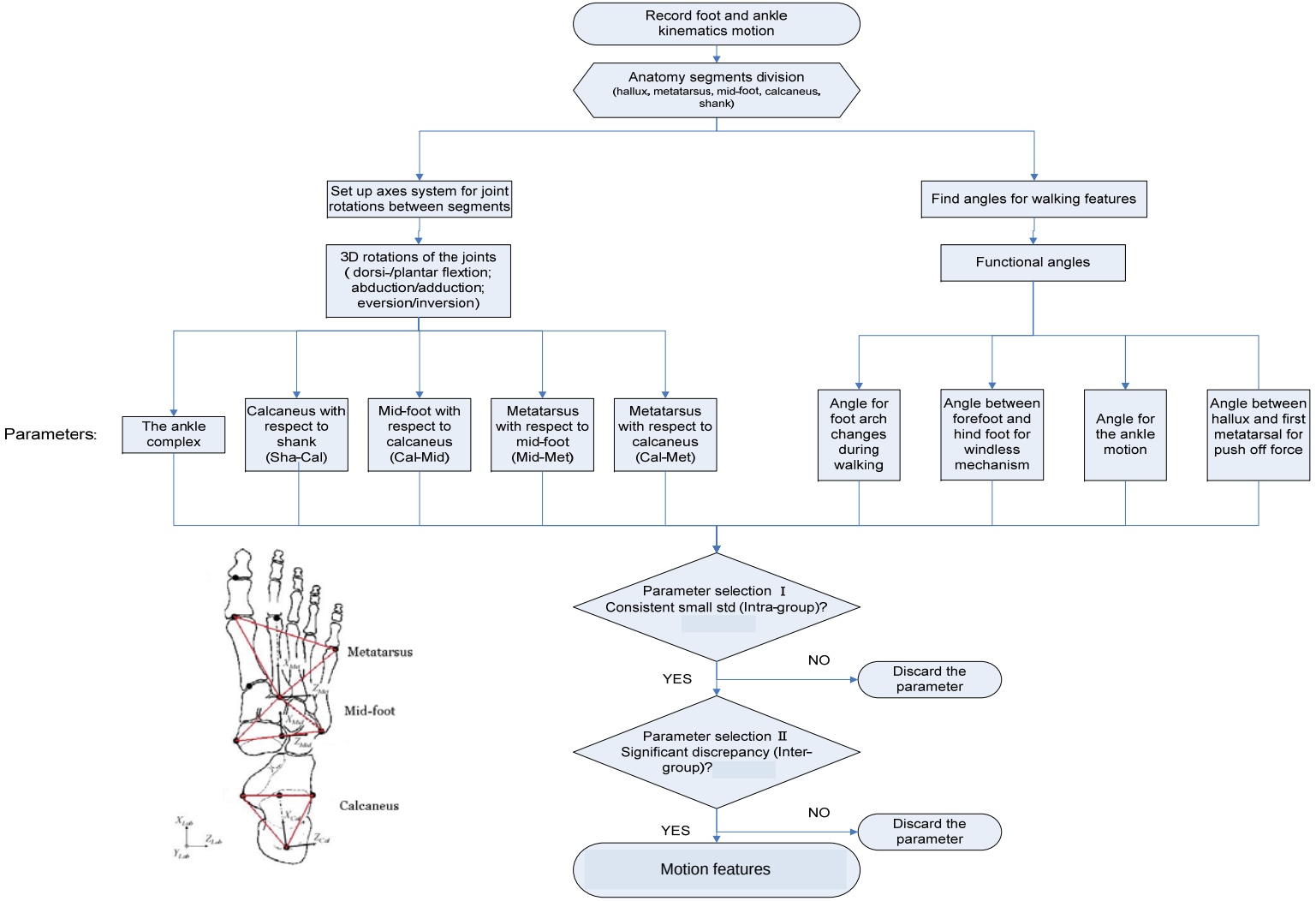

Figure 5.24: Details of the motion features extracted from 3D foot multi-segment motion

CHAPTER 6 APPLICATION OF FOOT MOTION FEATURES ON WALKING STABILITY DESCRIPTION

With the introduced method for foot motion features extraction in Chapter 5, the multi-segment foot joint angles and functional angles are extracted for describing foot and ankle kinematic behavior characteristics during walking. This chapter will apply these foot motion features to investigate the foot behavior during different walking conditions. Most of the previous studies focused on normal walking on the flat platform, and few studies have been conducted on the foot and ankle kinematic adaption to less stable walking conditions. This study aims to investigate detailed foot and ankle motion during stance phase with proposed motion features when subjected to less stable walking situations.

6.1 Introduction

It is necessary to evaluate walking stability to prevent possible falls and to check influence of some training programs for pre-disabled patients [34, 83, 84]. There is increasing evidence to show that foot and ankle characteristics may affect performance in balance and functional tests [82]. Significant differences in temporal parameters and sagittal plane ankle kinematics have been reported [83, 84]. Less stable walking tends to have lower speed, smaller toe clearance and smaller ankle dorsi/plantar-flexion. However, traditional gait analysis considers the foot as a single rigid body with no intrinsic motion [85, 86]. It is still unclear that how the segments of the foot (such as heel, metatarsals and mid-foot) function during less stable walking conditions. The single-rigid-body foot model does not provide sufficient information regarding the kinematic behavior of the foot. In addition, earlier research has shown that the foot

joints are susceptible to dysfunction and injury [58, 72, 87, 88]. Little is known about the adaption of intrinsic foot segment motion to less stable walking conditions.

Multi-segment foot models are increasingly utilized and shown in the increasing number of publications (more than 40 papers) [89]. Foot models are proposed dividing the foot into different segments [5, 6, 58-60, 72, 73, 77, 87, 88, 90], mostly separating the foot into hind-foot (heel), metatarsals, toes and sometimes mid-foot. Most of the previous studies worked on self-selected walking speed on normal walking situation. A few papers investigated detailed foot kinematics under certain conditions recently [62, 91, 92]. Kirsten [93] studied the effects of surface slope on multi-segment foot kinematics in healthy adults and found significant differences such as peak hind-foot plantar-flexion and sagittal plane range of motion (ROM). Pazit [94] compared foot kinematics in people with normal and flat arched feet. Greater peak fore-foot plantar-flexion, fore-foot abduction, decreased peak fore-foot adduction and a trend towards increased rear-foot eversion was notified. Foot multi-segment kinematics on cross-slope walking [95], anticipated medial cutting turns conditions [76] have also been investigated. Multi-segment foot models were applied on different applications, but not yet on the walking stability.

Through Chapter 5, foot motion features were extracted for walking behavior and foot function description. Since little is known about segmental adaptations essential to maintain both balance and forward locomotion. The purpose of this study is to apply the foot motion features, including foot intersegment rotational angles and functional angles, on walking stability indication, and to determine kinematic adaptations of the foot multi-segments to designed less stable walking conditions. Understanding of foot segment motions could help in the design of training programs, prostheses and walking aids [1, 96-98].

6.2 Experiment design

Different experiments are designed to provide less stable walking conditions, by changing walking environment. By reducing surface area during walking [31], walking on single beam and double beams are proposed as two walking conditions for an increased risk of falls and lower extremity injuries. Additionally, reduced muscular weaknesses, foot flexibility would obstruct gait competence and increase fall risk [95, 99]. By involving disturbance to muscle activities, dragging weights are added on subjects' ankles as another less stable walking condition. These three walking conditions will be compared with normal walking to obtain foot and ankle kinematic features that correlate with walking stability. Thus, totally the following four walking conditions are performed by each subject. In each condition, the subjects are to perform at least four trials.

1. Normal Walking: the subjects walk normally while data being recorded. The subjects walk at self-selected speed with barefoot.

2. Double Beam: subjects are to balance themselves and complete the trial by walking on two separate beams from one end to the other at their own desired speed with barefoot. By walking on a slightly elevated (40mm height) and reduced surface area (40mm width) path as shown in Figure 6.1, the walking might be less stable.

3. Single Beam: the subjects will walk on the "single" beam with barefoot. Due to the decreased base of support, the subject has to maintain its center of gravity while walking in an elevated straight line path as shown in Figure 6.2.

4. Dragging of Ankle Weights: subjects are tied with at least 2.45kg of weights at their ankle (the weights should give heavy feeling). They have to drag the weights from one end to the other end of the platform during the process of the motion capture as seen in Figure 6.3.

The subject will proceed to do trails of Normal Walking, following by Double Beam, Single Beam, and Dragging of weights. The weights attached will be adjusted according to stride strength of each subject. As different people will have different level of stride strength, weights will be increased if the subject has stronger strides. The motion data were collected from 10 young healthy subjects (6 males and 4 females ; average age 23.5 ±2.2 years; average weight 63.6 ±14.5 kg; average height 170 ±9.3 cm). Subjects walk at self-selected speed. Data are used for analysis.

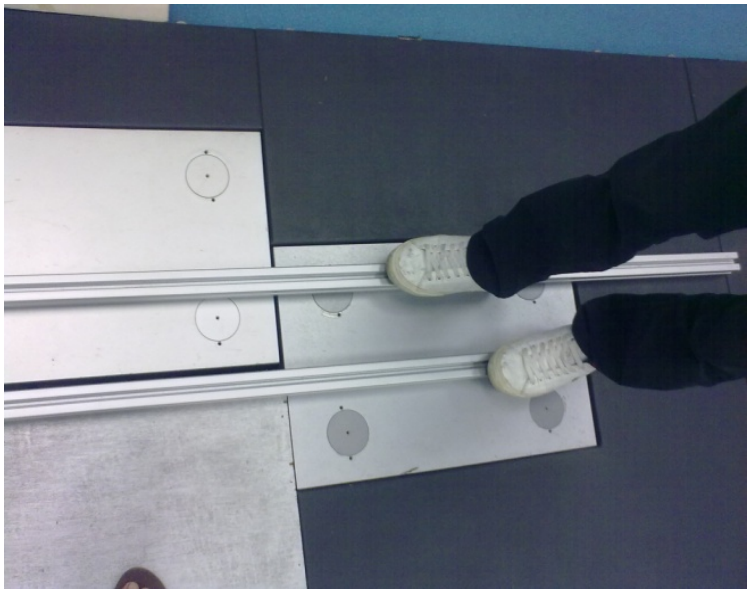

Figure 6.1: Double Beam condition

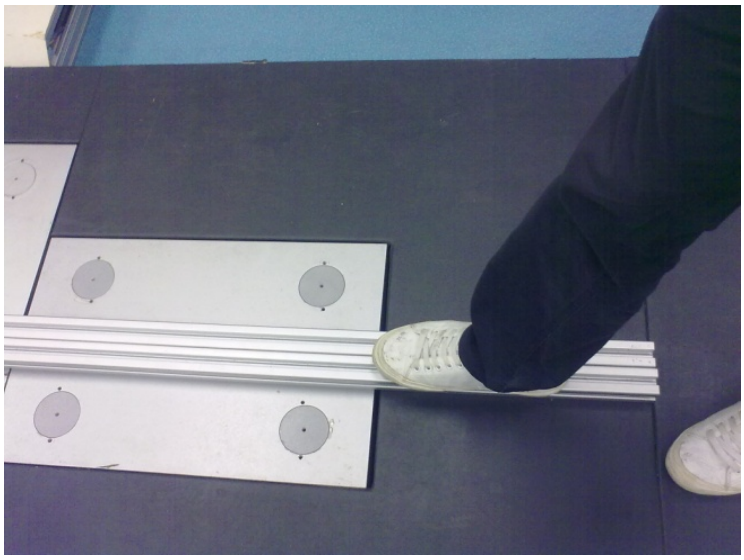

Figure 6.2: Single Beam condition

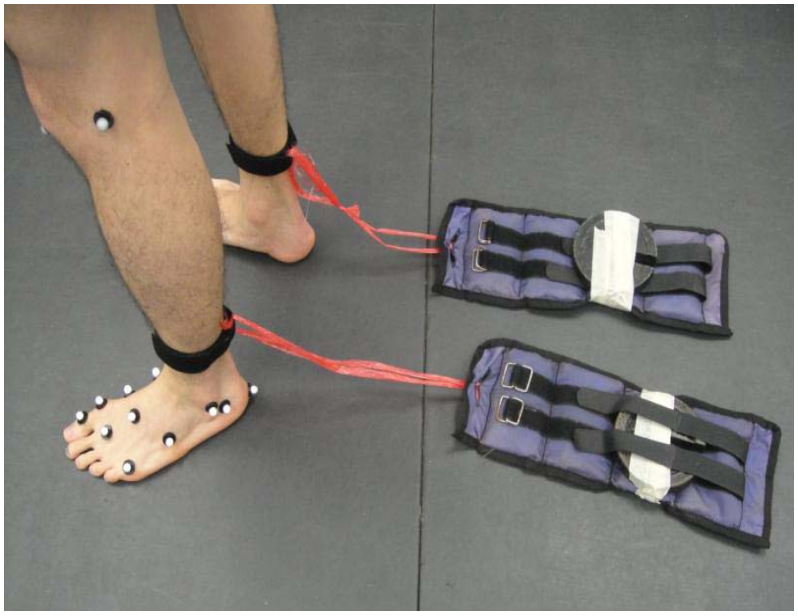

Figure 6.3: Dragging of Weights Condition

In this study, the multi-segment foot model used is the same as the one in Chapter 5 [5]. Detailed foot and ankle motions are captured with the multi-segment foot model, involving five rigid segments: shank, hind-foot (calcaneus/heel), mid-foot (tarsals: cuneiforms, navicular and cuboid), fore-foot (metatarsus) and the whole foot. The subjects will be attached with 16 spherical 9.5 mm diameter markers using double sided adhesive tapes. The markers are attached on the critical anatomical landmarks to assist in analyzing the multi-segmented foot. The main apparatus of the experiment consists of six Vicon cameras (Vicon MX13 Camera). The recording rate is set at 100 hertz which is not too little to pick up the markers and not too much which may record high level of noise. The captured volume is 2 m long, 1 m wide and 0.7 m high. Accuracy was estimated at around 0.6 mm on calibration residuals.

6.3 Data collection and analysis

6.3.1 Foot motion features

Foot motion features are calculated and analyzed based on data collected. The model can provide joint motions between shank and foot (Shank-Foot), shank and heel

(Shank-Heel), heel and mid-foot (Heel-Mid), mid-foot and metatarsal (Mid-Met), and heel and metatarsal (Heel-Met). Totally 15 joint rotation angles (JRAS) are calculated because each joint motion are presented by three joint rotation angles in sagittal, coronal and transverse planes respectively. Additionally, two functional angles are also calculated as complementation to represent specific physical functions of foot motion during walking: the foot arch changes and the push off feature during propulsive phase as shown in Figure 6.4.

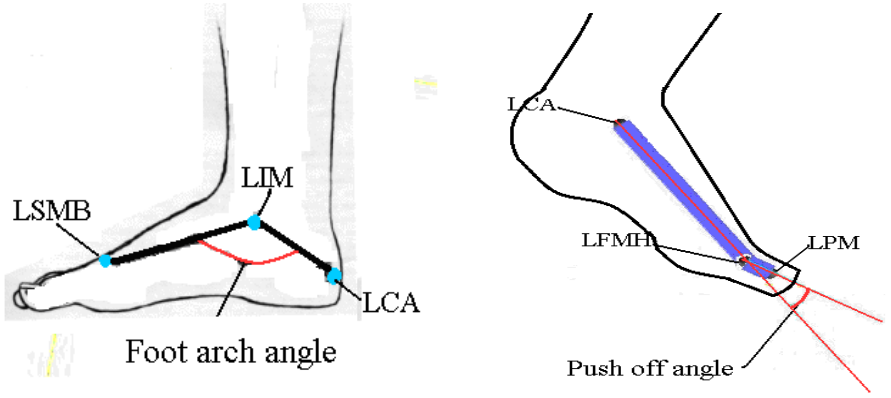

Figure 6.4: Arch angle (left) and push off angle (right)
LSMB: left 2nd metatarsal base; LCA: left central ridge of the calcaneus posterior surface marker; LIM: mid-point of the malleolus medial and lateral markers; LFMH: left foot first metatarsal head; LPM: left proximal phalanx marker of the hallux

6.3.2 Statistical analysis

The recorded motion data are calculated by Vicon software-"Bodybuilder", further processed by "MATLAB". All data were normalized in time through linear interpolation to 100% stance phase. The reference position for each trial is defined as the angle value of the mid-stance phase time during subjects' walking. The mid-stance time here is chosen as the mid-time of the time when both the hallux and calcaneus are contacting the ground, which is calculated according to the hallux marker and the calcaneus posterior surface marker.

For each walking condition (normal, single beam, double beam or ankle weights),

the angle patterns of all trials (30 trials: for each subject we choose at least 3 trials for analysis and 10 subjects are tested) are averaged point to point for visualization of the common features of the walking condition. For all trials of each walking condition, values on the same percentage of one stance time are averaged as the mean value of this time point and will be plotted to form an averaged angle pattern [5]. Comparison will be made between the normal walking and each less stable walking condition with T-test at different stance phase time and events: 3%, 10%, 20%, 50% 70%, 80%, 90% and 98% of stance. In every stance, 3% of the stance is considered at the initial contact (IC) phase. 10% of the stance is at the heel strike (HS) phase. 20% of the stance is at the foot flat (FF) phase. 50% of the stance is at the mid stance (MS) phase. 70% and 80% of the stance are at the heel off (HO) phase. 90% and 98% of the stance are at toe off (TO) phase. This average method will neutralize the peak values and smoother the angle patterns, and show the general trends.

For each walking trial, the Range of Motion (ROM), Maximum (and its time index i.e. when it reaches its max), Minimum (and its time index) and gradient value of the interested angles are also calculated [93]. Mean and standard deviation (STD) of these values (ROM, Max, etc.) for all trials are then calculated. Max Index and Min Index refers to the relative percentage of time (during stance phase) to reach the peak and minimum. This mean and STD values are obtained from the extreme values of each trial, thus this method is aiming to highlight the significant differences between walking conditions.

As this project deal with human walking, there will be a vast range of difference among individuals. The p-value will be used as the value that will show significant difference, seen in Figure 6.5. A p-value of 0.01(denoted by * significant difference) and 0.001 (denoted by ** i.e. very significant difference) will be used.

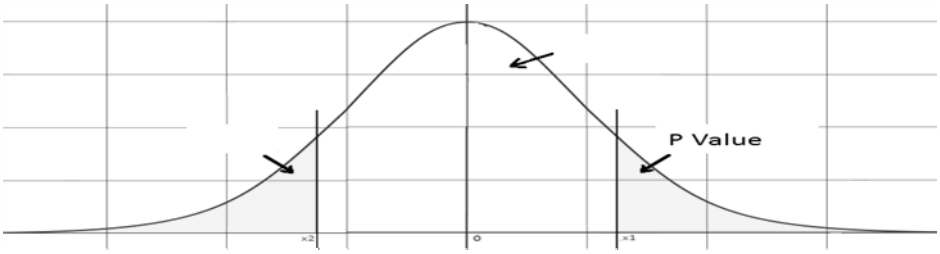

Figure 6.5: Typical T-test curve and P-value

As the T-test needs two groups of data, the values reflected from the data of each less stable walking condition are being compared with the normal walking (i.e. Normal Walking V.S. Double Beam) in order to find out significant differences between the two. The differences will be used to indicate the foot adaptations to less stable walking condition.

6.4 Results of motion features

According to previous study, angles larger than 4˚ and time differences longer than 5% of stance time are regarded as clinically significant [100]. When the p-value is smaller than 0.01, we mark it with (* i.e. significant difference), and when the p-value is smaller than 0.001, we mark it with (** i.e. very significant difference). The performance of different foot motion features, including functional angles and joint rotational angles, will be discussed.

6.4.1 Arch angle

Figure 6.6 shows the averaged angle pattern of the feature of arch change for the four walking conditions. Table 6.1 lists the change of arch angle with significant difference between normal walking and less stable walking conditions at the gait events. For less stable walking conditions, the foot arch is more contracted at heel strike (HS). This possibly indicates that the foot is more carefully controlled when

landing. The foot arch is less contracted at toe off (TO) and this may result in smaller push off force. However, most of the differences are smaller than 4˚.

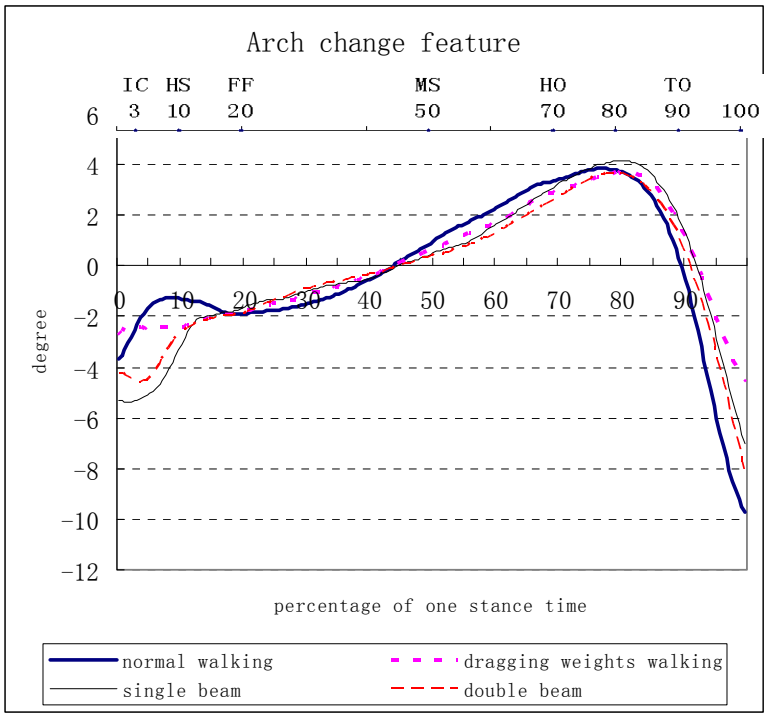

Figure 6.6: Arch change feature for four walking conditions (+,extension;-contraction). (Standard deviations are not shown to improve clarity)

Table 6.1: Comparison of averaged arch angle values at some gait events between normal walking and each less stable walking condition

	Arch angle			
	Normal	Double	Single	Dragging
	Mean (STD)	Mean (STD)	Mean (STD)	Mean (STD)
IC(3%)	-2.54 (3.77)	-4.55* (2.41)	-5.53** (3.28)	
HS(10%)	-1.28 (3.32)		-3.84* (2.3)	
MS(50%)	0.89 (0.74)	0.36* (0.64)	0.41* (0.53)	
98%	-9.72 (3.8)		-6.09* (4.81)	-4.61** (4.55)

IC: initial contact; HS: heel strike; MS: mid stance; HO: heel off; TO: toe off; When the p value is smaller than 0.01, it is marked with (*), and when the p value is smaller than 0.001, it is marked with (**).Value are in degrees

Table 6.2 shows the comparison of typical values for arch angle and push off angle between normal walking and each less stable walking condition; the Range of

Motion (ROM), Maximum and its time index (i.e. when it reaches its max), Minimum and its time index and gradient value of the interested angles. Angle changes with significant differences are listed. Compared with normal walking, there is about 3˚ significant decrease (** i.e. $p<0.001$, very significant difference) in the Range of Motion (ROM) for the double beam walking according to Table 6.2. In addition there is a delay of the time when the foot comes to be mostly extended (* i.e. $p<0.01$, significant difference). The single beam walking is just like the double beam condition, and there is a delay of the time when the foot comes to be mostly extended (* significant difference). This could mean that it took a longer time for one to transit to push off. This signifies that the arch angle maintains at the stance for a longer period during the single beam condition. For the walking with dragging weights, there is significant reduction of about 4˚ in ROM (* significant difference). The reduction is mainly due to decreased contraction at toe off (** very significant difference). Furthermore, the gradient of this angle pattern decreases as well. The angle pattern is smoother. As introduced in the statistical analysis section, values in Table 6.1 are averaged feature values among trials of all tested subjects, and would mild the angle pattern. Values in Table 6.2 contain extreme values compared among all trials of all tested subjects. Thus those values in Table 6.1 are relatively smaller than those in Table 6.2, which highlights the extreme values.

6.4.2 Push off angle

Figure 6.7 shows the averaged angle patterns of the push off feature for the four walking conditions. Table 6.3 lists the comparison of this angle pattern at some gait events between normal walking and each less stable walking condition. In this table, feature values at some gait events (e.g.: IC, HO and TO) of each less stable walking (totally three conditions) is compared with the feature values of normal walking, for

the push off feature. Mean and standard deviation of push off angle feature at some gait events that show significant differences are listed in the table (* i.e. $p<0.01$, significant difference; ** i.e. $p<0.001$, very significant difference). Push off angles decrease significantly at HS (Normal: 18.92˚; Double: 9.96˚; Dragging: 4.73˚), HO (80%, Normal: 12.52˚; Double: 4.7˚; Single: 5.05˚; Dragging: 8.41˚) and TO (98%, Normal: 46.24˚; Single: 23.29˚; Dragging: 34.79˚). There are less relative motions between hallux and metatarsals. The foot is more rigid and flat during less stable walking. It is very obvious that the power used for push off decreases from normal walking to less stable walking conditions. The ROM differences of push off angle between normal walking and each less stable walking conditions are larger than 4˚.

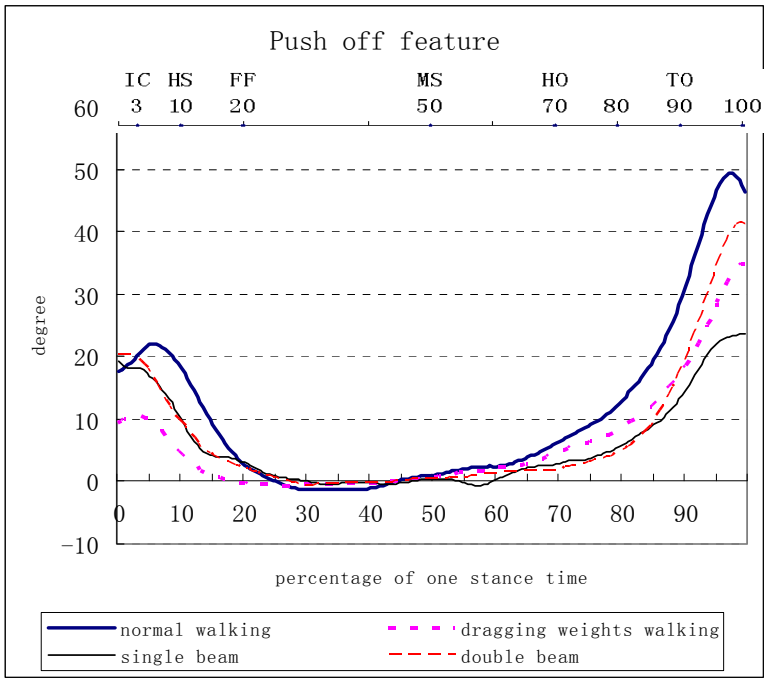

Figure 6.7: Averaged push off feature for four walking conditions

From Table 6.2, the push off feature, ROM decreases 13˚ (*) and the maximum value of the push off angle decreases 12˚ for the double beam walking,. For single beam walking, there is also a significant decrease in ROM (around 25˚ **) and the maximum push off angle also significantly decreased (from 59.13˚ to 34.57˚, around 24.5˚ **). For walking with dragging weights, there is a dramatic decrease (around 23˚

**) in ROM and the maximum push off angle is largely decreased (**) as well.

Table 6.2: Comparison of typical values between normal walking and each less stable walking condition for arch angle and push off angle

		Normal Mean (STD)	Double Mean (STD)	Single Mean (STD)	Dragging Mean (STD)
Arch Angle	**ROM(˚)**	15.45 (4.02)	12.40** (3.04)		9.83** (2.33)
	Max Index (of one stance time)	0.62 (0.28)	0.78* (0.12)	0.77* (0.13)	
	Min(˚)	-10.24 (3.67)			-5.35** (2.74)
	Gradient	1.27 (0.74)			0.86* (0.42)
Push Off Angle	**ROM(˚)**	67.12 (16.9)	54.12* (20.2)	42.32** (18.48)	42.24** (15.44)
	Max(˚)	59.13 (15.6)	47.60** (15.08)	34.57** (16.56)	36.60** (14.65)
	Gradient	6.41 (2.42)		4.81* (2.93)	4.45* (2.59)

Table 6.3: Comparison of averaged push off angle values at some gait events between normal walking and less stable walking conditions

	Push off angle			
	Normal Mean (STD)	Double Mean (STD)	Single Mean (STD)	Dragging Mean (STD)
IC(3%)	19.59 (17.84)			10.28* (10.96)
HS(10%)	18.92 (19.05)	9.96* (16.2)		4.73** (7.85)
HO(70%)	6.02 (3.68)		2.61* (5.6)	
80%	12.53 (5.54)	4.7* (8.09)	5.05* (7.1)	8.41* (6.71)
TO(90%)	29.68 (11.41)		13.22** (11.71)	17.84** (9.89)
98%	46.24 (18.48)		23.29** (18.96)	34.79* (16.2)

Gait events: IC: initial contact; HS: heel strike; MS: mid stance; HO: heel off; TO: toe off; When the p value is smaller than 0.01, it is marked with (*), and when the p value is smaller than 0.001, it is marked with (**).Value are in degrees

The results show that the ROM of push off angle has been significantly reduced during all less stable walking conditions. It clearly depicts that less effort is put to generate push off power, probably means less power in transition to swing phase. This could also indicate that subjects might be more focused on keeping their walk steady.

6.4.3 Shank-foot (foot motion relative to the shank)

Figure 6.8 shows the averaged shank-foot angle pattern of the four walking conditions. Table 6.4 lists the angles with significant difference between normal walking and less stable walking conditions at some gait events. In this table, feature values at some gait events (e.g.: IC, HO and TO) of each less stable walking (totally three conditions) is compared with the feature values of normal walking, for the shank-foot and shank-heel features in the sagittal, coronal and transverse planes. Mean and standard deviation of motion features at some gait events that show significant differences are listed in the table (* i.e. $p<0.01$, significant difference; ** i.e. $p<0.001$, very significant difference). From the table, it could be noticed that the sagittal plane angle decreases significantly from stable to less stable walking conditions at TO (98%).

Table 6.5 shows the comparison of typical values between normal walking and each of the three less stable walking condition. For double beam walking, the sagittal dorsi/plantar-flexion ROM significantly decreases (* significant difference) and the decrease mainly due to the reduced plantar-flexion (**) at toe off (TO). In addition, there is an around 6% stance time delay (**) in reaching the maximum dorsi-flexion. This indicates that the foot is more flat off the ground. In the coronal plane, the foot is significantly less inverted (*) during heel strike (HS) and toe off (TO). The reduced motion in the coronal plane signifies the more rigid and controlled foot. Smaller foot contact surface during walking may lead to the foot less supinated at toe off.

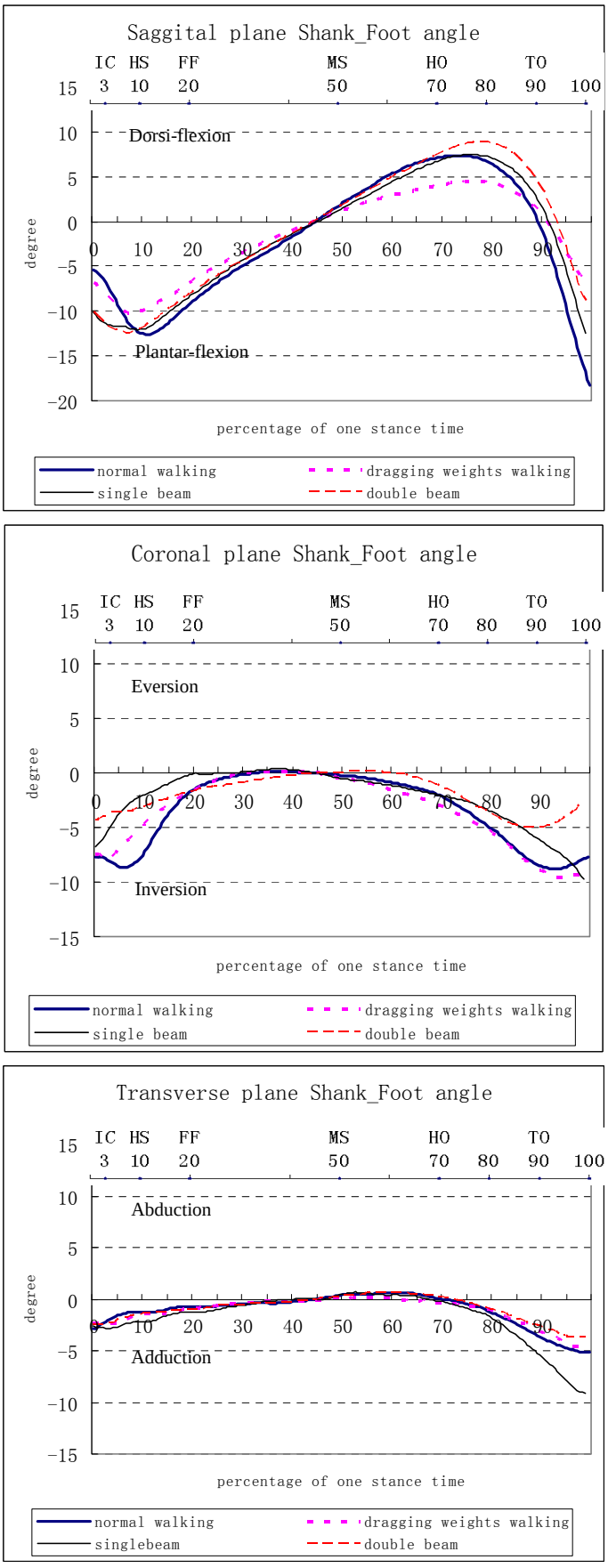

Figure 6.8: Averaged shank-foot angles in sagittal, coronal and transverse planes for four walking conditions

Table 6.4: Comparison of typical values between normal walking and each less stable walking condition for shank-foot angle and shank-heel angle

	Shank-foot(Sagittal)				Shank-foot(Coronal)				Shank-foot(Transverse)			
	Normal	**Double**	**Single**	**Dragging**	**Normal**	**Double**	**Single**	**Dragging**	**Normal**	**Double**	**Single**	**Dragging**
	Mean (STD)	Mean (STD)	Mean (STD)	Mean (STD)	Mean (STD)	Mean (STD)	Mean (STD)	Mean (STD)	Mean (STD)	Mean (STD)	Mean (STD)	Mean (STD)
IC(3%)	-6.75 (3.42)	-10.89** (4.41)	-10.99* (5.26)									
HS(10%)	-12.42 (3.51)			-10.02** (2.32)	-7.51 (4.33)	9.96* (16.2)	-2.28** (4.5)	-4.93* (2.79)				
FF(20%)	-9.12 (2.55)			-6.77** (1.6)	-1.63) (2.33)	-3.27** (4.43)						
MS(50%)	1.89 (0.89)		1.05* (1.12)	1.11* (0.98)								
HO(70%)	7.17 (2.52)			4.06** (2.57)								
80%	6.49 (2.91)			4.36** (3.67)								
TO(90%)	-0.5 (4.62)	4.76* (5.95)	2.92* (4.97)		-8.45 (2.88)	-5.11** (3.48)	-5.82* (4.24)		-3.67 (1.66)	-2.56* (2.13)	-5.04* (3.03)	
98%	-18.33 (6.21)	-8.85** (8.17)	-12.43* (8.18)	-7.47** (7.3)	-8.1 (4.5)	-3.63** (5.26)			-5.07 (2.91)		-8.66** (3.29)	
	Shank-heel(Sagittal)				**Shank-heel(Coronal)**				**Shank-heel(Transverse)**			
HS(10%)	-13.61 (4.33)		-11.14* (3.11)	-10.23** (3.07)	-2.1 (1.71)			-0.98* (1.06)				
FF(20%)	-9.68 (3.43)			-6.78** (2.56)	-1.46 (1.06)	-0.89** (1.09)		-0.59** (0.91)				
MS(50%)	1.92 (1.09)		0.99* (1.25)		0.29 (0.49)		-0.13* (0.5)					
HO(70%)	6.97 (3.33)			3.86** (2.96)								
80%	6.44 (3.82)			4.05** (4.18)								
TO(90%)					-2.01 (1.48)			-0.89* (1.83)				
98%	-9.95 (6.13)	-2.63** (7.49)	-5.40* (7.29)	-3.73** (6.5)	-4.55 (2.45)	-2.56** (2.05)		-2.17** (2.54)				

Gait events: IC: initial contact; HS: heel strike; MS: mid stance; HO: heel off; TO: toe off; When the p value is smaller than 0.01, it is marked with (*), and when the p value is smaller than 0.001, it is marked with (**).Value are in degrees

For the single beam walking, the sagittal dorsi/plantar-flexion ROM is reduced (*), and the maximum dorsi-flexion is delayed (**). This depicts the late transition

from foot flat to toe off, this may also be one reason of the smaller push off power. In the transverse plane, the ROM has significant increased (**). The increase is largely the result of higher adduction/supination (**) at toe off. This phenomenon is typically observed for single beam walking condition; the foot has to be more adducted contacting the narrower base of support to provide the push off force.

For dragging with ankle weights walking, there is about 10˚ decrease in ROM (**) of sagittal dorsi/plantar-flexion and a decline of more than 3˚ in maximum dorsi-flexion. The decrease of ROM is also mainly due to the decrease of plantar-flexion (around 7˚ **) during toe off. The smaller range of motion of dorsi/plantar could suggest that the ankle rotation is more controlled and rigid throughout the stance for stabilizing.

6.4.4 Shank-heel (heel motion relative to the shank)

According to Figure 6.8 and Figure 6.9, the sagittal plane shank-heel angle patterns are similar with shank-foot ones in the three less stable walking conditions, especially for the sagittal plane angles. This indicates that the heel plays a key role for the shank-foot sagittal plane motion. In Tables 6.4 and 6.5, Shank-heel sagittal plane ROMs are smaller and are mainly due to smaller plantar-flexion at toe off (e.g.: TO 98%). This signifies that the foot is more controlled and flat during heel strike and toe off. The heel is generally less inverted/supinated during toe off at less stable walking conditions. The shank-heel transverse plane motions are small.

For the double beam walking, the sagittal plane angle has similar pattern with the shank-foot one. The plantar-flexion decreases at heel strike and toe off; the heel strike is also more conservative. In the coronal plane, the ROM decreases significantly, but less than 4˚ as shown in Table 6.5. Heel is less inverted (*) at toe off, which may partly contributes to smaller push off force. The ROM of shank-heel transverse plane motion

decreases, which may be due to the smaller base of support.

Table 6.5: Comparison of typical joint motion values between normal walking and each less stable walking condition

		Normal	Double	Single	Dragging			Normal	Double	Single	Dragging
		Mean (STD)	Mean (STD)	Mean (STD)	Mean (STD)			Mean (STD)	Mean (STD)	Mean (STD)	Mean (STD)
Shank-foot (Sagittal)	**ROM(˚)**	27.92 (4.78)	24.81* (4)	25.24* (4.42)	17.34** (3.28)	**Heel-mid (Sagittal)**	**ROM(˚)**	19.04 (6.97)	13.71* (3.65)		11.97** (5.35)
	Max(˚)	8.49 (3.49)			5.11** (3.09)		Min(˚)	-13.54 (5.81)			-7.81** (5.48)
	Max Index (of one stance time)	0.73 (0.036)	0.79* (0.054)	0.77** (0.058)		Heel-mid (Transverse)	ROM(˚)	10.18 (3.72)			6.59** (3.03)
							Max(˚)	4.75 (3.72)		2.94 (2.73)	
	Min(˚)	-19.42 (4.63)	-15.09** (3.63)		-12.23** (3.07)		Min(˚)	-5.42 (3.45)			-3.01** (2.34)
Shank-foot (Coronal)	Min(˚)	-12.065 (3.73)	-8.49* (4.95)			Mid-Met (Sagittal)	ROM(˚)	11.22 (7)			6.91* (4.48)
Shank-foot (Transverse)	ROM(˚)	8.39 (2.79)		11.80** (3.1)			Min(˚)	-7.35 (5.91)			-3.89* (3.72)
	Min(˚)	-6.63 (2.59)		-9.80** (2.83)							
						Mid-Met (Coronal)	Max(˚)	3.34 (2.43)			1.50** (1.39)
Shank-heel (Sagittal)	**ROM(˚)**	26.277 (6.34)		22.89 (6.05)	18.28** (4.56)	**Heel-Met (Sagittal)**	**ROM(˚)**	20.7 (6.87)	15.64* (6.47)	15.56** (6.08)	14.10** (5.54)
	Max Index (of one stance time)	0.72 (0.051)	0.77 (0.072)	0.77* (0.075)			**Min(˚)**	-15.68 (6.15)		-10.77** (3.71)	-9.60** (5.84)
	Min(˚)	-17.676 (3.97)	-13.95* (3.9)		-12.20** (3.57)	**Heel-Met (Transverse)**	ROM(˚)	13.85 (3.82)			9.67** (2.83)
Shank-heel (Coronal)	**ROM(˚)**	7.12 (2.56)	4.86** (1.4)		4.69** (1.58)		**Max(˚)**	7.6 (4.13)		4.84* (3.55)	
	Min(˚)	-5.84 (2.71)	-3.65** (1.36)		-3.51** (1.76)		**Min(˚)**	-6.25 (3.54)		-8.57* (4.62)	-2.80** (2.18)
Shank-heel (Transverse)	**ROM(˚)**	9.565 (4.61)	6.49** (2.67)	6.85* (2.16)	6.56* (2.88)	**Stance**	**Time(s)**	0.77	0.92	0.94	1.03**

When the p value is smaller than 0.01, it is marked with (*), and when the p value is smaller than 0.001, it is marked with (**). The ROM, Maximum and Minimum value are in degrees; Maximum index and Minimum index are in percentage of one stance time. Angle features that have significant differences in more than (including) two conditions are bolded.

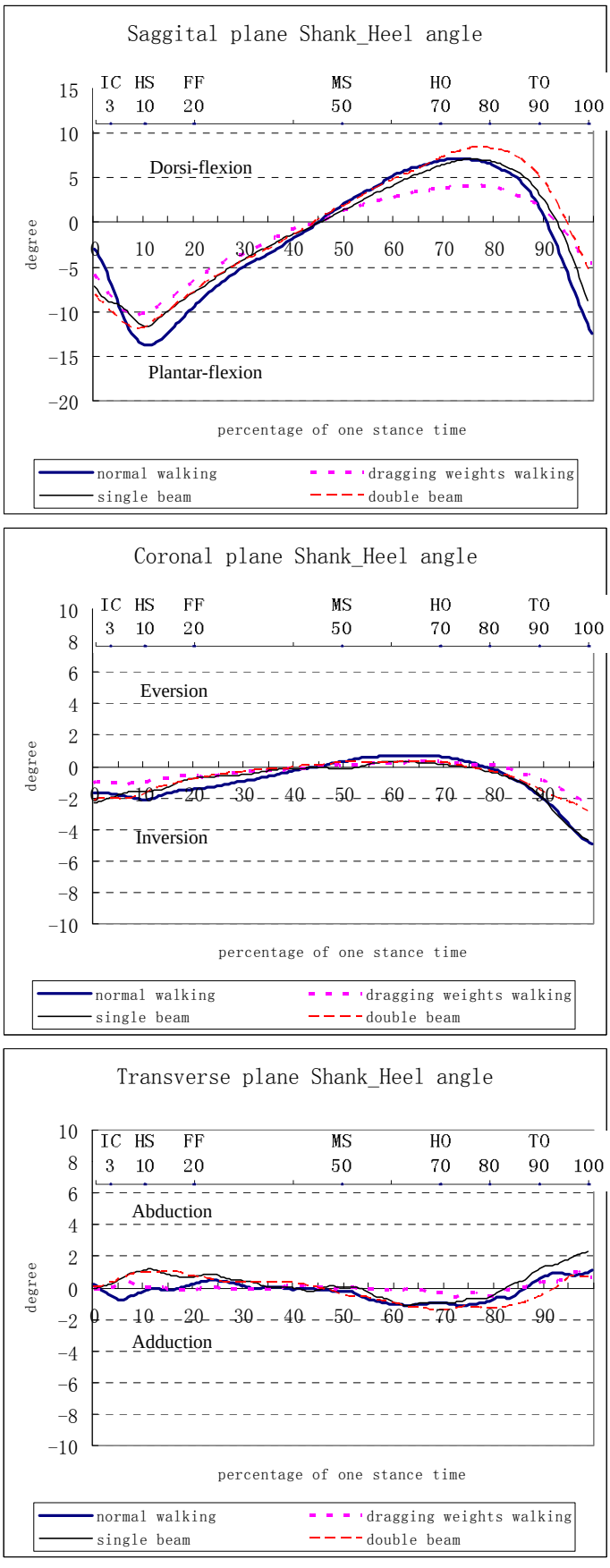

Figure 6.9: Averaged shank-heel angles in sagittal, coronal and transverse planes for four walking conditions

For single beam walking, shank-heel motions in sagittal plane also show similar patterns and significant differences as the shank-foot ones. There is a time delay (*) of reaching maximum dorsi-flexion. This indicates a longer foot flat phase and a shorter toe off phase. According to Table 6.5, the shank-heel transverse plane ROM also decreases (*).

For walking with dragging weights, sagittal plane ROM reduces (**) and is mainly due to decreased plantar-flexion (**). The ROM of shank-heel angle in coronal and transverse plane also decreases (*). Foot is less inverted and adducted at toe off. These two motions mean that the foot is less supinated at toe off and will result in smaller push off power. The smaller supination may be a conservative strategy for stabilizing.

6.4.5 Heel-mid (Mid-foot motion relative to the heel)

Figure 6.10 presents the averaged heel-mid angle pattern of the four walking conditions. Table 6.6 lists the angles with significant difference between normal and each less stable walking condition at the gait events. Sagittal plane heel-mid angle is less plantar-flexed at toe off (TO:98%). From Table 6.5, for double beam walking, sagittal plane ROM is decreased (*). There is more plantar-flexion when landing and less plantar-flexed at toe off. In the coronal plane, there is less inversion at toe off. In the transverse plane, motions do not show significant differences as seen in Table 6.5, 6.6 and Figure 6.10.

For single beam walking, the ROM in the sagittal plane is smaller. In the transverse plane, the maximum abduction decreases for around 2˚ and the inversion at toe off increases. This may due to the narrower contacting surface that constrains the coronal and transverse plane motions.

For walking with dragging weights, there is smaller peak plantar-flexion (** very

significant difference) which largely contributes to the reduction of the sagittal plane ROM (**). Furthermore, the transverse plane ROM is decreased (**) as well. There is less adduction during heel strike and toe off (TO). The foot seems to be maintaining the neutral position in the transverse plane.

Table 6.6: Comparison of typical values between normal walking and each less stable walking condition for heel-mid angle, mid-met angle and heel-met angle

	Normal	Double	Single	Dragging	Normal	Double	Single	Dragging	Normal	Double	Single	Dragging
	Mean (STD)	Mean (STD)	Mean (STD)	Mean (STD)	Mean (STD)	Mean (STD)	Mean (STD)	Mean (STD)	Mean (STD)	Mean (STD)	Mean (STD)	Mean (STD)
		Heel-mid(Sagittal)				**Heel-mid(Coronal)**				**Heel-mid(Transverse)**		
IC(3%)	-2.64 (4.5)	-5.05* (3.84)	-6.99** (2.68)									
HS(10%)	0.57 (4.38)	-2.15* (2.98)	-3.44** (2.66)		-3.78 (1.92)	-2.47* (2.43)			-1.24 (3.14)			0.34** (2.28)
FF(20%)					-0.71 (1.51)	-1.56* (1.91)						
80%									-0.75 (2.7)			0.95** (1.78)
98%	-10.96 (4.8)	-7.64* (4.91)	-7.55* (5.39)	-5.91** (5.54)	-5.67 (3.12)	-2.56** (2.05)	-8.06** (2.96)		-2.46 (5.2)			0.26* (3.06)
		Mid-met(Sagittal)				**Mid-met(Coronal)**				**Mid-met(Transverse)**		
IC(3%)					-4.07 (4.16)	-1.21** (4.21)			2.86 (5.36)	-1.21** (4.21)		
HS(10%)					-0.48 (1.84)	-0.82** (2.74)	-0.33** (3.16)		1.9 (3.33)	-0.82** (2.74)		
HO(70%)					-0.82 (1.38)	0.15* (1.16)			-1.0 (1.42)	0.15* (1.16)		
80%					-1.88 (1.5)	0.29** (1.65)	-0.73* (1.73)		-0.60 (1.82)		-2.15** (1.51)	
TO(90%)					-1.66 (1.8)	0.68** (1.85)			0.11 (2.47)		-2.62** (2.03)	
98%					0.94 (2.56)			-1.82** (3.65)	2.93 (3.24)	-0.18* (3.54)	-2.56** (4.16)	-0.05* (3.01)
		Heel-met(Sagittal)				**Heel-met(Coronal)**				**Heel-met(Transverse)**		
HS(10%)	-0.98 (3.96)		-4.03* (3.8)		-4.30 (3.66)		-0.32** (4.44)	-2.58* (3.33)				
TO(90%)	-2.03 (3.8)			-0.08* (3.3)					-0.46 (4.5)	-2.56* (2.13)	-5.04* (3.03)	2.49* (3.78)
98%	-11.08 (4.06)	-7.21** (4.02)	-6.74** (5.11)	-5.63** (4.11)	-3.08 (5.34)		-10.42** (6.76)		-3.45 (4.85)		-8.66** (3.29)	0.93** (4.94)

Gate events: IC: initial contact; HS: heel strike; MS: mid stance; HO: heel off; TO: toe off; When the p value is smaller than 0.01, it is marked with (*), and when the p value is smaller than 0.001, it is marked with (**).Value are in degrees.

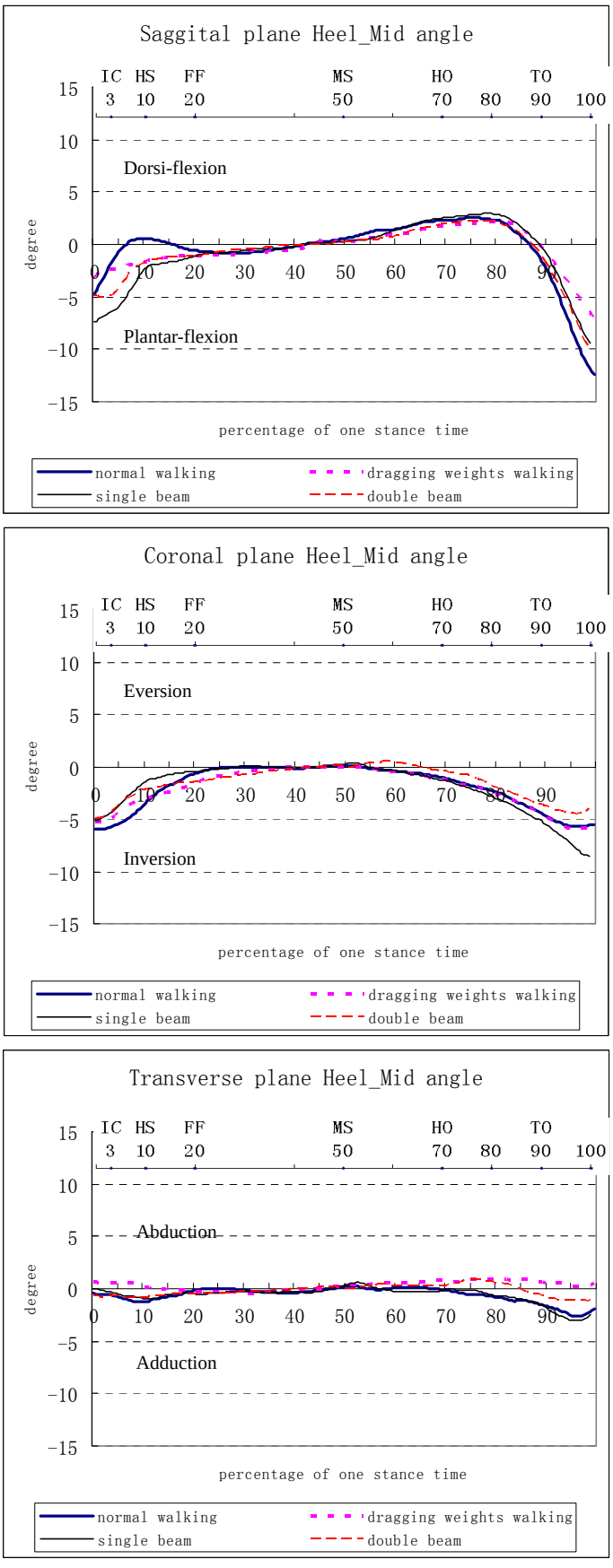

Figure 6.10: Averaged heel-midfoot angles in sagittal, coronal and transverse planes for four walking conditions

6.4.6 Mid-met (Metatarsal motion relative to the mid-foot)

In Figure 6.11, the averaged mid-met join motions have relatively small ROM in all sagittal, coronal and transverse planes. For both single beam walking and double beam walking, the data does not show significant differences as shown in Figure 6.11 and Table 6.5. Values in Table 6.6 are all very small and do not have clinically significance (<4˚). This shows that the mid-met motions are relatively small. This may also indicate that the mid-met do little in assisting the adaptation for single and double beam walking situations.

For walking with ankle weights, there is a reduction in sagittal plane ROM (*) while this decrease is mainly due to the smaller peak plantar-flexion. As for the coronal plane, the metatarsal is less everted at toe off (**). Compared with hind-foot changes, the fore-foot has relatively mild changes, subjected to less stable walking conditions.

6.4.7 Heel-Met (Metatarsal motion relative to the heel)

From Figure 6.12, Table 6.5 and 6.6, there is less plantar-flexion (**) at toe off (TO: 98%). Heel-met motion is the combined motions of heel-mid and mid-met. Because no significant differences are shown in mid-met sagittal plane motion, heel-mid may mainly contribute to the reduced sagittal plane ROM of heel-met.

For double beam walking, the dorsi/plantar-flexion ROM in the sagittal plane decreases (*). For single beam walking, ROM decreases in the sagittal plane (**), which is largely due to decreased plantar-flexion (**) at toe off (TO). Compared with the double beam walking, single beam walking shows more significant differences and may need more fore-foot function for stabilizing. In the transverse plane, abduction decreased at heel strike (*) and adduction increased at toe off (*). This phenomenon is in accordance with the single beam condition when the tested subject is trying to

follow the beam track.

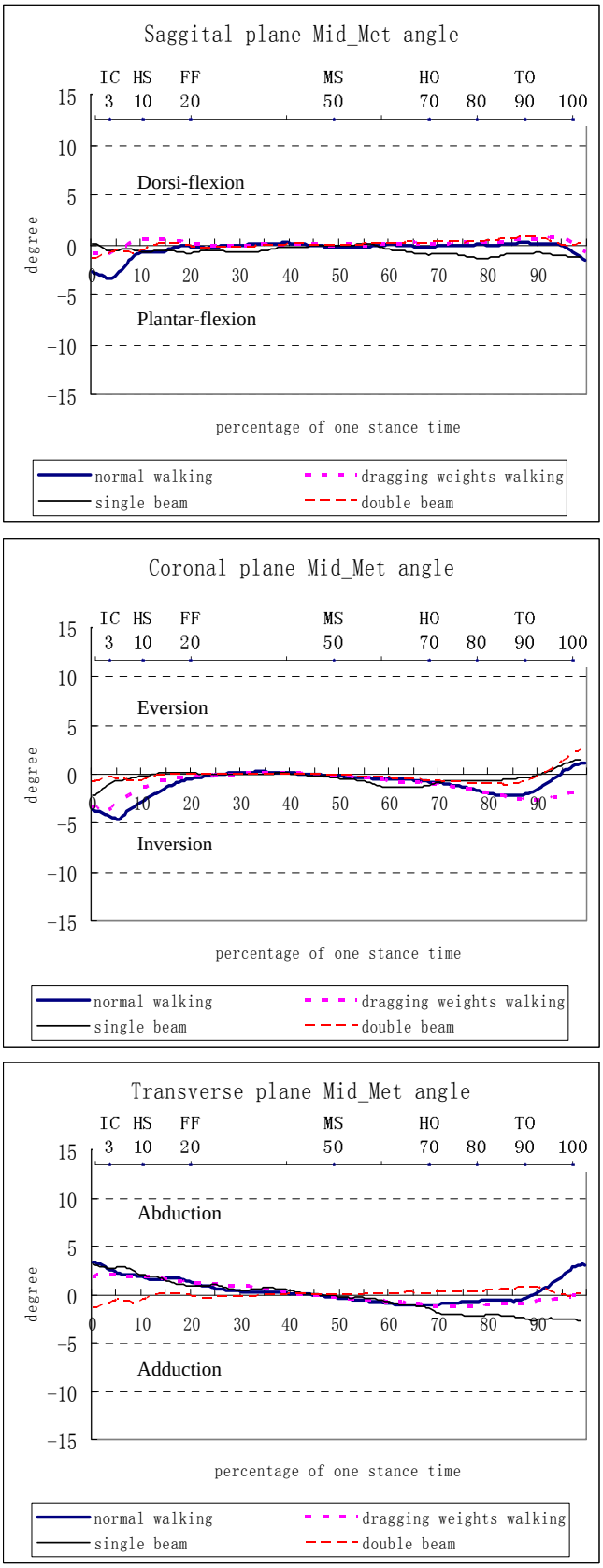

Figure 6.11: Averaged midfoot-metatarsal angles in sagittal, coronal and transverse planes for four walking conditions

For walking with dragging weights, the sagittal plane angle shows similar changes (**) as in the single beam walking, but with more significant changes, seen from Table 6.5, 6.6 and Figure 6.12. In the transverse plane, the ROM decreases significantly (**) and this is mostly caused by decreased adduction at toe off. This could result in smaller supination and reduced push off power.

6.4.8 Stance duration and toe clearance

In addition by looking at the stance duration, the normal walking takes around 0.77s. There are increases in the stance time for double (0.99s), single beam walking conditions (0.94s **) and walking with dragging weights condition (1.03s **). This phenomenon is in accordance with previous studies [80, 101], and less stable walking tends to be slower. It could be due to the need of more time to stabilize the foot before toe off and get ready to transit to swing phase. By longer contacting the ground, subjects could better control their center of gravity.

In addition, for walking with dragging weights, toe clearance (toe clearance from the floor during swing) is also calculated. The maximum toe clearance decreases from 46.97mm for normal walking to 29.82mm for walking with dragging weights, with a t-test value of 0.0021 (*). The significant reduction depicts a “flat-footed” landing and toe off. The Push off angle also features a lower power generated for toe off and could probably suggest small toe clearance during swing phase.

6.5 Discussion of motion features

In this study, foot motion features are applied on walking stability indication. Previous studies involving multi-segment foot models mostly focused on the foot function during normal walking on the flat platform [5, 6, 59, 76, 91]. Multi-segment

foot model is innovatively applied here for investigating how foot segments function when subjected to certain less stable conditions.

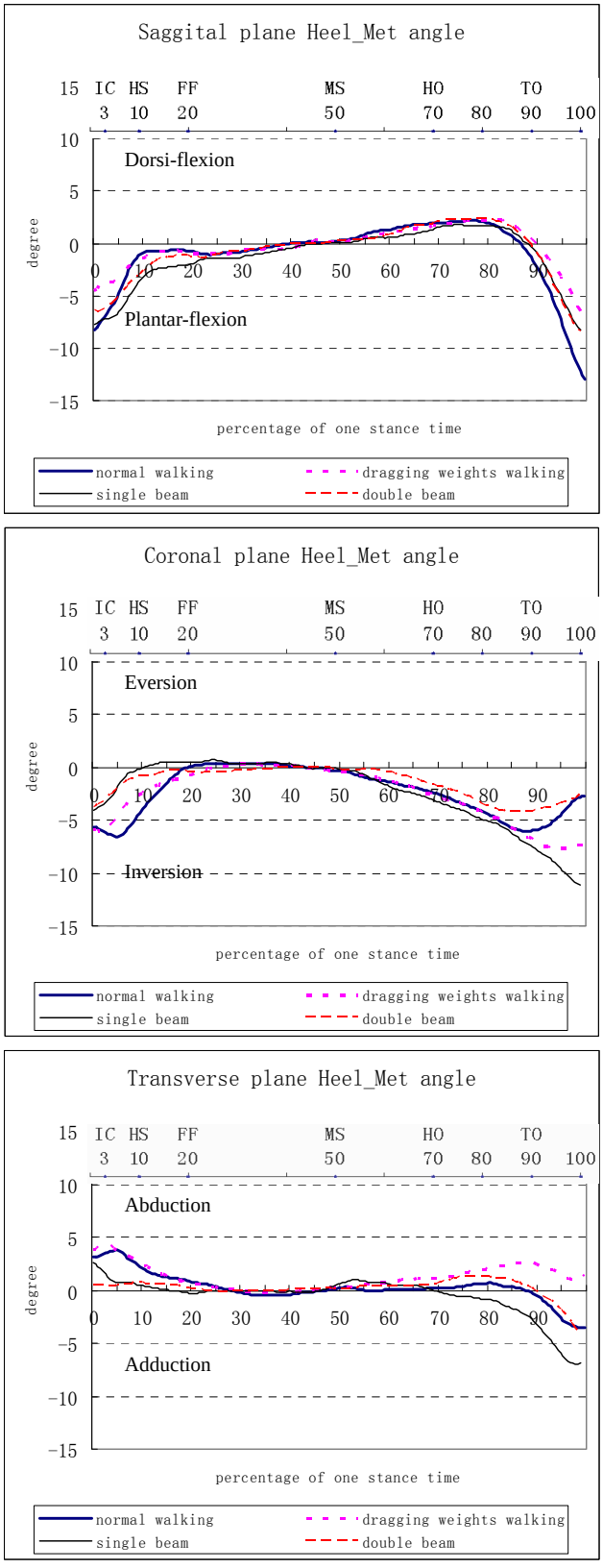

Figure 6.12: Averaged heel-metatarsal angles in sagittal, coronal and transverse planes for four walking conditions

Different experiments are designed to provide less stable walking conditions by involving the reduced base of support, foot flexibility, and muscular weaknesses using single beam, double beam and walking with dragging weights. Leardini's multi-segment foot model is applied here to examine inter-segment foot function in normal and less stable walking conditions. Further, two other functional angles, stance time and toe clearance are also calculated as complementary features. T-test is used to find significant difference between normal walking and each less stable walking condition. In general, the normal walking foot motions observed in our study are consistent with the previous study [5]. In addition, our results reveal significant differences in these motion feature patterns between the normal walking and less stable walking.

The most obvious phenomenon appears in the features of push off angle and the ROM of the shank-foot sagittal plane angle. When subjected to less stable conditions, the push off power reduces significantly and the ROM of shank-foot dorsi/plantar-flexion also decreases. The reduced push off power could be clearly reflected from decreased push off angle ROM and peak angles, thus the push off feature is one of the most obvious features for walking stability estimation. These results agree with a recent study [82], they concluded that foot plantar-flexor strength of the hallux is important determinants of balance.

The shank-foot motion is the result of combined function of the shank, heel, mid-foot and metatarsals. There is significant decrease (more than 4˚) in ROM of heel-met and heel-mid in the sagittal plane for designed less stable walking conditions. These motions were not reported before. It could be deduced that the hind-foot may slightly more occupy in stabilizing the foot, because it has more significant changes than the fore-foot, in Table 6.5. Additionally, the reduced sagittal plane ROM is

mainly due to decreased peak plantar-flexion at toe off. The companying phenomenon is that foot is more flat to maximize plantar foot surface contact. This also leads to smaller push off force.

Another noticeable phenomenon is the time delay of the peak dorsi-flexion. This delay also provides the evidence that the push off is delayed, which quite means less power could be generated during the toe off for the swing. This in turn may lead to slower swing and less impact on the next heel strike.

The above phenomena are also observed in the elderly walking [102]. Thus these features might be typical features for dynamic instability and could be applied for walking stability estimation, such as to detect pre-disabled patients, elderly with low and high fall risks.

Shank-heel coronal and transverse plane show significant differences for two designed walking conditions, but the differences are smaller than 3˚. Less inversion and less adduction occur at toe off phase for both double beam and dragging weights walking. The heel is less supinated at toe off. For less stable walking trials, coronal and transverse plane motions may serve for both maximize the base of support and placing the COM towards the center [82].

This study provides evidence that 3D foot motion features could well describe walking behavior and foot dynamic functions. The 3D foot motion features could depict the dynamic foot behavior in detail. With the 3D foot motion feature patterns, people can imagine the dynamic foot behavior vividly and the foot posture at every time frame could be pictured. In addition, there are significant differences in mutli-segmental foot mechanics during various stability conditions. Foot and ankle must accommodate to changes in stability. This study reveals how foot segments function when subjected to less stable walking conditions. Thus the 3D foot motion

could well depict foot behavior during walking, and indicate walking stability with motion features. During less stable walking, it should be highlighted that the most obvious phenomenon appears in reduced ROM of push off angle and shank-foot sagittal plane angle. The time delay of the peak dorsi-flexion of shank-foot sagittal plane angle is also another noticeable phenomenon when subjected to less stable walking. The foot tends to be less inverted and adducted at toe off phase. Our results also indicate that heel-met (fore-foot and hind-foot) sagittal plane motion should also be investigated for walking stability. Hind-foot may occupy more for stabilizing than fore-foot. The study could be benefit for estimation of walking stability for the elderly and patients with walking instability, as well as design of training programs, shoe-integrated sensor system, prostheses and walking aids [96].

There is a vast area of interest of this project, leading to many possible methods of studying walking stability. There are also many more possible conditions of walking stability. More subjects could be tested for normalizing the data to enhance the quality of the data analysis. More angles could be explored to compliment the analysis of the data. The largest error may come from marker positions; however according to [79], the error is overall acceptable.

6.6 Pattern recognition using fuzzy logic system with selected motion features

According to previous discussion, many motion features were obtained and analyzed for their angle patterns during four walking conditions. Some features showed distinctive differences between different walking conditions, while some features show no significant differences. Although some differences are noticeable, it might not be straight forward sometimes for human to differentiate the four walking

conditions with the data from these features. If more walking conditions to be involved and analyzed, the overwhelming data could bring difficulties in recognition of the distinction among these walking conditions. Thus there is a need to find a systematic method for data analysis and pattern recognition.

In this section, in order to prove the efficiency of the proposed motion features in Section 6.4 and assist human beings to distinguish four walking conditions from measured data of motion features, fuzzy logic system trained by nearest neighborhood clustering is proposed. Application shows the proposed method is effective and able to automatically distinguish the four walking conditions.

6.6.1 Fuzzy logic system

In this thesis, a singleton fuzzy logic system whose general configuration depicted in Figure 6.13 is considered. There are four components in a fuzzy logic system, namely fuzzifier, fuzzy rule base, fuzzy inference engine, and defuzzifier.

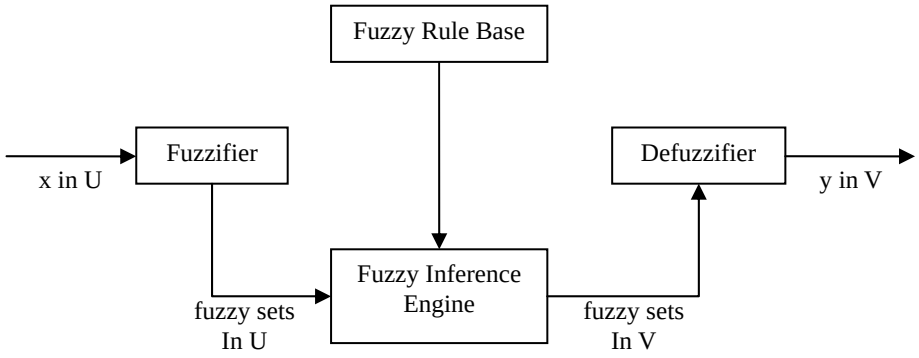

Figure 6.13: Basic configuration of a fuzzy logic system

Fuzzifier

The fuzzifier maps a crisp point $\mathbf{x} = (x_1, ..., x_n) \in \mathbf{U}$ into a set of fuzzy sets $A_{x_i} (i = 1, 2, ..., n)$ in $\mathbf{U}$. In the singleton fuzzification, the input fuzzy set A_{x_i} has only a single point of nonzero membership, that is, $\mu_{A_{x_i}}(x_i) = 1$ for $x_i = x_i'$ and

$\mu_{A_{x_i}}(x_i) = 0$ for all other $x_i \in \mathbf{U}$ with $x_i \neq x_i'$.

Fuzzy rule base

The fuzzy rule base consists of a group of fuzzy IF-THEN rules. The rules can be extracted from numerical data or provided by experts. Consider a fuzzy logic system having n inputs and one output, then the lth rule in the rule base can be written as

$$R^l: \text{ IF } x_1 \text{ is } F_1^l \text{ and} \cdots \text{and } x_n \text{ is } F_n^l, \text{ THEN } y \text{ is } G^l,$$

where l = 1, 2, …, M. $x_i (i = 1, 2, ..., n)$ and y are the inputs and output to the fuzzy logic system respectively. F_i^l and G^l are labels of antecedent and consequent fuzzy sets in **U** and R, respectively. This rule represents a fuzzy relation between the input space **U** and output space R.

Fuzzy inference engine

The fuzzy inference engine combines fuzzy IF-THEN rules and provides a mapping from input fuzzy sets in **U** to output fuzzy set in R. Each rule is interpreted as a fuzzy implication. Using the sup-star compositional rule of inference, the output consequent set corresponding to rule R^l of a singleton fuzzy logic system can be expressed as

$$\mu_{B^l}(y) = \sup_{\mathbf{x} \in \mathbf{U}} [\mu_{F_1^l \times \cdots \times F_n^l \to G^l}(\mathbf{x}, y) * \mu_A(\mathbf{x})] \qquad (6.1),$$

where $\mu_{F_1^l \times \cdots \times F_n^l \to G^l}(\mathbf{x}, y)$ is fuzzy implication. $*$ denotes the t-norm corresponding to the conjunction “and” in fuzzy rules.

Defuzzifier

The defuzzifier performs a mapping from fuzzy sets to a crisp point. There are several possible choices of this mapping, such as maximum defuzzifier, center average defuzzifier and modified center average defuzzifier. In this thesis, the center average

defuzzifier, which is defined as follows, is used.

$$y = \frac{\sum_{l=1}^{M} \bar{y}^l \mu_{B^l}(y)}{\sum_{l=1}^{M} \mu_{B^l}(y)} \tag{6.2}$$

Where $\bar{y}^l$ is the center of the consequent set G^l.

For a singleton fuzzy logic system, if product implication, product t-norm, center average defuzzification, and Gaussian membership function are used, the singleton fuzzy logic system can be expressed as

$$y = \frac{\sum_{l=1}^{M} \bar{y}^l [\Pi_{i=1}^{n} \exp(-(\frac{x_i - x_i^l}{\sigma_i^l})^2)]}{\sum_{l=1}^{M} [\Pi_{i=1}^{n} \exp(-(\frac{x_i - x_i^l}{\sigma_i^l})^2)]} \tag{6.3},$$

where x_i^l and σ_i^l are adjustable parameters of Gaussian membership function.

6.6.2 Adaptive fuzzy logic system

Suppose that given N input-output pairs $(\mathbf{x}^l, y^l), l = 1, 2, ..., N$, the task in this subsection is to construct a fuzzy logic system which can match all the N pairs to any given accuracy. The fuzzy logic system could be

$$f(\mathbf{x}) = \frac{\sum_{l=1}^{N} y^l \exp(-(\frac{|\mathbf{x} - \mathbf{x}^l|}{\sigma})^2)}{\sum_{l=1}^{N} \exp(-(\frac{|\mathbf{x} - \mathbf{x}^l|}{\sigma})^2)} \tag{6.4}.$$

Theorems in [103, 104] has shown that by proper choosing the parameter σ, the above fuzzy logic system can match all the N input-output pairs to any given accuracy. The σ is a smoothing parameter: the smaller the σ, the smaller the matching error, but less smooth the $f(\mathbf{x})$ becomes. Thus, the σ should be properly chosen to provide a balance between matching and generalization. Because σ is a one-dimensional parameter, it is not difficult to determine.

In fuzzy logic system design, the most challenging part is to choose the membership functions. To alleviate the challenge, nearest neighborhood clustering is used to train the fuzzy logic system. Thus, the designed fuzzy logic system can adapt itself according to the given data. The adaptive fuzzy logic system is constructed through following steps.

Step 1: starting with the first input-output pair $(\mathbf{x}^1, y^1)$, establish a cluster center $\mathbf{x}_0^1$ at $\mathbf{x}^1$, and set $A^1(1) = y^1$, $B^1(1) = 1$. Select a radius *r*.

Step 2: suppose that when the *k*th input-output pair $(\mathbf{x}^k, y^k), k = 2,3,...,$ is considered, there are *M* clusters with centers at $\mathbf{x}_0^1, \mathbf{x}_0^2, ..., \mathbf{x}_0^M$. Compute the distances of $\mathbf{x}^k$ to these *M* cluster centers, $|\mathbf{x}^k - \mathbf{x}_0^l|$, *l*=1,2,…*M*, and let the smallest distance be $|\mathbf{x}^k - \mathbf{x}_0^{l_k}|$, that is, the nearest cluster to $\mathbf{x}^k$ is $\mathbf{x}_0^{l_k}$. Then

(a) If $|\mathbf{x}^k - \mathbf{x}_0^{l_k}| > r$, establish $\mathbf{x}^k$ as a new cluster center $\mathbf{x}_0^{M+1} = \mathbf{x}^k$, set $A^{M+1}(k) = y^k$, $B^{M+1}(k) = 1$, and keep $A^l(k) = A^l(k-1)$, $B^l(k) = B^l(k-1)$, for *l*=1,2,…*M*.

(b) If $|\mathbf{x}^k - \mathbf{x}_0^{l_k}| \le r$, do the following:

$$A^{l_k}(k) = A^{l_k}(k-1) + y^k \tag{6.5}$$

$$B^{l_k}(k) = B^{l_k}(k-1) + 1 \tag{6.6}$$

and set

$$A^l(k) = A^l(k-1) \tag{6.7}$$

$$B^l(k) = B^l(k-1) \tag{6.8}$$

for *l*=1,2,…*M* with $l \neq l_k$.

Step 3: the adaptive fuzzy system at the *k*th input-output pair is computed as

$$f_k(\mathbf{x}) = \frac{\sum_{l=1}^{M} A^l(k) \exp(-\frac{|\mathbf{x}-\mathbf{x}_0^l|^2}{\sigma^2})}{\sum_{l=1}^{M} B^l(k) \exp(-\frac{|\mathbf{x}-\mathbf{x}_0^l|^2}{\sigma^2})} \tag{6.9}$$

if $\mathbf{x}^k$ does not establish a new cluster. If $\mathbf{x}^k$ establishes a new cluster, change the M in the above equation to M+1.

The radius r determines the complexity of the adaptive fuzzy system. For smaller r, more clusters are generated resulting in a more complex nonlinear regression at the price of more computation to evaluate it. Because r is a one-dimensional parameter, an appropriate r could be found by trial and error. Codes are written in "Matlab" to enable the fuzzy logic system trained by nearest neighborhood algorithm introduced in this section.

6.6.3 Motion pattern recognition with adaptive fuzzy logic system

In this subsection, several motion features previously proposed are employed to distinguish the four walking conditions: normal walking, single beam walking, double beam walking and walking with dragging weights. Measured data of these motion features are used to train the adaptive fuzzy logic system.

According to the discussion in Section 6.4, some motion features could show significant differences among walking conditions. Shank-foot sagittal plane angle pattern has similar phenomenon with the shank-heel sagittal plane angle pattern. Thus only shank-foot sagittal plane angle features are used as training features. The same happens to the heel-mid and heel-met motion. Because heel-mid motion contributes to heel-met motion, only heel-met features will be used to avoid repeated overwhelming information. Finally 13 motion features are chosen as inputs to the adaptive fuzzy logic system. The 13 chosen motion features are arch change angle ROM, push off angle ROM, push off angle maximum value, shank-foot sagittal plane angle ROM,

shank-foot sagittal plane angle index of maximum value, shank-foot sagittal plane angle minimum value, shank-heel coronal plane angle ROM, shank-heel coronal plane angle minimum value, shank-heel transverse plane angle ROM, heel-metatarsal sagittal plane angle ROM, heel-metatarsal sagittal plane angle minimum value, heel-metatarsal transverse plane angle ROM and heel-metatarsal transverse plane angle minimum value. As the fuzzy logic system is multi-input single-output system, the output to the fuzzy logic system is chosen as the indicator of the four walking conditions. The value of the indicator is set as 1 for the normal walking, 2 for the single beam walking, 3 for the double beam walking, and 4 for the walking with dragging weights. Since the structure, rules and membership functions of the adaptive fuzzy logic system are automatically generated through nearest neighborhood clustering, the only parameters which have to be set are σ and *r*.

For each walking condition, 20 sets of data with each set of data corresponding to 13 selected motion features were used for training of the fuzzy logic system. Thus totally 80 sets of data were used including the four walking conditions. After one round of training, the training data was used to test the performance of the adaptive fuzzy logic system in walking condition recognition. The confusion matrix when $\sigma = 4$ and *r*=10 for training data is shown in Table 6.7. A confusion matrix is a table including memberships predicted by a predictive model. In pattern recognition, confusion matrix is used to mark classification performance. The σ and *r* values are selected by trial and error, and the selected values could provide good similarity of the predicted type to the actual type during training. The value of the indicator is set as 1 for the normal walking, 2 for the single beam walking, 3 for the double beam walking, and 4 for the walking with dragging weights. After the training of the fuzzy logic system, the types that are wrongly identified are bolded in Table 6.7. The error rate is the percentage of

wrongly recognized type among all values used for training. For example, for the normal walking in Table 6.7, besides the bolded two values, all the other values could be rounded to 1, so the error rate is 2/20 and equals to 10%. Thus the error rate is 10% for the normal walking, 10% for the single beam walking, 20% for the double beam walking, and 15% for the walking with dragging weights. The error rate is relatively higher for the double beam walking condition, and this might due to the fact that the motion feature values of the double beam walking and single beam walking are quite similar. The single beam walking, double beam walking and walking with dragging weights are three designed less stable walking conditions, which have similar features to some extent. The walking with dragging weights has some similar features with the double beam walking.

For each walking condition, another 5 sets of data which were not used during the training were used for testing of the performance of the adaptive fuzzy logic system. The confusion matrix when $\sigma = 4$ and r=10 is shown in Table 6.8. For example, for the first row, feature data from normal walking is as input to the fuzzy logic system, and the output indicator is supposed to be 1 as defined. The types that are wrongly identified are bolded. The error rate is nearly 0% for the normal walking, 20% for the single beam walking, 40% for the double beam walking, and 20% for the walking with dragging weights. By just looking into the feature values, it is very difficult to classify these four walking conditions. However, the fuzzy logic system can automatically and effectively recognize different gait patterns although certain error rate exists.

In conclusion, the adaptive fuzzy logic system has good performance in motion pattern recognition for different walking conditions. The selected motion features could well indicate the differences among different walking conditions. In future works, more walking conditions, such as the ones of the elderly people and patients with foot

dysfunctions, could be involved. Motion feature data of more walking conditions could be used to set up a feature database. This would in future help to prescribe different problems in patients' gait.

Table 6.7: Confusion matrix for training data

Normal	1	1.0032	1.0007	1	1	1	**2.5194**	1	1	1
	1	1	**1.999**	1.0034	1	1	1	1	1	1
Single beam	2.0045	**3.2504**	2.0004	2.2857	2.2857	2.3333	2.0004	2.3328	2.2898	2.0006
	3	2	2	2	2	2	2.1917	2	2.3256	2.2857
Double beam	3.4001	2.9986	**2.3273**	**2.299**	2.9997	3.3066	**2.3087**	2.9997	2.8319	3.2748
	1.806	2.9999	3.4996	2.9995	3	3.2573	2.9992	2.9998	3.1172	3
Dragging weights	3.8267	3.6015	3.9988	3.8096	3.998	3.6767	4	3.9997	**3.3973**	**3.3117**
	3.9983	3.9998	4	3.9996	3.5747	3.9999	4	4	3.9996	**3.1317**

Table 6.8: Confusion matrix for test data

Normal	1.0021	1	1	1.0008	1.3329
Single beam	2.0099	**2.8691**	2.4333	2.0084	2.1501
Double beam	3	2.915	3.3916	**2.4661**	2.998
Dragging weights	3.8908	3.6994	3.9897	**3.2683**	3.9769

6.7 Summary

Previous chapter developed a standard method and proposed features for detailed foot motion measurement for normal walking. As to the author's knowledge, very few studies have been performed to investigate the detailed foot motions when subjected to less stable walking conditions. This chapter aims to apply the detailed foot motion features for different foot behavior description, and to test these features' effectiveness on foot behavior characteristics. Three different situations are designed in enabling the subjects to walk in less stable conditions; walking on single beam, double beams and walking with dragging weights. Motion cameras are applied to collect foot and ankle kinematic data for analysis. Results show that during less stable walking conditions, the features of push off power at toe off decreases significantly and most segmental joints' range of motion (ROM) reduces significantly. Heel-met (fore-foot and hind-foot)

sagittal plane motion could also be further investigated for walking stability. The hind-foot tends to have more function in stabilizing than the fore-foot. This study reveals how foot segments function when subjected to less stable walking conditions. Foot and ankle must accommodate to changes in stability. Although motion features which show significant differences between walking conditions are listed, it is still a bit implicit and troublesome for people to classify different walking conditions by directly reading the feature values. Adaptive fuzzy logic system trained by nearest neighborhood clustering is proposed, and is able to automatically distinguish the four walking conditions. Results show the proposed method is effective and reliable. Compared with other pattern recognition methods, adaptive fuzzy logic system has the advantage of combining human expert knowledge and automatic machine training. Understanding of foot segment motions could be benefit in the design of training programs, prostheses and walking aids.

In conclusion, this chapter applied the foot motion features to successively depict different walking conditions, normal walking and less stable walking conditions. Significant differences of the motion features exist between normal walking and each less stable walking condition. Training of an adaptive fuzzy logic system with motion feature data for gait pattern recognition was performed, and the results also showed the effectiveness of proposed motion features on classifying different walking conditions. For future study, obtained foot motion features related to walking stability could be applied on the elderly people and patients with risk of falls. More motion features of different walking styles from different group of patients could be measured and analyzed. More gait patterns could be automatically classified with fuzzy logic system. Efforts could also be put on obtaining these stability features without motion cameras, and finally integrated in shoes to daily monitor foot behavior.

CHAPTER 7 DEVELOP A MULTI-SEGMENT FOOT MODEL TO INVESTIGATE FOOT SEGMENT FEATURES

Computational modeling offers a cost-effective alternative to study the behavior of the human body mechanisms. Modeling and simulation of foot kinetics and kinematics could provide better understanding and visualization of walking behavior. In previous chapters, foot multi-segment pressure function and multi-segment motion function was individually investigated by conducting experiments and data analysis. However, if other information is needed, experiments need to be redesigned. Through the model, simultaneously looking into foot kinetics and kinematics could help to better understand foot dynamic behavior from a new perspective. The dynamic foot model could present the relationship between foot pressure/force and foot motion. Furthermore, with verified foot dynamic model, diverse simulations with different kinematics (e.g. walk, jump, turn and dance) or contacting environment (e.g. slope walking and step walking) could be investigated. At present, most of existed walking models consider the foot as one rigid segment. In this study, foot multi-segment behavior during walking will be modeled and investigated. In this chapter, effort is put on building a multi-segment foot model to study various foot segment behaviors, and studying foot motion features and foot pressure/force features simultaneously through modeling with an existing software package LifeMOD. Combined foot segment kinetic and kinematic features could be analyzed for different walking conditions. Changes of each kinematic feature will be discussed with respect to the changes of kinetic features. The relationship between foot segment features could be better understood.

7.1 Introduction of LifeMOD

The LifeMOD Biomechanics Modeler is used to perform multi-body analysis and is a plug-in module to the ADAMS (Automatic Dynamic Analysis of Mechanical Systems). It can also combine the physical environment with the created human body for dynamic contacts.

For a model building, LifeMOD can achieve modeling of body, joints, motions, and forces. It has many good features as a dynamic modeling tool. The modeling procedure is presented in Figure 7.1 [105].

To build a LifeMOD model, the first step is to create body segments. For the body segments creation, segment sizes and mass properties can be scaled according to your own problem and demand. Another important feature of LifeMOD body segment building is that default individual segments, such as the foot segment, can be refined into more segments according to the real bone structure for detailed modeling. This allows the investigator to create a model with better fidelity. For this study, feet can be refined into detailed sub-segments, and thus a multi-segment foot model could be built with LifeMOD.

As to the joints creation, a standard set of joints can be automatically created and each joint degree of freedom can be modified to include stops, friction, forces, torques, etc. The joints function as an essential component of the LifeMOD model. For walking trial modeling, the joints are mainly used to record the kinematic motion and stabilize the model during the inverse dynamics simulation, and to drive the model and provide joint friction stiffness for a forward dynamics simulation. The investigator can also modify the posture of the model joint axes.

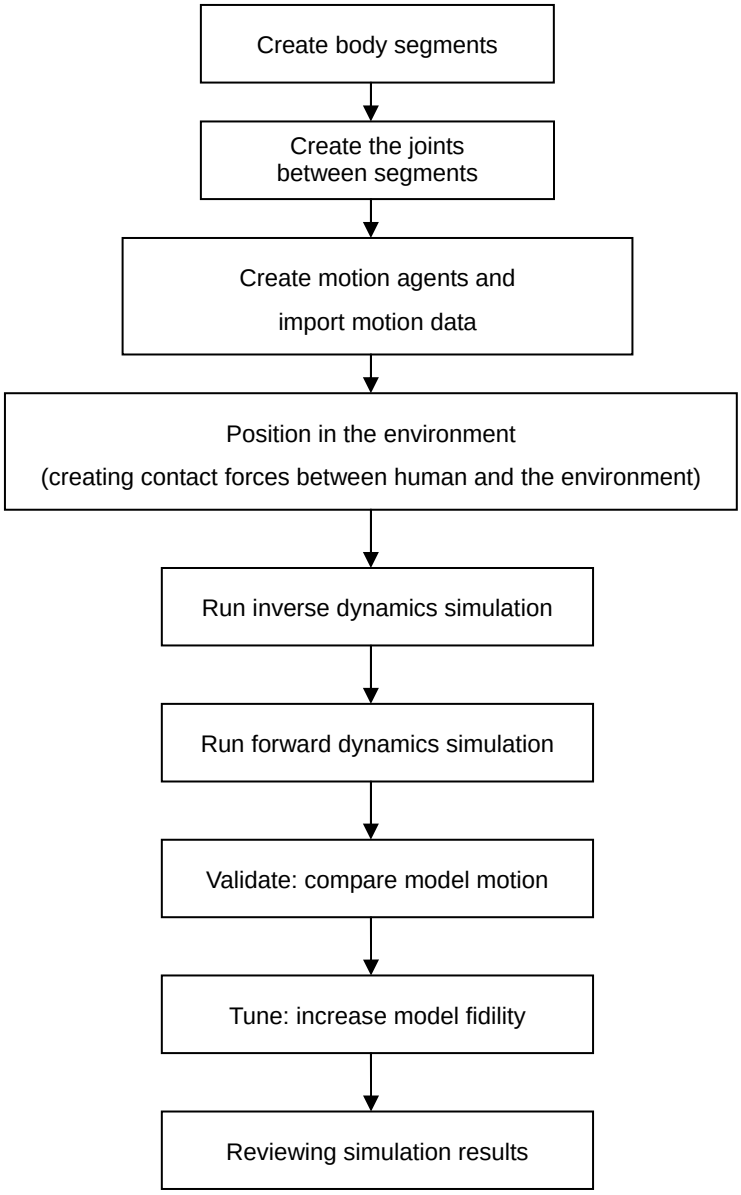

Figure 7.1: LifeMOD biomechanics modeling process

Then the motion data can be imported to the model. LifeMOD has a standard interface for motion movement of human body modeling. If the experiments are performed with LifeMOD standard marker sets, markers could be created on the model automatically after importing the motion input data. The human model is automatically matched with the marker sets according to an energy minimization principle. Marker trajectories from the motion capture system could drive the model by a method of motion agent, which are attached to the model using springs. The stiffness properties

of the springs rely on the relative accuracy of markers' placement because the motion agents are located at the motion capture sensors (marker set positions for motion capture). The passive model must be driven with and external force and motion agents are added to the model to drive the model to capture the simple joint angle histories. The motion agents can guide the model to track the segment motion in the motion input file. The motion agents just influence the motion of the model, since the model is also depended on the joint limits, environment and so on.

The simulation of LifeMOD includes two main parts: inverse dynamics simulation and forward dynamics simulation. The inverse dynamics simulation is performed to capture the motion of the model and joints, and the model is driven by motion agents under the control of joint limits, external forces, etc. Before the inverse dynamics simulation, contact forces such as the ground reaction forces could be added to the model.

In the forward dynamics simulation, the previous joints' record will be replaced with contractile elements to drive the human model to match the recorded motion. The forward dynamics simulation is then performed with the model guided by the internal forces, such as joint torques, and external forces like gravity and contact, etc. For the forward dynamics simulation, PD-servo controllers can also be created to allow the human model to track the recorded motion with joint torques at each joint degree of freedom. The trained driver elements are PD-servo actuators which minimize the error between the desired instantaneous joint angle and the recorded model joint angle. This is accomplished by multiplying *P* gain times the error and *D* gain times the derivative of the error.

After the forward dynamics simulation, results such as joint function, force action and magnitudes could be obtained and analyzed. Investigators can view the simulation

results with detailed animations, kinematics and kinetics plots. Joint and segment displacements, velocities and accelerations can be plotted and displayed. The model kinetics output, such as joint torques, joint forces and contact forces, can also be achieved. For better understanding of LifeMOD features, a LifeMOD tutorial example is presented in the Appendix B.

7.2 Proposed modeling objectives and scopes

From the previous sections, there are many useful features in LifeMOD. For example, the body segments could be refined to the scale of the investigator' needs, the ground reaction forces could be used as boundary information to make the model more real, and experimental motion data could be imported to train the model, etc. It is also a feasible way of investigating joint motions and contact forces of human body during different activities and this modeling method does not need much programming background.

In Chapter 4, foot pressure patterns during walking in different conditions can be recorded with F-scan mobile system. Pressure under different foot segments can also be calculated from pressure patterns. In Chapter 5 and 6, multi-segment foot motions could be obtained via Vicon motion cameras capture in different walking conditions. These data could be used as input and verification for LifeMOD modeling. Combining all the above information, the relationship among foot multi-segment kinematics, kinetics and walking behavior could be effectively developed if a dynamic multi-segment foot model [106, 107] is built. Additionally, more information will be obtained through modeling, such as joint forces. In LifeMOD modeling, previously foot was always regarded as only one rigid segment, and the foot function could not be well investigated. With a single foot segment model, the relationship between detailed foot kinematics and foot kinetics is not yet known. The objective of this chapter is to

investigate the foot segment behaviour characteristics with a multi-segment foot model using LifeMOD biomechanics modeller, and to explain dynamic relationship between foot pressure feature/force and foot motion feature from modelling perspective. Through this study, the foot segment features will be better understood.

To achieve the objective, a LifeMOD model with detailed multi-segment foot will be built according to the procedures as shown in Figure 7.1. Human walking motions in different walking conditions obtained from Vicon cameras are needed to be imported into the LifeMOD model. Foot plantar pressure could also be simultaneously recorded in different walking conditions for future model verification. The model would be tuned by comparing the simulation results of forces under feet segments (e.g.: the metatarsals and heel) with the forces calculated from foot plantar pressure. If they do not coincide with each other, we need to go back to further refine our model by choosing different parameters and so on. If they coincide well, the model is ready to do further simulation of lower body activities to investigate foot segment kinematics and kinetics features. By observing the force pattern and foot motion, we will finally link the foot segment (metatarsals and heel) force features and motion features during different walking conditions, which form the foot segment features.

Here we choose two different walking conditions including normal walking and walking with dragging weights. As in our previous studies, walking with dragging weights is considered as one less stable walking condition and it is quite similar to the walking of elderly population. The study of Silder, A., et. al [108] suggested that age-related shifts in joint kinetics do not arise as a result of increased passive hip joint stiffness, but seem to be reflected in ankle plantar-flexor weakness. Adding dragging weights is one way of increasing ankle weakness. Thus it is chosen as a typical walking condition for the LifeMOD modeling. In Chapter 6, foot motion features

during four walking conditions for 10 tested subjects were discussed, including the normal walking and walking with dragging weights. The motion data patterns are relatively consistent for the 10 tested subjects. Here we choose one set of normal walking motion data and one set of dragging weights walking motion data as the inputs to LifeMOD for corresponding dynamic modeling.

7.3 LifeMOD modeling for normal walking

The study starts with the building of normal walking model for foot kinematics and kinetics.

7.3.1 Build a LifeMOD model for normal walking trial

The basic LifeMOD process is listed in the Figure 7.1. The first step of modeling is to import SLF model file and to generate basic model segments as shown in the user interface in Figure 7.2. The tested subject's information can be imported to the model. The subject here is 25 years old with weight at 64kg and height at 170cm. A part of or complete set of body segments can be generated by default and could be further refined to individual bones. In our model, only lower body segments are needed for the walking simulation as shown in Figure 7.3. The lower body segments include lower torsal, hip, shank and foot segment.

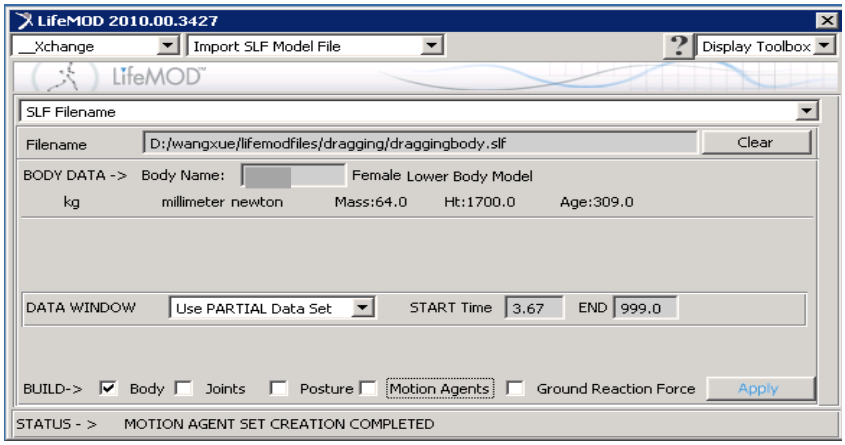

Figure 7.2: Import SLF model file with subject information

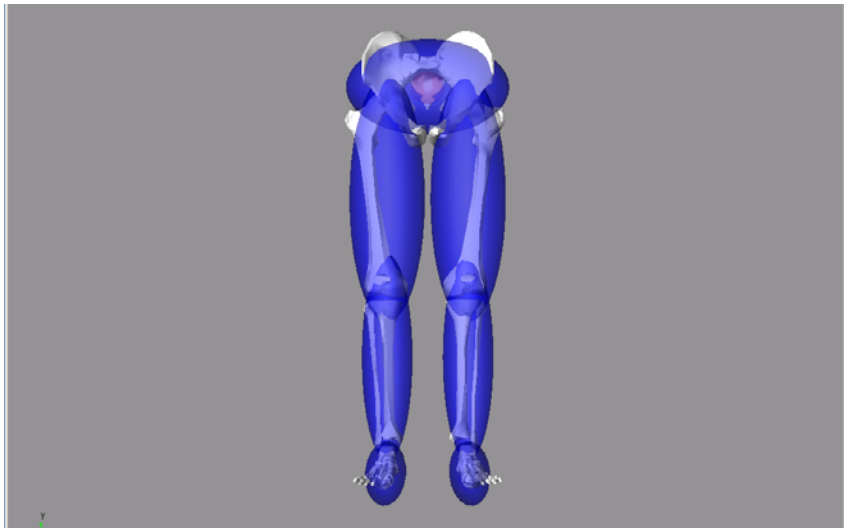

Figure 7.3: Lower body segments (foot is initially generated as one rigid segment)

The generated lower body structure by default only uses one ellipsoid segment for each foot. As seen in previous chapters, one-segment foot model cannot depict detailed foot motion and the foot model looks quite unrealistic. Further, the default model is unable to correctly present contact forces between foot segment and ground. To better understand foot function during walking, foot should be further refined into more segments, including toes, metatarsals, mid-foot and heels. This can greatly improve the reality of the walking model. It can be achieved by zooming in to the feet segment and bringing up the single segment creation panel as shown in Figure 7.4. The center position, orientation of the single segment and ellipsoid size can be defined in the model. The parameters are set according to the tested subjects' measurement. The details of the parameters are listed in Table 7.1. Hallux exerts most function among toes. In this study, only hallux is modeled in our model.

Table 7.1: Parameters for refined left foot segments

	Location (mm)			Orientation (degree)			Ellipsoid size (mm)		
	x	y	z	x	y	z	x	y	z
Heel	96	-826	24	0	0	0	65	100	95
Mid-foot	112	-828	94	40	20	300	70	50	60
Metatarsals	110	-840	145	270	170	90	100	42	65
Hallux	90	-840	180	180	-180	0	30	19	33

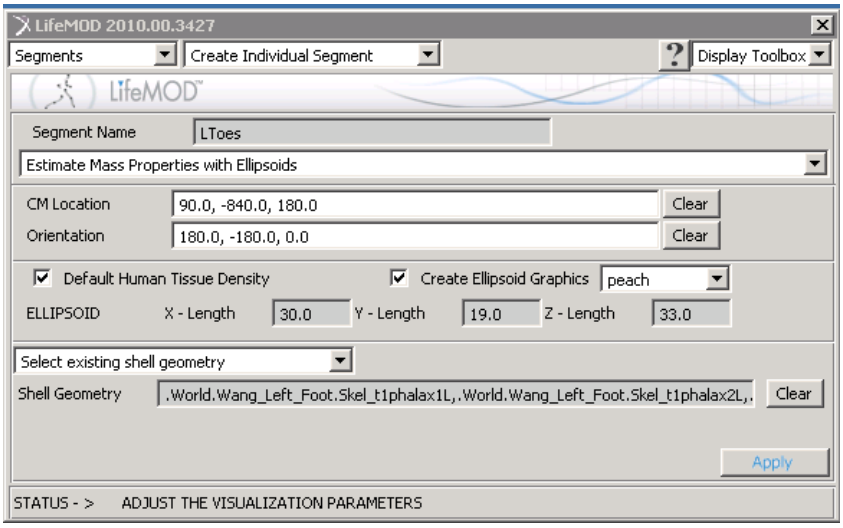

Figure 7.4: Single segment creation panel in LifeMOD

After the four single segments are created, they are linked to each other as shown in Figure 7.5. The original single foot segments are deleted as shown in Figure 7.6.

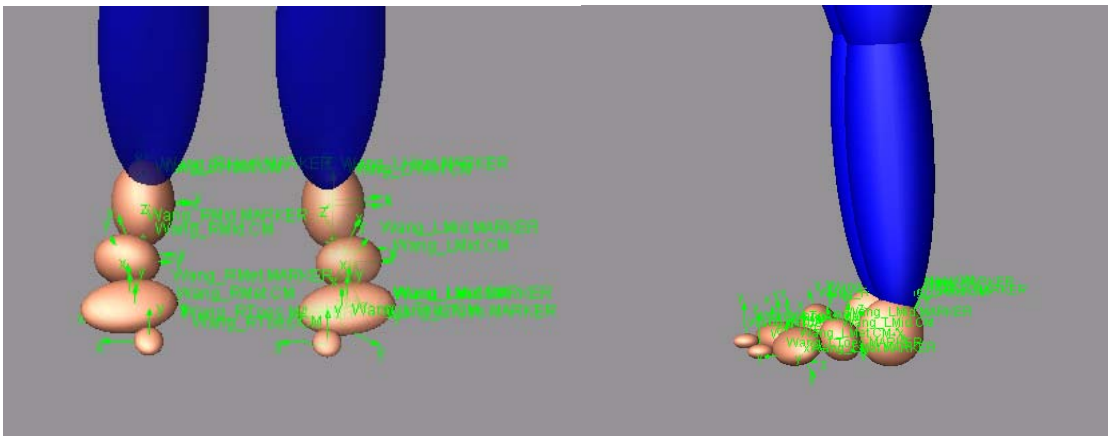

Figure 7.5: Refined foot segments

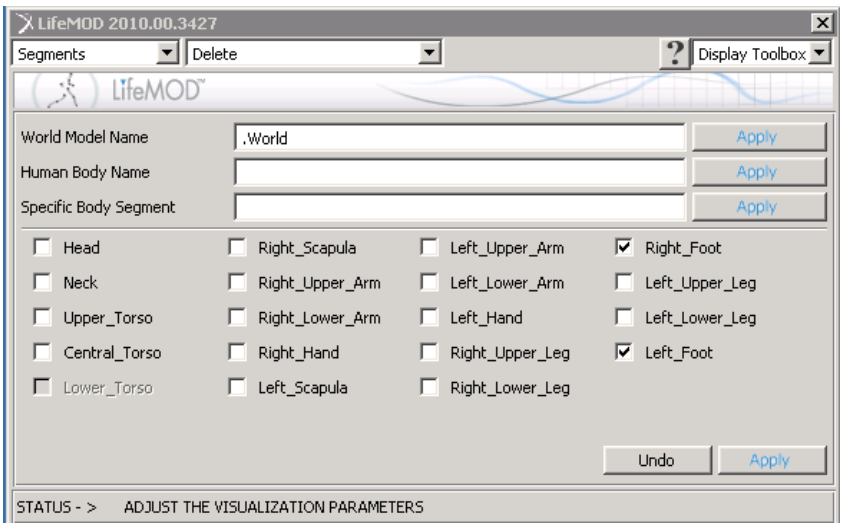

Figure 7.6: Segment delete panel

The next step is to create the joints between segments. The joint can be viewed as a tri-axis hinge and each degree of freedom can be specified separately. Specific stiffness, damping, angular limits and limit stiffness values can be chosen for a passive 6 DOFs joint. According to LifeMOD modeling experiences, damping is usually set as 10% of stiffness value. These joints are used to record the joint angulations in an inverse dynamics analysis while the model is being simulated. The creation of joints also includes two small steps. The first one is to create basic joint set; here the hip and knee joints are generated with parameters selected referring to previous tutorial and literature on joints [109, 110]. After the setting, the joint stiffness and damping parameters may still need to be adjusted for stabilizing the model. Figure 7.7 shows the user interface of basic joint set creation panel. The second one is to create individual joints between previous created refined foot segments: joint between shank and heel, joint between heel and mid-foot, joint between mid-foot and metatarsals, and joint between metatarsals and hallux [111-114]. The joint in the LifeMOD is used to provide resistance and stabilize the model. Figure 7.8 presents user interface of the individual joint creation panel. The created joint set for the lower body model with detailed foot structure is shown in Figure 7.9. Joint position is set at suitable position between two adjacent segments. These positions could also be adjusted manually.

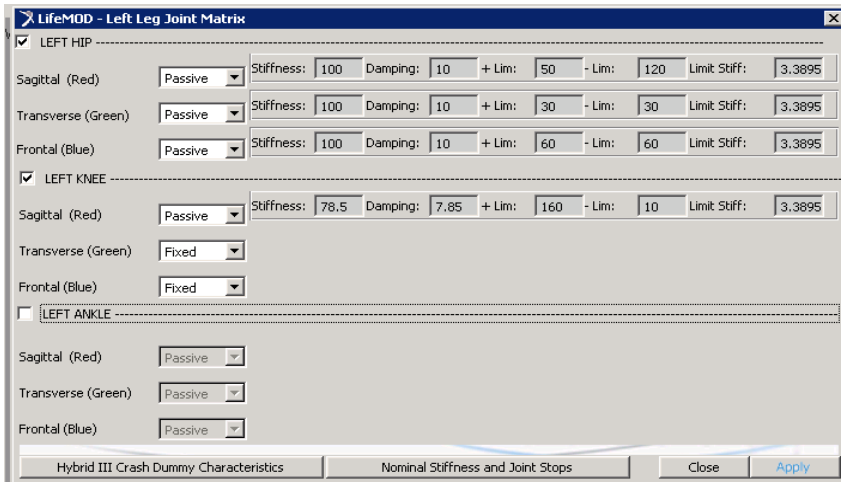

Figure 7.7: Create basic joint set

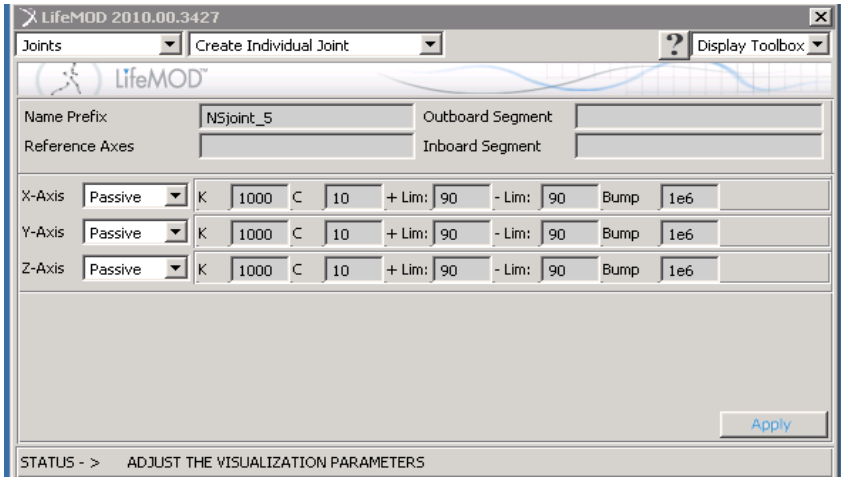

Figure 7.8: Create individual joint

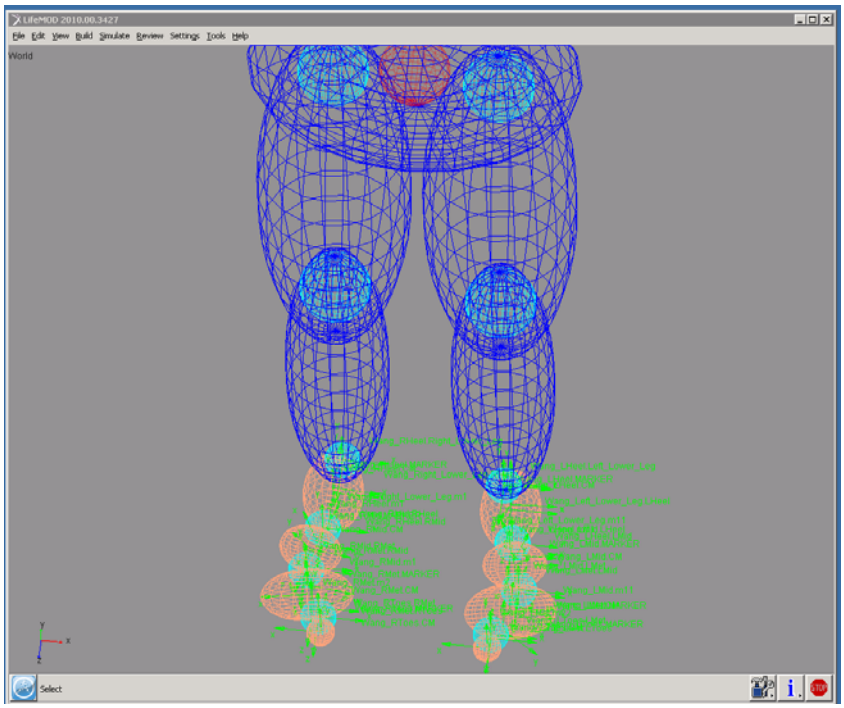

Figure 7.9: Created joint set

In an inverse-dynamics simulation, the motion captured data will drive the model to follow its motion. During the process, joints can learn angulation patterns, when the model is being driven by the motion capture data. Then the joints repeat the kinematics of the captured motion data, and serve as actuators for the forward dynamics simulations.

After the segments and joints are built, the motion agents could be added to the model to drive the model during inverse dynamics simulation. The model is passive

and must be driven or manipulated with an external force. The model could be trained with expected trajectory. In the motion agent process, two kinds of motion agents are used in this study. The first kind is a standard marker set ‘Helen Hayes (Davis) Marker Placement’ with 15 markers distributed around the subject’s lower body [105]. The other ones are augmented markers, which are positioned in specified positions for better accuracy and special investigation. In this study, foot is our main concern, and 15 additional augmented markers are added on the left foot and left knee region to provide a detailed foot kinematics. Experiments are conducted to obtain the foot motion and pressure simultaneously. The motion data is used as input to train the LifeMOD model, and the pressure data is used for verification of the model output. The experiment set up is shown in Figure 7.10.

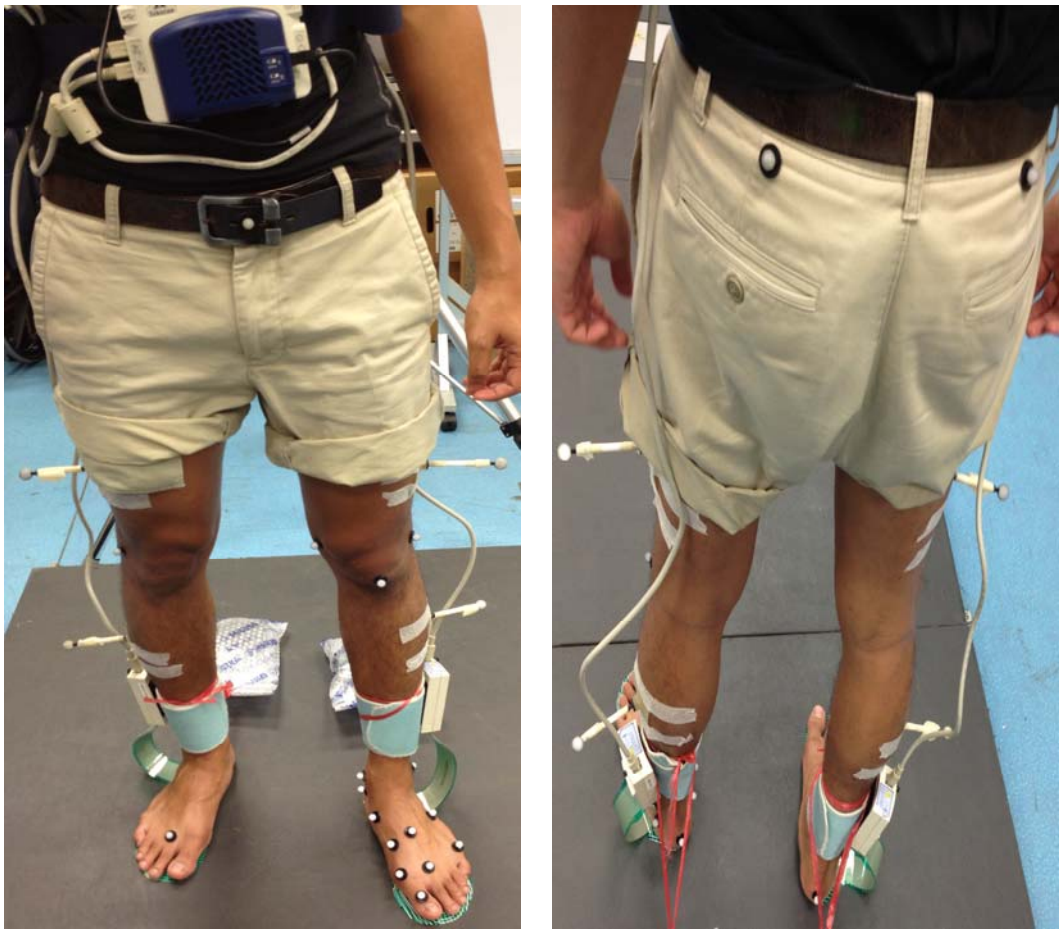

Figure 7.10: Experiment set up for measuring both foot motion and pressure during walking

The recorded marker trajectories during walking are saved as '.slf' file, which is to be imported to LifeMOD to drive the model. After the importing of motion data process, the model is shown in Figure 7.11.The darker points around the model body is the motion agents and the lighter points (some distance to the body) are the imported motion data. A synchronization and equilibration could be performed for the markers and motion agents. The motion agents are synchronized with the motion data points. After this step, motion agents created can drive the model to the specific posture, according to the motion data trajectory, as shown in Figure 7.12.

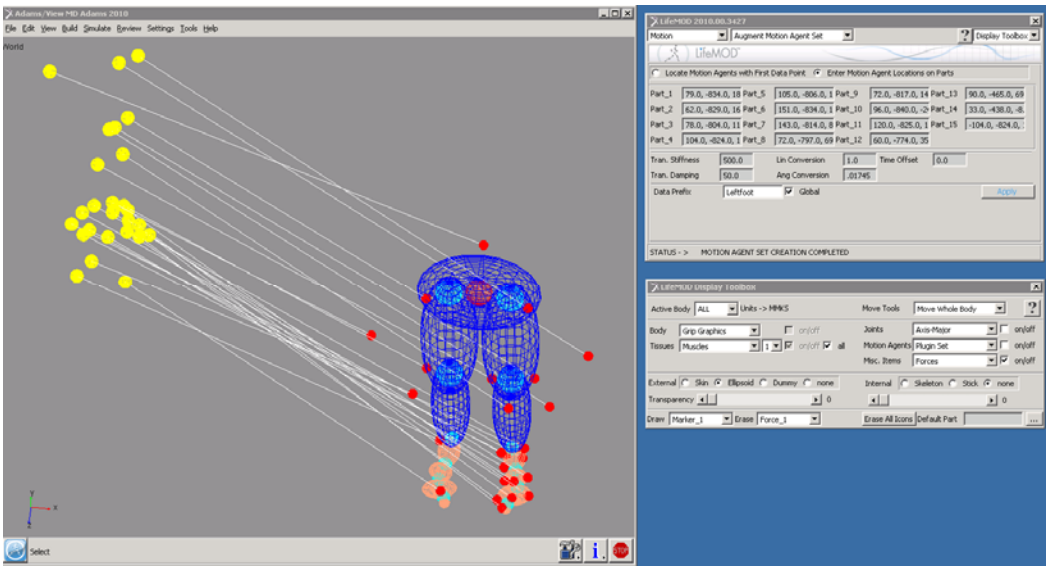

Figure 7.11: Motion agents (standard and augmented motion agents)

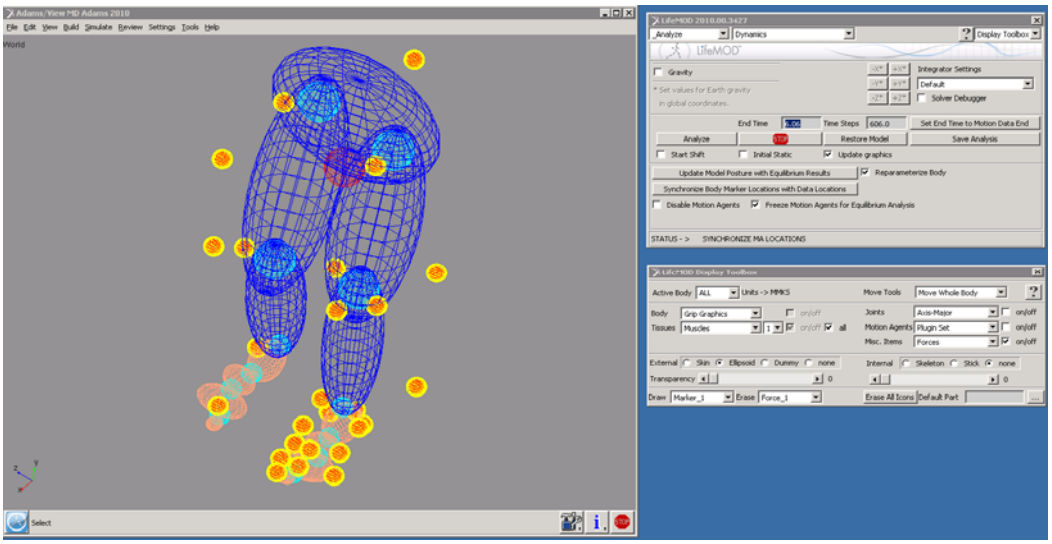

Figure 7.12: Motion agents after equilibration

The next step is to create contacts between foot segments and ground. Ground should be generated under the model's feet so that individual contact between the ground and each foot segment is created. According to LifeMOD tutorial [105], the general function of contact force is given as

$$F = k * g^{a} + \mu(g, \mu_m, g_m)\, dg/dt \tag{7.1}$$

where F is the contact force, k is the basic contact stiffness; g is the penetration of one geometry into another; a is a positive real value to consider the dependence of the penetration deformation; μ is the damping which depends on the penetration g; μ_m corresponding to the maximum damping value; g_m corresponding to the maximum penetration value; dg/dt is the penetration velocity. These parameters can be set to the model, as shown in Figure 7.13. The parameters were verified to give realistic contact forces between feet and ground [115]. Figure 7.14 shows the model after contacts are added.

The next step is running the Inverse-Dynamics Simulation. Using this developed model with passive joints and motion agents, inverse dynamics simulation can be run for the model to record experimental motion trajectories, as shown in Figure 7.15.

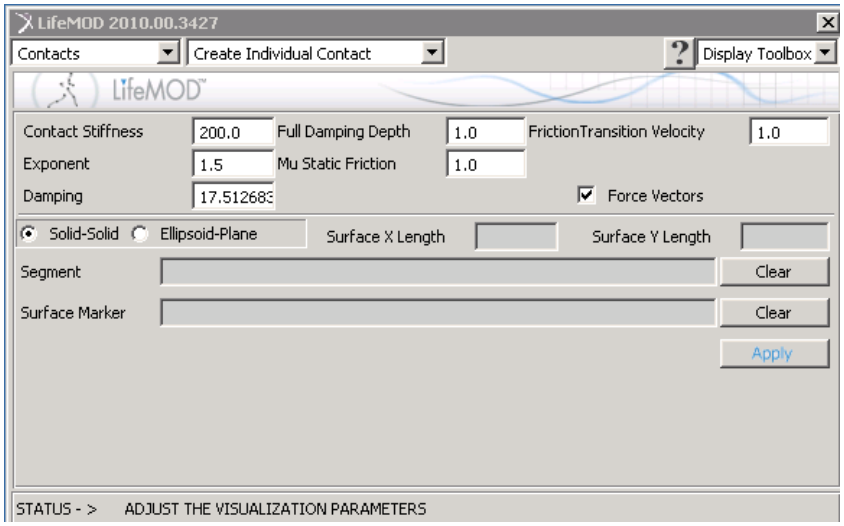

Figure 7.13: Contact parameters used in the feet floor interactions

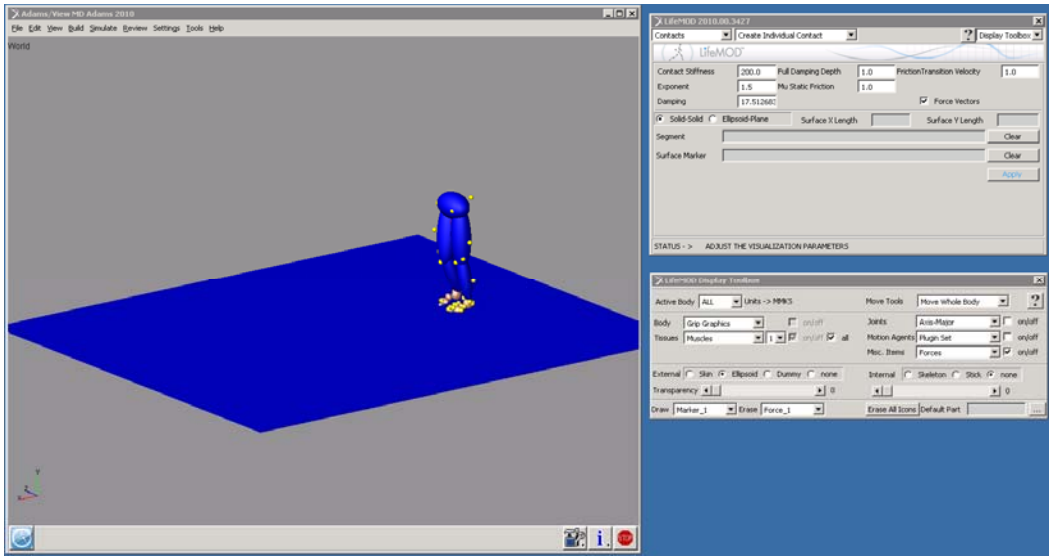

Figure 7.14: Create contacts between foot segments and ground

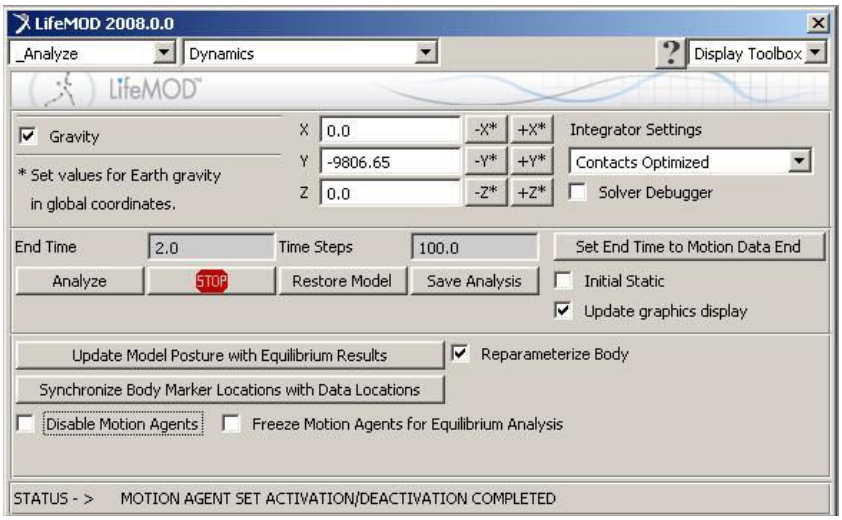

Figure 7.15: Analyze panel set to run inverse-dynamics simulation

Next is to run the forward dynamics simulation. With the joints motion history recorded from the inverse-dynamic simulation, it is now used in linear PD-Servo formulation to produce a force to recreate the motion history. The motion agents will be deactivated before running the forward-dynamics simulation. Finally, the results of joints trajectory, joints forces, and contacts between each foot segments and the ground could be simulated and displayed.

The LifeMOD modeling process is quite standard and could be relatively easily implemented. Thus LifeMOD is a relatively convenient tool for dynamics modeling

and simulation.

7.3.2 Simulation results for normal walking

Motion data obtained from experiments could drive the model during the inverse-dynamic modeling. The motion camera data of the posture would be obtained, simultaneously with the Tekscan foot plantar pressure data under feet. After building the model by loading the file of motion camera data, the forces under specific regions of feet can be simulated. These forces could be compared with the forces calculated from the plantar pressure data. If these two data coincide, our model is verified to be effective in linking the foot motion and foot pressure information. Several normal walking trials' pressure data are listed in the Appendix C for a better understanding of the typical segmental force pattern for the normal walking. For a typical normal walking, the forces are almost evenly distributed on the heel and metatarsals during the stance phase, and there is a normal push off force at the hallux at toe off phase.

As a comparison with the multi-segment foot model, a single segment foot model was built firstly, simulation results are shown in Figure 7.16. The dotted line is the force under the left foot and the real line is the force under the right foot. No clear pattern can be recognized. The foot modeling using single ellipsoid does not work well as compared with the real case. Thus, multi-segment foot segments model are needed.

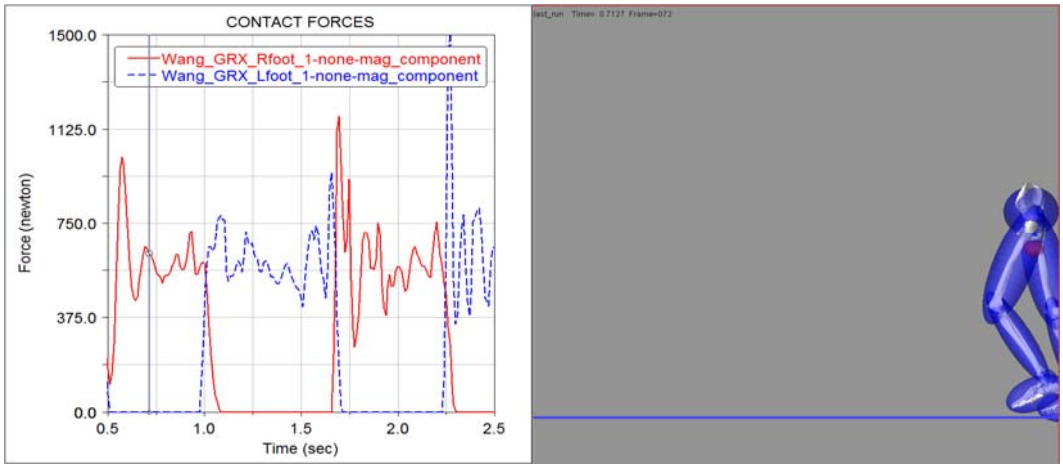

Figure 7.16: Normal walking simulation result for contact forces with single segment foot

Simulation results shown in Figure 7.17 are for model with the refined foot segments. The blue line is the force under the heel; the red line is the force under metatarsals; the black line is the force under hallux and the yellow line (here is constant zero value) is the force under mid-foot. Clear force pattern can be recognized.

A comparison between simulation results and experimental results are shown in Figure 7.18. Differences are reasonably small. The simulated results and experimental results are quite comparable. The force patterns of foot segments for the modeled normal walking trial have similar patterns with force patterns of other normal walking trials as shown in appendix C.

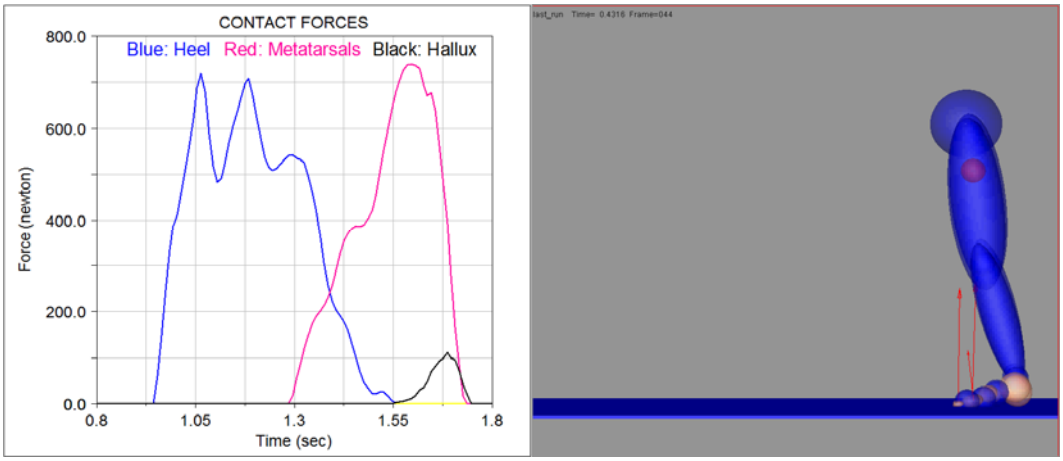

Figure 7.17: Normal walking simulation result for contact forces of refined foot model

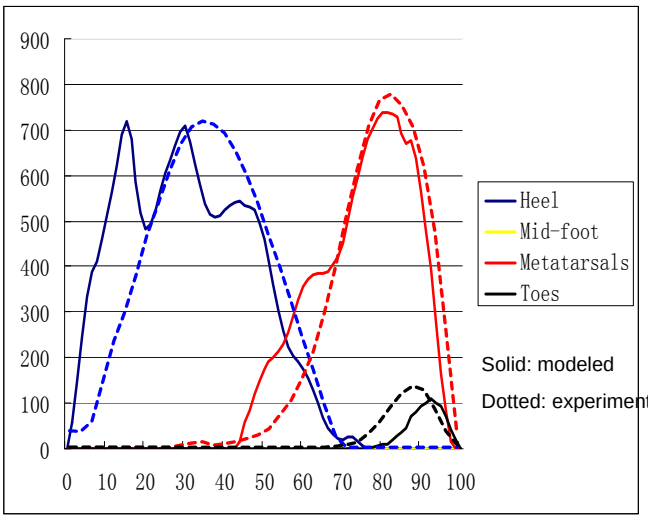

Figure 7.18: Contact force comparison between simulated results and experimental results (X axis: percentage of stance phase; Y axis: force values)

Comparison is also made between simulated ankle joint motion and experimental joint motion as shown in Figure 7.19. The pattern is very similar. The small differences might due to joint stiffness and damping settings in the model. Thus the modeling with LifeMOD is an effective method for foot behavior study during normal walking and can provide good kinetics and kinematics information.

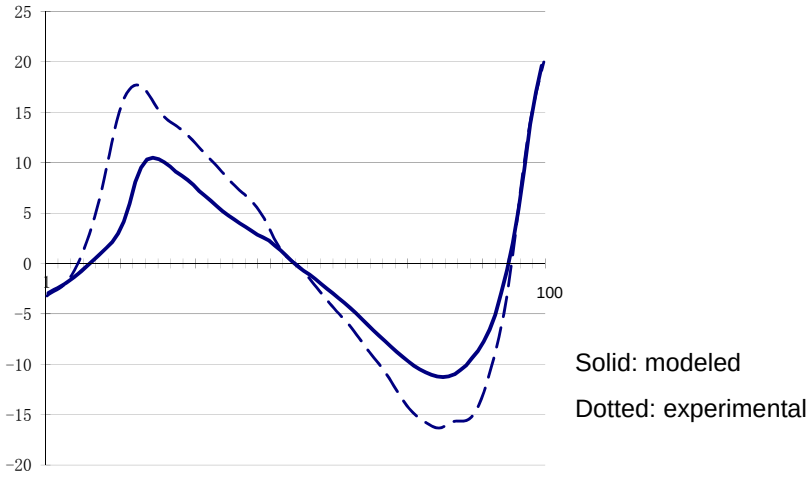

Figure 7.19: Ankle joint motion comparison between simulated results
(X axis: percentage of stance time; Y axis: degree)

7.3.3 Data analysis for normal walking

Previous section shows the simulated results by the model built from LifeMOD, and the results match reasonable well with experiment data. LifeMOD modelling and simulation could provide a better visualised interface for interpreting the foot segment features, combing foot kinetics and kinematics features. The kinematic features in discussion include joint rotation angles in sagittal, coronal, and transverse planes. The kinetic features in discussion involve the forces under foot segments of heel, mid-foot, metatarsal and hallux. Changes of each kinematic feature will be analyzed with respect to the changes of kinetic features. The relationship between foot segment features could be better understood.

SHANK – HEEL (Sagittal)

In Figure 7.20, the plot of Shank-Heel sagittal plane angle feature versus contact forces is presented. Before the mid-stance time, the force is mainly exerted on the heel segment. The maximum plantar-flexion of the heel segment happens near the time when the heel force reaches its peak value. The maximum dorsi-flexion of the heel segment happens near the time when the metatarsal segment's force reaches its peak value. In Figure 7.21 (a), the force on the heel reaches maximum value just before the left foot reaches mid-stance (MS). This phenomenon shows the heel segment is more responsible for absorbing the weight of the body at this moment. The force on the metatarsal starts to gradually increase just after MS as shown in Figure 7.21 (b). This is because the center of gravity (CG) of the body now has been shifted continuously forward.

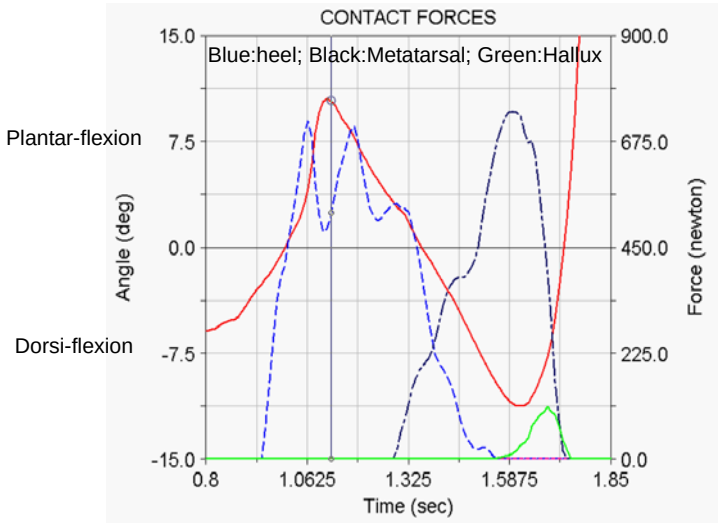

Figure 7.20: Shank-Heel sagittal plane angle feature (red line) VS contact forces

In Figure 7.21 (c), after the heel off (HO) position of the left foot, the dorsi-flexion is reaching its maximum. In this moment, force on the metatarsal is increasing towards its peak value, because at this moment the only contact with the ground is mostly on the metatarsal. This means that the whole body weight is now acting on the metatarsal as it counters the forces from the ground. In addition, the

forward acceleration of the whole body is also produced from this contact face. Thus the motion features' changes are corresponding to the pressure/force features' changes.

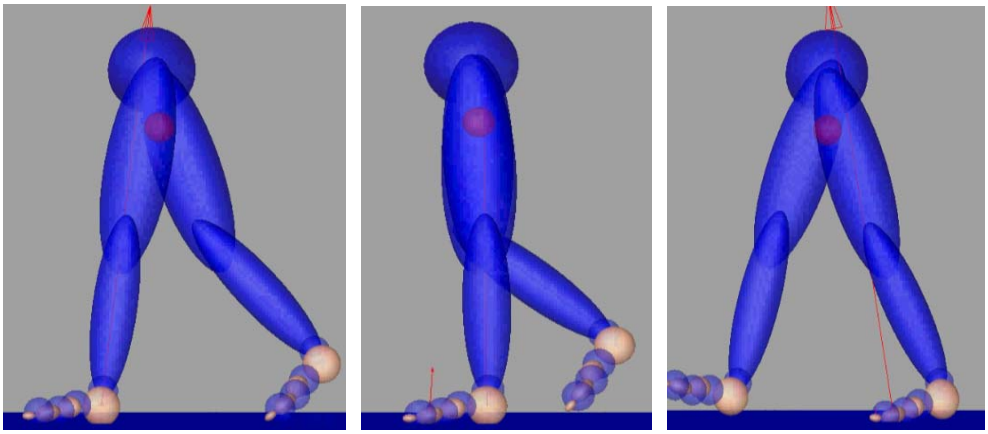

(a) (b) (c)

Figure 7.21: Foot and ankle motion before mid-stance, at mid-stance and after mid-stance

The force on the hallux starts to increase gradually as it is propelling the left foot forward and it will start to decrease when the right foot is ready in contact with the ground. The decrease in pressure on the hallux shows that weight is being shifted to the right foot and the left foot is at the toe off (TO) period of the stance phase.

SHANK – HEEL (Coronal)

In the coronal plane, the Shank-Heel angle feature pattern versus the contact forces is shown in Figure 7.22. Eversion starts to increase gradually as the force acting on the metatarsal increases as shown in Figure 7.22 and Figure 7.23. Due to eversion, the forces acting on the foot mainly fall on the medial foot side. Whereas for the elderly population, it usually occurs on their lateral side. In that case, the eversion might be smaller than the young healthy people's.

Before the TO phase, inversion occurs when the pressure on the hallux starts to decrease. The foot is supinating at TO. Inversion causes the hallux to shift upwards as the foot is going to TO, reducing the contact from the ground. As a result, the force on

the Hallux decreases.

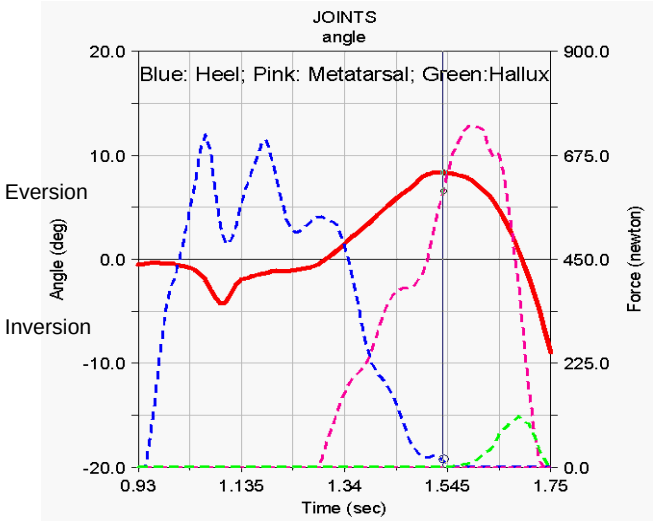

Figure 7.22: Shank-Heel coronal plane angle feature (red line) VS contact forces

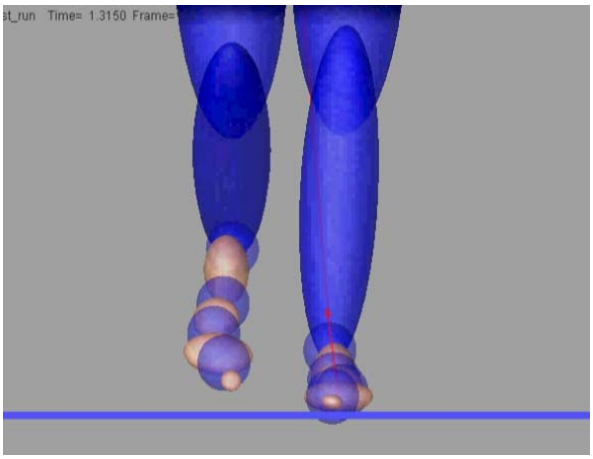

Figure 7.23: Eversion starting to occur

SHANK – HEEL (Transverse)

At the mid-stance, the heel transverse plane angle feature is in neutral as shown in Figure 7.24. In the figure, the adduction and abduction are referring to the angles at the mid-stance. After the TO phase, the heel starts to adduct (abduction decreases) slightly. Force on the metatarsal is decreasing because the foot is getting ready for push off, and the contact to the ground is slowly being transferred to the hallux. Hence force on the hallux increases as the force on metatarsal decreases. Then the heel continues to be adducted and force on the hallux decreases at toe off.

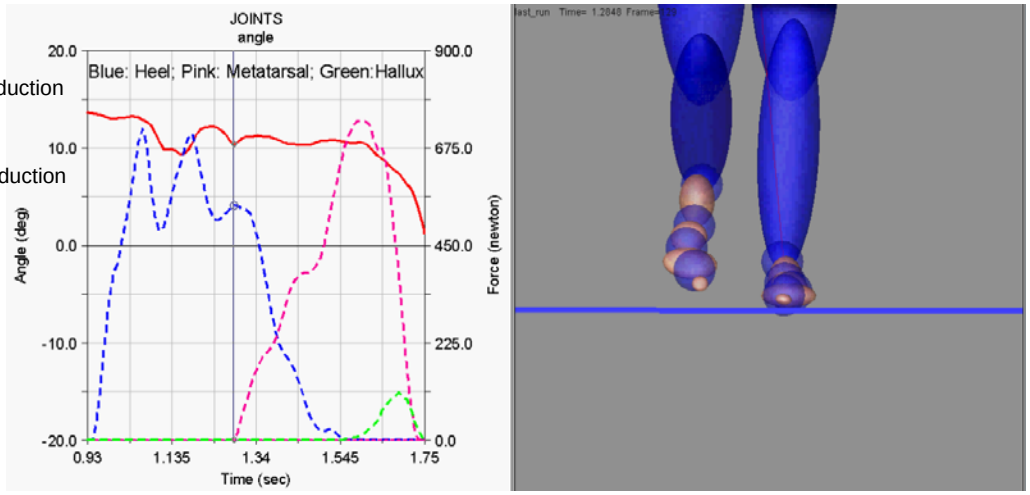

Figure 7.24: Foot is nearly neutral in the transverse plane

HEEL – MIDFOOT (Sagittal)

Figure 7.25 represents the Heel-Midfoot sagittal plane angle feature versus ground reaction forces on foot segments, with the line in red for the joint rotation angle, and the rest of the colors are the forces for heel (blue), metatarsal (pink) and hallux (green). At HO, dorsi-flexion occurs on the mid-foot relatively to the heel. There is an increase in the hallux's force. As the dorsi-flexion angle of mid-foot relative to the heel decreases, forces on the hallux decreases as well. This may indicate that the heel and mid-foot sagittal plane angle influence the hallux segment force.

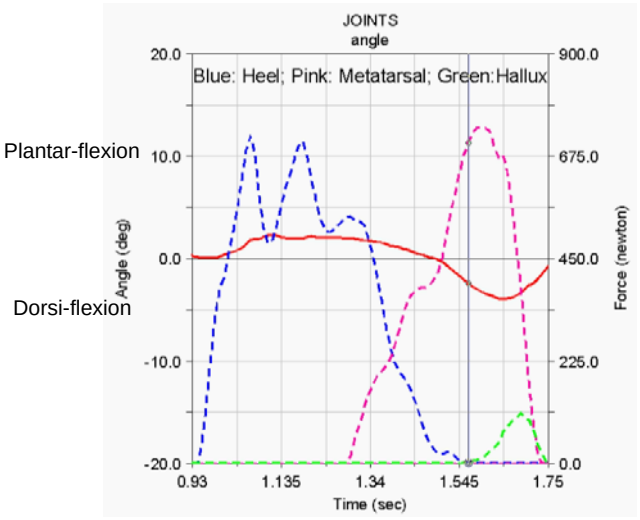

Figure 7.25: Heel-Midfoot sagittal plane angle feature (red line) VS contact forces

HEEL – MIDFOOT (Coronal)

In Figure 7.26, the Heel-Midfoot coronal plane angle feature does not show any significant phenomenon throughout the whole stance. Results give an almost constant reading.

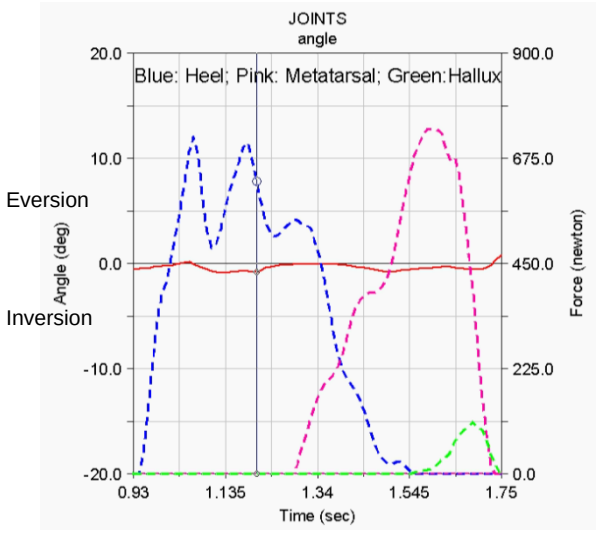

Figure 7.26: Heel-Midfoot coronal plane angle feature (red line) VS contact forces

HEEL – MIDFOOT (Transverse)

Just before TO, the mid-foot is adducting slightly. Simultaneously, the force on the hallux also decreases. However, the angle changes are small.

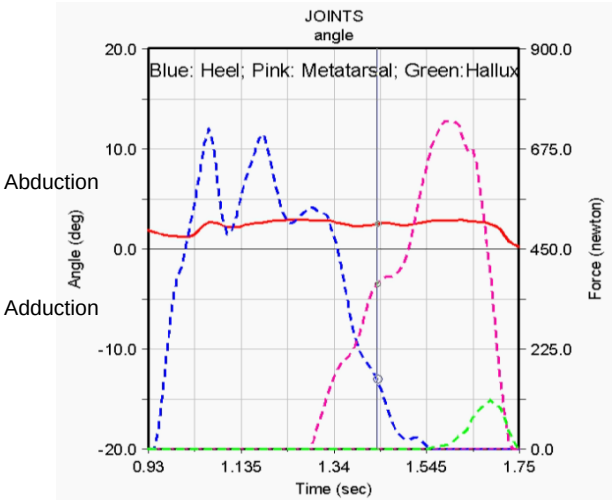

Figure 7.27: Heel-Midfoot transverse plane angle feature (red line) VS contact forces

MIDFOOT - METATARSAL (Sagittal)

Figure 7.28 represents the Midfoot-Metatarsal sagittal plane angle feature versus ground reaction forces on foot segments. When the metatarsal is initially contacting the ground, the foot is still plantar-flexed, as well as the sagittal plane midfoot-metatarsal angle, shown in Figure 7.29. The plantar-flexion starts to decrease because the metatarsal segment starts contacting with the ground with respect to the mid-foot, simultaneously force on the metatarsal and hallux starts to increase.

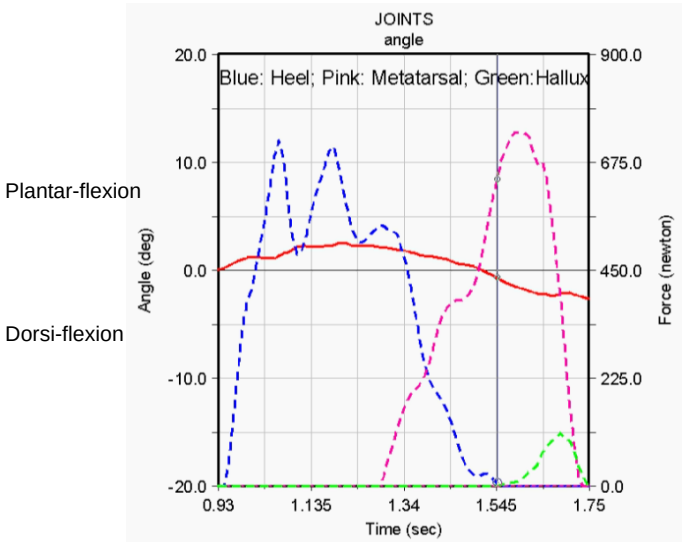

Figure 7.28: Midfoot-Metatarsal sagittal plane angle feature (red line) VS contact forces

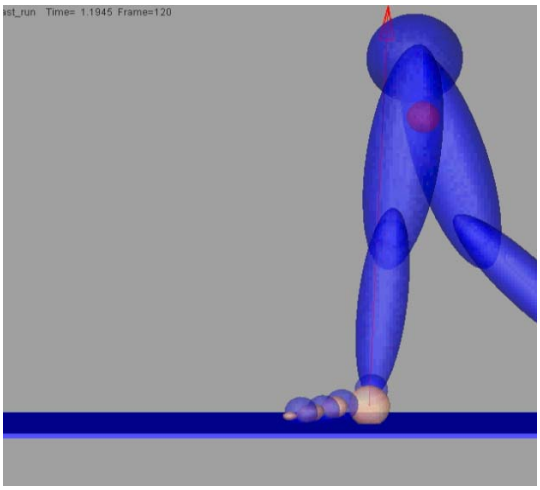

Figure 7.29: Metatarsal initial contact with ground

MIDFOOT - METATARSAL (Coronal)

An almost constant reading in the Midfoot-Metatarsal coronal plane angle feature

throughout the stance is shown in Figure 7.30. The mid-met coronal plane angle keeps almost constant throughout the phase. There are no noticeable changes for this angle feature during the whole stance phase.

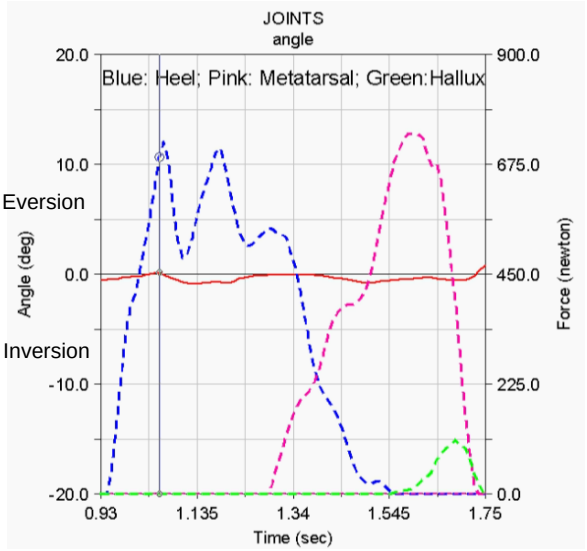

Figure 7.30: Midfoot-Metatarsal coronal plane angle feature (red line) VS contact forces

MIDFOOT - METATARSAL (Transverse)

This Midfoot-Metatarsal transverse plane angle feature versus contact forces under foot segments are shown in Figure 7.31. The pattern is similar with the Heel-Midfoot transverse one. The angle changes are smaller than 5 degree.

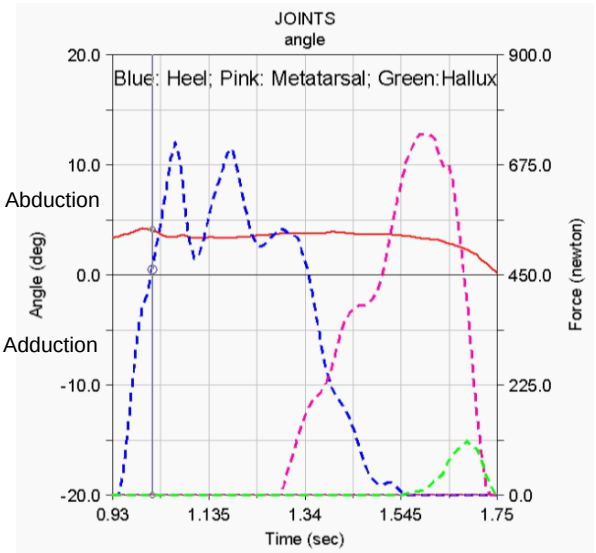

Figure 7.31: Midfoot-Metatarsal transverse plane angle feature (red line) VS contact forces

METATARSAL – HALLUX (Sagittal)

The sagittal plane angle feature between metatarsal and hallux is presented in Figure 7.32. At MS, when the hallux starts to be dorsi-flexed gradually in Figure 7.33, the force on the metatarsal starts to increase gradually. Even though the hallux is in contact with the ground, the force on the hallux is negligible.

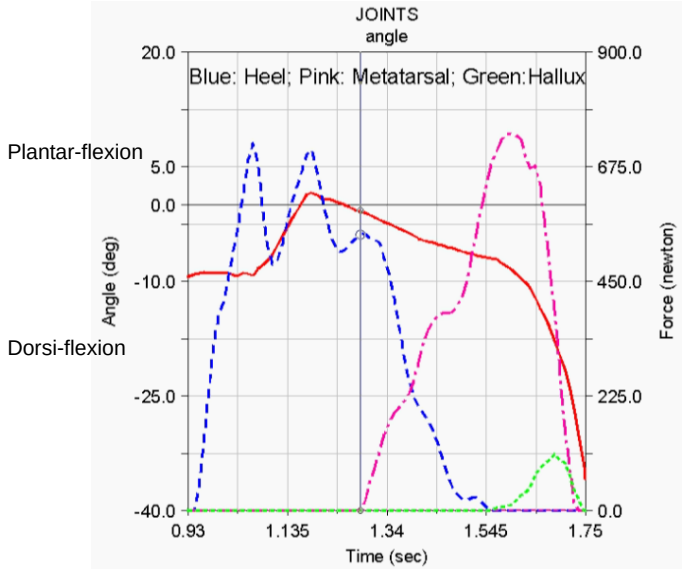

Figure 7.32: Metatarsal-Hallux sagittal plane angle feature (red line) VS contact forces

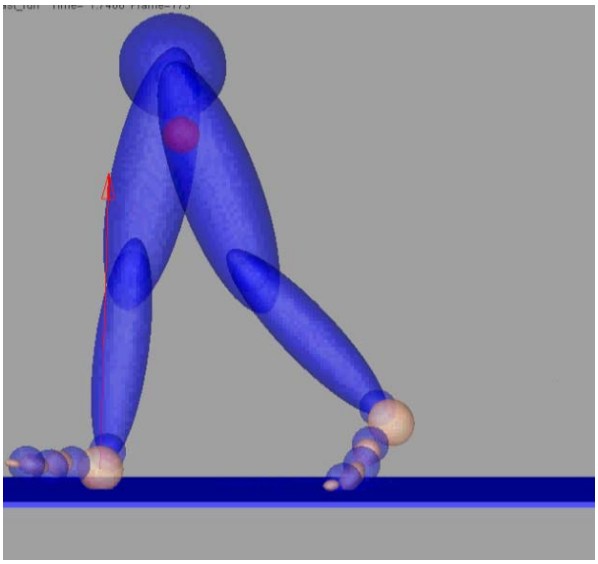

Figure 7.33: Dorsiflexion at maximum on Hallux before TO

After HO, as the gradient in the dorsi-flexion starts to increase significantly, the

force on the hallux also begins to increase gradually from zero. Just slightly before the TO, the dorsi-flexion of the hallux is at maximum as shown in the Figure 7.32 and 7.33. This phenomenon is due to the necessary push-off required by the hallux to propel the foot forward. The metatarsal-hallux dorsi-flexion feature greatly influences the metatarsal force and hallux force.

7.3.4 Discussion of the normal walking model

Through LifeMOD modeling, the foot segment motion features and corresponding foot segment contact forces during normal walking could be well visualized and investigated. The relationship between foot motion features (joint rotation angles) and foot segment forces could be better understood.

From the normal walking, it is observed that the foot motion is rather flexible and relaxed. The force acting on the various segments of the foot appears to be well distributed. The foot tends to be generally in plantar-flexion at heel strike. The maximum shank-heel plantar-flexion at heel strike is accompanying peak force on the heel segment. The maximum shank-heel dorsi-flexion and maximum heel-mid dorsi-flexion happens near the time when the peak metatarsal force occurs. Different foot segments are collaborating with each other. Heel-mid sagittal plane angle feature changes in the dorsi-flexion after heel off, and this accompanies with the changes in the hallux force. Large metatarsal-hallux sagittal plane angle occurs at heel off and toe off. At mid-stance, when the hallux starts to be dorsi-flexed gradually, the force on the metatarsal starts to increase gradually. After heel off, as the gradient in the dorsi-flexion starts to increase significantly, the force on the hallux also begins to increase gradually from zero. Thus this angle feature pattern could influence the metatarsal force and hallux force.

In the coronal plane, the heel goes from inversion to eversion, then inversion

during the stance phase. The eversion happens concurrently with the increased metatarsal force, and thus has some effect on the pattern of the metatarsal force. The inversion occurs at toe off phase and leads to the decreased force on the hallux, to some extent. In the transverse plane, the shank-heel coronal plane angle feature got adducted at toe off phase, and the hallux force also decreases.

In conclusion, a multi-segment foot model is built with LifeMOD for the foot segment motion and segment force analysis. Clearer relationship between foot kinetic features and kinematic features during normal walking are understood with the lifeMOD model.

7.4 LifeMOD modeling for walking with dragging weights

To better understand foot kinematic and kinetic behavior during walking, another case is studied in LifeMOD. Walking with dragging weights is considered as one less stable walking condition, which also has many similar phenomena with the walking of elderly population [116]. In the next part, a walking model with dragging weights will be developed with LifeMOD.

7.4.1 Build a LifeMOD model for walking with dragging weights

The modeling process is same with the normal walking one. Just one more process of adding dragging weights is needed before the inverse dynamics simulation. The weights are added similar with the weights during experiments, which is 2.45kg. Individual contacts between weights and ground are to be built. The dragging weights are added as shown in Figure 7.34. The size of the dragging weights is modeled as 8 cm wide, 12 cm long and 3.5 cm high.

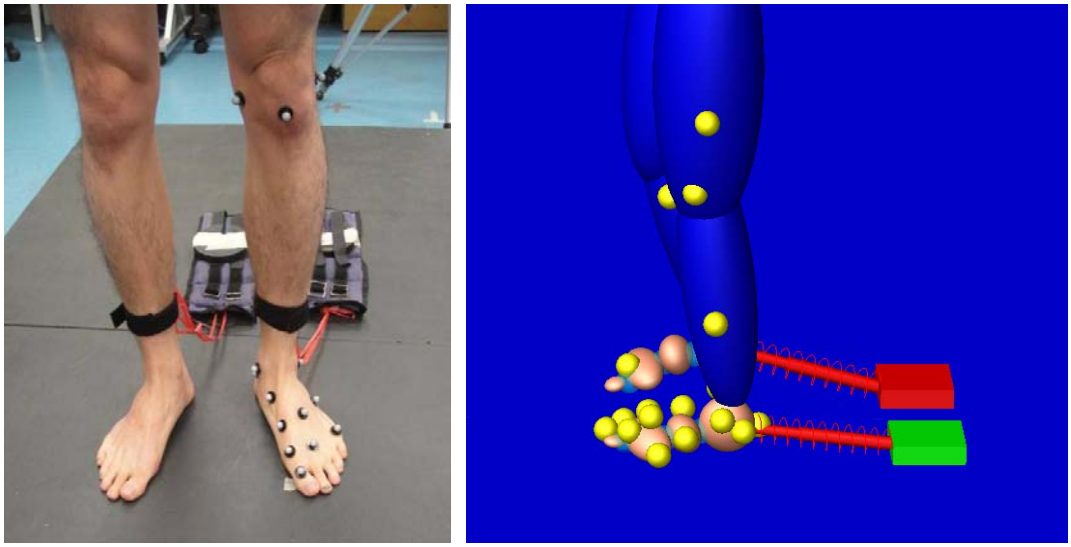

Figure 7.34: Walking with dragging weights (Left: experiments; Right: LifeMOD modeling)

7.4.2 Simulation results for walking with dragging weights

Experimental force data of several walking trails with dragging weights are listed in the Appendix C for a better understanding of the typical segmental force pattern for the walking with dragging weights. For a typical walking with dragging weights, the forces are mainly exerted on the heel during the stance phase. There is nearly no push off force at the hallux at toe off phase.

Forces under each foot segments of the left foot for two subsequent strides are shown in Figure 7.35. A comparison between simulation results and experimental results are shown in Figure 7.36. The simulated and experimental contact forces under foot segments have quite similar pattern. Comparison is also made between simulated ankle joint motion and experimental joint motion for the walking with dragging weights as shown in Figure 7.37. The modeled ankle angle also has similar pattern with experiment measured ankle angle. The ankle angle range of motion is much smaller than the normal walking one. This result agrees with the observation also, the ankle is more rigid during dragging weights.

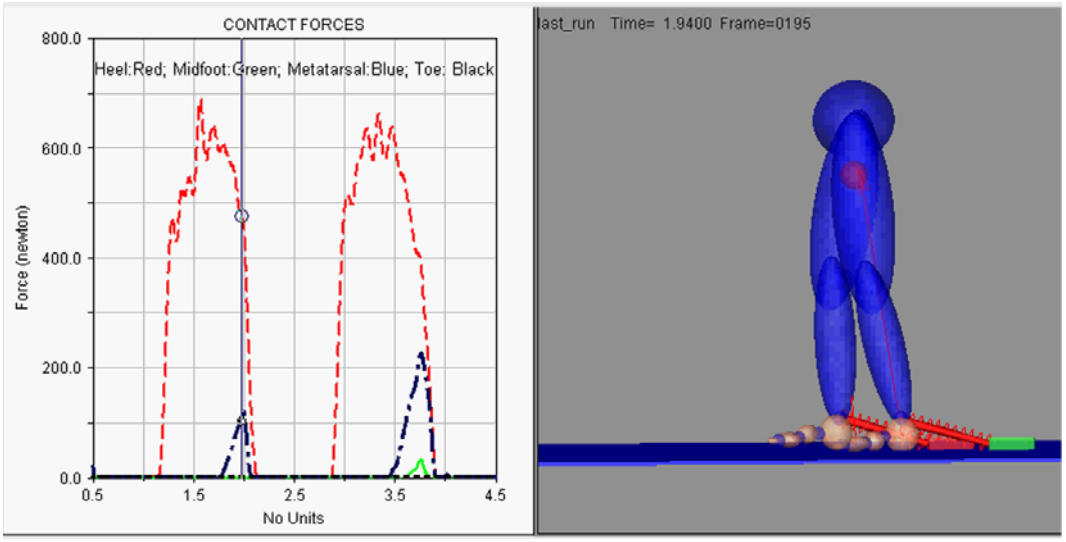

Figure 7.35: Walking with dragging weights simulation result for contact forces of refined foot model

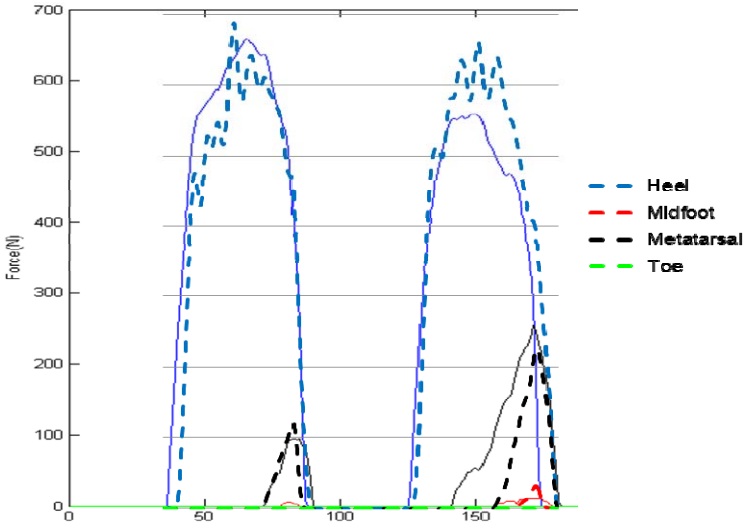

Figure 7.36: Contact force comparison between simulated results (Dotted) and experimental results (Solid) (X axis: time steps; Y axis: force values)

For simulation of both normal walking and walking with dragging weights, the modeled ankle joint motion ROM is smaller than the experimental one. This could be because of the joint stiffness differences between the model and the tested subject.

In summary, the modeling with LifeMOD is an effective method for foot behavior study and can provide good kinetics and kinematics information.

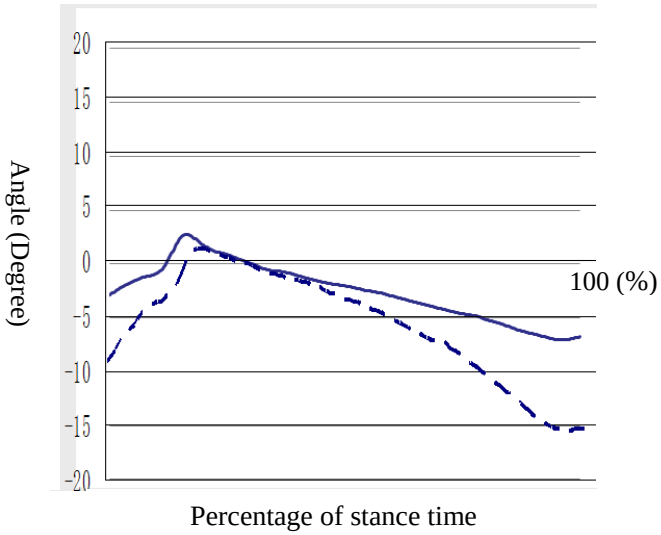

Figure 7.37: Ankle joint motion comparison of one stance between simulated results (solid) and experimental results (dotted) for walking with dragging weights

7.4.3 Data analysis for walking with dragging weights

The force patterns between foot segments and ground are quite different with the one in normal walking. The forces mainly exerts on the heel and metatarsals. There is also force on the mid-foot for dragging weights walking, which is more than the force on the mid-foot for normal walking. That may indicate that tested subject have more lateral deviation during walking with dragging weights and encounters more unstable walking. Because the force is very small and random on the mid-foot, attention is mainly put on the forces under the heel and metatarsals. Changes of each kinematic feature will be analyzed with respect to the changes of kinetic features. The relationship between foot segment features could be better understood.

SHANK – HEEL (Sagittal)

In Figure 7.38, the Shank-Heel sagittal plane angle feature and contact forces under foot segments are plotted. At the HS phase, the heel is slightly plantar-flexed relative to the shank. At heel strike, the force acting on the heel starts to increase. This motion is almost similar to the normal walking; however, the range of motion is much

smaller than in normal walking. This is possibly because the weights being strapped to ankle restricts the foot motion. The dragging weights also influence the muscle activities and thus bring less stability to the walking.

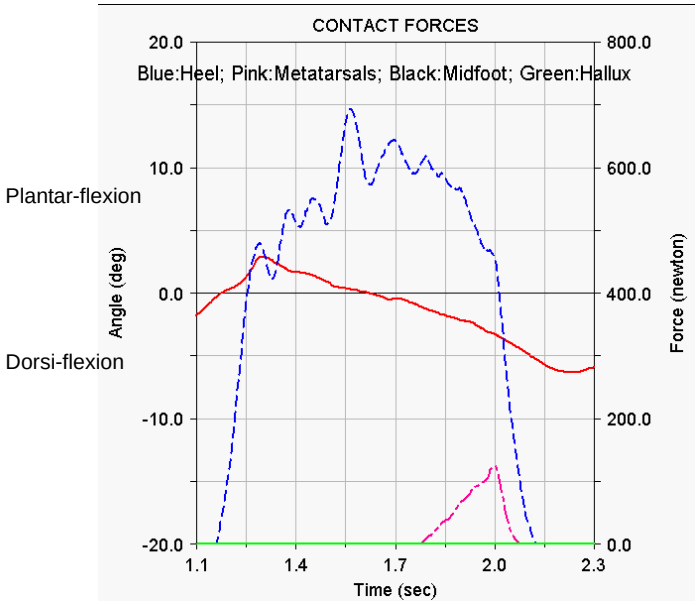

Figure 7.38: Shank-Heel sagittal plane angle feature (solid, red line) VS contact forces (Walking with Weights)

Figure 7.39 (a) presents the model at HS phase and the heel is slightly plantar-flexed. In Figure 7.39 (b), the graph shows that the force on the heel is at its maximum at mid-stance. The presences of the weights have made motion to be less stable and the muscles in the foot segment are constantly working hard. At the MS, the right foot is positioned beside the left foot. The entire weight of the body is now supported by the left foot and particularly the left heel is absorbing most of the reacting forces from the ground. Little force is acting on the metatarsal yet. However, the force on the metatarsal starts to increase just after MS for the normal walking. This could be because of the more controlled and rigid foot with very stiff and rigid ankle during the walking with dragging weights.

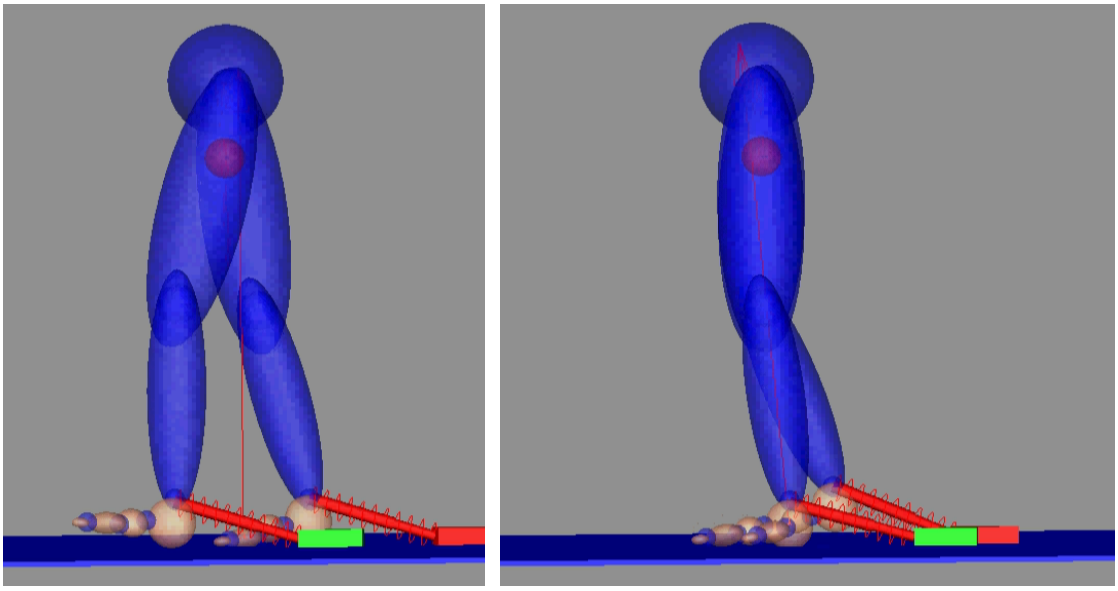

(a) (b)

Figure 7.39: Left foot at Heel Strike and Mid-stance (Walking with weights)

SHANK – HEEL (Coronal)

The Shank-Heel coronal plane angle feature and contact forces are plotted in Figure 7.40. Generally the angle changes are small. After the MS, eversion starts to occur and continues to increase as shown in Figure 7.41. During the eversion phase, the force of contact between the metatarsal and the ground increases gradually. This phenomenon is similar with the normal walking one, and larger heel eversion might contribute to larger force on metatarsals.

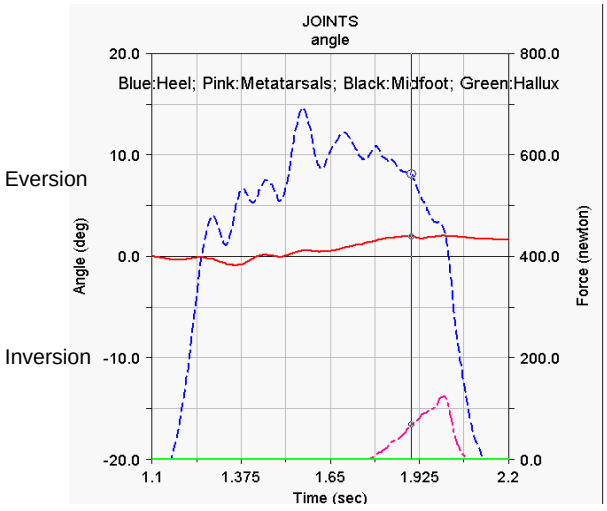

Figure 7.40: Shank-Heel coronal plane angle feature (solid, red line) VS contact forces (Walking with Weights)

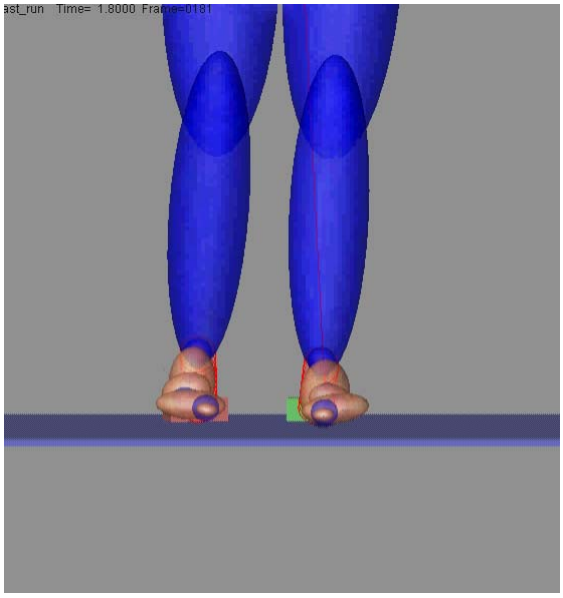

Figure 7.41: Heel eversion after MS (Walking with Weights)

SHANK – HEEL (Transverse)

In Figure 7.42, the shank-heel transverse plane angle feature was relatively constant with a small range of motion. This could also indicate the more rigid and controlled foot during walking with dragging weights.

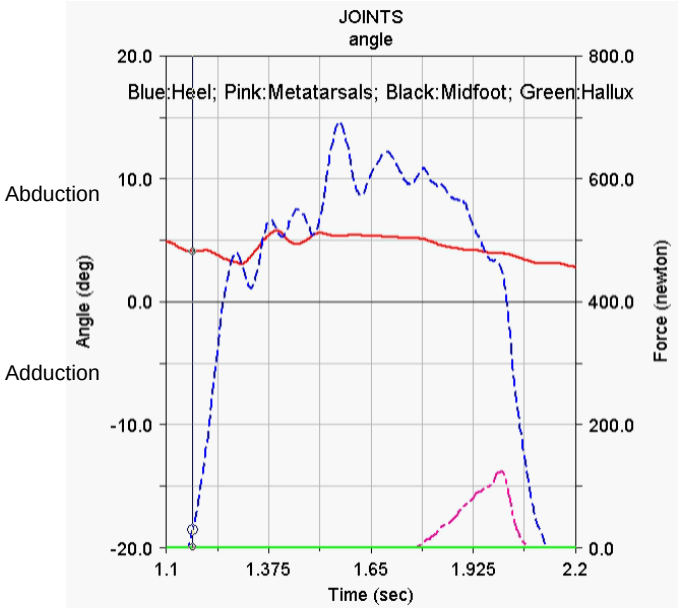

Figure 7.42: Shank-Heel transverse plane angle feature (solid, red line) VS contact forces (Walking with Weights)

HEEL – MIDFOOT (Sagittal)

Figure 7.43 presents the Heel-Midfoot sagittal plane angle feature pattern versus the contact forces under foot segments during walking with dragging weights.

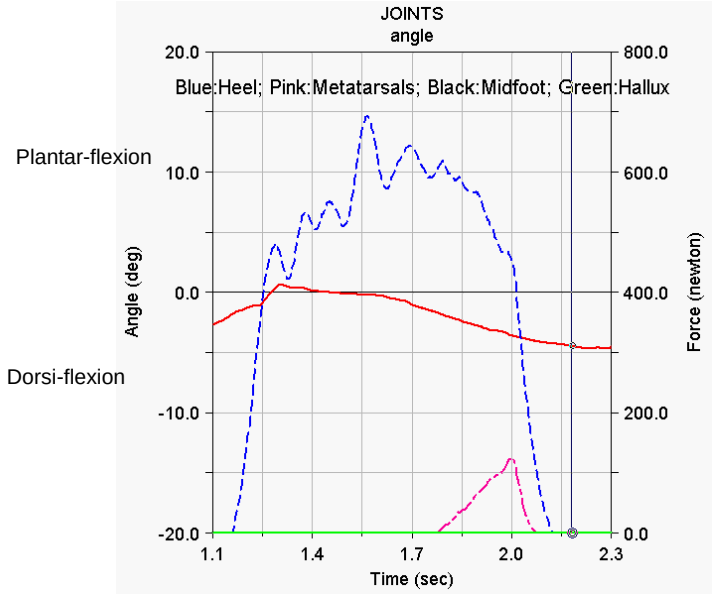

Figure 7.43: Heel-Midfoot transverse plane angle feature (solid, red line) VS contact forces (Walking with Weights)

It is different with the normal walking, where the mid-foot is in plantar-flexion at the heel strike. For walking with dragging weights, the body needs to be slightly pushed forward to lead the weights ahead and to be in a stable and more comfortable position. After the MS phase, the mid-foot gradually increases in dorsi-flexion. This phenomenon is similar with the shank-heel sagittal plane angle.

HEEL – MIDFOOT (Coronal)

Shown in Figure 7.44, the Heel-Midfoot coronal plane angle range of motion is very small, smaller than five degrees. Similar with the normal walking, there is actually a transition in the coronal plane angle from inversion to eversion and then back to inversion. Near the time when eversion has reached its peak, the force on the metatarsal starts to increase.

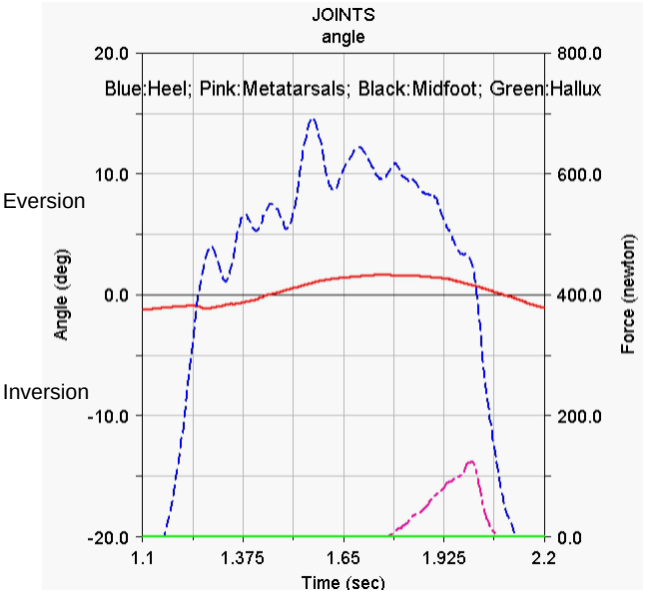

Figure 7.44: Heel-Midfoot coronal plane angle feature (solid, red line) VS contact forces (Walking with Weights)

HEEL – MIDFOOT (Transverse)

Similarly as the shank-heel transverse plane angle feature, the Heel-Midfoot transverse plane angle keeps almost constant throughout the phase. This could also indicate the more rigid and controlled foot during walking dragging weights.

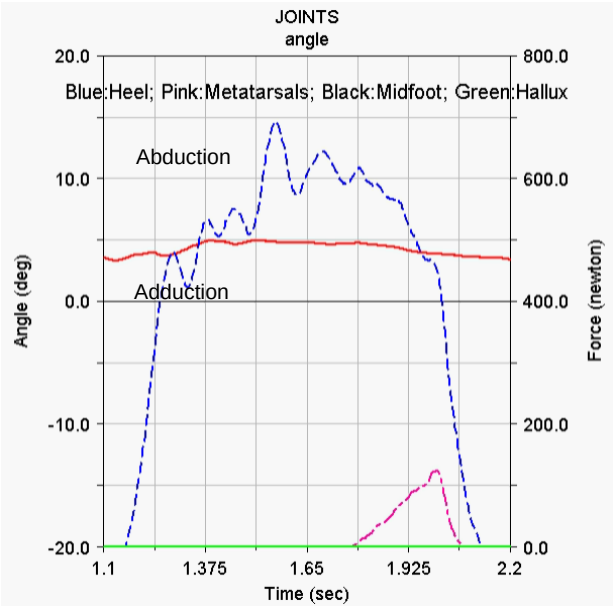

Figure 7.45: Heel-Midfoot transverse plane angle feature (solid, red line) VS contact forces (Walking with Weights)

MIDFOOT - METATARSAL (Sagittal)

Because of the dragging weights effect, the foot is very stiff and rigid. This is to help maintain the stability of the foot. The Midfoot-Metatarsal sagittal plane angle ROM is very small, around 3 degrees, seen in Figure 7.46.

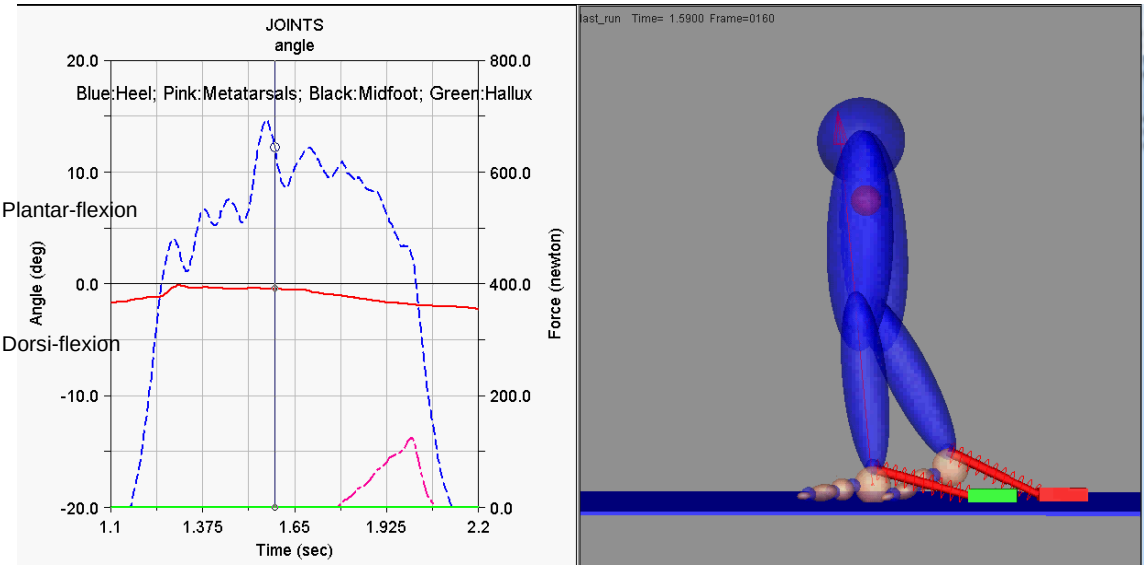

Figure 7.46: Midfoot-Metatarsal sagittal plane angle feature (solid, red line) VS contact forces (Walking with Weights)

The force on the metatarsal would only start to take effect when the right foot has crossed the path of the left foot. From the force pattern, it indicates that the heel is exerting more prominent function during the whole stance phase for walking with dragging weights. The heel takes most of the force, and the metatarsal shares some of the force for balance and distribution, shown in Figure 7.47.

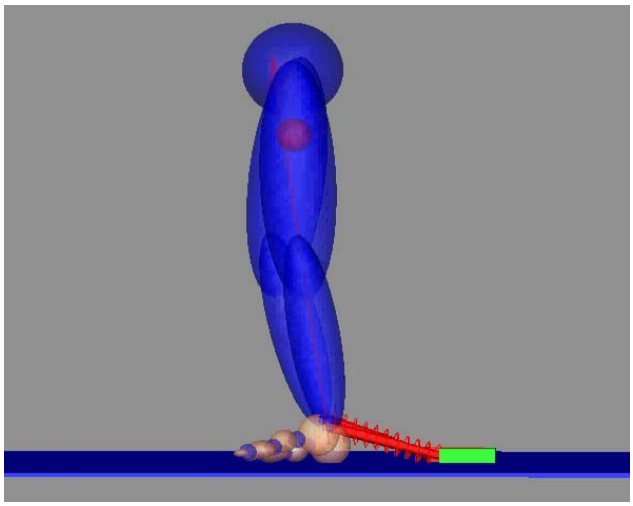

Figure 7.47: Force distribution on the left foot near mid-stance (Walking with Weights)

MIDFOOT - METATARSAL (Coronal)

As in Figure 7.48, the Midfoot-Metatarsal coronal plane angle ROM is very small, around 2 degrees. At HS, slight inversion starts to gradually decrease until MS. The inversion starts to increase again at TO.

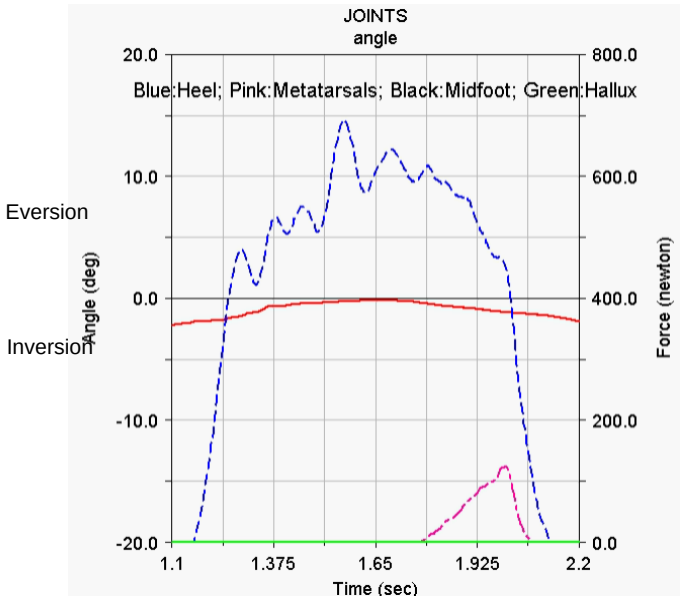

Figure 7.48: Midfoot-Metatarsal coronal plane angle feature (solid, red line) VS contact forces (Walking with Weights)

MIDFOOT - METATARSAL (Transverse)

In Figure 7.49, results show almost constant angle value throughout the stance. Thus there are no noticeable changes for the Midfoot-Metatarsal transverse plane angle feature. This could reflect that the foot is rigid and controlled during walking with dragging weights.

METATARSAL – HALLUX (Sagittal)

There is no significant change in rotational angle in the hallux throughout the whole stance as shown in Figure 7.50. The tested subject is concentrating on dragging the weights ahead, which depends more on the hind-foot. Thus hallux was involved very little throughout the stance. Smaller push off force is a similar phenomenon which also happens in the walking of elderly population. The angle pattern depends not only

on the motion imported to the model, but also depends on the joint stiffness defined to the model. The joint stiffness could influence the extent of the model's following the driving motion data.

Compared with normal walking, the walking with dragging weights tends to weight more on the heel. This coincides with the dragging effect. The ankle range of motion is significantly reduced.

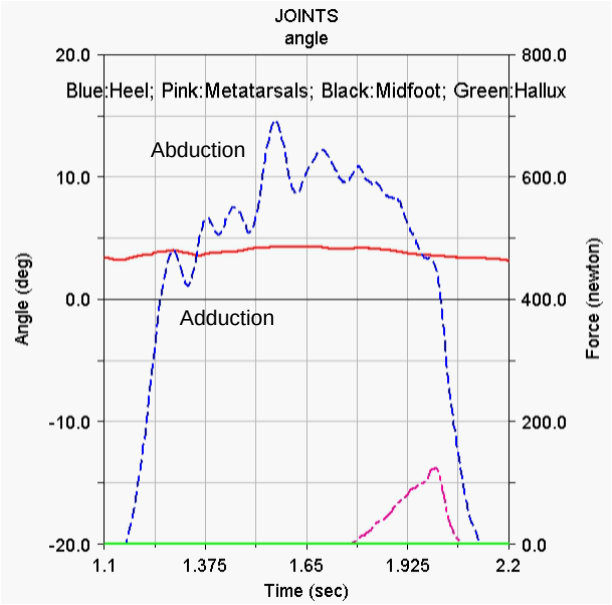

Figure 7.49: Midfoot-metatarsal transverse plane angle feature (solid, red line) VS contact forces (Walking with Weights)

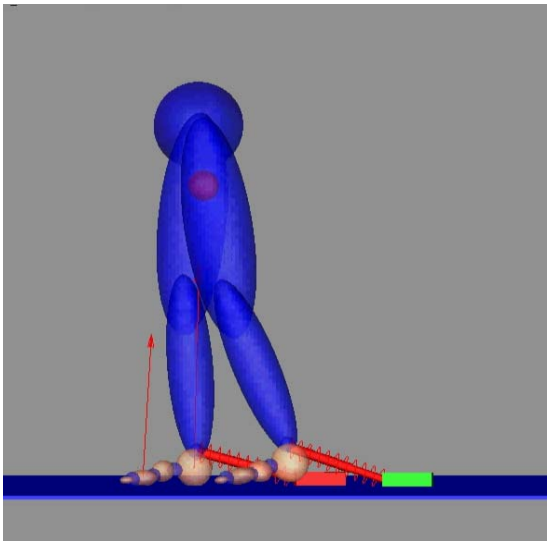

Figure 7.50: Hallux, metatarsal and mid-foot during TO

7.4.4 Discussion of the dragging weights walking model

Through LifeMOD modeling, the foot segment motion and corresponding foot segment contact forces during dragging weights walking could be well visualized and investigated. For the walking with dragging weights, the force on the heel takes up about 80% of the force and around 20% of the force by the metatarsal. This shows the heel plays a very crucial role in this type of walking condition. It is also observed that the position of the body seems to be slightly hinged forward. Most the time, the foot tends to be in dorsi-flexion and hardly any plantar-flexion in all stances. Due to the dragging of the weights, this position actually helps to maintain stability during walking and help in the aid of propelling the foot forward. Similar with the normal walking, the maximum heel dorsi-flexion also happens with the increased force on metatarsals. In the coronal plane, the foot motion is also from inversion to eversion and inversion again during stance; however, the range of motion is much smaller than the normal walking one. Lastly, because the foot is dragging the weights, the foot naturally becomes rigid controlled and stiff. Compared with the normal walking, the heel segment exerts more function for the walking with dragging weights. In addition, the kinematic features' ROM reduces for better stabilization during walking with dragging weights.

7.5 Summary

The multi-segment foot models are developed and simulated with LifeMOD models for normal walking and walking with dragging weights. Kinematic segment motion data is imported to the model and the kinetic segment force data are regarded as the output. Simulation results of foot segment forces are quite comparable with experiment data. The model is proved to be a good tool for linking the foot kinetics and kinematics. The relationship between foot motion features (joint rotation angles)

and foot segment forces could be better understood.

From the normal walking, it is observed that the segment foot motion is rather flexible and relaxed. The force acting on the foot segments appears to be well distributed and not biased. For the walking with dragging weights, the force on the heel segment takes up about 80% of the total force, and around 20% of the total force is shared by the metatarsal segment. This shows the heel segment plays a very crucial role in this type of walking condition. During the walking with dragging weights, the foot naturally becomes rigid controlled and stiff.

In conclusion, LifeMOD modeling and simulation could be a useful tool for investigating the foot kinetics and kinematics simultaneously during different walking conditions. A detailed multi-segment foot model is built with LifeMOD, and the multi-segment foot model can output forces under each foot segment. Thus relationship between foot segment motions and foot segment forces is possible to be studied with the model. Features of both foot kinetics and kinematics and their relationship could be better visualized. The multi-segment foot model built with LifeMOD provides a new perspective of understanding foot segment behavior characteristic. The foot segment kinematics information is well linked with the segment foot kinetics information. Another advantage of LifeMOD is its function of adding environment contacts. With the established foot model, various dynamic behaviors in various environments could be modeled and simulated. In addition, the LifeMOD modeling process is quite standard and could be easily implemented. The multi-segment foot model built in this study could possibly function as a toolbox in LifeMOD for the relationship between segment foot kinetics and kinematics.

CHAPTER 8 CONCLUSIONS AND FUTURE WORKS

8.1 Conclusions

The objective of this thesis is to study the foot behavior during walking based on foot kinetics and kinematics; to extract useful foot dynamic features from foot pressure and foot motion, and to model the foot dynamics with LifeMOD. Useful features obtained from the foot dynamic behavior study could help to indicate normal and pathological gait, and will benefit clinical problems related to walking problems or foot dysfunctions. For this objective, this thesis extracted features from foot kinetics and kinematics for the foot behavior characteristics during walking. For the foot kinetics, pressure features are extracted for the whole foot pressure function and multi-segment foot pressure function. Then these features' effectiveness is checked through designed walking conditions. For the foot kinematics, foot motion features are extracted to describe the whole foot motion characteristics and multi-segment foot motion characteristics. These features are then applied in different walking conditions for their effectiveness on foot behavior indication. For a better understanding of foot segment features, an innovative multi-segment foot model is built with LifeMOD biomechanics modeler to combine foot kinetic and kinematic features for foot segment behavior description and software realization.

Through this study, kinetic and kinematic features are extracted for the foot behaviour characteristics description. For the foot kinetics, useful foot pressure features that can effectively describe different walking conditions are extracted from plantar pressure patterns. Features that can describe the whole foot COP trajectory are firstly extracted, and the features that can indicate the whole foot pressure repeatability

between strides are proposed. From the foot plantar pressure analysis, among all the discussed features, AP-COP motion and NCSS can well indicate the walking stability differences. In addition, foot segment pressures under heel, mid-foot, metatarsals and toes are also calculated and discussed. For the foot kinematics, detailed foot segment motions are investigated and motion features are extracted for describing foot behavior characteristics, from the whole foot motion perspective and the segment foot motion perspective. A standard method and proposed features for detailed foot motion measurement is developed for normal walking. Joint motions between sub-defined foot segments are firstly measured with a multi-segment foot model as the motion features. The results of the joint rotation angle feature patterns are generally consistent with previous studies. Consistency and repetition of joint rotation angle features are discussed according to ASD and CMC values. New dynamic reference positions are proposed as the foot mid-stance time positions during walking. The proposed reference positions perform well for variance reduction among subjects. In addition, functional angles are proposed for directly describing some foot mechanism during walking and regarded as motion features. The functional angles perform well for the whole foot behavior characteristics description and could be easier understood. The functional angles are not based on segments and sagittal, coronal and transverse planes, and could be more flexible and intuitive for understanding the whole foot mechanism.

Except the individual kinetic and kinematic features, the combined information of foot kinetics and kinematics could help to better understand foot dynamic behavior from a new perspective. A detailed foot model is built with four foot segments for simulation of normal walking condition and walking with dragging weights condition. Features of both foot kinetics and kinematics could be better visualized for each foot segment. For example, the maximum shank-heel dorsi-flexion and maximum heel-mid

dorsi-flexion happens near the time when the peak metatarsal force occurs. Each foot segment kinetic and kinematic features could be well investigated through the multi-segment foot model.

As to the author's knowledge, very few studies have been performed to investigate the detailed foot motions when subjected to less stable walking conditions. Thus this thesis applied the detailed foot motion features for describing less stable walking conditions. Different walking conditions (normal walking, walking on single beam, walking on double beams and walking with dragging weights) are designed to test the effectiveness of the proposed motion features for foot behavior characteristics. Results show that during less stable walking conditions, the features of push off power at toe off decreases significantly and most segmental joints' range of motion (ROM) reduces significantly. Heel-Met (fore-foot and hind-foot) sagittal plane motion could also be further investigated for walking stability. The hind-foot tends to have more function in stabilizing than the fore-foot. This study reveals how foot segments function when subjected to less stable walking conditions. To find an automatic and systematic method for data analysis and pattern recognition, adaptive fuzzy logic system trained by nearest neighborhood clustering is proposed. Compared with other pattern recognition methods, adaptive fuzzy logic system has the advantage of combining human expert knowledge and automatic machine training. Results show the proposed method is effective and reliable, and is able to automatically distinguish the four walking conditions. This also verifies that the proposed features can describe foot kinematics behavior characteristics.

Another focus of this thesis is the multi-segment foot model for segment foot behavior characteristics. Previously, the foot was always modeled as one rigid segment. In this study, an innovative mutli-segment foot model is built with LifeMOD

biomechanics modeler for investigating foot segment kinematic and kinetic features. Two walking conditions are modeled for comparison: normal walking and walking with dragging weights. The model integrated the foot segment motion and foot segment force. Changes of each kinematic feature are discussed with respect to the changes of kinetic features. Clearer relationship between foot kinetic features and kinematic features are understood with the lifeMOD model. The innovative multi-segment foot model is of acceptable reliability and complexity. The LifeMOD modeling process is quite standard and could be easily implemented. The multi-segment foot model built in this study could possibly function as a toolbox in LifeMOD for the relationship between segment foot kinetics and kinematics.

In conclusion, this study is a systematic and comprehensive study focused on the foot behavior during walking. Useful foot dynamic features are extracted to describe foot dynamic behavior from the study of foot kinetics (foot pressure), kinematics (foot motion analysis), and modeled the multi-segment foot dynamics with LifeMOD. This study could be beneficial in the design of rehabilitation training programs, prostheses and walking aids, etc. This study would possibly serve as a start point to achieve dynamic foot behavior/feature database for people with different walking styles and patients with foot problems or walking difficulties. The proposed fuzzy logic method is also potential to be applied to effectively and automatically distinguish more walking conditions in the database.

8.2 Future works

However, this study is a still at the start point. Many future works could be done. The proposed parameters from both foot pressure and foot motion are meaningful to describe walking features of a group of people, here young healthy subjects. For future study, obtained effective features (e.g.: NCSS, ankle dorsi/plantar-flexion ROM and

hallux push off angle) could be applied on different group of people, such as the elderly people and patients with risk of falls or foot dysfunctions. For specific group of patients, certain proposed features might be able to better indicate the walking characteristics than the other features. Data could be analysed and accumulated. Feature database could be set up and complemented with more groups of patients involved. For the most important and effective motion features, efforts could be put on obtaining these features without motion cameras. Instead, certain sensors (e.g. gyroscopes, accelerometers) could be applied to record these features. This could not only reduce costs, but also potential to be finally integrated in shoes for daily walking monitor. With the daily supervision, as long as the subject's walking is identified as abnormal, the subject could be warned to be more careful during walking, and could also go for clinics, or perform some physical rehabilitation to improve his/ her walking. This could also benefit the shoe design industry for multi-functional shoe design.

Foot pressure is not only dependent on the foot motion, but also influenced by the foot pat tissue, individual bone structure. In future study, these factors could be considered to improve the fidelity. For the LifeMOD modelling, besides the normal walking and walking with dragging weights situations, many other conditions could also be modelled and investigated. Models could also be refined with adding muscles, tendons and ligaments. Special LifeMOD model could also be built and applied for specific clinical requirement. Walking styles of any group of patients with foot dysfunctions could be imported to LifeMOD to train the model during inverse dynamics simulation. This could be very helpful to understand the whole body mechanism, reaction and consequences for certain walking problems.

Hopefully this project would be able to help the society by providing a relatively standard and thorough method for investigating dynamic foot behaviour characteristics, and being able to help people determine if they have any walking problems in future. However, much further work could be done to make the project more justifiable and reliable. Additionally, there would always be room for improvements.

REFERENCES

1. Weatherall, M., *Multifactorial risk assessment and management programmes effectively prevent falls in the elderly.* Evidence-Based Healthcare and Public Health, 2004. **8**(5): p. 270-272.
2. Aminian, K., et al., *Evaluation of an ambulatory system for gait analysis in hip osteoarthritis and after total hip replacement.* Gait & Posture, 2004. **20**(1): p. 102-107.
3. Chaler, J., et al., *Suspected feigned knee extensor weakness: Usefulness of 3D gait analysis. Case report.* Gait & Posture. **32**(3): p. 354-357.
4. Santos-Rocha, R. and A. Veloso, *Comparative study of plantar pressure during step exercise in different floor conditions.* Journal of Applied Biomechanics, 2007. **23**(2): p. 162-168.
5. Leardini, A., et al., *Rear-foot, mid-foot and fore-foot motion during the stance phase of gait.* Gait and Posture, 2007. **25**(3): p. 453-462.
6. Jenkyn, T.R. and A.C. Nicol, *A multi-segment kinematic model of the foot with a novel definition of forefoot motion for use in clinical gait analysis during walking.* Journal of Biomechanics, 2007. **40**(14): p. 3271-3278.
7. Pont, M.-P., et al., *Cutaneous sensory nerve injury during surgical approaches to the foot and ankle: A cadaveric anatomic study.* Foot and Ankle Surgery, 2007. **13**(4): p. 182-188.
8. Bus, S.A., J.S. Ulbrecht, and P.R. Cavanagh, *Pressure relief and load redistribution by custom-made insoles in diabetic patients with neuropathy and foot deformity.* Clinical Biomechanics, 2004. **19**(6): p. 629-638.

9. Chen, H., B.M. Nigg, and J. de Koning, *Relationship between plantar pressure distribution under the foot and insole comfort.* Clinical Biomechanics, 1994. **9**(6): p. 335-341.

10. Actis, R.L., et al., *Multi-plug insole design to reduce peak plantar pressure on the diabetic foot during walking.* Medical and Biological Engineering and Computing, 2008. **46**(4): p. 363-371.

11. Orendurff, M.S., et al., *Regional foot pressure during running, cutting, jumping, and landing.* American Journal of Sports Medicine, 2008. **36**(3): p. 566-571.

12. Ray, J., D. Needham, and D. Snyder. *Utilizing gaitline velocity in dynamic gait analysis*. in *Southern Biomedical Engineering Conference - Proceedings*. 1997. Biloxi, MS, USA: IEEE.

13. Okita, N., et al., *An objective evaluation of a segmented foot model.* Gait and Posture, 2009. **30**(1): p. 27-34.

14. Chen, W.-P., F.-T. Tang, and C.-W. Ju, *Stress distribution of the foot during mid-stance to push-off in barefoot gait: a 3-D finite element analysis.* Clinical Biomechanics, 2001. **16**(7): p. 614-620.

15. Cavanagh, P.R., et al., *Method for Design and Manufacture of Insoles*. 2005: United States. p. 20p.

16. Cavanagh, P.R., et al., *Reduction of plantar heel pressures: Insole design using finite element analysis.* Journal of Biomechanics, 2006. **39**(13): p. 2363-70.

17. Cheung, J.T.-M. and M. Zhang, *Parametric design of pressure-relieving foot orthosis using statistics-based finite element method.* Medical Engineering and Physics, 2008. **30**(3): p. 269-277.

18. Lemmon, D., et al., *The effect of insoles in therapeutic footwear-a finite element approach.* Journal of Biomechanics, 1997. **30**(6): p. 615-20.

19. Cheung, J.T.M. and M. Zhang, *A 3-dimensional finite element model of the human foot and ankle for insole design.* Archives of Physical Medicine and Rehabilitation, 2005. **86**(2): p. 353-358.

20. Chen, W.-P., C.-W. Ju, and F.-T. Tang, *Effects of total contact insoles on the plantar stress redistribution: A finite element analysis.* Clinical Biomechanics, 2003. **18**(6): p. 17-24.

21. Tsung, B.Y.S., et al., *Effectiveness of insoles on plantar pressure redistribution.* Journal of Rehabilitation Research and Development, 2004. **41**(6 A): p. 767-774.

22. Guldemond, N.A., et al., *The effects of insole configurations on forefoot plantar pressure and walking convenience in diabetic patients with neuropathic feet.* Clinical Biomechanics, 2007. **22**(1): p. 81-87.

23. Zequera, M., S. Stephan, and J. Paul. *Effectiveness of moulded insoles in reducing plantar pressure in diabetic patients*. 2007. Lyon, France: Institute of Electrical and Electronics Engineers Computer Society, Piscataway, NJ 08855-1331, United States.

24. Zequera, M.L., et al. *Study of the plantar pressure distribution on the sole of the foot of normal and diabetic subjects in the early stages by using a hydrocell pressure sensor*. 2003. Cancun, Mexico: IEEE.

25. Karkokli, R. and K.M.V. McConville. *Design and development of a cost effective plantar pressure distribution analysis system for the dynamically moving feet*. 2006. New York, NY, United States: Institute of Electrical and Electronics Engineers Inc., Piscataway, NJ 08855-1331, United States.

26. Nyska, M., et al., *Planter foot pressures in pregnant women.* Israel Journal of Medical Sciences, 1997. **33**(2): p. 139-146.

27. Rougier, P.R., *What insights can be gained when analysing the resultant centre of pressure trajectory?* Neurophysiologie Clinique, 2008. **38**(6): p. 363-373.

28. Murray, M.P., A.A. Seireg, and S.B. Sepic, *Normal postural stability and steadiness: quantitative assessment.* Journal of Bone and Joint Surgery - Series A, 1975. **57**(4): p. 510-516.

29. Thigpen, M.T., et al., *Adaptation of postural responses during different standing perturbation conditions in individuals with incomplete spinal cord injury.* Gait and Posture, 2009. **29**(1): p. 113-118.

30. Biswas, A., E.D. Lemaire, and J. Kofman, *Dynamic gait stability index based on plantar pressures and fuzzy logic.* Journal of Biomechanics, 2008. **41**(7): p. 1574-1581.

31. Hof, A.L., M.G.J. Gazendam, and W.E. Sinke, *The condition for dynamic stability.* Journal of Biomechanics, 2005. **38**(1): p. 1-8.

32. Lee, H.J. and L.S. Chou, *Detection of gait instability using the center of mass and center of pressure inclination angles.* Archives of Physical Medicine and Rehabilitation, 2006. **87**(4): p. 569-575.

33. Lee, H.J. and L.S. Chou, *Balance control during stair negotiation in older adults.* Journal of Biomechanics, 2007. **40**(11): p. 2530-2536.

34. Granata, K.P. and T.E. Lockhart, *Dynamic stability differences in fall-prone and healthy adults.* Journal of Electromyography and Kinesiology, 2008. **18**(2): p. 172-178.

35. Hsue, B.J., F. Miller, and F.C. Su, *The dynamic balance of the children with cerebral palsy and typical developing during gait. Part I: Spatial relationship between COM and COP trajectories.* Gait and Posture, 2009. **29**(3): p. 465-470.

36. Hsue, B.J., F. Miller, and F.C. Su, *The dynamic balance of the children with cerebral palsy and typical developing during gait. Part II: Instantaneous velocity and acceleration of COM and COP and their relationship.* Gait and Posture, 2009. **29**(3): p. 471-476.

37. Huang, S.C., et al., *Age and height effects on the center of mass and center of pressure inclination angles during obstacle-crossing.* Medical Engineering and Physics, 2008. **30**(8): p. 968-975.

38. Lafond, D., M. Duarte, and F. Prince, *Comparison of three methods to estimate the center of mass during balance assessment.* Journal of Biomechanics, 2004. **37**(9): p. 1421-1426.

39. Betker, A.L., Z.M.K. Moussavi, and T. Szturm, *Ambulatory center of mass prediction using body accelerations and center of foot pressure.* IEEE Transactions on Biomedical Engineering, 2008. **55**(11): p. 2491-2498.

40. Hof, A.L., *Comparison of three methods to estimate the center of mass during balance assessment.* Journal of Biomechanics, 2005. **38**(10): p. 2134-2135.

41. Chao, L.P. and C.Y. Yin, *The six-component force sensor for measuring the loading of the feet in locomotion.* Materials and Design, 1999. **20**(5): p. 237-244.

42. Savelberg, H.H.C.M. and A.L.H.D. Lange, *Assessment of the horizontal, fore-aft component of the ground reaction force from insole pressure patterns by using artificial neural networks.* Clinical Biomechanics, 1999. **14**(8): p. 585-592.

43. Pappas, I.P.I., T. Keller, and S. Mangold. *A Reliable, Gyroscope based Gait Phase Detection Sensor Embedded in a Shoe Insole*. in *Proceedings of IEEE Sensors*. 2002. Orlando, FL.

44. Pappas, I.P.I., et al., *A reliable gait phase detection system.* IEEE Transactions on Neural Systems and Rehabilitation Engineering, 2001. **9**(2): p. 113-125.

45. Pappas, I.P.I., et al., *A Reliable Gyroscope-Based Gait-Phase Detection Sensor Embedded in a Shoe Insole.* IEEE Sensors Journal, 2004. **4**(2): p. 268-274.

46. Morley, R.E., Jr., et al., *In-shoe multisensory data acquisition system.* IEEE Transactions on Biomedical Engineering, 2001. **48**(7): p. 815-20.

47. Joseph Paradiso, E.H., Kai-yuh Hsiao, *The CyberShoe: A Wireless Multisensor Interface for a Dancer's Feet*. 1999, International Dance and Technology: Tempe AZ.

48. Diss, C.E., *The reliability of kinetic and kinematic variables used to analyse normal running gait.* Gait and Posture, 2001. **14**(2): p. 98-103.

49. Revill, A.L., et al., *Variability of the impact transient during repeated barefoot walking trials.* Journal of Biomechanics, 2008. **41**(4): p. 926-930.

50. Smith, B.T., et al., *Evaluation of force-sensing resistors for gait event detection to trigger electrical stimulation to improve walking in the child with cerebral palsy.* IEEE Transactions on Neural Systems and Rehabilitation Engineering, 2002. **10**(1): p. 22-29.

51. Morris, M.E., et al., *The biomechanics and motor control of gait in Parkinson disease.* Clinical Biomechanics, 2001. **16**(6): p. 459-470.

52. Kimmeskamp, S. and E.M. Hennig, *Heel to toe motion characteristics in Parkinson patients during free walking.* Clinical Biomechanics, 2001. **16**(9): p. 806-812.

53. Lemaire, E.D., A. Biswas, and J. Kofman, *Plantar pressure parameters for dynamic gait stability analysis.* Conference proceedings: Annual International Conference of the IEEE Engineering in Medicine and Biology Society. IEEE

Engineering in Medicine and Biology Society. Conference, 2006. **1**: p. 4465-4468.

54. Mordaunt, P. and A.S.M. Zalzala, *Towards and Evolutionary Neural Network for Gait Analysis.* IEEE (2002) 1922-1927, 2008.

55. Deluzio, K.J. and J.L. Astephen, *Biomechanical features of gait waveform data associated with knee osteoarthritis: An application of principal component analysis.* Gait & Posture, 2007. **25**(1): p. 86-93.

56. Rozumalski, A. and M.H. Schwartz, *Crouch gait patterns defined using k-means cluster analysis are related to underlying clinical pathology.* Gait & Posture, 2009. **30**(2): p. 155-160.

57. Johnson, J., et al., *Kinematic analysis of the adult foot and ankle.* Gait and Posture, 1996. **4**(2): p. 179-180.

58. Leardini, A., et al., *An anatomically based protocol for the description of foot segment kinematics during gait.* Clinical Biomechanics, 1999. **14**(8): p. 528-536.

59. MacWilliams, B.A., M. Cowley, and D.E. Nicholson, *Foot kinematics and kinetics during adolescent gait.* Gait and Posture, 2003. **17**(3): p. 214-224.

60. Buczek, F.L., et al., *Impact of mediolateral segmentation on a multi-segment foot model.* Gait and Posture, 2006. **23**(4): p. 519-522.

61. Curtis, D.J., et al., *Intra-rater repeatability of the Oxford foot model in healthy children in different stages of the foot roll over process during gait.* Gait and Posture, 2009. **30**(1): p. 118-121.

62. Rao, S., et al., *Comparison of in vivo segmental foot motion during walking and step descent in patients with midfoot arthritis and matched asymptomatic control subjects.* Journal of Biomechanics, 2009. **42**(8): p. 1054-1060.

63. Scott, S.H. and D.A. Winter, *Biomechanical model of the human foot: Kinematics and kinetics during the stance phase of walking.* Journal of Biomechanics, 1993. **26**(9): p. 1091-1104.

64. Ren, L., et al., *A generic analytical foot rollover model for predicting translational ankle kinematics in gait simulation studies.* Journal of Biomechanics. **43**(2): p. 194-202.

65. Cheung, J.T.-M., et al., *Three-dimensional finite element analysis of the foot during standing.* Journal of Biomechanics, 2005. **38**(5): p. 1045-1054.

66. Chen, W.-P., C.-W. Ju, and F.-T. Tang, *Effects of total contact insoles on the plantar stress redistribution: a finite element analysis.* Clinical Biomechanics, 2003. **18**(6): p. S17-S24.

67. Zultowski, I. and A. Aruin, *Carrying loads and postural sway in standing: The effect of load placement and magnitude.* Work, 2008. **30**(4): p. 359-368.

68. Hyunho, C., et al. *Biomechanical effects of the weight of side loaded carriage in walking - Correlation between body Center of Mass (COM) and joint moments*. in *ICBPE 2006 - Proceedings of the 2006 International Conference on Biomedical and Pharmaceutical Engineering*. 2006. Singapore.

69. Al Nazer, R., et al., *Flexible multibody simulation approach in the analysis of tibial strain during walking.* Journal of Biomechanics, 2008. **41**(5): p. 1036-1043.

70. Ong, W.W., *Investigating gait stability via the assessment of plantar pressures*, in *Mechanical Engineering, National University of Singapore*. 2009, NUS: Singapore.

71. Mekjavic, I.B., et al. *Phase Change Material in Hiking Boots Does Not Minimise the Risk of Cold Injury*. 2005. Slovenia.

72. Kadaba MP, R.H., Wootten ME, Gainey J, Gorton G, Cochran GV, *Repeatability of kinematic, kinetic, and electromyographic data in normal adult gait.* J Orthop Res, 1989. **6**(7): p. 849-60.

73. Nester, C., et al., *Foot kinematics during walking measured using bone and surface mounted markers.* Journal of Biomechanics, 2007. **40**(15): p. 3412-3423.

74. Wang, R., et al., *One year follow-up after operative ankle fractures: A prospective gait analysis study with a multi-segment foot model.* Gait and Posture, 2010. **31**(2): p. 234-240.

75. Twomey, D., et al., *Kinematic differences between normal and low arched feet in children using the Heidelberg foot measurement method.* Gait and Posture, 2010. **32**(1): p. 1-5.

76. Jenkyn, T.R., et al., *A comparison of subtalar joint motion during anticipated medial cutting turns and level walking using a multi-segment foot model.* Gait & Posture, 2010. **31**(2): p. 153-158.

77. Rao, S., C. Saltzman, and H.J. Yack, *Segmental foot mobility in individuals with and without diabetes and neuropathy.* Clinical Biomechanics, 2007. **22**(4): p. 464-471.

78. Simon, J., et al., *The Heidelberg foot measurement method: Development, description and assessment.* Gait and Posture, 2006. **23**(4): p. 411-424.

79. Long, J.T., et al., *Repeatability and sources of variability in multi-center assessment of segmental foot kinematics in normal adults.* Gait and Posture, 2010. **31**(1): p. 32-36.

80. Laughton, C.A., et al., *Aging, muscle activity, and balance control: Physiologic changes associated with balance impairment.* Gait and Posture, 2003. **18**(2): p.

101-108.

81. Berry, S.D., et al., *Falls as Risk Factors for Fracture*, in *Osteoporosis (Third Edition)*. 2008, Academic Press: San Diego. p. 911-921.

82. Spink, M.J., et al., *Foot and Ankle Strength, Range of Motion, Posture, and Deformity Are Associated With Balance and Functional Ability in Older Adults.* Archives of Physical Medicine and Rehabilitation, 2011. **92**(1): p. 68-75.

83. Gross, M.M., et al., *Effect of muscle strength and movement speed on the biomechanics of rising from a chair in healthy elderly and young women.* Gait & Posture, 1998. **8**(3): p. 175-185.

84. Scott, G., H.B. Menz, and L. Newcombe, *Age-related differences in foot structure and function.* Gait & Posture, 2007. **26**(1): p. 68-75.

85. Kuo, A.D., *The six determinants of gait and the inverted pendulum analogy: A dynamic walking perspective.* Human Movement Science, 2007. **26**(4): p. 617-656.

86. Jordan, K., et al., *Stability and the time-dependent structure of gait variability in walking and running.* Human Movement Science, 2009. **28**(1): p. 113-128.

87. Johnson, J., et al., *Kinematic analysis of the adult foot and ankle.* Gait & Posture, 1996. **4**(2): p. 179-180.

88. Kidder, S., et al., *Repeatability of kinematic data in normal foot and ankle motion.* Gait & Posture, 1996. **4**(2): p. 180-180.

89. Deschamps, K., et al., *Body of evidence supporting the clinical use of 3D multisegment foot models: A systematic review.* Gait & Posture, 2011. **33**(3): p. 338-349.

90. Simon, J., et al., *The Heidelberg foot measurement method: Development, description and assessment.* Gait & Posture, 2006. **23**(4): p. 411-424.

91. Twomey, D., et al., *Kinematic differences between normal and low arched feet in children using the Heidelberg foot measurement method.* Gait & Posture, 2010. **32**(1): p. 1-5.

92. Wang, R., et al., *One year follow-up after operative ankle fractures: A prospective gait analysis study with a multi-segment foot model.* Gait & Posture, 2010. **31**(2): p. 234-240.

93. Tulchin, K., M. Orendurff, and L. Karol, *A comparison of multi-segment foot kinematics during level overground and treadmill walking.* Gait & Posture, 2009. **31**(1): p. 104-108.

94. Levinger, P., et al., *A comparison of foot kinematics in people with normal- and flat-arched feet using the Oxford Foot Model.* Gait & Posture, 2010. **32**(4): p. 519-523.

95. Damavandi, M., P.C. Dixon, and D.J. Pearsall, *Kinematic adaptations of the hindfoot, forefoot, and hallux during cross-slope walking.* Gait & Posture, 2010. **32**(3): p. 411-415.

96. Morris, S.J. and J.A. Paradiso. *Shoe-integrated sensor system for wireless gait analysis and real-time feedback*. 2002. Houston, TX, United States: Institute of Electrical and Electronics Engineers Inc.

97. Hannula, M., A. Sakkinen, and A. Kylmanen. *Development of EMFI-sensor based pressure sensitive insole for gait analysis*. 2007. Warsaw, Poland: IEEE.

98. Kyoungchul, K., B. Joonbum, and M. Tomizuka. *Detection of abnormalities in a human gait using smart shoes*. 2008. San Diego, CA, USA: SPIE - The International Society for Optical Engineering.

99. Pollard H, S.P., McHardy A., *Lateral ankle injury: literature review and report of two cases.* Aust Chiropr Osteopathy, 2002. **10**(1): p. 10.

100. Benedetti, M.G., Leardini A. Bianchi L, Berti L, Giannini S., *Comparisons of outputs of different models for foot kinematics.* Proc Int Foot Ankle Biomech Congr, 2008. **91**: p. 1.

101. Kang, H.G. and J.B. Dingwell, *Effects of walking speed, strength and range of motion on gait stability in healthy older adults.* Journal of Biomechanics, 2008. **41**(14): p. 2899-2905.

102. Jessica Rose, J.G.G., ed. *Human walking*. 3rd ed. 2006, Lippincott Williams & Wilkins: Philadelphia.

103. Wang, L.-X., *A Course in Fuzzy Systems and Control*. 1997, Englewood Cliffs, NJ: Prentice-Hall.

104. Wang, L.-X., *Adaptive Fuzzy Systems and Control*. 1994, Englewood Cliffs, NJ: Prentice-Hall.

105. *LifeMOD Online Manual*. 2010 [cited 2011 December]; Available from: http://www.lifemodeler.com/LM_Manual/.

106. Dawe, E.J.C. and J. Davis, *(vi) Anatomy and biomechanics of the foot and ankle.* Orthopaedics and Trauma. **25**(4): p. 279-286.

107. Valderrabano, V., et al., *Chapter 8b - Anatomy and Biomechanics of the Ankle and Foot*, in *Musculoskeletal Disorders in the Workplace (Second Edition)*. 2007, Mosby: Philadelphia. p. 341-350.

108. Silder, A., B. Heiderscheit, and D.G. Thelen, *Active and passive contributions to joint kinetics during walking in older adults.* Journal of Biomechanics, 2008. **41**(7): p. 1520-1527.

109. Carvalhais, V.O.d.C., et al., *Validity and reliability of clinical tests for assessing hip passive stiffness.* Manual Therapy. **16**(3): p. 240-245.

110. Granata, K.P., S.E. Wilson, and D.A. Padua, *Gender differences in active*

musculoskeletal stiffness. Part I.: Quantification in controlled measurements of knee joint dynamics. Journal of Electromyography and Kinesiology, 2002. **12**(2): p. 119-126.

111. Gabriel, R.C., et al., *Dynamic joint stiffness of the ankle during walking: Gender-related differences.* Physical Therapy in Sport, 2008. **9**(1): p. 16-24.

112. Davis, R.B. and P.A. DeLuca, *Gait characterization via dynamic joint stiffness.* Gait & Posture, 1996. **4**(3): p. 224-231.

113. Faber, F.W.M., et al., *Doppler imaging of vibrations as a tool for quantifying first tarsometatarsal joint stiffness.* Clinical Biomechanics, 2000. **15**(10): p. 761-765.

114. Oleson, M., D. Adler, and P. Goldsmith, *A comparison of forefoot stiffness in running and running shoe bending stiffness.* Journal of Biomechanics, 2005. **38**(9): p. 1886-1894.

115. Aerts, P., et al., *The mechanical properties of the human heel pad: A paradox resolved.* Journal of Biomechanics, 1995. **28**(11): p. 1299-1308.

116. Rose, J.G., *Human walking.* 2005, Lippincott williams and wilkins: United states.

APPENDIX A RESULTS OF FOOT PRESSURE FEATURES

Graphs are plotted for each individual feature to observe the trends of mean and standard deviations across the four walking conditions, A for normal walking, B for walking with eyes closed, C for walking after being spun in the chair with eyes open, D for walking after being spun in the chair with eyes closed. Here results from the other four tested subject's calculated experiment values are listed.

Table A.1: Mean and standard deviation of six features for Subject 3

Experiment:		A	B	C	D
Feature 1: AP Motion, Normalised	Mean	1.304	1.344	1.342	2.608
	Std Dev	0.476	0.757	0.832	2.275
Feature 2: ML Motion, Normalised	Mean	0.870	1.502	1.460	1.723
	Std Dev	0.000	1.491	0.557	0.944
Feature 3: ML Range	Mean	2.623	4.507	3.994	6.334
	Std Dev	1.271	3.163	1.311	3.066
Feature 4: Cell Triggering, Normalised	Mean	1.594	1.495	1.937	1.883
	Std Dev	0.355	0.471	0.049	0.350
Feature 5: Stride Time	Mean	1.150	1.117	1.033	1.158
	Std Dev	0.000	0.026	0.026	0.132
Feature 6: Double Support time	Mean	0.267	0.292	0.258	0.358
	Std Dev	0.026	0.020	0.038	0.097

Table A.2: Mean and standard deviation of six features for Subject 4

Experiment:		A	B	C	D
Parameter 1: AP Motion, Normalised	Mean	0.992	1.883	1.317	2.564
	Std Dev	0.019	1.185	1.021	0.866
Parameter 2: ML Motion, Normalised	Mean	1.992	2.677	2.317	3.074
	Std Dev	0.905	1.111	0.530	0.888
Parameter 3: ML Range	Mean	7.308	8.606	7.786	7.656
	Std Dev	2.705	2.376	2.231	3.021
Parameter 4: Cell Triggering, Normalised	Mean	1.984	1.573	1.325	1.369
	Std Dev	0.039	0.482	0.523	0.532
Parameter 5: Stride Time	Mean	1.008	1.058	1.008	0.975
	Std Dev	0.020	0.020	0.020	0.042
Parameter 6: Double Support time	Mean	0.233	0.283	0.200	0.242
	Std Dev	0.041	0.026	0.000	0.038

Table A.3: Mean and standard deviation of six features for Subject 5

Experiment:		A	B	C	D
Parameter 1: AP Motion, Normalised	Mean	2.584	2.455	2.899	3.536
	Std Dev	0.672	0.780	1.270	1.214
Parameter 2: ML Motion, Normalised	Mean	2.461	2.157	3.035	2.556
	Std Dev	0.727	0.793	1.077	0.564
Parameter 3: ML Range	Mean	7.605	7.485	7.327	7.019
	Std Dev	1.687	1.641	2.555	1.773
Parameter 4: Cell Triggering, Normalised	Mean	1.167	1.218	1.620	1.483
	Std Dev	0.410	0.438	1.227	0.352
Parameter 5: Stride Time	Mean	1.288	1.163	0.958	1.242
	Std Dev	0.048	0.038	0.227	0.107
Parameter 6: Double Support time	Mean	0.304	0.288	0.233	0.292
	Std Dev	0.014	0.057	0.052	0.038

Table A.3: Mean and standard deviation of six features for Subject 6

Experiment:		A	B	C	D
Parameter 1: AP Motion, Normalised	Mean	1.262	2.600	1.109	2.476
	Std Dev	0.733	1.052	0.675	1.442
Parameter 2: ML Motion, Normalised	Mean	1.673	2.712	1.142	2.227
	Std Dev	0.614	1.240	0.121	0.400
Parameter 3: ML Range	Mean	4.968	5.399	3.523	4.969
	Std Dev	1.992	2.741	2.164	2.699
Parameter 4: Cell Triggering, Normalised	Mean	1.113	1.119	1.317	1.209
	Std Dev	0.395	0.372	0.402	0.509
Parameter 5: Stride Time	Mean	1.054	1.046	0.883	1.117
	Std Dev	0.054	0.072	0.088	0.075
Parameter 6: Double Support time	Mean	0.233	0.271	0.158	0.233
	Std Dev	0.033	0.026	0.049	0.026

APPENDIX B LIFEMOD MODELING EXAMPLE

Here is one selected LifeMOD modeling tutorials and from which the features and application of lifeMOD are presented clearly [105]. Part of these applications can prove that LifeMOD can solve the problems of detailed foot modeling during walking. Here one typical modeling example is presented, shown in Figure B.1.

In this following tutorial, a human model performs a twisting motion on the ground. The model is driven using motion capture data and ground reaction forces. A force plate is used to obtain the ground reaction force at the bottom of the foot to get an accurate boundary condition of the interface contacting force between that foot and floor. The model firstly processes the equilibrium training. Then the model is driven by the motion agents during inverse-dynamics simulation and the joints are trained. At forward dynamic simulation, the trained model is interacting with the environment and shows kinematic and kinetics results.

In this tutorial, LifeMOD could simulate ground reaction force with different kinds of upper body motion as twisting in this case. However, only standard marker sets are used in this tutorial.

For the simulation results, plots of joints force could be obtained for the needs of the investigator. In the Figure B.2, sample plots of the lower body joints forces are presented.

LifeMOD is a very suitable modeling tool, by which we can import motion trajectories from real experiments and achieve the goals of investigating the relationship between foot motion and ground reaction forces. The modeled ground reaction forces, in Figure B.3, can be compared with real experiment data to improve the modeling.

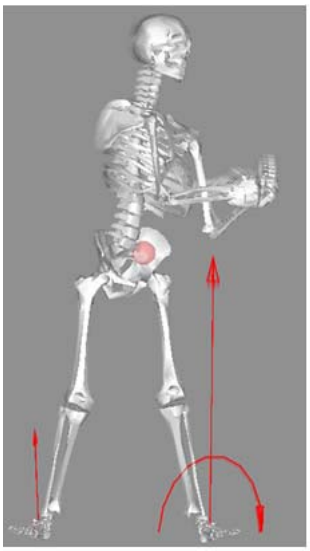

Figure B.1: The twisting with ground reaction force

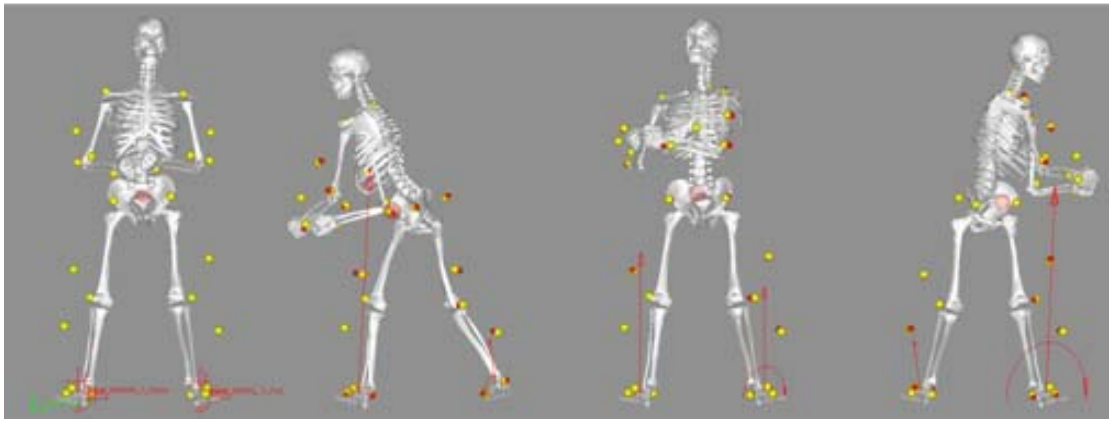

Figure B.2: Successive animation frames from the inverse-dynamics simulation

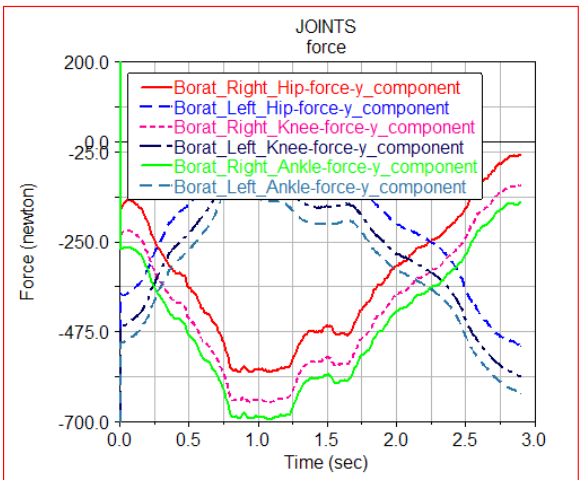

Figure B.3: Plot of the forces the joints are exerting on the lower body model

APPENDIX C FORCE PATTERN DURING NORMAL WALKING AND WALKING WITH DRAGGING WEIGHTS

For a typical normal walking, the forces are almost evenly distributed on the heel and metatarsals during the stance phase, and there is a normal push off force at the hallux at toe off phase. Here are foot force patterns during normal walking for three tested subjects.

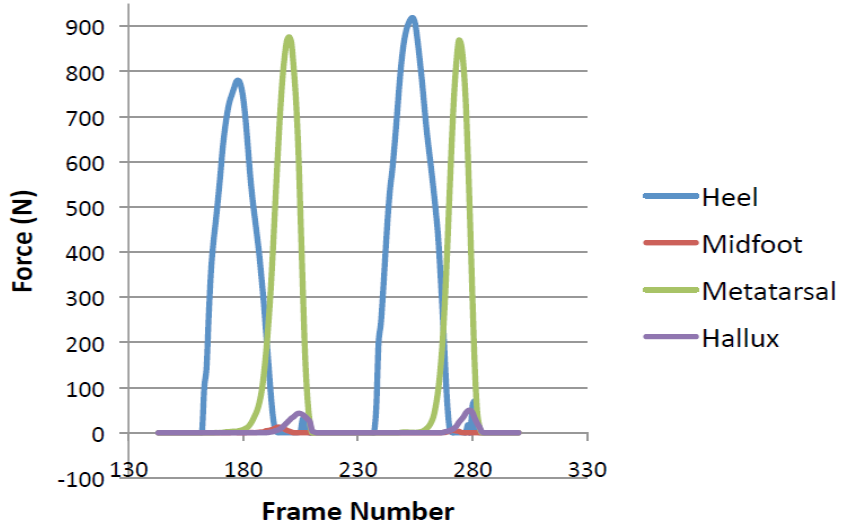

Figure C.1: Normal walking forces under foot segments during two stances of subject 1

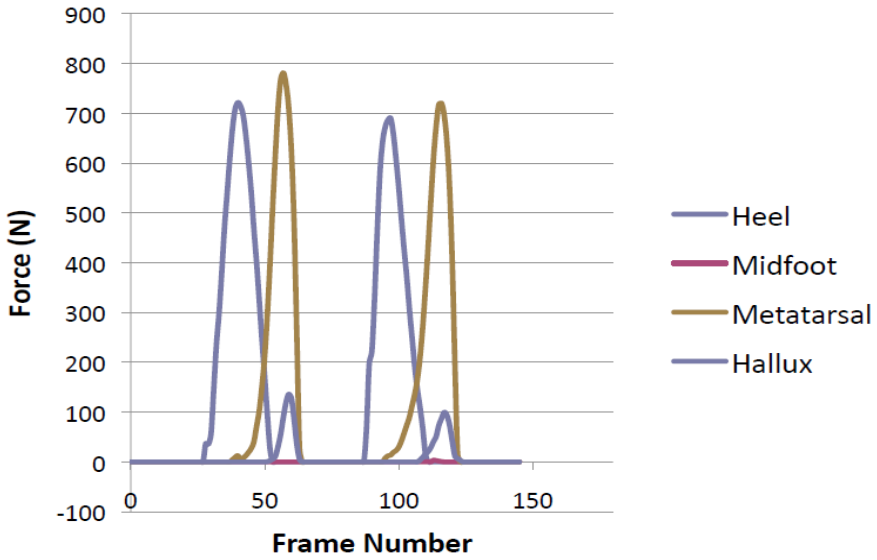

Figure C.2: Normal walking forces under foot segments during two stances of subject 2

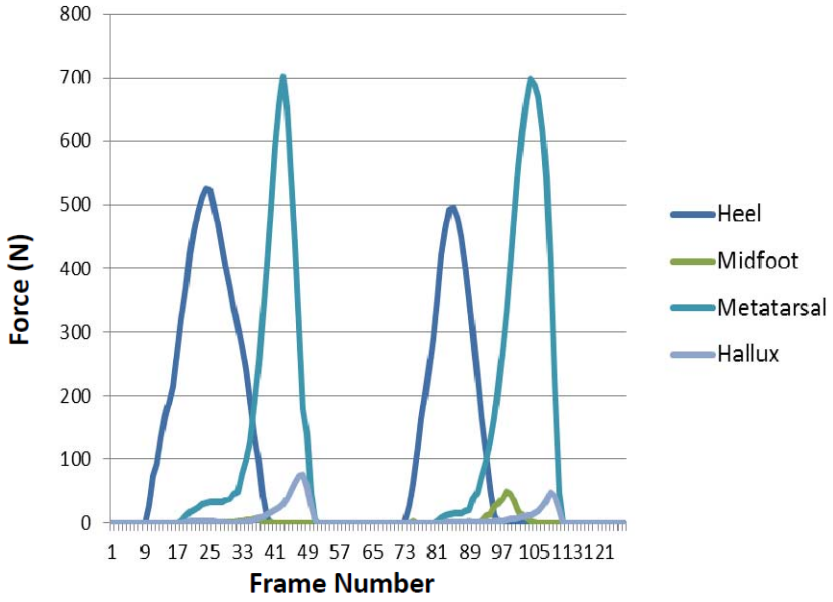

Figure C.3: Normal walking forces under foot segments during two stances of subject 3

For a typical walking with dragging weights, the forces are mainly exerted on the heel and during the stance phase. There is nearly no push off force at the hallux at toe off phase. Here are force patterns during walking with dragging weights for three tested subjects.

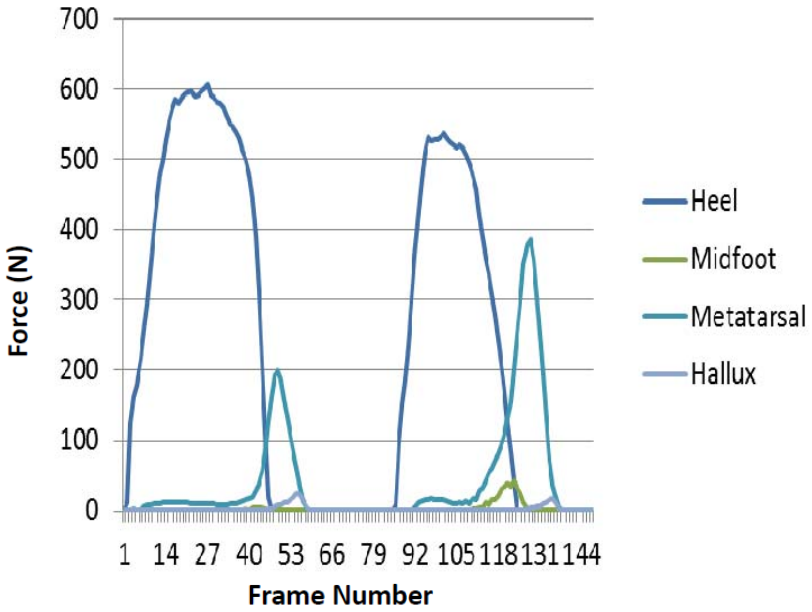

Figure C.4: Dragging weights walking forces under foot segments of subject 1

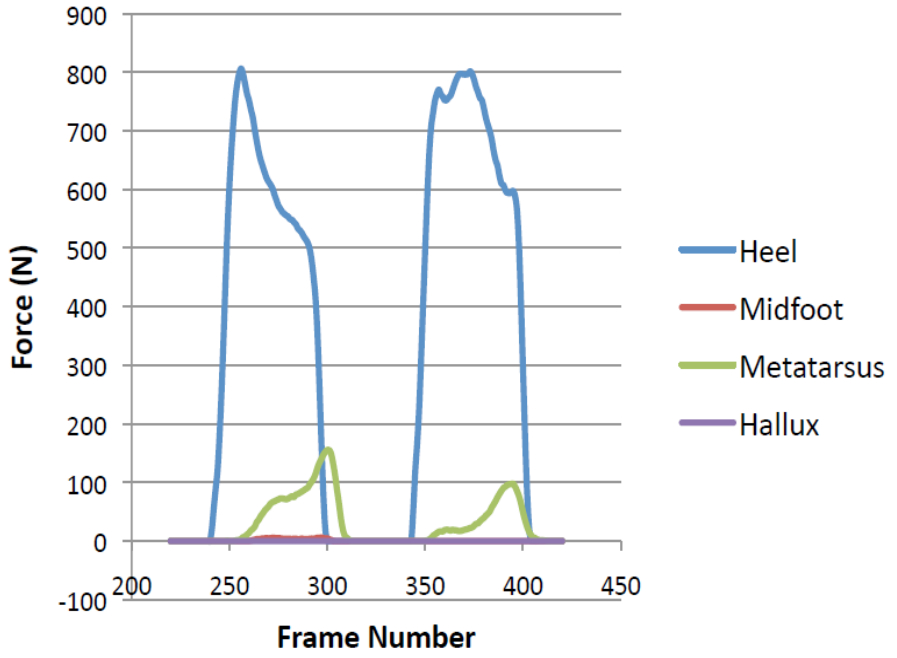

Figure C.5: Dragging weights walking forces under foot segments of subject 2

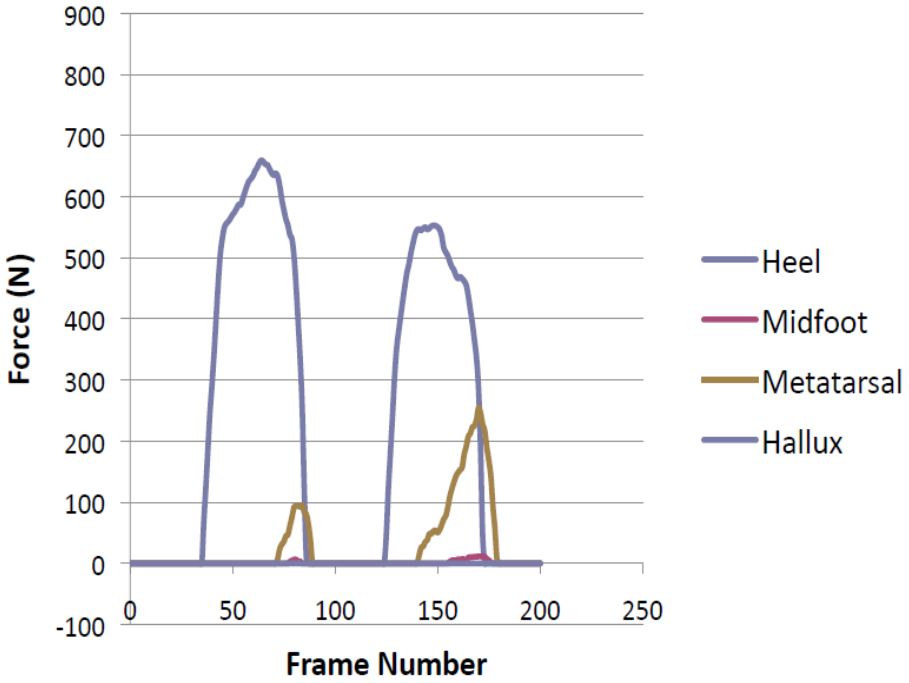

Figure C.6: Dragging weights walking forces under foot segments of subject 3